Investigating the Role of von Willebrand Factor in Regulating Macrophage Biology and Innate Immunity

Trinity College Dublin
Coláiste na Tríonóide, Baile Átha Cliath
The University of Dublin

A thesis submitted to the University of Dublin, Trinity College, for the Degree of Doctor of Philosophy in the School of Medicine.

Submitted August 2019

Clive Drakeford

Haemostasis Research Group,
Trinity College Dublin.

Declaration of Originality

I declare that this thesis has not been submitted as an exercise for a degree at this or any other university and it is entirely my own work.

I agree to deposit this thesis in the University's open access institutional repository or allow the Library to do so on my behalf, subject to Irish Copyright Legislation and Trinity College Library conditions of use and acknowledgement.

I consent to the examiner retaining a copy of the thesis beyond the examining period, should they so wish (EU GDPR May 2018).

Clive Drakeford

Acknowledgments

I would like to express my thanks and gratitude to my supervisor Prof. James O'Donnell, whose expertise and support has undoubtedly guided me though this thesis and my time as a PhD student. Furthermore, I sincerely thank Dr Fredrick Sheedy for his guidance and generosity of time providing huge insights into macrophage immunology. Additionally, I would also like to thank Dr Ross Murphy for his help and support throughout. Finally, I wold like to convey the importance of Dr Sonia Aguila to this work. Sonia was both a mentor and close friend of mine throughout my PhD, providing me with continuous support, expertise and laughs.

No matter what difficulties arose during the past 4 years Kate Barton was invaluable to me. I would like to truly thank her for her devoted support no matter how big or small the situation. Kate's continuous encouragement and generosity is truly remarkable. May I also thank all my family and friends for all their unquestionable advice and support.

To everyone in the Irish Centre of Vascular Biology and MCT. In particular, a thank you to Alain, Judi, Jamie, Sean, Thomas, Soracha, Michelle and Roger.

Abstracts leading to Oral presentations

2018

A novel role for von Willebrand factor promoting pro-inflammatory responses in macrophages

Clive Drakeford, Sonia Aguila, Alain Chion, Eamon Breen, Mariana Cervantes, Frederick J Sheedy & James S O'Donnell

Haematology Association of Ireland, Annual Meeting

Winer of Presidents Prize

A novel role for von Willebrand factor promoting pro-inflammatory responses in macrophages

Clive Drakeford, Sonia Aguila, Alain Chion, Eamon Breen, Mariana Cervantes, Frederick J Sheedy, James S O'Donnell

Hemostasis, Gordon Research Seminars.

2016

The binding of VWF augments macrophage TLR (2/4) signalling – an emerging role for VWF in macrophage biology and vascular haemostasis.

Clive Drakeford, Frederick J Sheedy, Sharee Basdeo, Alain Chion, Sonia Aguila, Joseph Keane and James O'Donnell

Haematology Association of Ireland, Annual Meeting

Abstracts leading to poster presentation

2018

A novel role for von Willebrand factor promoting pro-inflammatory responses in macrophages

Clive Drakeford, Sonia Aguila, Alain Chion, Eamon Breen, Mariana Cervantes, Frederick J Sheedy, James S O'Donnell

Hemostasis, Gordon Research Conference

2017

A Novel Role for Von Willebrand Factor in Macrophage Biology

Clive Drakeford, Sonia Aguila, Frederick Sheedy, Alain Chan, Soracha Ward, Jamie O'Sullivan and James O'Donnell

Royal College of Surgeons, Research Day.

Publications

von Willebrand Factor regulates macrophage metabolism to promote a pro-inflammatory phenotype.

Clive Drakeford, Sonia Aguila, Alain Chion, Eamon Breen, Mariana P. Cervantes, Annie M. Curtis, Joe Keane, Padraic Fallon, Roger J.S. Preston, Jamie M. O'Sullivan, Ross Murphy, Frederick J. Sheedy and James S. O'Donnell.

Manuscript Completed

A novel role for the macrophage galactose-type lectin receptor in mediating von Willebrand factor clearance.

Ward SE, O'Sullivan JM, Drakeford C, Aguila S, Jondle CN, Sharma J, Fallon PG, Brophy TM, Preston RJS, Smyth P, Sheils O, Chion A, O'Donnell JS.

Blood. 2018 Feb 22;131(8):911-916. doi: 10.1182/blood-2017-06-787853

Targeting von Willebrand Factor-Mediated Inflammation.

Drakeford C, O'Donnell JS.

Arterioscler Thromb Vasc Biol. 2017 Sep 37(9):1590-1591. doi: 10.1161/ATVBAHA.117.309817

Plasmin Cleaves Von Willebrand Factor at K1491-R1492 in the A1-A2 Linker Region in a Shear- and Glycan-Dependent Manner *In Vitro*.

Brophy TM, Ward SE, McGimsey TR, Schneppenheim S, Drakeford C, O'Sullivan JM, Chion A, Budde U, O'Donnell JS.

Arterioscler Thromb Vasc Biol. 2017 May 37(5):845-855. doi: 10.1161/ATVBAHA.116.308524

N-linked glycans within the A2 domain of von Willebrand factor modulate macrophage-mediated clearance.

Chion A, O'Sullivan JM, Drakeford C, Bergsson G, Dalton N, Aguila S, Ward S, Fallon PG, Brophy TM, Preston RJ, Brady L, Sheils O, Laffan M, McKinnon TA, O'Donnell JS.

Blood. 2016 Oct 13;128(15):1959-1968. doi: 10.1182/blood-2016-04-709436

Summary

The plasma multimeric glycoprotein von Willebrand factor (VWF) plays a critical role in primary haemostasis by tethering platelets to exposed collagen at sites of vascular injury. Recent studies have suggested that VWF may play an important role in regulating inflammatory responses. In particular, data from clinical trials have demonstrated that patients with reduced plasma VWF levels are significantly protected against ischemic heart disease and stroke. In addition, studies performed in a number of animal inflammation models (including, sepsis, dermatitis, stroke and malaria) have reported a pathogenic role for VWF. Critically however, the biological mechanisms through which VWF exerts its immuno-modulatory effects remain poorly understood.

Interestingly, recent studies have shown that VWF can bind to macrophages. Furthermore, a number of specific macrophage receptors have been implicated in regulating the binding of VWF, including the low density lipoprotein receptor-related protein-1 (LRP1), scavenger receptor class A member 1 (SR-A1) and macrophage galactose-type lectin (MGL). Given the importance of macrophages in regulating innate immune responses, we hypothesized that VWF binding might influence macrophage biology and thereby impact upon inflammatory responses.

Initially, we confirmed that full-length VWF, as well as a series of truncated VWF fragments, could bind to macrophages. This binding was observed under static conditions, but was significantly enhanced in the presence of ristocetin. Importantly, we further showed that VWF binding to macrophages triggered

significant pro-inflammatory signalling and activation. Treatment of both human and murine macrophages with VWF resulted in activation of MAP-kinase and NF-kB pathways, leading to the enhanced expression of a panel of pro-inflammatory cytokines. Macrophages treated with VWF adopted a M1 phenotype, confirmed by cell surface marker expression and inflammasome activation. Additionally, we observed that VWF altered functional aspects of macrophage biology such as phagocytosis and chemotaxis capacity.

In order for macrophages to generate a pro-inflammatory response, significant metabolic changes must occur. In particular, a marked upregulation in macrophage glycolysis is required to meet the need to rapidly generate increased energy. In keeping with the pro-inflammatory effects of VWF-binding, we observed significant effects upon macrophage immuno-metabolism. Thus, VWF treatment significantly elevated macrophage glycolysis and induced modifications in mitochondrial biogenesis. Importantly however, in contrast to LPS, these pro-inflammatory changes induced by VWF were strictly time-dependent.

The ability of damage and pattern associated molecular pathways to promote macrophage glycolysis has been attributed to HIF-1α activation. We demonstrated that the VWF time-dependent glycolytic changes included HIF-1α activation. Furthermore, we demonstrated that the VWF pro-inflammatory effect was at least in part mediated though LRP1 signalling Finally, we established a novel direct link between VWF/LRP1 dependent p38 signalling and early glycolytic changes, as inhibition of p38 fully attenuated VWF dependent glycolysis and HIF-1α activation.

Cumulatively, our novel findings define an entirely novel biological role for VWF in modulating macrophage function, and thereby establish a novel link between primary haemostasis and innate immunity.

Abbreviations

AA + R Antimycin A and Rotenone

ADAMS13 A Disintegrin and Metalloproteinase with a Thrombospondin Type 1 Motif Member 13

AKT Protein kinase B

Ang-2 Angiopoietin-2

APC Allophycocyanin

APC-Cy7 Allophycocyanin Cy7

ApoE Apolipoprotein E

ATP Adenosine Triphosphate

BCA Bicinchoninic acid

BFA Brefeldin A

BMDM Bone Marrow Derived Macrophages

bPEI Branched Polyethylenimine

BSA Bovine Serum Albumin

BV Blue Violet

$CaCl_2$ Calcium Chloride

CCL2 Chemokine Ligand 2

CCL3 Chemokine Ligand 3

CCL4 Chemokine Ligand 4

CD11b Cluster of Differentiation 11b (ITGAM, Integrin alpha M)

CD14 Cluster of Differentiation 14

CD16 Cluster of Differentiation 16

CD18 Cluster of Differentiation 18

CD206 Cluster of Differentiation 206

CD3 Cluster of Differentiation 3

CD36 Cluster of Differentiation 36

CD38 Cluster of Differentiation 38

CD49b Cluster of Differentiation 49b

CD63	Cluster of Differentiation 63
CK	Cysteine Knot
CLEC4M	C-type Lectin Domain Family 4 Member M
CLP	Cecum Ligation and Puncture
CMV	Cytomegalovirus
CXCL1	Chemokine (C-X-C motif) Ligand 1
CLCL2	Chemokine (C-X-C motif) Ligand 2
DAMP	Damage Associated Molecular Pattern
DAPI	6-diamidino-2-phenylindole
DC	Dendritic Cells
DDAVP	1-desamino-8-D arginine vasopressin
DMEM	Dulbecco`s Modified Eagle Media
DTT	Dithiothreitol
E. Coli	*Escherichia* coli
EC	Endothelial Cell
ECL	Enhanced Chemiluminescence
ECAR	Extracellular Acidification Rate
ECM	Experimental Cerebral Malaria
EDTA	Ethylenediaminetetraacetic acid
EEA1	Early Endosome Activation Marker 1
ELISA	Enzyme-Linked Immunosorbent Assay
FADH	Flavin Adenine Dinucleotide
FBS	Fetal Bovine Serum
FCCP	Carbonyl Cyanide p-trifluoromethoxyphenylhydrazone
FITC	Fluorescein Isothiocyanate
FPLC	Fast Protein Liquid Chromatography
FVIII	Factor VIII
Gal	Galactose
GalNAc	N-acetylgalactosamine
GAPDH	Glyceraldehyde 3-phosphate dehydrogenase

GLUT1	Glucose Transporter 1
GM-CSF	Granulocyte Macrophage – Colony Stimulating Factor
GPIb-IX-V	Glycoprotein Ib-IX-V Receptor Complex
GPIbα	Glycoprotein 1bα
HEK293	Human Embryonic Kidney Cells 293
HEPES	Hydroxyethyl-1-piperazineethanesulfonic acid
HIF-1α	Hypoxia-Inducible Factor 1-alpha
HMWM	High Molecular Weight Multimers
HRP	Horseradish Peroxidase
ICD	Irritative Contact Dermatitis
ICH	Intracranial Haemorrhage
ICV	Immune Complex Vasculitis
IE	Infected Erythrocytes
IHD	Ischemic Heart Disease
IL-10	Interleukin 10
IL-13	Interleukin 13
IL-18	Interleukin 18
IL-1β	Interleukin 1 beta
IL-4	Interleukin 4
IL-6	Interleukin 6
IL-8	Interleukin 8
INF-γ	Interferon- γ
iNOS	Inducible Nitric Oxide Synthases
KC	Keratinocyte Derived Chemokine
LAL	Llimulus amebocyte lysate
LAMP	Lysosome Associated Membrane Protein
LDLR	Low Density Lipoprotein Receptor
LDS	Lithium Dodecyl Sulphate
LRP1	Low Density Lipoprotein Receptor-Related Protein 1
LSEC	Liver Sinusoidal Endothelial Cells

LTA	Lipoteichoic acid
Ly-6G	Lymphocyte Antigen 6 Complex Locus G6D
M-CSF	Macrophage Colony Stimulating Factor
MA-ARDC	Malaria Acquired - Acute Respiratory Distress Syndrome
MDA-5	Melanoma Differentiation-Associated Protein 5
MFI	Mean Fluorescence Intensity
MGL	Macrophage Galactose Lectin
MHCII	Major Histocompatibility Complex Class II
$MnCl_2$	Manganese Chloride
MRC	Maximum Respiratory Capacity
NADPH	Nicotinamide Adenine Dinucleotide Phosphate
NET	Neutrophil Extracellular Trap
Neu/Gal	Sialic acid and galactose removal
Neu-VWF	Desialylated VWF
NK	Natural Killer Cells
NLRP3	NACHT, LRR and PYD Domains-Containing Protein 3
NOD	Nucleotide-Binding Oligomerization Domain-Containing Protein
NS	Not Significant
OCR	Oxygen Consumption Rate
Oligo	Oligomycin
OPG	Osteoprotegerin
PAMP	Pathogen Associated Molecular Pattern
PBMC	Peripheral Blood Mononuclear Cell
PBS	Phosphate Buffered Saline
pd-VWF	Plasma Derived – Von Willebrand Factor
PE	Phycoerythrin
PE-Cy7	Phycoerythrin Cy7
Pentahis	Penta Histidine Tag
PFA	Paraformaldehyde
PFK1	6-phosphofructo-1-kinase

PFKFB3	6-phosphofructo-2-kinase/fructose-2,6-biphosphatase 3
PHD3	Prolyl Hydroxylase 3
PI3-kinase	Phosphoinositide 3-kinase
PKM2	Pyruvate Kinase M2
PLA	Proximal ligation assay
P.falciparum	Plasmodium Falciparum
PMA	Phorbol 12-myristate 13-acetate
PMN	Polymorphonuclear
PNGase F	Peptide-N-Glycosidase F
PNGase-VWF	N-linked glycan Removal
PSGL-1	P-selectin Glycoprotein Ligand-1
PVDF	Polyvinylidene Fluoride
PVP	Polyvinylpyrrolidone
Rac1	Receptor for Activated C Kinase 1
RAP	Receptor Associated Protein
RIG-1	Retinoic Acid-Inducible Gene – I
RIPA	Radioimmunoprecipitation Assay
rmM-CSF	Recombinant Mouse Macrophage – Colony Stimulating Factor
ROS	Reactive Oxygen Spices
RPMI Media	Roswell Park Memorial Institute Media
RT-qPCR	Real Time Quantitative Reverse Transcription
r-VWF	Recombinant VWF
SDS-PAGE	Sodium Dodecyl Sulphate - Polyacrylamide Gel Electrophoresis
SEM	Slandered Error of the Mean
SEPA	Secreted Embryonic Alkaline Phosphatase
Siglec-5	Sialic Acid-Binding Immunoglobulin-Like Lectin-5
SNARE	Soluble N-ethylmaleimide-sensitive factor activating protein receptor
SOC	Super Optimal Broth
SR-A1	Scavenger Receptor A1
SRC	Spare Residual Capacity

TBS	Tris Buffered Saline
TBS-T	Tris Buffered Saline Tween
TCA	Tricarboxylic Acid
TLR	Toll Like Receptor
TMB	Tetramethylbenzidine
TNF-α	Tumour Necrosis Factor alpha
TTP	Thrombotic Thrombocytopenic Purpura
VWD	Von Willebrand Disease
VWF	Von Willebrand Factor
VWF:Ag	Von Willebrand Factor Antigen
VWFpp:Ag	Von Willebrand Factor Propeptide:Antigen
WPB	Weibel Palade Bodies

Contents

Table of figures

Table of Tables

1.0 Introduction

1.1: VWF synthesis, secretion and function

1.1.1 Biosynthesis of von Willebrand Factor

1.1.1.1 The *VWF* gene

The gene encoding VWF is located on chromosome 12 (12p13.2). It spans approximately 180kb and is composed of 52 exons, of which exon 28 is the largest comprising 1.4kb.(1,2),(3) The initial 17 exons of the *VWF* gene encode the signal peptide and a large VWF propeptide (VWF:pp).(4) The remaining exons (18-52) encode the mature VWF subunit. Furthermore, a large *VWF* pseudogene (containing a duplication of exons 23-24) is located on chromosome 22 (22q11.2).(5)

1.1.1.2 Tissue distribution of VWF

VWF is synthesised within endothelial cells (EC) and megakaryocytes as a pre-proVWF primary translation product containing 2813 amino acids.(4,6,7) This product consists of a signal peptide of 22 residues, a VWF:pp of 741 residues, followed by the mature VWF subunit of 2050 residues. Interestingly, the transcription of VWF within EC varies between different tissues. VWF expression is highest in the arteries and venules of the kidneys and lungs, but significantly lower in other tissues including spleen and liver.(8) In addition, higher *VWF* mRNA is seen in larger arteries.(9)

1.1.1.3 Domain structure of VWF

VWF circulates as a large multidomain protein, composed of several repeating regions (A-D). Previous studies reported that VWF was composed of a series of domains arranged in the order D1-D2-D'-D3-A1-A2-A3-D4-B1-B2-B3-C1-C2-CK.(10) However, following more recent electron microscopy studies, the structural organisation of the VWF domains has been re-annotated to D1-D2-D'-D3-A1-A2-A3-D4-C1-C2-C3-C4-C5-C6-CK.(11) The cleaved VWF pro-peptide is represented by regions D1-D2 (Figure 1.1).

Importantly, individual domains of VWF have specific functions. For example the A domains of VWF have been shown to mediate collagen and platelet binding. The VWF A1 domain has a large positive charge that facilitates the interaction with negatively-charged platelet GP-1bα.(12) Importantly, heparin also binds to the positivity charged A1 domain.(13) The A3 domains are involved in anchoring VWF to collagen type I and III while the A1 domain is important for supporting interactions with collagen type IV.(14–17) The A2 domain of VWF is important because it contains the ADAMTS13 cleavage site (Tyr1605-Met1606).(18,19) Finally, the D'D3 domains of VWF allow it to bind to pro-coagulant FVIII in the circulation.(20)

Figure 1.1 VWF domain organisation

Structural organisation of domains in pro-VWF monomer

1.1.1.4 Dimerization and multimerization

Within the endoplasmic reticulum, VWF monomers undergo C-terminal dimerization. In this process, two pro-VWF subunits covalently combine though the formation of disulphide bonds between the CK (cysteine knot) domains.(21)(22) VWF dimers then move to the trans-Golgi network where they undergo another round of N-terminal disulphide bond formation to generate multimeric VWF chains (Figure 1.2).(23)(24) Importantly, this interaction requires the low pH and high Ca^{2+} concentration that are present within the Golgi.(23,25) Ultimately, this process generates heterogeneous pools of VWF multimers up to 60 subunits in length (Figure 1.2).(25,26)(27,28) Following multimerization within the Golgi, the D1-D2 domains are cleaved to generate mature VWF and the VWF propeptide (D1-D2).(26) The VWF:pp remains non-covalently associated with VWF until it is secreted into the circulation.(26,29)

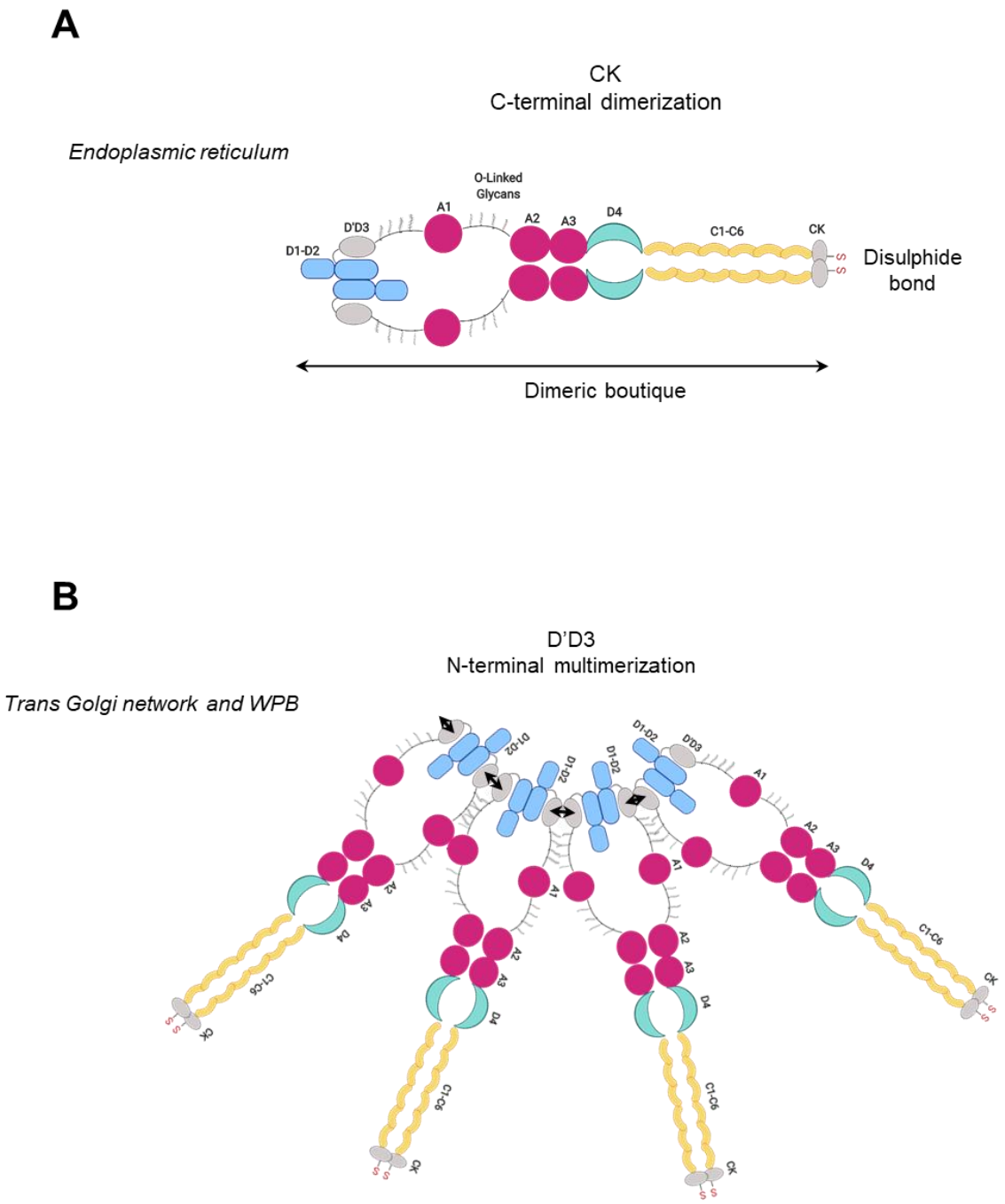

Figure 1.2 VWF dimerization and multimerization

Dimerization and multimerization of VWF monomers to form high molecular weight multimers. **A:** C-terminall CK dimerization, and alignment. **B:** N-terminal D'D3 dimeric bouquets multimerization.

1.1.1.5 Glycosylation

During its synthesis within EC and megakaryocytes, VWF undergoes complex post-translational modification, including significant N- and O-linked glycosylation. Within the ER, N-linked glycosylation commences with the transfer of a pre-formed mannose-rich glycan core structures onto specific VWF asparagine residues.(30,31) 13 N-linked glycan sites have been described within the mature VWF monomer, with a further 4 in the VWF:pp (Figure 1.3).(32,33) As VWF moves though the ER these glycan structures are progressively remodelled by a series of glycosyltransferase and glycosidase enzymes.(34) Furthermore, some of the N-linked glycans (N1515, N2223, N2290, N2400, and N2790) are also terminally sulphated.(33)

Unlike N-linked glycans which are distributed across the VWF monomer, O-linked glycans are predominantly found within two clusters located at the N- and C-terminal ends of the A1 domain (cluster 1 and cluster 2 respectively).(32,35,36) The O-linked glycans of human VWF are simple mucin structures that are formed though sequential glycan addition in contrast to the pre-formed to N-linked core structures (Figure 1.3).(37,38) The majority of both the N- and O-linked glycans of VWF are terminally sialylated, such that the complex glycan chains are capped by sialic acid.(33,36,39) Furthermore, the O-linked glycans of VWF have also recently been shown to express terminal bi- and tri-sialic acid structures.(36) Interestingly, some of the N- and O-linked glycans of human VWF have also been shown to express terminal ABO blood group glycan structures.(33,36,39) These ABO(H)

determinants have been observed on 13% of the N-glycans and 1% of the O-glycans of human plasma-derived VWF.(39) In addition, expression of ABO(H) structures has also been shown to vary between different N-glycan sites on VWF, with highest expression on N2635.(33)

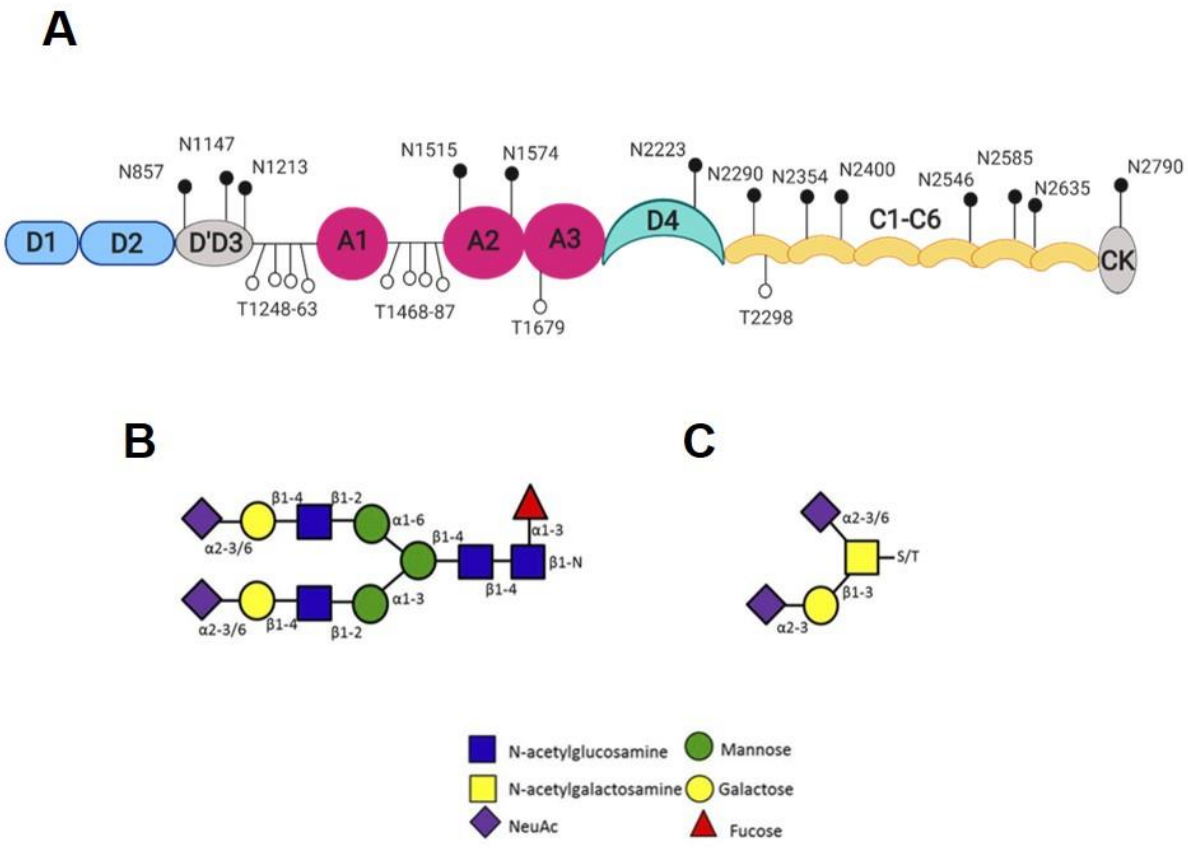

Figure 1.3: VWF glycosylation

A: Location of N-linked (closed circles) and O-linked (open circles) glycans within VWF. **B:** Typical N-linked VWF glycan structure. **C:** Typical O-linked glycan structure.

1.1.2 VWF storage and secretion

1.1.2.1 Intracellular packaging

Some of the VWF synthesized within EC is stored within dedicated storage organelles called Weibel Palade bodies (WPB).(40–42) The formation of WPB is critically dependent upon the presence of VWF.(43,44) Consequently, WPB are not present in EC in the absence of VWF.(43,44) In addition to VWF, a number of other haemostatic and pro-inflammatory proteins are also stored within WPB. These include Interleukin-8 (IL-8), P-selectin, angiopoietin-2 (Ang-2) and osteoprotegerin (OPG).(45–50) In addition to being stored within WPB in EC, VWF and VWF:pp are also stored together within platelet α-granules.(51) However, in contrast to WPB, the formation of platelet α-granules is not dependent on VWF.

1.1.2.2 VWF endothelial cell secretion

VWF synthesised within EC can be secreted through constitutive, basal and regulated pathways (Figure 1.4). The majority of endothelial VWF is released into the circulation through basal secretion composed of both ultra large and high molecular weight structures. (40,52–54) This VWF release is spontaneous and gives rise to the plasma concentration of VWF. Importantly, basal release of VWF does not result in the formation of long EC anchored platelet decorated VWF strings, but binds collagen and platelets at site of injury. (55–57) Extended VWF string structures arise following EC activation and consequent WPB secretion which provide a platform for platelet decorated stings to from.(58,59) Trauma induced activation of EC, results in increased intercellular Ca^{2+} concentrations that induces

cAMP to drive WPB clustering in the EC perinuclear region. WPB begin to fuse together to form secretory pods enabling secretion of bundles of high multimeric weight multimers (HMWM) ultra large VWF to be released.(55),(58,59) In pathological conditions whereby VWF is cleared rapidly, 1-desamino-8-D arginine vasopressin, (a derivative of vasopressin that acts on EC V2 receptors to increase intracellular cAMP) is used to artificially drive VWF release, restoring plasma levels.

Finally, VWF can also be released from EC through a constitutive secretory pathway.(54,60) Synthesised low molecular weight and dimeric VWF derived from the trans-Golgi network which do not enter tubules to from WPB can be constitutively secreted basolaterally through small anterograde carriers.(61,62) Importantly this is a non-stimulated process which occurs continually, giving rise to a pool of basolateral VWF in which the function is not known.(62)

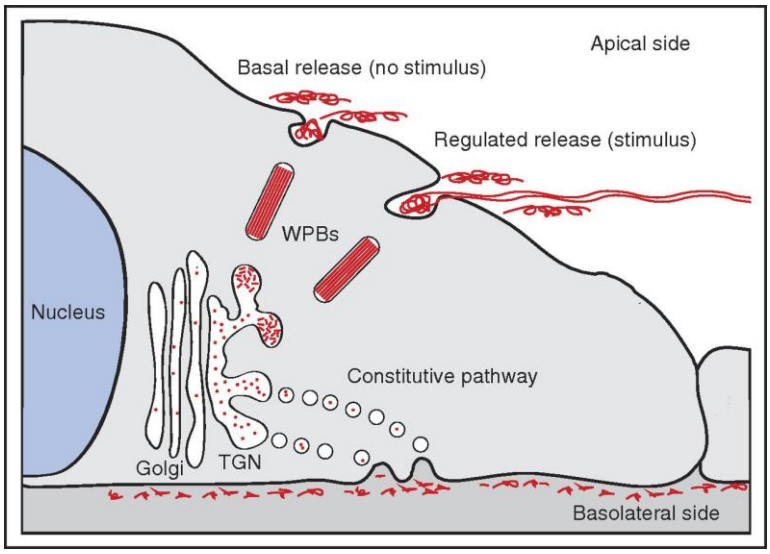

Figure 1.4 VWF endothelial secretory pathways

Schematic representation of apical WPB regulated and basal secretion pathways. Additional depiction of basolateral constitutive secretion. (Bierings & Voorberg, 2016)(63)

1.1.3 VWF haemostatic function

VWF plays a number of critical roles in maintaining normal haemostasis, depicted in Figure 1.5. Injury to the blood vessel wall results in exposure of subendothelial collagen. Circulating plasma VWF binds to the exposed collagen. Under sheer stress, the tethered VWF undergoes conformational changes that expose the A1 domain, and thereby enable VWF binding to the platelet GP1bα surface receptor.(18,28,64–70) Following this initial platelet tethering, further platelets are recruited as a result of GPIIb/IIIa activation and subsequent fibrinogen crosslinking.(71) Platelet activation also results in the release of high molecular weight multimeric VWF stored within platelet α-granules. The importance of VWF in haemostasis is demonstrated by the fact that von Willebrands disease (VWD) constitutes the commonest inherited human bleeding disorder. In VWD, qualitative and/or quantitative VWF deficiency can result in a significant bleeding phenotype.(72)

Von Willebrands Disease	
Type	**Description**
1	Partial quantitative deficiency of VWF
2	Qualitative VWF defects
2A	Deceased platelet adhesion, with deficiency of high molecular weight multimers
2B	Enhanced affinity for platelet GPIbα
2M	Decreased VWF dependent platelet adhesion with normal multimers
2N	Decreased VWF binding for FVIII
3	Complete deficiency of VWF

Table 1.1: von Willebrand Disease Types

ADAMTS13 (A Disintegrin and Metalloprotease with Thrombo Spondin type 1 repeats) is a circulating metalloprotease synthesised in hepatic stellate cells.(73,74) ADAMTS13 plays an important role by regulating VWF multimer distribution in normal plasma. This regulation occurs as ADAMTS13 cleaves VWF at a specific site (Tyr1605 and Met1606) within the A2 domain.(75–77) Thus in normal conditions, haemostasis requires a balance between VWF-dependent platelet aggregation on the one hand, versus ADAMTS13 cleavage of UL-VWF multimers on the other.(58) ADAMTS13 deficiency and subsequent increased UL-VWF results in thrombotic microangiopathy thrombotic thrombocytopenic purpura (TTP).(78) Conversely, enhanced ADAMTS13 proteolysis of UL-VWF is seen in some patients with type 2A VWD and is associated with significant bleeding.(79)

VWF further contributes to haemostasis as it is maintains normal plasma levels of pro-coagulant FVIII. VWF functions as a carrier molecule for FVIII, protecting it from premature proteolysis and circulatory clearance.(80–82) The importance of this interaction is highlighted in VWD type 2N patients, where mutations within in VWF D'D-3 decrease affinity for FVIII and result in a bleeding phenotype.(83)

It is possible to modify the conformation of VWF under static conditions using ristocetin. Ristocetin is an antibiotic previously used for the treatment of staphylococcal infections, however it now used for a number of VWF haemostatic assays. Putatively, VWF circulates with the A1A2A3 domain in a closed conformation, preventing spontaneous platelet aggregation through VWF A1–platelet GPIbα axis. (69) Furthermore, within circulation the A2 domain binds

directly to the A1 domain shielding its interaction with platelet GP1bα.(66,67) Importantly, the A1 domain is connected flexibly to D'D3 C-terminally by a linker of 6.4 nm and N-terminally to A2 by a linker of 6.2 nm.(27) These linkers a mucin like, and are heavily glycosylated. (27,36) Force from shear stress exerted on VWF is driven through these flexible linkers to structured regions N- and C- terminally of the A1 disulphide bond allowing for conformational changes in this region to facilitate A1 GPIbα interaction.(70,84) Ristocetin is used to artificially induces similar conformational changes within the A1 domain, mimicking sheer stress. (85–87) Alternatively, snake venom botrocetin is used for similar effects.(88)

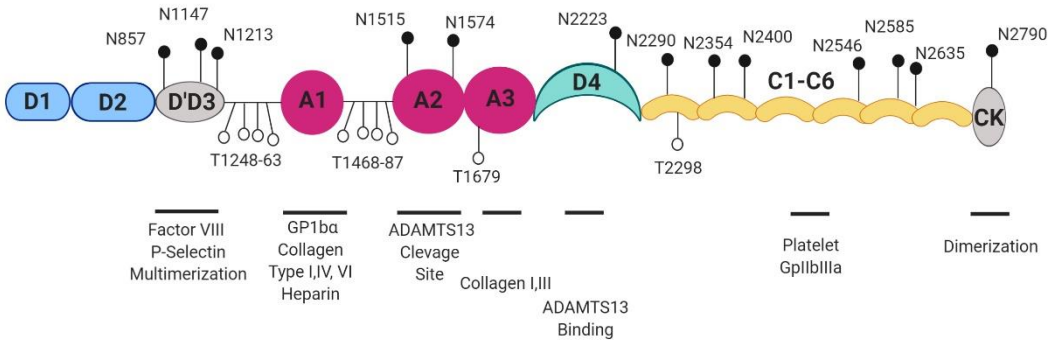

Figure 1.5: Location of haemostatic function on VWF

Schematic representation of VWF glycans and domain specific function.

1.2: Macrophage and innate immunity

Immunity can divided into both adaptive and innate responses. Adaptive immunity refers to a highly specialised immune response composed of T and B cells, while innate immunity is a rapid and nonspecific response to damage or infection. (Figure 1.6) Macrophages are a crucial component of the innate immune system facilitating a rapid response to injury or damage. Macrophages express a broad spectrum of both membrane bound and intercellular receptors allowing them to recognise both foreign pattern associated molecule patterns (PAMPS) and damage associated molecular patterns (DAMPS).(89) Crucially, macrophages are highly specialised at phagocytosing both DAMPS and PAMPS and regulating other immune cells.

Macrophages possess remarkable heterogeneity, in terms of their phenotype and tissue population.(90) Unique micro-environments give rise to individual macrophage populations with distinct functions.(91) Kupffer cells are resident within the liver, glia cells are resident within the brain, alveolar macrophages are located in the lungs and osteoclasts within the skeletal system.(90) Furthermore, depending on the local environment macrophages are polarized into two functional subsets, the classically activated pro-inflammatory M1 cells, and the alternative anti-inflammatory M2 cell. (92)

The M1 macrophage is characterised by its ability to promote a type 1 immune response. Typically, the cell is capable of producing pro-inflammatory cytokines and chemokines (TNF-α, IL-1β and MCP-1), increase reactive oxygen species

generation and antigen presentation.(93–95) Furthermore, M1 macrophages display increased glucose consumption and enhanced glycolysis.(96) Alternatively, M2 macrophages display a distinct ability to induce a type 2 immune response. M2 cells are associated with anti-inflammatory, homeostatic functions such as wound healing and expression of anti-inflammatory cytokines (IL-4, IL-13).(97) Furthermore, M2 cells maintain an increased arginase activity, and decreased glycolytic capacity.(96) Despite clear differences in these subpopulations, it is important to note that macrophages are highly plastic and continually change from one functional phonotype to another.(92)

Macrophages sense infection, recruit circulating monocytes, proliferate in order to eliminate infection and finally convert to their suppressive cell type in an attempt to restore tissue homeostasis. In order for macrophages to recognise both damaged and pattern associated molecular patterns they express a diverse range of receptors, including Toll Like Receptors (TLR), NOD like receptors (NLR), C-type lectin receptors and retinoic acid inducible gene-1 like receptors.(98–101) Activation of these receptors induces signalling cascades resulting in changes in many processes such as cytokine production, metabolism and antigen presentation.

TLRs are a family of 12 receptors that recognise a diverse range of ligands. TLR1, TLR2, TLR4 TLR5 and TLR6 are located on the cell surface, while TLR3, TLR2 and TLR9 are found within intracellular vesicles. (102) Importantly each TLR recognises distinct ligands; TLR1 and TLR2 recognise triacylated and diacylated lipoprotein,

TLR4 recognises LPS, TLR3 recognises double stranded RNA and TLR7 and TLR8 recognise single stranded RNA.(102) Majority of the TLR have similar and conserved signalling pathways, involving the myeloid differentiation primary response gene 88 (MYD88) adapter proteins, TIR-domain-containing adaptor inducing interferon β (TRIF), TIR-domain containing adaptor protein (TIRAP) and TRIF-related adaptor molecule (TRAM) which ultimately drive transcription factor activation.(102)

C-Type lectin receptors are another large family of transmembrane proteins crucial for sensing both DAMPS and PAMPS.(103) Importantly C–type lectin receptors can have alternative functions, driving an inflammatory response or dampening macrophage activation. C-type lectins signal though spleen tyrosine kinase (Syk) and immunoreceptor tyrosine-based activation motifs (ITAMS) to induce an effect.(103)

As macrophages are phagocytic cells, they contain a number of cytosolic NOD like receptors (NLR).(104) NLR are large multidomain proteins essential for recognising structures of gram-positive bacteria like peptiglycan.(105) Two major NLRs are NOD1 and NOD2, which drive activation of receptor interacting serine threonine kinase 2 (RIP2) leading to MAPkinase or NF-Kb activation. Additional members of the NLR family also include NLRP1, NLRP3 and NLRP4. These NLRs can form the inflammasome through complexing with caspase 1 leading to the possessing on IL-18 and IL-1β.(106)

Activation of a macrophage by induction of these receptors generates an inflammatory response.(107,108) Secretion of chemokines will result in the recruitment of inflammatory monocytes to the infected area, but moreover the production of IL-12 or IL-23 will promote T-helper 1 and T-helper 17 cell response respectively to kill invading pathogens.(109,110) Alternatively, macrophage production of IL-4 or IL-13 will drive the recruitment of T helper 2 cells.(111) Importantly, macrophages themselves produce reactive oxygen sepsis or nitric oxide that directly kill invading pathogens.(112)

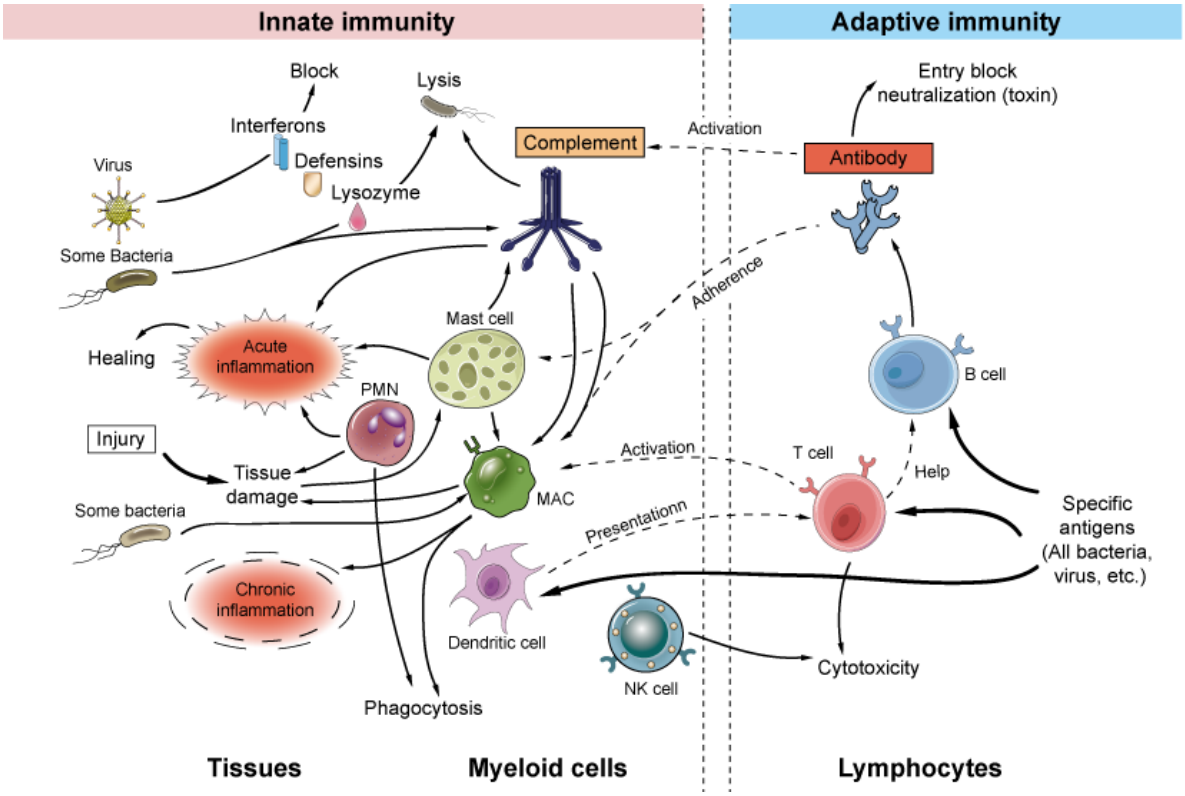

Figure 1.6: Overview of innate and adaptive immune response

Simplified representation of innate and adaptive cell and response to infection and tissue damage. Image from creative diagnostics, Innate and Adaptive Immunity.

1.3: The role of VWF in inflammation and inflammatory disease

In humans, there are five distinct classes of white blood cells or leucocytes. These cells function as part of the innate and adaptive immune systems, thereby providing protection against infectious disease and other pathogens. Leucocytes can be subdivided into two groups – the polymorponuclear leucocytes (PMNs including neutrophils, eosinophils and basophils) and mononuclear leucocytes (including monocytes and lymphocytes) respectively. Both neutrophils and monocytes/macrophage are important in phagocytosis. Accumulating data has demonstrated that VWF can interact with a number of these leucocytes through several different mechanisms as summarised in Figure 1.7.

1.3.1 VWF interaction with PMN leucocytes

Pendu *et al* reported that immobilised VWF bound to freshly isolated PMNs that had been activated with PMA (100nM for 15 minutes) under static conditions.(113) Under these experimental conditions, PMNs adhered as efficiently to VWF as to fibrinogen. Furthermore, PMN adhesion to immobilised VWF was also observed under conditions of flow $50s^{-1}$ (physiological shear $10s^{-1}$-$2000s^{-1}$).(113) Interestingly, PMN interaction with VWF under shear conditions involved a combination of two distinct steps. This was characterised by an initial short-lived transient binding deceleration step, followed by a subsequent second more stable adhesion.(113) This second stable VWF-adhesion step was markedly increased

(approximately 10-fold) when PMNs were pre-activated with PMA stimulation.(113)

Subsequent studies demonstrated that VWF directly binds to a number of important PMN surface receptors. In particular, VWF was shown to bind to P-selectin glycoprotein ligand-1 (PSGL-1) in a botrocetin-dependent manner, suggesting that shear-induced conformational changes in the A1 domain may be required for optimal PSGL-1 binding.(113) In addition, binding of both the D'D3 and A1A2A3 domains of VWF to leucocyte β2-integrins was also observed.(114–116) Cumulatively, these data demonstrate that VWF binds to PMNs under both static and shear conditions, and suggest that different regions of the VWF monomer may be involved. Although the physiological and pathological importance of this VWF-PMN interaction remains unclear, these initial data led to the hypothesis that VWF is not only important in normal haemostasis, but might also play functional roles in leucocyte biology and inflammatory processes.

1.3.2 VWF interaction with monocytes / macrophages

In addition to demonstrating that VWF could interact with PMNs, Pendu *et al* further showed that immobilised VWF could also bind to primary human monocytes pre-treated with PMA for 15 minutes. Similarly, binding to PMA activated monocytic cell lines U937 and THP1 was also observed.(113) Subsequently, a number of different groups have shown that macrophages play a key role in regulating VWF clearance *in vivo*. Thus, macrophage depletion with

either gadolinium or clodronate is associated with significantly prolonged survival of VWF. (117–120) *In vitro* studies have confirmed that primary human macrophages bind VWF in a dose-dependent and saturable manner.(113,117,118) Furthermore, macrophage binding was followed by VWF uptake and degradation.(117) Several groups have reported that VWF binding to macrophages is significantly enhanced in the presence of shear stress or ristocetin, suggesting that VWF conformation plays a critical role in regulating macrophage-mediated clearance.(121,122)

A number of different macrophage surface receptors have been shown to bind to VWF. These include the low-density lipoprotein receptor-related protein-1 (LRP1); the scavenger receptor class A member I (SR-A1); the macrophage galactose-type lectin (MGL); sialic acid-binding immunoglobulin-like lectin (Siglec-5): and the Galectins-1 and -3 (Gal-1 and Gal-3).(119,121–124) For some of these receptors, studies have defined at least in part the mechanisms underpinning VWF binding. For example, *in vitro* studies have demonstrated that cluster IV of the extracellular domain of LRP1 can bind to VWF and that LRP1.(122) Moreover, the binding of wild type VWF to LRP1 occurs only in the presence of shear stress or ristocetin, suggesting that VWF needs to be at least partially unfolded in order to interact with LRP1.(122) LRP1 binding can also be accelerated by truncation of the N-linked glycans of VWF.(118) In keeping with the importance of shear, the A1 domain of VWF has been shown to be play a key role in modulating interaction with LRP1.(118,122) Nevertheless, recent data suggest that additional domains of VWF (including D'D3 and D4) may also contribute to LRP1 binding.(121) Similarly,

Wohner *et al* have shown that VWF also binds to purified SR-A1 in a dose-dependent manner, and that multiple different domains of VWF (including the D'D3 region, the A1 domain and the D4 domain) are involved in binding.(121) However, in marked contrast to LRP1, binding of VWF to SR-A1 can occur under static conditions, without the need for either shear stress or ristocetin.(121) Finally, *in vitro* studies have confirmed binding of the VWF glycoprotein to a number of C-type lectin receptors, including MGL, Siglec-5 and several members of the galectin family.(119,124)

1.3.3 VWF regulates leucocyte extravasation

Initial studies to investigate a putative role for VWF in inflammation were performed using *VWF*$^{-/-}$ mice. The data derived from these studies performed need to interpreted with care given that *VWF*$^{-/-}$ mice lack Weibel-Palade bodies, and consequently also have inherent P-selectin EC storage abnormalities. In view of this fact, Petri *et al* utilised VWF blocking antibodies in order to investigate whether VWF may be involved in modulating the inflammatory response in a murine model of thioglycollate-induced experimental peritonitis.(125) In the presence of the VWF-blocking antibodies, recruitment of PMNs into the inflamed peritoneum was significantly attenuated.(125) Furthermore, the authors showed that VWF also influenced PMN extravasation in another murine inflammation model involving keratinocyte-derived chemokine (KC)-stimulated exposed cremaster muscle.(125) In both murine models, the ability of the VWF-blocking antibody to reduce neutrophil extravasation was critically dependent upon the presence of platelets and GPIbα.(125) Collectively, these data suggest that VWF not only binds to PMN, but also modulates extravasation through a platelet-dependent mechanism. Interestingly, the ability of VWF to promote PMN extravasation was shown to be independent of any effects upon PMN rolling or adhesion to the luminal surface of EC. Rather, platelet recruitment to VWF strings on inflamed EC was proposed to increase EC barrier permeability, thereby leading to enhanced PMN diapedesis.(125) Consequently, PMN extravasation was inhibited in the absence of VWF. It remains unclear how VWF modulates vascular extravasation. Interestingly

however, the tight junction protein claudin-5 has been reported to be negatively regulated by VWF.(126)

In addition to these platelet-dependent effects of VWF in promoting leucocyte extravasation, data from other animal models suggests that VWF may also have direct platelet-independent effects. In particular, Hillgruber *et al* showed that VWF-blocking antibodies significantly attenuated neutrophil recruitment in murine models of immune-complex-mediated vasculitis (ICV) and irritant contact dermatitits (ICD) respectively.(127) In contrast to the critical need for platelet GPIbα in regulating VWF-induced neutrophil extravasation into inflamed peritoneum, the authors further demonstrated that the ability of VWF to promote neutrophil recruitment in these cutaneous inflammation models was platelet-independent.(127) Instead, a direct effect of VWF in regulating EC permeability was observed, even in the absence of platelets and leucocytes.(127) Further studies will be required to define the biological mechanisms underlying this VWF effect on EC barrier integrity is modulated

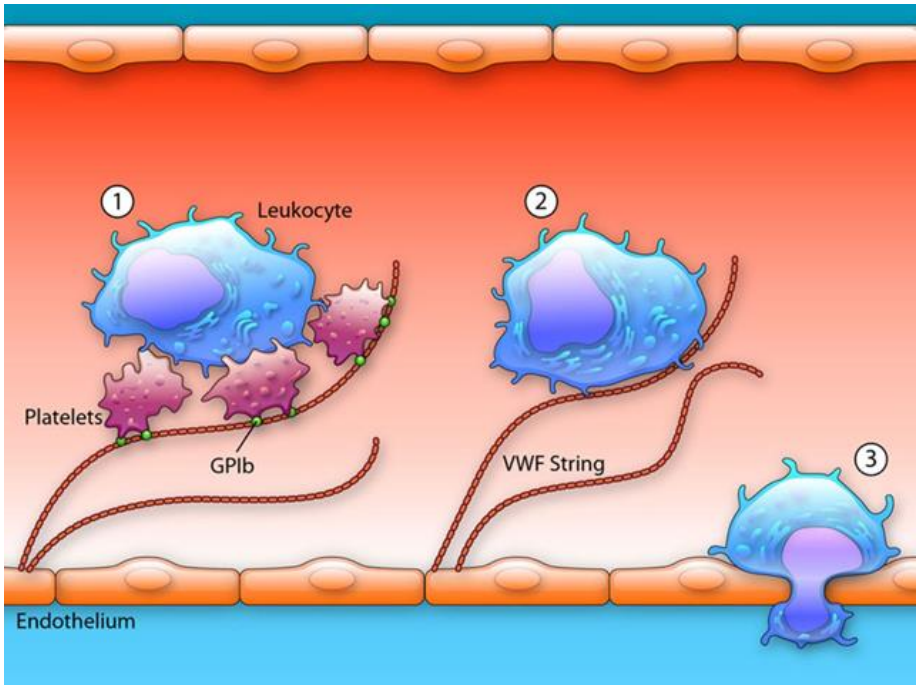

Figure 1.7: VWF modulates inflammation through multiple different mechanisms.

1: VWF released from activated endothelial cells, or bound to collagen at sites of vascular injury, interacts with platelet GPIbα (glycoprotein Ibα) and recruits platelets. The VWF-tethered platelets subsequently enable neutrophil recruitment. **2:** VWF can also recruit leucocytes in a platelet-independent manner by directly interacting with leukocyte cell surface receptors including β2-integrins and P-selectin glycoprotein ligand-1. **3:** VWF regulates endothelial wall permeability and influences leukocyte extravasation.

1.3.4 VWF and NETosis

Neutrophil extracellular traps (NETs) are part of the innate immune response to invading pathogens. In a process called NETosis, chromatin with bound anti-microbial proteins is expelled from neutrophils and then functions to sequester and neutralise invading pathogens.(128,129) Recent studies have demonstrated that the A1 domain of VWF can binds to NETs though a mechanism similar to GP1bα.(130) Furthermore, imaging of venous, coronary and cerebral thrombi have all demonstrated colocalization between VWF and NETS.(131–134) For example, microscopic characterisation of cerebral thrombi has demonstrated that they are composed of distinct regions. Some regions within the thrombous are composed mainly of fibrin and red blood cells.(135) Conversely, other areas consist mainly of platelets, neutrophils and are enriched in VWF.(135) These different regions within the thrombus may have clinical relevance with respect to the efficacy of therapeutic thrombolysis. Importantly, the dense VWF and neutrophil regions have been reported to be resistant to tPA thrombolysis.(135) However, Savchenko *et al,* recently reported that digestion of VWF and DNA using co-administration of ADAMTS13 and DNase leads to the reduction of myocardial infarction size and leukocyte infiltration when compared to classical thrombolysis.(136)

The VWF-NET complex may also have an anti-microbial role. Putatively, NETs exert strong antibacterial activity though immobilising and killing bacteria via bound myeloperoxidase and neutrophil elastase. However, NET bound VWF may enhance bacterial immobilisation. For example, Pappelbaum *et al*, have shown that both

the VWF A1 and A3 domains can directly enhance Staphylococcus aureus adhesion onto EC.(137,138)

1.3.5 VWF and complement

The complement cascade functions as a rapid innate immune response to infection and comprises three independent activation pathways – (i) classical antibody induced activation (ii), lectin receptor induced activation and (iii) alternative microbial particle activation.(139) Importantly, all three pathways converge on the activation of C3 convertase.(139) Recent studies have highlighted a new role for VWF in linking primary haemostasis with complement activation. Kolm *et al*. demonstrated that VWF binds to C1q released by apoptotic cells.(140) Importantly, VWF was also detected in C1q positive regions within the glomeruli of systemic lupus erythematosus patients.(140) Furthermore, the binding of C1q to VWF induced conformational changes within A1 that enhanced platelet binding (Figure 1.8).(140) The observed direct interaction between VWF and C1q may contribute to the pathology of complement-mediated inflammatory diseases. Conversely, VWF appears to have a regulatory role further downstream in the complement cascade. Due to the inflammatory potential of the complement pathway, it is tightly regulated by Factor 1. Factor 1 cleaves C3b into the inactive iC3b, halting cascade progression.(141) Interestingly, VWF acts as a cofactor for Factor 1, facilitating iC3b generation and complement inactivation (Figure 1.8).(142) Curiously, UL-VWF cannot act as a Factor 1 co-factor and this effect is a mediated by lower molecular weight VWF.(142)

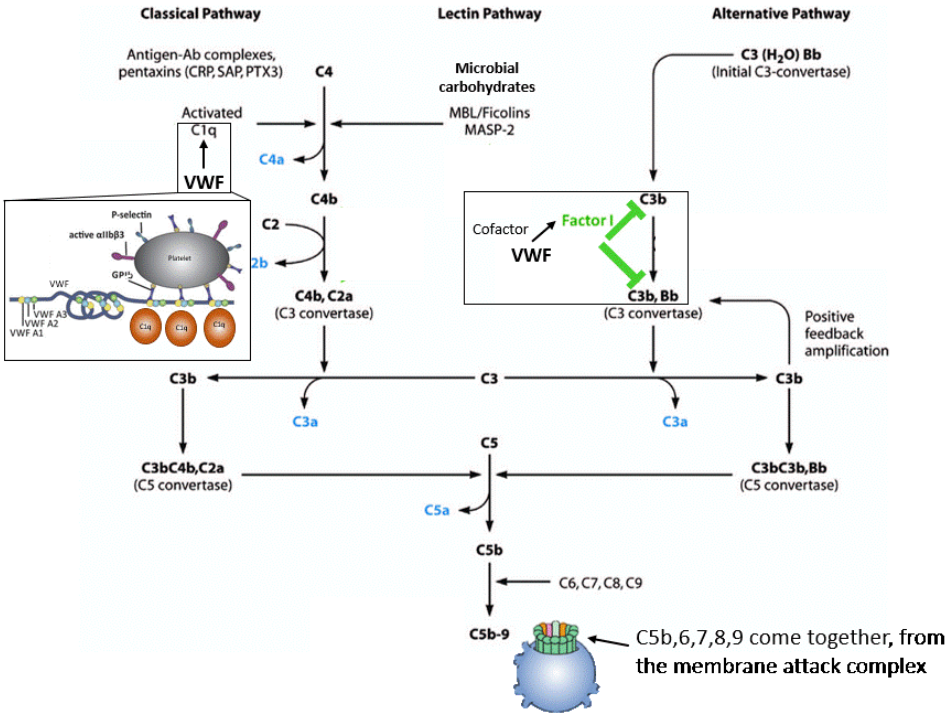

Figure 1.8: Schematic representation of the crossover between VWF and complement cascades.

The complement cascades is initiated by the classical, lectin and alternative pathways which results in the assembly of the membrane attack complex. Classical pathway activator C1q can bind to VWF A1 domain and facilitate platelet aggregation. Furthermore, VWF can also act as a cofactor for complement inhibitor Factor 1.

1.3.6 VWF in the pathogenesis of inflammatory disorders

In view of the accumulating evidence that VWF directly interacts with various leucocytes through a variety of different mechanisms, it is interesting to consider whether VWF may have a role in modulating inflammatory responses. This exciting hypothesis is supported by *in vivo* data form a series of different animal disease models.

1.3.6.1 VWF in murine sepsis models

To investigate the potential pathological importance of VWF in regulating inflammatory responses, Lerolle *et al,* used the well-established caecal ligation and puncture (CLP) model. This model involves severe multi-microbial sepsis that results in a sustained cytokine response, and has been proposed to constitute a model of human sepsis. Interestingly, significantly improved overall survival was observed in *VWF*$^{-/-}$ mice compared to *VWF*$^{+/+}$ wild type controls.(143) The mechanisms underlying the improved survival in the *VWF*$^{-/-}$deficient mice remains unclear, but importantly the CLP-induced decrease in leucocyte count was significantly less in the *VWF*$^{-/-}$ cohort.(143)

Kasuda *et al,* also investigated the role of VWF in modulating inflammation using a murine CLP sepsis model. In contrast to the previous study, they observed that overall survival was significantly decreased in *VWF*$^{-/-}$ mice compared to wild type controls, however it was restored by the administration of human VWF.(144) A significant reduction in circulating and peritoneal invading neutrophils was

observed in *VWF*$^{-/-}$.(144) The explanation for this conflicting data remain unclear, but likely reflect significant differences in the two CLP models employed.

1.3.6.2 VWF in malaria pathogenesis

Infection with *Plasmodium falciparum* (*P. falciparum*) is the principal cause of lethal cerebral malarial.(145) *P. falciparum* infects erythrocytes which then become sequestered within the microvasculature of organs including the brain and kidney.(145) Activation of EC results in upregulation of specific adhesion proteins (including CD36, intercellular adhesion molecule-1, E-selectin and P-selectin).(146) This EC activation occurs early in the pathogenesis of severe malaria infection and plays a critical role in regulating the cytoadhesion of infected erythrocytes (IE) to EC surfaces.(147)

Previous studies have demonstrated that severe *P. falciparum* infection is associated with a marked increase in plasma VWF and VWF:pp levels.(148) Furthermore, studies performed in healthy volunteers have confirmed that the increase in plasma VWF levels develops at an early stage following *P. falciparum* infection, before IE can be seen in peripheral blood.(149) Interestingly, clinical studies have also demonstrated an accumulation of pathological hyper-adhesive UL-VWF multimers in patients with severe malaria. (148,150,151) Collectively, these observations have led to the proposal that VWF may play a direct role in the pathogenesis underlying the development of cerebral malaria. In keeping with this hypothesis, plasma VWF and VWF:pp levels have been shown to inversely correlate with platelet count and overall outcome.(150,152) Studies performed in a murine

model of experimental cerebral malaria (ECM) have provided further evidence that VWF may be important in malaria pathobiology. Interestingly, *VWF*$^{-/-}$ mice were shown to be protected against cerebral malarial following *P. berghei* infection.(151) Enhanced blood brain barrier permeability is strongly implicated in the pathogenesis of cerebral malaria and importantly, permeability was markedly increased in WT mice when compared to *VWF*$^{-/-}$.(151),(153–155) All together, these data suggest that VWF is not merely a biomarker of EC activation, but rather is directly involved in the pathogenesis of cerebral malarial.

Recent studies have investigated the role of VWF in another murine model of malaria associated acute respiratory distress syndrome (MA-ARDS). The pathology of MA-ARDS results from increased permeability of the alveolo-capillary membrane due to inflammatory damage.(156) P*. berghei* NK65-E (PbNK65) does not induce cerebral malaria, but does result in pulmonary inflammation with protein rich interstitial.(156) Following infection with this murine strain of malaria, a significant increase in plasma VWF levels was again observed.(156) However, in contrast with previous results, significantly decreased overall survival was observed in *VWF*$^{-/-}$ compared to WT controls.(156) In addition, a significant decrease in alveolar permeability and increased lung parasitemia load were seen in the *VWF*$^{-/-}$ mice.(156) Together, these data suggest that VWF may play a number of important roles in relation to the pathogenesis underlying severe malaria infection. Moreover, the relative importance of these different VWF roles may vary according to the properties of the infecting malaria strain.

1.3.6.3 VWF in the pathogenesis underlying ischaemic heart disease

Ischemic heart disease (IHD) results from reduction in blood supply to the heart and is usually caused by stenosis or occlusion of the coronary arteries. Atherosclerosis is a major cause of this narrowing. A number of different meta-analyses and systematic reviews have reported that elevated levels of VWF are associated with an increased risk of IHD.(157–160) Conversely, patients with inherited VWD appear to be relatively protected from IHD development.(161,162) Studies using both *VWF*$^{-/-}$ or *ADAMTS13*$^{-/-}$ mice have investigated whether VWF plays a direct role in the pathogenesis underlying IHD (Figure 1.9). Interestingly, studies performed in *VWF*$^{-/-}$*LDLR*$^{-/-}$ double knockout mice demonstrated significantly reduced atherosclerotic lesions compared to *VWF*$^{+/+}$*LDLR*$^{-/-}$ controls.(163) In addition, the distribution of plaque lesions in the mice was also different depending upon the presence or absence of VWF. In VWF replete mice, plaque lesions were confined to arterial branch points. Conversely, in the absence of VWF, plaque lesions were evenly distributed along arteries.(163) These differences may be affected at least in part by the fact that EC stores of P-selectin are also lost in *VWF*$^{-/-}$ mice.

It is well established that atherosclerosis is predominantly an inflammatory disorder, whereby damage to the vascular wall results in monocyte/macrophage recruitment.(164,165) These phagocytic cells subsequently develop into cytotoxic foam cells. The core of the lesion becomes necrotic, with the death of immune and smooth muscle cells, perpetuating the inflammatory response.(165–169)

Importantly, a significant reduction in macrophage accumulation within atheromatous plaques was also observed in *VWF*$^{-/-}$ mice.(163) Similarly, studies performed using *ADAMTS13*$^{-/-}$ mice have also provided data supporting the hypothesis that VWF may be important in IHD.(170) Importantly, macrophage recruitment into plaque lesions was significantly increased in *ApoE*$^{-/-}$/*ADAMTS13*$^{-/-}$ when compared to *ApoE*$^{-/-}$/*ADAMTS13*$^{+/+}$ controls.(170)

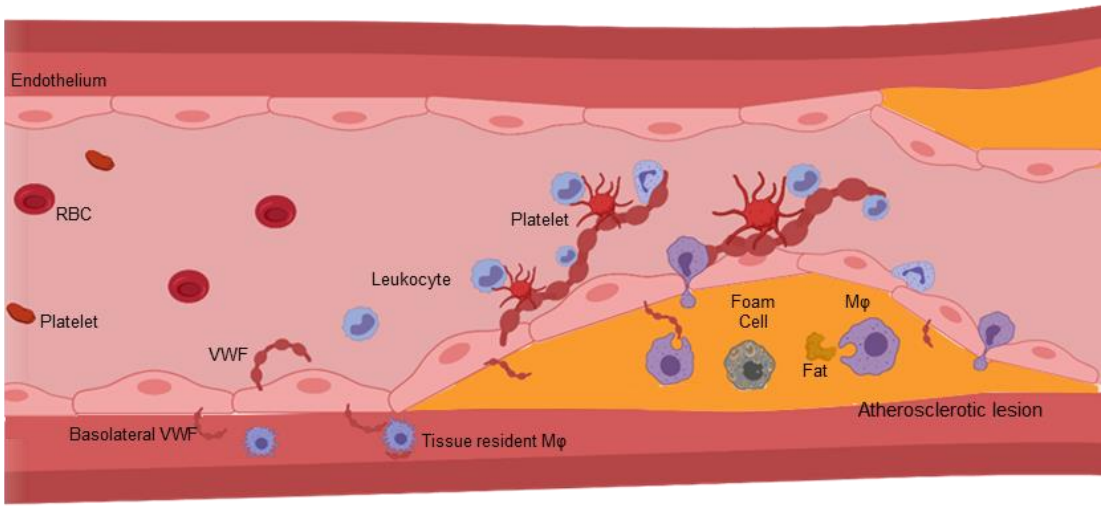

Figure 1.9: Schematic representation of endothelial VWF release during atheroserotic plaque development.

Atheroserotic lesion progression drives endothelial activation and VWF release. VWF tethers platelets and leukocytes promoting leukocyte extraversion into inflammatory lesion core.

1.3.6.4 VWF in Stroke pathobiology

A critical biological mechanism underlying stroke-associated pathology is reperfusion injury. Thus, the initial period of brain ischemia is followed by a period of rapid microglial activation.(171–173) In addition, there is a marked infiltration of peripheral neutrophils, monocytes, macrophages and T-cells resulting in profound inflammatory damage.(174) Accumulating data from both animal models and human studies suggests that the VWF-ADAMTS13 axis may be important in this process. Plasma VWF levels are significantly elevated in patients following both ischaemic or haemorrhagic stroke and have been significantly correlated with neurological functional outcomes.(175) Conversely, patients with VWD are relatively protected against stroke.(161,176,177) Studies in murine stoke models have reported that cerebral infarct volumes are significantly reduced in *VWF*$^{-/-}$ mice compared to wild type controls.(178,179) Interestingly, *VWF*$^{-/-}$ mice were still protected from stroke associated damage when mice were re-supplemented with mutated VWF that could not support collagen or GPIbα binding.(179) However, *VWF*$^{-/-}$ mice lost their protective phenotype when VWF defective in binding GPIIb/IIIa was re-perfused. Thus, the ability of VWF to interact with collagen and GPIbα but not GPIIb/IIIa is essential in mediating ischemic stroke pathology.(179) This data was confirmed as infarct development and size was reduced following inhibition of the VWF-GPIbα axis. Interesting, studies using chimeric mice further suggest that platelet-derived VWF (in addition to EC-derived) is crucial for mediating ischemic stroke pathology.(180) Moreover, in line with these data, it has

also demonstrated that deletion of *ADAMTS13* augments ischemic injury. (181,182)

Strokes can be either ischaemic or haemorrhagic in origin. Both types of stoke have been associated with significant reperfusion injury. In a murine model of haemorrhagic stroke, induction of intracerebral haemorrhage resulted in the release of large amounts of VWF.(183) Furthermore, intracerebral treatment with VWF decreased pericyte load and increased blood brain barrier permeability.(183) Importantly, following intracerebral haemorrhage VWF treatment exacerbated cerebral inflammation. The presence of VWF was also associated with increased chemokines CXCL1 CX3CL1, myeloperoxidase and the pro-inflammatory cytokines IL-6 and IL-1β.(183) Furthermore, enhanced microglial activation and neutrophil accumulation were also noted.(183) Importantly, specific inhibition of VWF significantly reduced haemorrhagic blood brain barrier permeability and improved neurological outcome in this murine model.(183)

1.4 Hypothesis and Aims

1.4.1 Hypothesis

The hypothesis of this thesis is: that VWF may alter innate immune responses by acting as a novel damage associated molecular pattern detected by macrophages. This would be yet another link between primary haemostasis and inflammation.

1.4.2 Aims

- Investigate how VWF interacts with macrophages.
- Determine if VWF macrophage interaction results in a pro-inflammatory response.
- Examine the alterations in macrophage metabolism following VWF interaction.
- Investigate the receptors and signalling pathways that might be involved in mediating macrophage response to VWF.

2.0 Material and Methods

2.1: Cell culture

2.1.1 Human primary monocyte isolation

Healthy donor buffy coats were obtained from the Irish Blood Transfusion Service. Buffy coats were diluted 1:3 (15ml into 30ml) in PBS $Ca^{2+}Mg^{2+}$ free (-/-) and gently layered onto histopaque (gradient 1077, Sigma-Aldrich, Ireland) at a 1:1 ratio (20ml:20ml). To obtain the peripheral blood mononuclear cell (PBMC) layer, the buffy coat-histopaque solution was centrifuged at 300g for 35 minutes with the brake removed. PBMCs were harvested by aspiration of the layer underneath the plasma-PBS followed by two wash steps using 50ml of PBS (calcium and magnesium free (-/-)).

Monocytes (defined by high $CD14^{High}$ and $CD16^{Low}$) were isolated from PBMCs using CD14 magnetic positive selection MicroBeads (Miltenyi Biotec, UK) in conjunction with a miltenyi LS magnetic column. PBMCs were incubated at 4^0C for 15 minutes with an anti-CD14 antibody conjugated to a magnetic nanoparticle ($1x10^8$ PBMC, 140µl anti-CD14 beads and 860µl monocyte isolation buffer (PBS 0.5% Bovine Serum albumin (BSA), 2mM EDTA, pH 7.2) and isolated through magnetic gradient separation column. Monocytic population was confirmed by detecting CD14 and CD16 expression by flow cytometry (Figure 2.1)

2.1.2 Human primary monocyte cell culture

Isolated monocytes were seeded at $2x10^5$ cells/ml in primary macrophage media (RPMI Glutmax, Gibo, ThermoFisher Scientific USA), 10% human serum (Type AB male, Sigma-Aldrich, Ireland), 100 IU/ml penicillin (Sigma-Aldrich, Ireland) and 100µg/ml streptomycin (Sigma-Aldrich, Ireland)). $1x10^5$ cells were seeded onto non-surface treated 48 well tissue culture plates (Falcon, USA). To facilitate differentiation, monocytes were cultured for 7-10 days replacing primary macrophage media every 3 days. Cells were cultured at 37^0C, 5% CO_2.

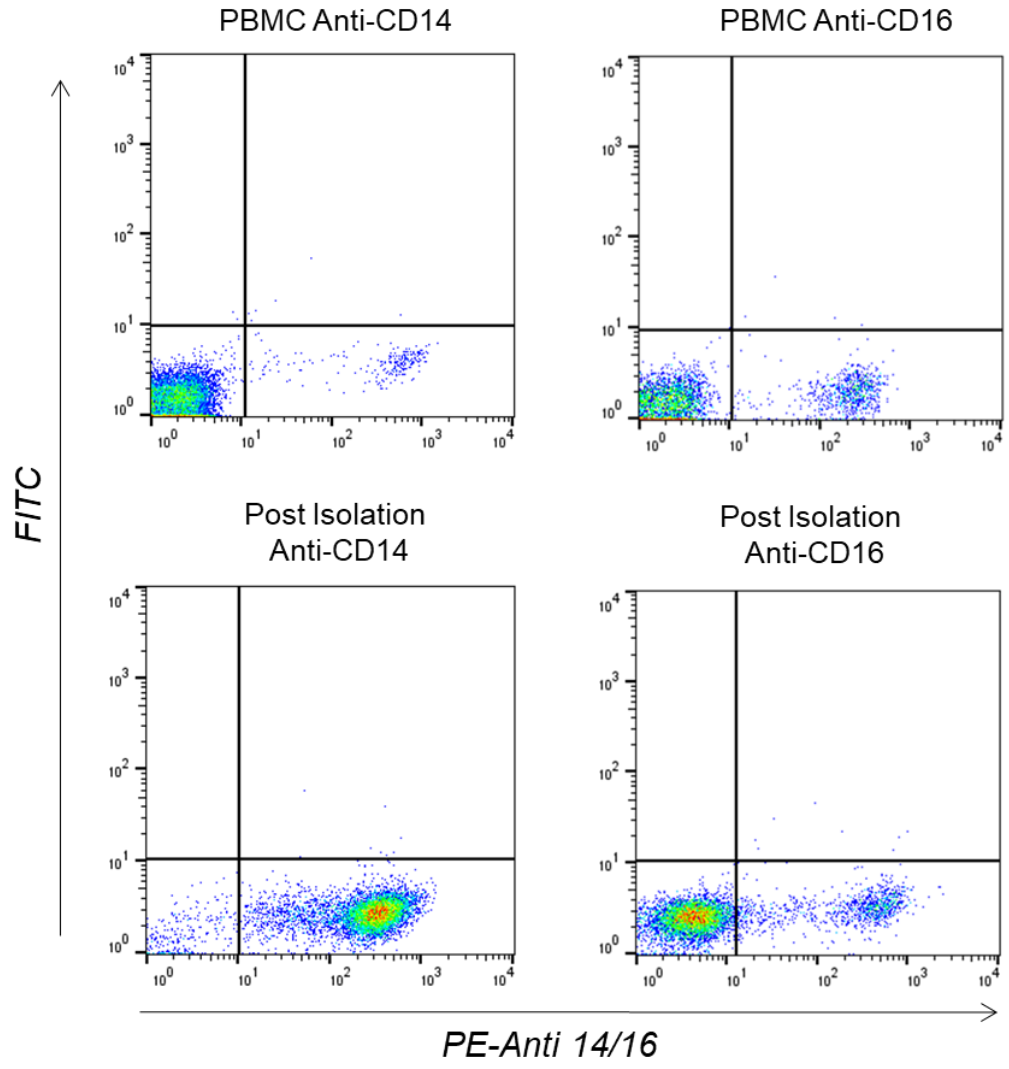

Figure 2.1: PBM CD14 CD16 expression pre- and post- isolation.

Flow cytometry analysis of PBMC CD14 or CD16 staining (PE) pre- and post-CD14 isolation. Pre isolation minimal PBMC are CD14 positive. Post isolation, cell population is monocytic $CD14^{High}$ $CD16^{Low}$.

2.1.3 Monocytic THP1

THP1 cells were obtained from ATCC (Authenticated Cell Cultures, Sigma-Aldrich, UK). Cells were cultured in RPMI Glutmax supplemented with 10% heat inactivated Foetal Bovine Serum (FBS: Gibco, USA), 100 IU/ml penicillin and 100ug/ml streptomycin (RPMI^{++}). Suspension THP1 cells were maintained at a density 3-10x10^{5}cells/ml in non-adherent plastic (Starstedt, Germany) and were cultured for two weeks prior use and not maintained beyond passage 20. For experimental use, cells were seeded onto adherent 48 well plates (Starstedt, Germany) or 8cm tissue culture grade petri dishes (Thermo Scientific, Ireland) at a density of 2x10^5 cells/ml and differentiated into adherent macrophages by culturing with 100nM para-Methoxyamphetamin (PMA, Sigma-Aldrich Ireland) for 72 hours.

2.1.4 RAW 264.7 macrophages

RAW 264.7 cells were obtained from American Type Culture Collection (ATCC, Sigma-Aldrich, UK) and maintained in Dulbecco's Modified Eagle's Medium (DMEM, Gibco, USA) supplemented with glucose (4.5g/l), 10% FBS, normocin (100µg/ml, Invivogen USA), L-glutamine (2mM, Sigma-Aldrich, USA), zeocin (200µg/ml, Invivogen, USA) and penicillin -streptomycin (100 U/ml-100 µg/ml). Cells were maintained at a density of 6x10^5 cells/ml up to passage 20. RAW 264.7 were incubated at 37^{0}C, 5% CO_2.

2.1.5 Bone marrow derived macrophages

To obtain bone marrow derived macrophages (BMDMs), female C57BL/6J mice aged between 6-12 weeks were scarified and the pelvis, femur, tibia and fibula were harvested. Soft tissue and cortical bone was removed and the marrow was extracted from the cavity with RPMI using and a 23-gauge needle. A single cell suspension was generated from the marrow and sieved through a 40µm nylon filter (Ibidi, Germany). Red blood cells were lysed in red cell lysis buffer (Sigma-Aldrich, Ireland) for 90 seconds and neutralised with RPMI (1:10 ratio). Cells were resuspended in 30ml of RPMI supplemented with 10% FBS, penicillin (100 IU/ml), streptomycin (100ug/ml) and recombinant murine (M-CSF, 25µg/ml, R&D systems USA). Cells were seeded into 8cm low adherent petri dishes (Thermo Scientific. UK) and cultured for 6-7 days. On day 3, an additional 3ml of supplemented RPMI was added. Following differentiation cells were detached and seeded overnight onto 48 well plates (Starstedt, Germany) at $1.5x10^5$cells/well in RPMI supplemented media for experimental use

2.1.6 HEK293(T)

Human Embryonic Kidney (HEK) 293 cell lines were obtained from ATCC (Sigma-Aldrich, UK) and cultured in DMEM (Sigma-Aldrich, UK) with 10% FBS, penicillin (100 IU/ml) and streptomycin (100ug/ml). These adherent cells were routinely cultured in T-175 flasks (Nunc, UK) and passaged at ~80% confluence.

2.2: Protein preparations

2.2.1 Purification analysis of plasma derived VWF

High purity plasma derived VWF (pd-VWF) was purchased from Haemtech (USA). Protein contamination was determined by coomassie (Sigma-Aldrich, Ireland) staining and endotoxin contamination determined using macrophage RAW Blue reporter cell line. RAW 264.7 cells stably express secreted embryonic alkaline phosphatase (SEPA) which is inducible by NF-Kb and AP-1 transcription factors. RAW cell express all TLRs (apart from TLR5), RIG-1, MDA-5, NOD1 and NOD2 whereby activation of these receptors induces expression of SEPA. Antibiotic selection using zeocin (Inviogen, USA) maintains the RAW cells containing SEPA plasmid. To test for the presence of endotoxin, RAW cells were seeded onto 96 well plate ($1x10^5$/well) overnight with VWF sample or positive control, LPS (100ng/ml, Sigma-Aldrich Ireland) or negative control (cell culture media). Following incubation, cell supernatants were harvested and combined with QUANTI-Blue (alkaline phosphatase substrate, Invivogen USA) at a ratio of 1:3 and incubated at 37^{o}C. The degree of Pattern Associated Molecular Patterns (PAMP) activation is directly proportional to the extent of SEPA production, indicative of endotoxin presence Cleavage of QUANTI-Blue by SEPA results in a colour change from pink to purple, which is measured by absorbance at 630λ.

2.2.2 Recombinant VWF expression and purification

2.2.2.1 Expression vector constructs

pcDNA VWF expression vector: pcDNA vector containing the full length VWF sequence was designed and constructed by Dr. Alain Chion (Irish Centre for Vascular Biology, RCSI). This vector contains a cytomegalovirus (CMV) immediate-early promoter ensuring high-level expression, SV40 origin driving episomal replication in T antigen expressing cells and a neomycin resistance gene to facilitate selection in mammalian cells. Finally, pcDNA encodes for the addition of a polyhistidine tag inserted C-terminally onto the recombinant protein. The vector also contains a PUC origin and ampicillin resistance gene to drive high-copy number replication selection in *E.coli* Details on sequence boundaries of inserted full length VWF and VWF truncated fragments can be found in Table 2.1.

pEXPR-IBA VWF expression vector: For the expression of VWF truncated domain fragments pEXPR-IBA-42 expression vector was utilised. This VWF vector was designed and constructed by Dr. Alain Chion. pEXPER-IBA-42 (IBA, Germany) vector backbone contains a neomycin gene for selection in mammalian cells and a CMV promoter. The vector also contains a pUC ORI and ampicillin gene for selection in *E.coli* production. pEXPR-IBA encodes for the addition of a polyhistidine tag inserted C-terminally onto the recombinant VWF protein. Table 2.2 provides details on the pEXPR-IBA VWF constructs used and sequence boundaries. The D'-D3 protein used in this study was a kind gift from Pfizer Ireland.

Construct	Details
pcDNA Full length VWF	Full length (residues 1-2813)
pcDNA D'A3 VWF	D'A3 domains (residues 786-1874)
pcDNA A1CK VWF	A1-CK domains (residues 1260-2813)

Table 2.1: pcDNA VWF expression vectors and VWF sequence boundaries

Construct	Details
pEXPR-A1A2A3-VWF	A1A2A3 domains (Glu1260- Phe1875)
pEXRP-A1-VWF	A1 domain (Glu1260 - Glu1463)
pEXRP-A2-VWF	A2 domain (Met1495 - Glu1672)
pEXRP-A3-VWF	A3 domain (Ser1671 - Phe1875)
pEXRP-A3-CK-VWF	A3 to CK domains (Ser1671 - Lys2813)

Table 2.2: VWF pEXRP VWF expression vectors sequences boundaries

2.2.2.2 Amplification and purification of VWF plasmid DNA.

To amplify VWF DNA expression vectors for transfection into mammalian cells, competent *E.coli* cells were transformed with the plasmid DNA. 10µl of Top 10-β competent *E.coli* cells (New England Biolabs, USA) were thawed on ice and incubated for 30 minutes with 0.5-1µL of the VWF expression vectors outlined in Table 2.1 and 2.2. Subsequently heat shock was performed at 42°C for 30 seconds followed by a 2 minute incubation on ice. 80µL of pre-warmed Super Optimal Broth (SOC) outgrowth media (Promega, USA) was added to the cells followed by 1 hour of shaking (225rpm) at 37^0C. The mixture was subsequently inoculated onto a LB-ampicillin agar plate and incubated at 37^0C overnight. Successful transformants were picked and inoculated into a 5mL starter culture of LB broth with ampicillin (100µg/ml: Fisher Scientific) for 8-10 hours at 37^0C with shaking (225rpm). This

culture was then expanded overnight to 200ml in LB broth with ampicillin incubated at 37^0C with shaking (225rpm). Cells were pelleted, and the plasmid DNA construct was isolated using a MaxiPrep Kit (Omega bio-tek, USA) as per manufactures instructions.

2.2.2.3 Expression of recombinant VWF

The production of all recombinant VWF proteins (with exception of commercial VONVENDI® preparation (Takeda, Japan)) were expressed in HEK293T cells by transient transfection. HEK293T cells were cultured as described in Section 2.1.6 and grown to 80-90% confluence in T-175 flasks (Gibco, USA). Prior to transfection, the cells were washed with PBS and 18ml of reduced serum Opti-MEM was added to each flask Transfection reagent, branched polyethylenimine (bPEI; Sigma-Aldrich, Ireland) was prepared at a working concentration of 1 µg/ml in 150mM NaCl. Similarly VWF plasmid DNA was diluted to 2 µg/ml in 150mM NaCl. Complex formation occurred following the dropwise addition of bPEI solution to DNA and incubated for 20 minutes at room temperature. Finally, 2ml of bPEI:DNA complex was added to each flask and incubated for 72hours. The harvested conditioned media was centrifuged at 4,000rpm for 30 minutes to remove cell debris and filtered (0.22µm PES filters, Merk Ireland). Transfection media containing truncated VWF variants were concentrated using a Pellicon XL Biomax 10 column (Millipore) on a Labscale TFF System (Millipore, USA) and buffered exchanged into binding buffer (Tris (20mM), NaCl (150mM) and imidazole (7mM) at pH 7.4) prior to nickel affinity purification.

2.2.2.4 Anion exchange chromatography

Anion-exchange chromatography was used to concentrate conditioned medium containing full length recombinant VWF (Figure 2.2). Using Fast Protein Liquid Chromatography (FPLC, AKTA, GE Healtcare, USA), conditioned media was loaded onto HiTrap Q HP column (Q-Sepharose High Performance; GE Healthcare, USA) in 20mM Tris, pH 7.4 at a flow rate of 1.5mL/min. A low salt buffer (20mM Tris, 100mM NaCl, pH 7.4) was used to wash the column at a flow rate of 2mL/min. Following extensive washing the immobilised VWF was subsequently eluted using a high salt buffer (20mM Tris, 500mM NaCl, pH 7.4) at a flow rate of 0.5mL/min. Eluted VWF was collected into 1ml fractions and dialysed to 20mM Tris pH 7.4 for subsequent purification by metal ion affinity chromatography.

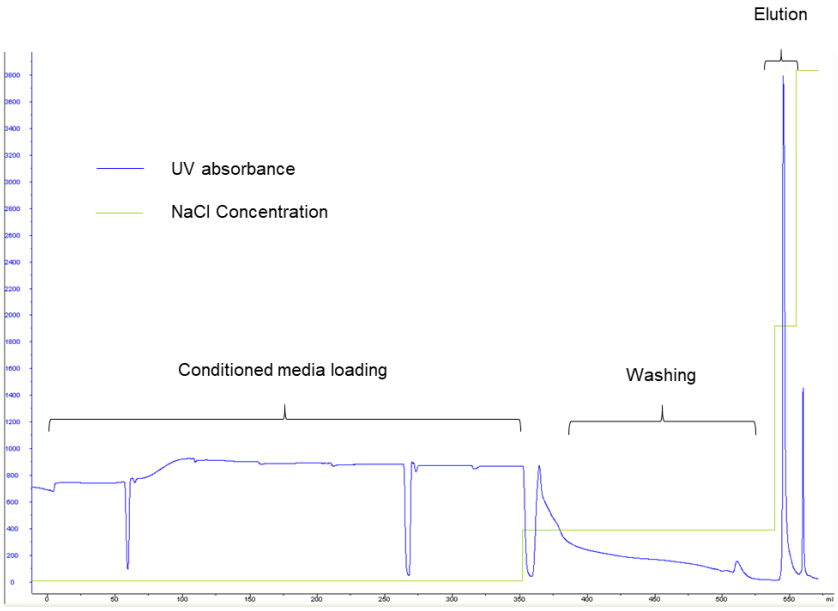

Figure 2.2: Anion exchange chromatography purification of recombinant VWF.

2.2.2.5 Purification using metal affinity chromatography

Following anion exchange, VWF constructs expressing a C-terminal polyhistidine tag were further purified by metal affinity chromatography. Sepharose bound nickel binds to the polyhistidine residues on recombinant protein, immobilising them. High concentrations of free histidine (imidazole) are then used to competitively elute bound proteins. HiTrap Chelating Column (GE Healthcare, UK) was charged with $NiCl_2$ (0.1M) at a flow rate of 0.5mL/min in. Concentrated conditioned medium dialysed into binding buffer (Tris (20mM), NaCl (150mM) and imidazole (7mM) at pH 7.4) and loaded on the charged column at a flow rate of 1mL/min. Following washing, bound recombinant VWF was eluted with elution buffer (Tris (20mM), NaCl (150mM) and Imidazole (300mM) at pH 7.4). Eluted fractions were dialyzed into 20mM Tris pH 7.4 and analysed for purity by coomassie staining (Figure 2.3).

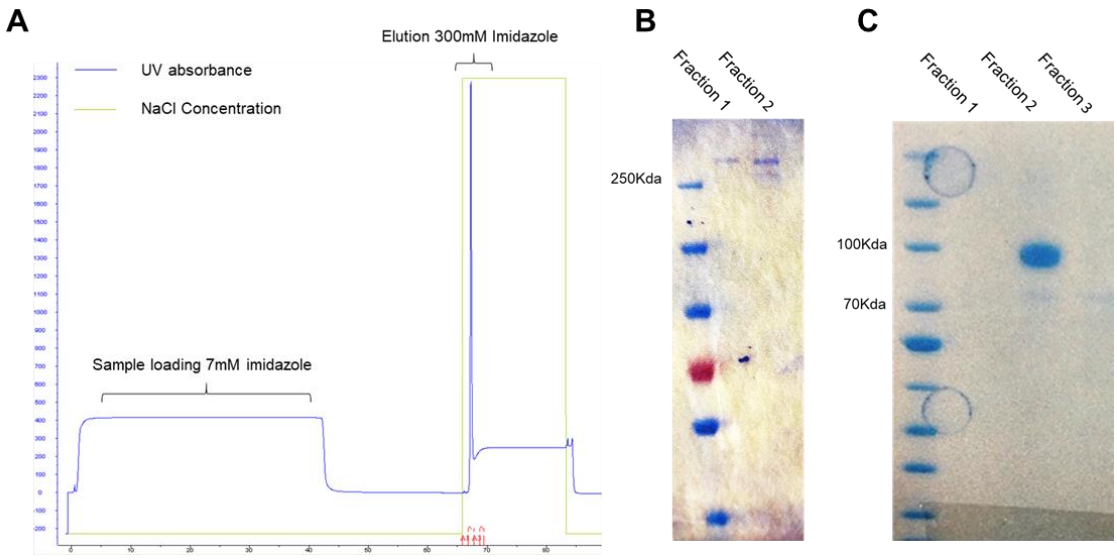

Figure 2.3: Metal affinity chromatography

A: Nickel purification of His-tagged VWF protein **B:** Coomassie staining of elution fractions 1 and 2, of purified recombinant full length VWF. **C:** Coomassie staining of elution fractions following A1A2A3-VWF purification.

2.2.3 Purification of plasma derived VWF from Fandhi®

Commercial concentrate Fandhiμ® (Grifols, Spain) was used as additional source of plasma derived VWF. Fandhi is a plasma concentrate containing VWF, FVIII, albumin and a number of excipients. Size exclusion chromatography was employed as a method to purify plasma-derived VWF from Fandhi. Size exclusion chromatography (gel filtration) elutes larger proteins first from the column while smaller proteins migrate slowly. Using a sepharose 2B-CL gel filtration column (600mm x 26mm, 320ml volume, Amersham Pharmacia) high, intermediate and low molecular weight multimer fractions were isolated. The column was pre-equilibrated with two column volumes of Tris-Citrate buffer (20mM Tris, 10mM

sodium citrate, pH 7.4) and 5-10ml of reconstituted Fandhi was added to the column at a flow rate of 0.5mL/min. Fractions were collected in citrate buffer at a flow rate of 1mL/min.

2.2.4 Analysis of VWF

2.2.4.1 SDS polyacrylamide gel electrophoresis (SDS-PAGE)

For purity analysis of VWF following purification protocol gel electrophoresis was performed. 50ng (western blot) or 1µg (Coomassie Blue staining) of purified VWF were diluted in LDS sample running buffer (4X TheremoFisher scientific, Life Technologies USA) and heated to 80^0C for 10 minutes. For reducing conditions, dithiothreitol (DTT, 0.1M, Thermofisher USA) was added. Samples were loaded onto pre-cast gradient gels (NuPAGE Bis-Tris 4-12% gels, Life Technologies USA) with a pre-stained high molecular weight marker (ThermoScientific, USA). Electrophoresis was performed at 160V for 1h in MOPS-SDS running buffer.

2.2.4.2 Coomassie staining and western blotting

Following SDS-PAGE the purity of VWF was determined by coomassie and western blot. Coomassie stain (0.1% Brilliant Blue: Sigma-Aldrich Ireland, 20% methanol, 10% acetic acid) was employed for the detection of non-specific total protein. Gels were washed in distilled H_20 for 30 minutes followed by a 30 minute incubation with coomassie stain. Subsequently 10% acetic acid was used to destain under gentle agitation.

For specific VWF detection, proteins were transferred from the SDS-PAGE gel surface to a methanol activated polyvinylidene fluoride membrane (PVDF, Immobilon-P; Millipore USA) using a wet electroblot system (Trans-Blot Electrophoretic Transfer Cell, Bio-Rad USA). A 1 hour transfer was completed at 100V in ice cold transfer buffer (Tris (25mM), glycine (192mM) , 0.2% SDS, 20% methanol). VWF fragments <100 KDa were transferred for 10 minutes using a SEMI-DRY power blotter (Thermo scientific, USA) system with 1-Step transfer buffer (Thermo scientific, USA). 3% BSA in PBS-T (0.1%) was used to block membranes for 1 hour at room temperature. VWF was detected with a rabbit polyclonal anti-human VWF-HRP (Dako, Denmark) diluted 1:5000 in 3% BSA PBS-T for 1 hour at room temperature with gentle agitation. Following three x five minute PBS-T (0.1%) washes VWF was detected using Enhanced chemiluminescence (ECL) substrate (ThermoFisher Scientific, USA) according to the manufacturer's instructions.

2.2.4.3 BCA protein quantification

Once pure recombinant protein was obtained, it was quantified using the BCA Protein Assay Kit (Thermo Scientific Pierce, USA). Bicinchoninic acid (BCA) assay is a colourimetric means of quantifying total protein concentration against a standard curve. BCA quantification is based on the reduction of $Cu2^{+}$ to Cu^{+} by peptides bonds of proteins. Thus, reduction of $Cu2^{+}$ is directly proportional to the total protein present. Subsequent chelation of Cu^{+} ion yields a colourimetric change with absorbance at 562λ.

2.2.4.4 Endotoxin removal and detection

Following protein purification, endotoxins were removed using EndoTrap HD columns (Hyglos, Germany). VWF protein preparations were applied over an affinity chromatography resin that immobilises endotoxin in a buffer containing 0.5mM $Ca2^{+}$ and 20mM Tris solution. Fractions were eluted by gravity flow and protein concentration re-determined by BCA.

To confirm endotoxin removal, endotoxin levels were determined pre and post treatment using RAW-Blue reported cell line as previously discussed (Section 2.1.4). Furthermore, endotoxin levels were also determined using ToxinSensor Gel Clot Endotoxin Assay (GenScript, USA, Appendix ii). Protein preparation were diluted 1:1 with reconstituted limulus amebocyte lysate (LAL) reagent at incubated for 30 minutes at 37^{0}C. The presence of endotoxin induces the formation of a gelatin clot in this assay.

2.3: Binding assays

2.3.1 Activated primary monocyte binding

Full length recombinant VWF or A1A12A3-VWF preparations were immobilised at indicated concentrations onto a 96 well Nunc Immuno -polysorb plate (Thermo Fisher, USA) overnight in carbonate buffer pH 9.6 (Na_2CO_3 (28mM), $NaHCO_3$(70mM)). Plates were blocked with 0.5% polyvinylpyrrolidone (PVP, Sigma-Aldrich, Ireland) in PBS for 2 hours at 37^{0}C. Healthy donor isolated monocytes ($2x10^{6}$cells/ml) were activated with PMA (100nM, Sigma-Alderch Ireland), $MnCl_2$

(1nM) and BSA (1%) for 30 minutes at 37^0C. Cells were washed and resuspended ($2x10^6$cells/ml) in RPMI media supplemented with $MnCl_2$ (1mM). Following blocking, plates were washed 3 times with PBS and 100µl of cells were added to each well and incubated for 30 minutes at 37^0C. Non-adhered cells were removed by sealing the plate and centrifuging upside-down at 500rpm for 1 minute. Remaining adhered cells were fix and stained with 4% paraformaldehyde (PFA, Sigma-Aldrich, Ireland) and 5µg/ml Hoechst (Sigma-Aldrich, Ireland) for 10 minutes at room temperature. VWF bound activated monocytes were imaged using Cytell imaging platform (GE life sciences, USA) in which nuclei were detected. Blank controls are represented by monocyte binding in the absence VWF or A1A2A3 or non-coated wells. Bound monocytes were quantified and graphed as the fold change in binding from control in which VWF positive counts were divided by counts from non VWF treated wells.

2.3.2 THP1 cell binding

THP1 monocytes were differentiated as described (Section 2.13) and VWF binding was determined by flow cytometry. Differentiated THP1 cells were detached from petri dishes by continuous ice cold PBS pipetting and subsequently divided between treatments ($5x10^5$ cells/flow tube). Alternatively, non PMA treated suspension monocytic THP1 cells were used. VWF variants of interest were incubated with THP1 macrophages in binding buffer (Hanks balanced salt solution supplemented with HEPES (10mM), $MnCl_2$ (1mM) and $CaCl_2$ (1mM) ± ristocetin (Helena, UK 1.5mg/ml) where indicated) for 30 minutes at room temperature. For

recombinant VWF variants, equimolar full length or domain fragments (300µM) were incubated with the cells. Cells were washed once in 2ml of ice cold binding buffer and centrifuged at 4^0C for 5 minutes at 1500 rpm. FC-receptors were blocked with 1/100 dilution of CD16/CD32 monoclonal antibody (ThermoFisher scientific, USA) for 10 minutes on ice. Various antibodies were used to stain for bound VWF, detailed in Table 2.3. Where applicable, cells were washed with 2ml of binding buffer between and after 30 minute incubations (on ice) with primary and secondary antibodies. Following staining, cells were fixed in binding buffer containing 1% PFA for 10 minutes on ice. Normal PE-IgG control (Bio-legend USA) was used to determine nonspecific binding. Baseline fluorescence was established using 0µg/ml VWF incubated with PE conjugated anti penta-his tag. Using flow cytometry (CyAn ADP Analyzer: Beckman, USA) bound VWF was quantified and staining was determined by changes in mean florescence intensity (MFI) from baseline fluorescence using Flowjo software (Flowjo, USA). VWF binding was represented by combined replicates of fold change in MFI in which fold change MFI was determined by the division of VWF positive MFI signal by background PE-IgG control (Fold Change = VWF treated cell MFI / 0mM VWF MFI) .

Detecting protein	Antibody	Species	Working Dilution
Recombinant VWF and fragments	PE conjugated anti-penta-his Tag (Bio-Legend)	Mouse IgG2a, κ	1/25
Plasma derived VWF	Anti-VWF polyclonal (Dako, Agilent)	Rabbit IgG	1/1000
Secondary	Polyclonal Alexa Fluor™ 488 anti-rabbit. (ThermoFisher Scientific)	Goat IgG	1/1000
Secondary	PE-IgG control (Bio-Legand)	Mouse IgG2a, κ	1/25

Table 2.3: Flow cytometry antibodies for detecting bound VWF.

2.3.3 Human primary macrophage cell binding

Human primary macrophages were differentiated from buffy coat isolated $CD14^{High}$ monocytes on 48 well low adherent plates (Starstedt, Germany) and detached by gentle scraping with the barrel of a 1ml syringe. Cells were pooled and equally divided between treatment flow tubes ($2x10^5$-$1x10^6$). VWF was incubated as previously described (Section.2.3.2) and detected with an Alexa Fluor™ 488 bound to a polyclonal anti-VWF as detailed in Table 2.3. Staining and flow cytometry was completed as described in Section 2.2.2. VWF binding was represented by combined replicates of fold change in MFI in which fold change MFI was determined by the division of VWF positive MFI signal by background Alexa Flour 488-IgG control.

2.4: Confocal microscopy

2.4.1 THP1 Cells

THP1 cells were differentiated as previously described (Section 2.1.3) onto 8-well chamber well slides (Lab-Tec, USA). Macrophages were treated with VWF or VWF truncated variants (10µg/ml) in binding buffer (RPMI glutmax, $CaCl_2$ (1mM), ± ristocetin (1mg/ml)) where indicated at room temperature or on ice to prevent internalisation depending on experimental conditions. Cells were washed once with binding buffer and fixed with 4% PFA for 10 minutes on ice. Fixed cells were neutralised with two washes of ammonium chloride (100mM), and subsequently washed 3 times with PBS. When indicated, permeabilization was performed using 0.1% TritonX (Sigma-Aldrich, Ireland) in PBS for 4 minutes. Following this, cells

were washed 3 times with PBS and blocked (3% BSA-PBS) for 30 minutes. Primary and secondary antibodies were diluted in 2% BSA-PBS in accordance with Table 2.4 and 2.5 and incubated for 45 minutes and 30 minutes respectively at room temperature. Cells were washed 4 times before and after secondary antibody incubation. Nuclei were stained with in situ DAPI mounting media (Sigma-Aldrich, Ireland) and slides were sealed. Imaging was completed using oil emersion Carl Zeiss 710 LSM confocal microscope (Carl Zeiss, Germany).

Detecting Antigen	Antibody Source	Dilution
VWF	Polyclonal rabbit IgG-anti-VWF (DAKO)	1/1000
EEA1	Polyclonal mouse IgG1-anti EEA1, (BD Transduction Laboratories)	1/100
LAMP	Monoclonal mouse anti-LAMP-1 (Santa Cruz)	1/50

Table 2.4: Confocal microscopy primary antibodies

Secondary Antibody	Dilution
Alexa 594 – anti-mouse	1/300
Alexa 488 - anti-rabbit	1/1000

Table 2.5: Confocal microscopy secondary antibodies

2.4.2 Human primary macrophages

Glass cover slips (18mm, 170µm) were cleaned in a sonicating water bath by serial immersion in dH_2O, chloric acid (1M), 50% ethanol, 75% ethanol and 100% ethanol for 30 minutes each. Coverslips were sterilised with a 30 minute UV exposer. BMDM ($3x10^5$/ml) or human primary monocytes ($2x10^5$/ml) were differentiated onto glass coverslips. Depending on experimental conditions, 10-20µg/ml of VWF was incubated for 30 minutes at room temperature with monocyte derived macrophages in binding buffer (RPMI glutmax, $CaCl_2$ (1mM)). Following 3 washes with binding buffer cells were then blocked for 30 minutes with 3% BSA and Fc-Blocker at a dilution of 1/100. Staining and imaging was completed in accordance with Section 2.4.1.

2.4.3 DuoLink® proximal ligation assay (PLA)

Duolink® PLA allows for detection of interacting proteins. Primary antibody's raised in different hosts bind to respective proteins of interest. Secondary "+" and "-" antibodies conjugated with DNA oligonucleotides bind to the individual primary antibodies. Hybridize connector oligos join the secondary oligos if in close proximity to each other (40nm), and fused by DNA ligase that forms a closed circular DNA template. DNA polymerase is added, in which the closed circle oligos acts as a primer for rolling circle amplification generating a single stranded sequence up to 1000 copies of the primer sequence, tether to the antibodies. Finally, ladled detection probes hybridize to the complementary sequence within the single stranded amplicon.

THP1 macrophages and BMDMs were differentiated onto chamber slides or cover slips as described in Sections 2.4.1 and 2.4.2 respectively. VWF was incubated with the cells in binding buffer (RPMI Glutmax, $CaCl_2$ (1mM) ± ristocetin (1.5mg/ml)) for 30 minutes at 37°C and cells were fixed with 1% PFA. Prior to duolink staining cells were blocked for 60 minutes with Duolink® blocking solution (Sigma-Aldrich, Ireland) at 37°C. Primary antibodies were diluted as per Table 2.6 in PBS 1.5% BSA and incubated for 2 hours at room temperature.

Primary Antibodies	Dilution
Polyclonal rabbit anti VWF (Dako)	1/1000
Monoclonal mouse [8G1] anti LRP1 (Abcam)	1/200

Table 2.6: Antibodies used for Duolink® proximal ligation assay

Following two x five minute washes with Duolink® wash buffer A (Sigma-Aldrich, Ireland), anti-mouse(+) and anti-rabbit(-) PLA probes (Sigma-Aldrich, Ireland) were diluted 1:5 with antibody diluent (Sigma-Aldrich, Ireland) and incubated with the cells for 1h at 37°C. Samples were washed for two x five minutes in Duolink® wash buffer A. Two circle forming DNA oligonucleotides were added and ligated onto secondary probes following a 30 minute incubation at 37°C with Duolink® ligase (1:40, Sigma-Aldrich, Ireland). The sample was washed in Duolink® wash buffer A for two x five minutes and the closed circular DNA template was amplification by Duolink® polymerase (1:80, Sigma-Aldrich, Ireland) for 100 minutes at 37°C in the dark. The sample was washed 2 x 10 minutes with Duolink® wash buffer B and slide mounted with Duolink® in situ DAPI mounting medium. Cells were imaged using Carl Zeiss LSM 710 confocal microscope (Carl Zeiss, Germany).

2.5: VWF glycosylation modification

2.5.1 N-Linked glycan removal - PNGase F

To remove the N-linked glycan structure from VWF, 5µg of VWF was incubated with 2µl of specific glycosidase enzyme, PNGase F (New England Biolabs, USA) with an appropriate volume of the supplied 10X glycobuffer Digestion was carried out overnight at 37^0C. PNGase F and cleavage products were removed from the preparation by molecular weight cut off spin columns (10 kda molecular weight cut off spin, Sartorius, Sigma-Aldrich Ireland). Digestion was confirmed by loss in VWF molecular weight as detected by western blot analysis.

2.5.2 Sialic acid removal - Neuraminidase

To remove terminal sialic acid residues from VWF N- and O-linked glycans 5µg of VWF was treated with cleaved with 6.25mU of α2-3,6,8,9 Neuraminidase (New England Bio-labs, USA). Digestion was carried out in 1x glycobuffer overnight in at 37^0C and loss of sialic acid residues was confirmed by molecular weight on SDS-Page and lectin binding performed by Dr Sonia Aguila (Irish Centre for Vascular biology).

2.6: Gene analysis

2.6.1 RNA isolation

To obtain sufficient a concentration of RNA following cell lysis, a minimum of $2x10^6$ primary cells were used. Cells were washed with PBS followed by lysis and homogenization with 1ml of TRIZOL (Sigma-Aldrich, Ireland) per 10 cm^2 culture dish. Lysates were frozen at -80^0C for a minimum of 1 hour and when defrosted 100µl of 1-bromo-3-chloropropane (Sigma-Aldrich, Ireland) was added per ml of TRIZOL. Phase separation was initiated by resting samples at room temperature for 15 minutes and subsequently centrifuging at 12,000g for 15 minutes at 5°C. Following the formation of 3 distinct layers, the RNA containing aqueous phase was aspirated without disturbing the organic or DNA containing phases. To precipitate RNA, 500µl of isopropanol (-20°C) was added to the aqueous phase per ml of TRIZOL and samples were allowed to stand at room temperature for 30 minutes. The RNA pellet was then formed by centrifuged for 10 minutes at 12,000g at 5°C. The supernatant was removed and RNA was washed with 1 ml of 75% ethanol per 1 ml of TRIZOL, centrifuged again and finally dissolved in 40µl of molecular grade water. RNA concentration and purity were determined by 260λ/280λ and 260λ/280λ ratios respectively.

2.6.2 cDNA synthesis

cDNA was synthesized from 100ng-200ng of RNA produced as in Section 2.6.1 in sterile nuclease-free tubes. All reagents were kept on ice (excluding reverse transcriptase -20) and sequentially added as per Table 2.7. Using a thermocycler,

primer annealing occurred for 10 minutes at 25°C, followed by DNA polymerization for 60 minutes at 42°C and finally terminated for 10 minutes at 70°C.

Total RNA	100-300ng
Random Hexamer Primer (TheremoFisher Scientific, USA)	1µl
Molecular Grade Water (TheremoFisher Scientific, USA)	Made up to 12.5µl
5X Reaction Buffer (TheremoFisher Scientific, USA)	4µl
RNase Inhibitor (TheremoFisher Scientific, USA)	0.5µl
dNTP (VWR, USA)	2µl
Reverse Transcriptase (TheremoFisher Scientific, USA)	1µl
Total Volume 20µl	

Table 2.7: cDNA synthesis reagents

2.6.3 Real time - qPCR (RT-qPCR)

Gene expression was determined by Quantitative reverse transcription PCR (RT-qPCR) following cDNA synthesis. 96 well plate (Thermofisher scientific, USA) PCR was setup in accordance to Table 2.8 and gene-specific primers (Sigma-Aldrich/IDT USA) were diluted 1/10 from stock 100µM concentrations. PCR reaction was completed using a 7500 real time PCR system (ThermoFisher, USA) following Table 2.9 setup. Changes in expression of genes of interest from untreated cells, or following LPS (100ng/ml) and/or VWF (10µg/ml) treatments were quantified by fold change-ΔΔCT from housekeeping genes β-Actin ($2^{-\Delta\Delta Ct}$). Ct meaning cycle threshold, is the PCR cycle value in which florescence has detectible above background levels. ΔCT represents the CT of gene of interest normalised to

housekeeping gene. (ΔCT = CT gene of interest – CT housekeeping gene) ΔΔCT refers to the normalisation of ΔCT to experimental control/untreated conditions (ΔΔCT = ΔCT gene of interest – ΔCT average of control). Primer sequences found in Table 2.10. Optimal gene expression was determined by time course analysis.

cDNA template	**0.5µl**
H_20	3.3µl
Forward Primer (Sigma-Aldrich/IDT)	0.6µl
Reverse Primer (Sigma-Aldrich/IDT)	0.6µl
Master Mix (Promega)	5µl
Total Volume 10µl	

Table 2.8: Real time-qPCR 96 well setup

Stage	**Time (Minutes)**	**Temperature (^OC)**
Holding	2	95
Denaturation	0.25	95
Annealing / Extension	1	58

Table 2.9: Real time-qPCR running settings for 40 cycles.

Human (5’-3’)				
ITGAM	**Forward**	GAGTTTGTCTCAACTGTGATG	**Reverse**	GTGAATCCGGAATTCTTCAG
ITGB2		CCAAGTTTGCTGAGAGTTAG		GGTTAATTGGTGACATCCTC
LRP1		GAGAATTATCTCTATGCCACC		CATACTGGTCGTTTTCACAG
MSR1		TCCCACTGGAGAAAGTGGTC		CTCCCCGATCACCTTTAAGAC
IL-1β		CTAAACAGATGAAGTGCTCC		GGTCATTCTCCTGGAAGG
IL-6		GCAGAAAAAGGCAAAGAATC		CTACATTTGCCGAAGAGC
TNFα		AGGCAGTCAGATCATCTTC		TTATCTCTCAGCTCCAGC
CCL2		AGACTAACCCAGAAACATCC		ATTGATTGCATCTGGCTG
CCL3		GCAACCAGTTCTCTGCATCA		TGGCTGCTCGTCTCAAAGTA
CCL4		GCTTTTCTTACACTGCGAGGA		CCAGGATTCACTGGGATCAG
NOS2		GCTCTACACCTCCAATGTGACC		CTGCCGAGATTTGAGCCTCATG
β-Actin		GACGACATGGAGAAAATCTG		ATGATCTGGGTCATCTTCTC
Murine (5’-3’)				
LRP1	**Forward**	ACTTTGGGAACATCCAGCAG	**Reverse**	GGTGGATGTGGTGTAGCTTG
β-actin		TGCTGTCCCTGTATGCCTCT		TTGATGTCACGCACGATTTC
TNFα		ACGTCGTAGCAAACCACCAA		GAGAACCTGGGAGTAGACAAGG
IL-6		ATGAAGTTCCTCTCTGCAAGAGACT		CACTAGGTTTGCCGAGTAGATCTC
PHD3		CAACTTCCTCCTGTCCCTCA		CCTGGATAGCAAGCCACCA

Table 2.10: Human and murine primer sequences for RT-PCR

2.7: Flow cytometry

2.7.1 M1 and M2 surface marker expression

BMDMs were generated over a 6-day period as previously described (Section 2.1.5) and seeded onto 48 well plates ($1.5x10^5$/well) overnight. All BMDMs were incubated in $RPMI^{++}$ supplemented with M-CSF (25ng/ml) and $CaCl_2$ (1mM) for 24 hours. Additionally, cells were incubated with INF-γ (20ng/ml, Gibco, USA) and LPS (100ng/ml Sigma-Aldrich, Ireland) to generate a M1 macrophage phenotype. Alternatively, IL-4 (40ng/ml PeproTech, USA), IL-13 (20ng/ml PeproTech, USA) and IL-10 (10ng/ml, PeproTech USA) were used to generate a M2 phenotype. BMDMs were also treated with plasma derived VWF (10μg/ml). Control cells did not receive additional agonists and remained in $RPMI^{++}$ supplemented with M-CSF (25ng/ml) and $CaCl_2$ (1mM). BMDM were washed with $RPMI^{++}$ media, lifted by scraping with the barrel of a 1ml syringe and using flow cytometry M1 and M2 populations were determined by the respective expression of CD38 and CD206. Fc receptors were block as previously described and cells were stained with an anti-CD11b PE (1/800 PE conjugated, Biolegand USA), anti-CD206 blue violet 421 (1/25, Biolegand, USA) and anti-CD38 APC (1/800, Biolegand, USA) for 30 minutes on ice. Cells were washed in $RPMI^{++}$ then fixed in 1% PFA for 10 minutes on ice and washed again. Macrophages were identified as CD11b positive cells and relative CD206 (M2) and CD38 (M1) expression determined. Changes MFI surface marker expression from control cells was determined using FlowJo software (FlowJo & BD, USA).

2.7.2 Reactive oxygen sepsis generation

BMDM were generated over 6 days as described (Section 2.1.5) and subsequently seeded onto 48 well plates ($1.5x10^5$/well) overnight with M-CSF (25ng/ml). BMDMs were washed and incubated with LPS (100ng/ml) or plasma derived VWF (10µg/ml) for 3 hours in $RPMI^{++}$ supplemented with $CaCl_2$ (1mM). Cells were washed in supplemented $RPMI^{++}$ and incubated with CellRox Deep Red (5µM, ThermoFisher Scientific, USA) and LiveDead stain (1/1000, TheremoFisher Scientific, USA) for 30 minutes at 37^0C. Prior to staining a control dead cell population was determined using 70% ethanol. Free amines from dead cells compromise the cell membrane and combine with LiveDead-488 yielding fluorescence. To quantify cellular reactive oxygen species CellRox was used. Once CellRox has undergone oxidation it exhibits a strong fluorescent signal. Following dead cell exclusion, CellRox signal was determined based in change in MFI from untreated BMDM population using FlowJo (FlowJo, USA).

2.7.3 Phagocytosis Assay

Human monocyte derived macrophages were allowed to differentiate as described in section 2.1.2 for 10 days in a 48 well, reduced adherence surface plate (Starstedt, Germany). A minimum of $6x10^5$ cells were used per treatment by combining 6-wells at $1x10^5$cells/well. Plasma derived VWF (10µg/ml) or LPS (100ng/ml) were incubated with cells for 30 minutes at 37^0C in $RPMI^{++}$ supplemented with $CaCl_2$ (1mM). Following this, $2.5X10^6$ of fluorescent *E.coli* particles labelled with Alexa Fluor® 488 (TheremoFisher Scientific, USA) were added for 1.5 hours per well.

Human macrophages were thoroughly washed in ice cold RPMI^{++}, detached and fixed in 1% PFA for 10 minutes.

The extent of intracellular phagocytosed fluorescence was determined by quenching the bound extracellular fluorescence using 0.2% trypan blue (Sigma-Aldrich, Ireland), pH 5.5 in PBS. Immediately prior to loading sample for flow cytometry, quenching buffer was added and changes in macrophage fluorescein isothiocyanate (FITC) MFI were determined. Data was quantified using FlowJo (Flowjo, USA).

2.7.4 *In vivo* lavage panel

2.7.4.1 Short time course treatment

Plasma derived VWF (2mg/kg) or equal volume sterile PBS was injected intraperitoneally into wile type female C57BL/J6 mice weighing 24g. Following a 3 hour incubation mice were culled by cervical dislocation and peritoneal lavage was performed with 5ml of PBS containing 3% BSA. Lavage fluid was harvested and on average $2x10^6$ cells were isolated per mouse. Cells were Fc blocked, stained and gated as per Table 2.11 and Figure 2.4 in 5% FBS in RPMI phenol red free (Gibco, USA) for 30 minutes on ice. Compensation was determined by single staining alone and no positive staining detected from IgG controls. Analysis was completed using FlowJo (Flowjo, USA).

Marker	Clone	Fluorophore	Dilution
CD3	17A2	Alexa-488 (BioLegend, USA)	1/20
F4/80	BM8	Brilliant Violet 421 (BV421, BioLegend, USA)	1/20
CD11c	N418	APC (BioLegend, USA)	1/20
CD122	5A4	PE (BioLegend, USA)	1/20
Ly-6C	RB6-8CH	Blue Violet 510 (BV510, Bio Legend, USA)	1/20

Table 2.11: Antibodies used for 3 hour *in vivo* lavage

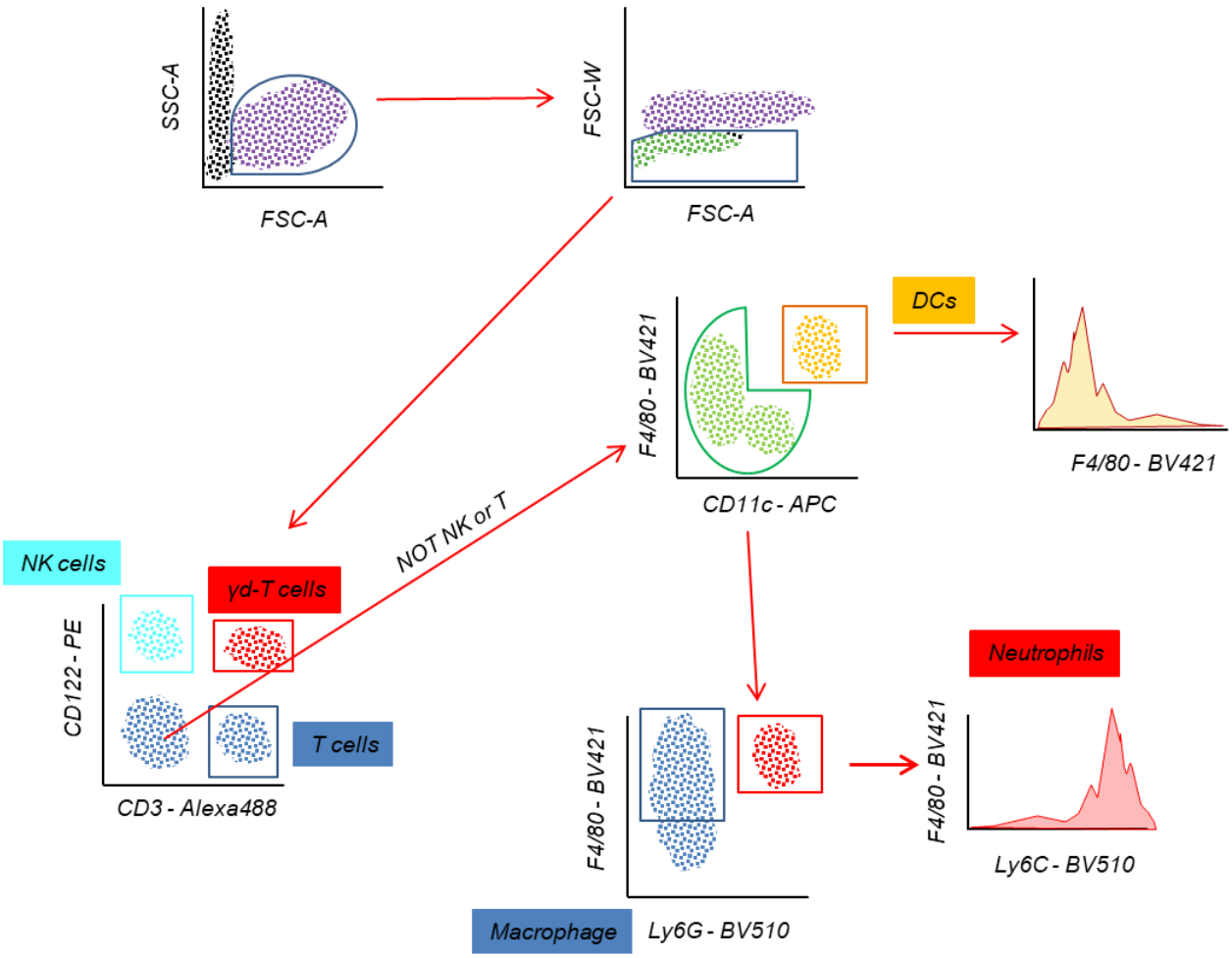

Figure 2.4: Short time course lavage gating strategy

2.7.4.2. Extended time course treatment

As per previous, plasma derived VWF (2mg/kg) or PBS was injected intraperitoneally into wild-type female mice and incubated for 24 hours. Peritoneal lavage was performed as per previous. Cells were stained for tissue resident and recruited macrophages using the antibodies outlined in Table 2.12. Resident peritoneal macrophages are MHC-II high while recruited are MHC-II low. Cell populations were gated based on the strategy illustrated in Figure 2.5.

Marker	Clone	Fluorophore	Dilution
CD3	17A2	Alexa-488 (BioLegend, USA)	1/20
F4/80	BM8	Brilliant Violet 421 (BV421, BioLegend, USA)	1/20
CD11c	N418	APC (BioLegend, USA)	1/20
MHC II	AF6-102.1	PE (BioLegend, USA)	1/20
Ly-6C	RB6-8C5	Blue Violet 510 (BV510, Bio Legend, USA)	1/20
CD49b	DX5	APC-Cy7 (BioLegend, USA)	1/20
CD11b	M1/70	PE-Cy7 (BioLegend, USA)	1/20

Table 2.12: Antibodies used for 24 hour *in vivo* lavage

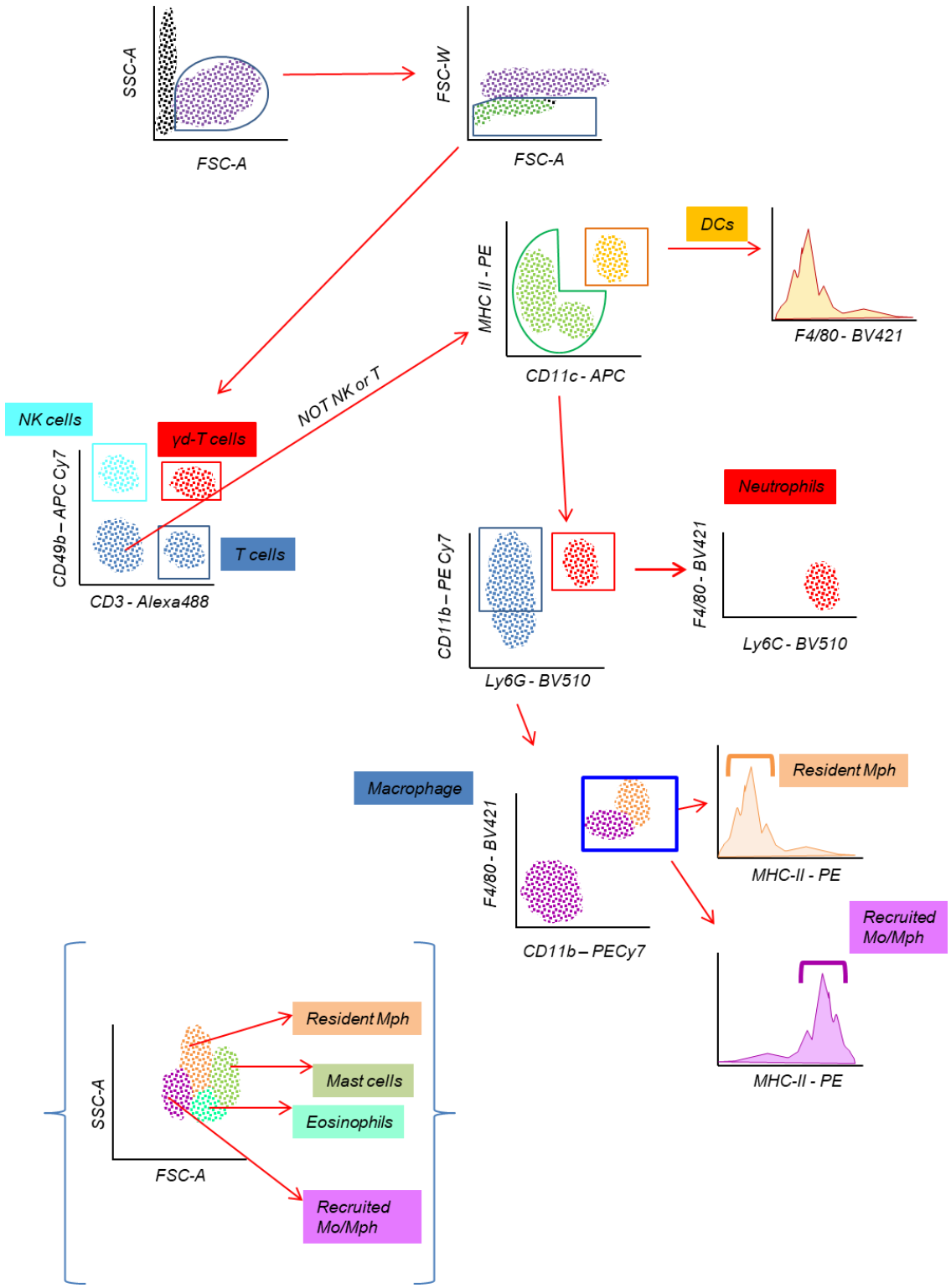

Figure 2.5: Extended time course lavage gating strategy

2.8: *In vitro* cell signalling and cytokine generation

2.8.1 MAPKinase and NF-κB

Human monocyte derived macrophages were differentiated onto 48 well plates as described and minimum of $3x10^5$ cells were used per treatment. BMDM were seeded overnight onto 48 well plates in $RPMI^{++}$ supplemented with M-CSF (25ng/ml) where a minimum of $3x10^5$ cells were also used per treatment. Cells were washed and treated where indicated with plasma derived VWF (10µg/ml), recombinant VWF (10µg/ml) or LPS (100ng/ml) for 25 minutes at 37^0C in $RPMI^{++}$ supplemented with $CaCl_2$ (1mM).

Cells were lysed on ice for 10 minutes with 40µl/well of radioimmunoprecipitation assay (RIPA) buffer (TheremoFisher scientific, USA) supplemented with Protease Inhibitor cocktail 1 (1/100, Merc Chemicals, USA) and Phosphatase Inhibitors Cocktail 2 & 3 (1/500, Sigma-Aldrich, Ireland). Following lysis, total protein was quantified by BCA reagent and normalised. 10-20µg of protein was resolved under reduced conditions by SDS-PAGE and transferred to PVDF membrane as per Section 2.2.4.1. Membranes were blocked for 1 hour at room temperature and primary antibodies (Table 2.13) were diluted in TBS-T (0.1%) - 5% BSA or milk in according to manufactures instructions. Membranes were incubated with HRP conjugated anti-mouse or anti-rabbit antibodies (1/1000-1/5000, R&D Systems, USA) in TBS-T (0.1%) 5% milk for 1 hour at room temperature. Three 5minute washes in TBS-T (0.1%) were carried out pre- and post-secondary antibody

incubation. Western blots were developed with enhanced chemiluminescence substrate (ThermoFisher Scientific, USA) using Amersham Imager (GE, USA)

Antibody	Epitope	Dilution
Rabbit monoclonal anti-phosop-p38 (CST, USA)	Thr180/Tyr182	1/1000
Rabbit polyclonal anti-p38 (CST, USA)	p38α, -β or -γ MAPK	1/1000
Rabbit monoclonal anti-phospho-NF-κB p65 (CST, USA)	Ser536	1/1000
Rabbit monoclonal anti-NF-κB p65 (CST, USA)	Glu498	1/1000
Mouse monoclonal anti-IκBα (CST, USA)	Amino-terminal Antigen	1/1000
Rabbit monoclonal anti-phospho-IκBα (CST, USA)	Ser32	1/1000
Rabbit polyclonal anti-JNK (CST, USA)	JNK1, JNK2 or JNK3	1/1000
Rabbit polyclonal anti-phospho-JNK (CST, USA)	Thr183/Tyr185	1/1000
Mouse monoclonal anti-B-actin (Sigma-Aldrich, Ireland)	N-terminal	1/3000

Table 2.13: Western blot primary antibodies

2.8.2 Hypoxia-inducible factor 1-alpha (HIF-1α) analysis

Differentiated BMDMs were seeded into 48 well plates and treated with VWF (10µg/ml) or LPS (100ng/ml) and where indicated ± p38 inhibitor SB202190 (50µM, Invivogen, USA) in RPMI^{++} supplemented with $CaCl_2$ (1mM) and M-CSF (25ng/ml) for 3 or 16 hours. Given the difficulty in detecting HIF-1α an alternative lysis protocol was used. Cells ($3x10^5$) were directly lysed (120µl) with SDS running buffer (1X) supplemented with DTT (0.1M) and benzonase (1/1000, Millipore, USA) on ice. Lysates were frozen at -80^{0}C for minimum of 1 hour and 5-10µl were resolved by

SDS-PAGE as per Section 2.2.4.1. Equal loading was confirmed using β-Actin. Protein was transferred onto nitrocellulose membrane using wet electroblot system for 1 hour at 100V in ice cold transfer buffer. Membranes were blocked with 5% milk with 0.05% sodium azide (Sigma-Aldrich, Ireland) in TBS-T (0.1%) at room temperature for 1 hour. The same blocking buffer was used to dilute the primary anti-HIF-1α antibody (1/1000, rabbit monoclonal anti-HIF-1α (Leu478) CST, USA) incubated overnight at 4^{O}C. Following extensive washing Secondary antibody (Anti-Rabbit, 1/2000, R&D USA) was incubated for 1 hour at room temperature in 5% milk TBS-T (0.01%) Imaging was completed in accordance to Section 2.8.1.

2.8.3 Low density lipoprotein receptor-related protein 1 (LRP1) analysis

Human monocyte derived macrophages were differentiated in 48 well plates. Macrophages ($3x10^5$) were treated with plasma derived VWF (10µg/ml) or LPS (100ng/ml) ± an LRP1 antagonist termed receptor associated protein (RAP, 200nM, R&D Systems USA) in $RPMI^{++}$ supplemented with $CaCl_2$ (1mM). Following a 25 minute incubation at 37^0C cells were lysed and samples resolved per Section 2.8.1.

Differentiated BMDMs were seeded into 48 well plates. Cells were treated with plasma derived VWF (10µg/ml) or LPS (100ng/ml) ± anti-LRP1 (mouse monoclonal anti-LRP1 (α chain) 200nM, Sigma-Aldrich, Ireland) in $RPMI^{++}$ supplemented with CaCl (1mM). Control cell were treated with anti-LRP1 alone or mouse IgG control (200nM, Santa Cruz, USA) Following a 25 minute incubation at 37^0C cells were lysed and samples resolved per Section 2.8.1.

To blot for LRP1, human monocyte derived macrophages, BMDMs or THP1 macrophages were lysed using RIPA buffer supplemented with Protease Inhibitor Cocktail 1 (1/100). Lysate was quantified using BCA, aliquoted and frozen at -20^{0}C. Before undertaking SDS-PAGE, sample-loading buffer was added to 10µg of cell lysate and samples were heated to 80^{0}C for 10 minutes in non-reducing conditions. PVDF membrane was blocked in 5% milk TBS-T (0.1%) and primary antibodies were diluted in accordance with Table 2.14 in 5% BSA TBS-T (0.1%). As per Section 2.8.1 secondary antibodies were applied and the membrane imaged.

Antibody	Recognition site	Dilution
Mouse monoclonal anti-LRP1 [5A6] (Abcam)	α-chain	1/1000
Mouse monoclonal anti-LRP1 [8G1] (Abcam)	β-chain	1/1000
Mouse monoclonal anti-LRP1 [Blocking 11] (Sigma-Aldrich)	α-chain	1/1000

Table 2.14: Anti-LRP1 antibodies

2.8.4 THP1 macrophages stimulation

THP1 cells were differentiated in 48 well plates according to Section 2.1.3. Cells were treated with plasma derived VWF (10µg/ml) or LPS (100ng/ml) for 25 minutes in RPMI^{++} supplemented with $CaCl_2$ (1mM). As per Section, 2.8.1 cells were lysed in RIPA buffer, resolved on SDS-PAGE and membranes imaged.

2.8.5 Inflammasome activation

Differentiated BMDM were seeded onto 48 well plates as described in Section 2.1.5. Cells were treated with plasma derived VWF (10µg/ml) or LPS (100ng/ml) in $RPMI^{++}$ supplemented with $CaCl_2$ (1mM) and M-CSF (25ng/ml) for 24 hours. To induce IL-1β cleavage, cells were washed with serum free RPMI and incubated with ATP (5µM, Invivogen, USA) for 1 hour. Supernatants were harvested and cells were lysed in RIPA buffer in accordance with Section 2.8.1.

Cell lysis was examined by SDS-PAGE whereby total protein was transferred to PVDF membrane as described in section 2.2.4. The PVDF membrane was blocked for 1 hour at room temperature in 5% milk TBS-T (0.1%) and probed overnight at 4^0C with anti-proIL-1β (1/1000, R&D systems, USA) in 5% BSA TBS-T (0.1%). Following washing with TBS-T (0.1%), the membrane was incubated with HRP conjugated anti-goat (1/2000: Jackson laboratories) in 5% milk TBS-T (0.1%) for 1 hour at room temperature.

The release of cleaved IL-1β from the cells was determined by ELISA (R&D systems, USA). Following the manufacturers instructions, the capture antibody was coated onto a Maxisorp 96-well microtiter plates (Nunc Thermo Scientific, USA) overnight at 4^0C washed with PBS-T (0.05%) and blocked for 1 hour at room temperature with 1% BSA. Recombinant mouse IL-1β (used as a standard) and cell supernatants were incubated for 2 hours at room. Plates were washed in triplicate in PBS-T (0.05%) before biotinylated IL-1β detection antibody and streptavidin-HRP were incubated for 1 hour and 20 minutes respectively. Levels of IL-1β were determined

following the addition of HRP substrate, TMB (1-Step Ultra TheremoFisher Scientific, USA). The reaction was terminated upon addition of H_2SO_4 (2N) and absorbance read at 450λ. Concentration of IL-1β calculated from the recombinant IL-1β standard curve.

2.8.6 Cytokine generation

Levels of TNF-α and IL-6 generated in BMDMs and primary human macrophages following VWF treatments were determined by ELISA. Human primary macrophages were incubated with plasma derived VWF (10μg/ml) and LPS (100ng/ml) in $RPMI^{++}$ supplemented with $CaCl_2$ (1mM) for 4 or 24 hours. BMDMs supernatants were harvested following 4 hours or 24 hour incubations where indicated with LPS (100ng/ml) or plasma derived VWF (10μg/ml). BMDM media was supplemented with M-CSF (25ng/ml) for these time points. Human TNF-α was determined using Ready Set Go ELISA KIT (TheremoFisher Scientific, USA) and human IL-6 levels were quantified by IL-6 ELISA (BioLegend, USA). Murine TNF-α levels were determined by DuoSet ELISA (R&D System, USA) and IL-6 by murine IL-6 ELISA (BioLegend, USA). Assays were completed in accordance manufactures instructions, similar to Section 2.8.5.

2.9: Macrophage tolerance

Differentiated BMDMs were seeded overnight onto 48 well plates at $1.5x10^5$ cell/well. Cells were stimulated with LPS (100ng/ml) or plasma derived VWF (10µg/ml) in $RPMI^{++}$ supplemented with M-CSF (25ng/ml) and $CaCl_2$ (1mM) for 8 hours followed by agonist wash out with supplemented $RPMI^{++}$ media. Cells were rested for a further 16 hours in cell culture media and subsequently re-stimulated at the same concentration with VWF or LPS for 4 hours. Supernatants were harvested at each step. Secreted TNF-α was used as an output of tolerance and quantified by ELISA as per Section 2.8.6.

2.10: Transmigration assays

Differentiated human macrophages were treated with LPS (100ng/ml), plasma derived VWF (10µg/ml) or recombinant VWF (10µg/ml) for 24 hours in $RPMI^{++}$ supplemented with $CaCl_2$ (1mM). Human monocytes were isolated using CD14 surface expression as described in Section 2.1.1 and resuspended in serum free RPMI supplemented with $CaCl_2$ (1mM). Using a 24 well hanging cell insert (Millicell, 0.8µm, PET, Millipore, USA) $2x10^6$ monocytes were placed in the upper chamber and 400µl of supernatants from 24 hour stimulation were placed in the lower chamber. The hanging insert was placed into the supernatants forming an interface for 2.5 hours. The upper chamber was removed and live migrated cells were stained with Cell Tracker Green (2.5µM, Invitrogen, TheremoFisher Scientific USA) for 20 minutes. Cells were washed and imaged using an epifluorescence NIKON Eclipse TS100 (Nikon, Japan). 6 images/well were taken across the diameter of the

well and cell counts were quantified using ImageJ (NIH, USA). Data was represented by fold increase from control untreated human macrophage supernatants.

2.11: Macrophage metabolism

2.11.1 Seahorse mitostress

Following differentiation, BMDMs were seeded into Seahorse XF96 culture plates (Agilent) at a density of $5x10^4$cells/well. Cells were stimulated with LPS (100ng/ml), plasma derived VWF (10µg/ml) or recombinant VWF (10µg/ml) for 3 hours or 16 hours where indicated in 50µl of $RPMI^{++}$ supplemented with $CaCl_2$ (1mM) and M-CSF (25ng/ml). Additionally, a 1 hour pre-treatment with p38 ATPase inhibitor SB202190 (50µM) prior to incubation with VWF or LPS was performed where indicated. Following treatment, BMDMs were washed and incubated at 37^0C with Seahorse phenol red-free basal media supplemented with pyruvate (1mM), glutamine (2mM) and glucose (10mM), pH 7.4 in a CO^2 free incubator for 40 minutes. To determine extracellular acidification and oxygen consumption rate (ECAR and OCR, respectively) markers of glycolysis and oxidative phosphorylation, Seahorse Mito Stress Kit (Agilent, USA) was used in Seahorse XFe96 Analyser (Agilent, USA). Basal rates of respiration were determined by ECAR and OCR prior to the addition of mitochondrial inhibitors. Oligomycin (1µM, oligo), an inhibitor of Complex V which decreases mitochondrial ATP generation thus decreasing OCR and increasing the demand from glycolysis.(184,185) Carbonyl cyanide p-trifluoromethoxyphenylhydrazone (1mM, FCCP), uncouples the mitochondrial

membrane, collapsing the proton gradient allowing electrons move freely driving oxygen consumption by complex IV.(186,187) Finally antimycin A and rotenone (0.5mM, AA + R) blocks complex III and I shutting down mitochondrial respiration, inducing a drop in OCR but increase in ECAR to sustain energy production. (188,189) Once the mitostress test was completed, data was normalized to total protein per well determined by BCA reagent. Alterations in metabolism were assessed by changes in OCR and ECAR in accordance with Figure 2.6 using Wave software 2.6.0 (United States).

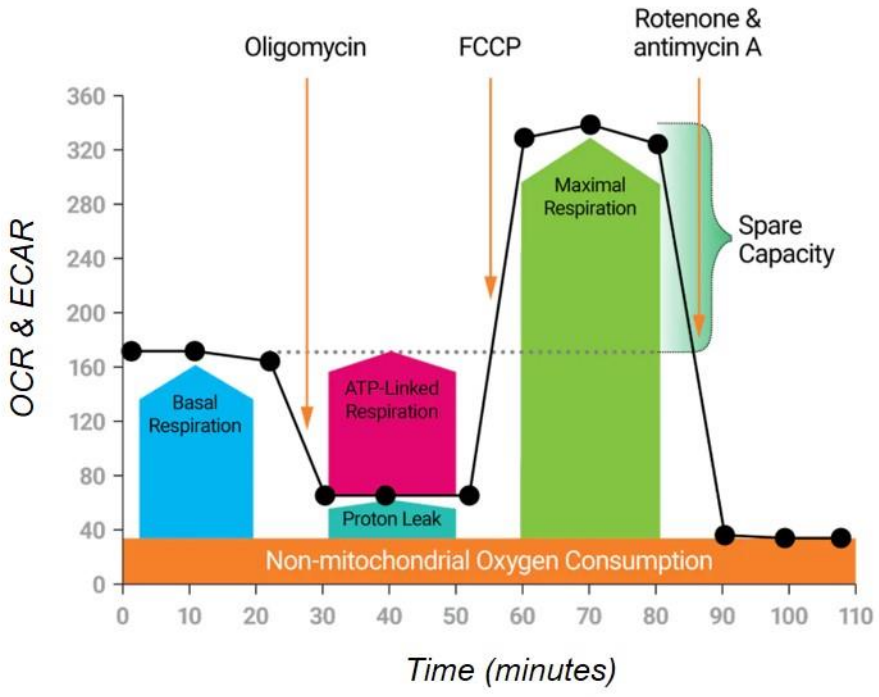

Figure 2.6: Mitostress test metabolic readouts

2.11.2 Mitochondrial morphology

Once differentiated, BMDMs were seeded onto live cell imaging 4-well culture dishes (Ibidi, Germany) at $1x10^5$cells/well overnight. Cells were treated with VWF (10µg/ml) or LPS (100ng/ml) for 3 or 16 hours in $RPMI^{++}$ supplemented with M-CSF (25ng/ml) and $CaCl_2$ (1mM). Cells are washed twice with media and stained with MitoTracker Red (1/1000, ThermoFisher Scientific, USA) for 30 minutes in serum free RPMI media. Following staining cells were thoroughly washed with cold PBS five times and serum free media was replaced for imaging. Mitochondrial morphology was determined using a Leica SP8 scanning confocal microscopy (Leica, Germany) where a minimum of 30 cells were taken per treatment. Images were analysed for mitochondrial morphology using Fiji ImageJ (NIH, USA) and an average 60 mitochondria were measured per cell. Mitochondrial fragmentation, representing the glycolytic form, was defined as <1µm in size.(190) Tubular formed mitochondrial which represents homeostatic conditions defined as those sized 1.1µm-2.9µm.(190) Finally elongated mitochondria, observed in aerobic states, defined as those >3µm in size.(190)

2.11.3 Cell viability

BMDMs seeded into 48 well plates at $1.5x10^5$/well and treated with plasma derived VWF (10µg/ml), recombinant VWF (10µg/ml), LPS (100ng/ml) or p38 inhibitor SB202190 (50µM) for 3 or 16 hours where indicated, in $RPMI^{++}$ supplemented with M-CSF (25ng/ml) and $CaCl_2$ (1mM). Cells were washed and incubated for 1-4 hours at 37^OC in 10% alamarBlue cell viability reagent (Bio-Rad, USA) media. Viability was

determined by metabolism of almarBlue in which living cells catabolise resazurin to fluorescent resorufin (absorbance λ = 600nm). Fluorescence values were normalised to total protein determined by BCA reagent.

2.12: Data Presentation and Statistical Analysis

All experimental data and statistical analysis were performed using the GraphPad Prism program (Graphpad Prism version 5.0 for Windows; GraphPad Software, Inc. San Diego, CA). Data were expressed as mean values ± standard error of the mean (SEM). Normal distribution was determined by D'Agostino–Pearson or Shapiro-Wilk tests. To assess statistical differences, data were analysed using Student's unpaired 2-tailed t test following F-Tests for equality of variances. For comparison of multimer means an Anova was preformed. For all statistical tests, P values <0.05 were considered significant.

3. Investigating the interaction between von Willebrand factor and macrophages

3.0: Introduction

Although the biological basis underpinning VWF clearance from the circulation remains poorly understood, previous studies have demonstrated that the liver and spleen represent the most important organs for VWF clearance.(117,191) In addition, accumulating data suggests that hepatic and splenic macrophages function as key cellular mediators of VWF clearance.(117,192,193) *In vivo* studies have shown that radiolabelled VWF co-localises with CD68+ macrophages in murine livers and that macrophage depletion significantly prolongs the survival of infused VWF.(117) Dose-dependent binding of human VWF to primary human macrophages and differentiated THP1 macrophages has also been confirmed *in vitro*.(121,194) A number of specific macrophage surface receptors have been implicated in regulating VWF binding and endocytosis. These include low-density lipoprotein receptor-related protein-1 (LRP1), scavenger receptor A1 (SR-A1) and the macrophage galactose lectin (MGL) receptor. (119,121,123)

The hypothesis that these specific macrophage receptors contribute to the physiological clearance of VWF is supported by a number of lines of evidence. First, *in vitro* binding studies using purified proteins has demonstrated that VWF binds to LRP1, SR-A1 and MGL.(118,119,122,123) Second, significantly increased plasma VWF:Ag levels have been observed in genetically engineered *MGL1*-deficient mice, as well as in macrophage-specific *LRP1* deficient mice. In addition, reduced VWF

propeptide to antigen ratios have been reported in *SR-A1*$^{-/-}$ mice, suggesting decreased VWF clearance *in vivo*.(121) Critically however, the molecular mechanisms through which these individual macrophage receptors interact with the complex multimeric glycoprotein, and their relative importance in regulating physiological and/or pathological VWF clearance have not been elucidated.

Although VWF clearance *in vivo* appears to be independent of multimer size, preliminary data suggest that specific VWF domains may be important in regulating macrophage-mediated clearance.(195) In particular, the A domains of VWF appear to be of particular importance in this context.(121,123) In the normal circulation, VWF released from the endothelium circulates in a globular conformation. Under conditions of shear stress, for example at sites of vascular injury, these VWF multimers unwind. As a result, conformational changes in the A1 domain occur that enable VWF binding to the platelet GPIbα receptor.(66,67,69) Previous studies have reached conflicting conclusions regarding the role of shear in regulating VWF interaction with macrophages. Initial studies demonstrated that VWF binding to macrophages was significantly increased in the presence of ristocetin, thereby suggesting that A domain conformational changes might influence macrophage interaction in a manner analagous to that of the VWF-platelet interaction.(117–119,121,196) Furthermore, VWF binding to the purified LRP1 receptor was also significantly increased in the presence of ristocetin.(122) In keeping with the hypothesis that VWF shear-dependent conformational changes might be an important regulator of macrophage interaction, a specific Type 2B VWD mutation

(V1316M) in the A1 domain has been shown to cause enhanced spontaneous binding to both platelets and LRP1.(122,197–199) In contrast however, more recent studies have reported that VWF can also interact with macrophages under static conditions.(117,122) In particular, *in vitro* studies suggest that VWF can interact with the SR-A1 receptor without the need for any shear-induced conformational changes.(122)

The significant differences reported in previous studies regarding the molecular mechanisms that regulate VWF binding and endocytosis by macrophages are likely attributable in part to differences in experimental methodologies. Nevertheless, understanding the mechanisms through which VWF binds to macrophages is critical in order to elucidate the physiological and pathological impotence of this interaction. Consequently, we first systematically investigated the VWF-macrophage interaction using a variety of different macrophage cell types and VWF preparations. In addition, the role of specific VWF domains and glycan determinants in modulating macrophage interaction were investigated.

3.1: Differentiation of THP1 macrophages

In initial experiments, conditions for differentiation of THP1 monocytes using PMA (100nM) exposure for either 24 hours or 72 hours were assessed. Following PMA treatment, the expression of macrophage-specific surface markers was assessed. Integrin alpha M is a macrophage marker composed of an α chain (CD11b) and a β_2 chain (CD18) that combine to form a hetero-dimeric integrin. Following PMA treatment for 24 hours, both *ITGAM* and *CD18* gene expression were significantly increased (Figure 3.1 A). Surface CD11b expression following PMA treatment was also confirmed using flow cytometry (Figure 3.1 B). PMA stimulation for 72h resulted in positive CD11b staining in THP1 macrophages. Based upon these experiments, and previous studies demonstrating that 72 hours PMA also up-regulates indicators of macrophage maturation (including lysosomal and mitochondrial formation and additional surface markers),(200) THP1 cells were treated with PMA for 72h hours in all subsequent experiments.

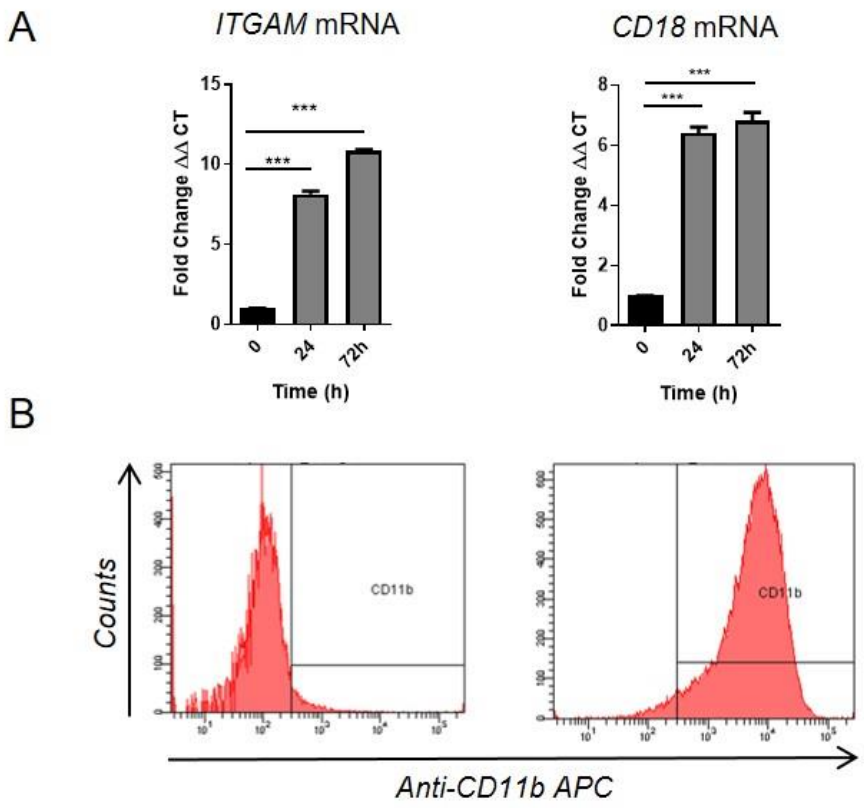

Figure 3.1: Differentiation of THP1 macrophages

A: THP1 macrophage markers CD11b and CD18 expression was determined RT-qPCR following PMA (100nM) treatment for either 24 or 72 hours respectively. The data presented are the means of three independent experiments ±SEM. Significance was determined by t-test (***p<0.001). **B:** Surface CD11b expression was determined by flow cytometry using an anti-CD11b APC tagged fluorophore following 72 hours PMA treatment.

3.2: VWF binds to human THP1 and murine RAW 264.7 macrophages

Following PMA differentiation, THP1 macrophages were incubated with human plasma derived (pd-VWF) for 30min on ice. Binding experiments were performed in the presence of ristocetin (1.5mg/ml) and detected using a polyclonal anti-VWF antibody. Dose-dependent binding of pd-VWF to THP1 macrophages was observed using flow cytometry (Figure 3.2 A). Furthermore, binding of pd-VWF was confirmed using confocal microscopy (Figure 3.2 B).

Further studies confirmed that pd-VWF also bound in a dose-dependent manner to the murine macrophage RAW 264.7 cell line (Figure 3.2 C). In this experiment, pd-VWF at the indicated concentrations was immobilised onto a microtiter plate and RAW 264.7 cells were then allowed to bind for 30min at room temperature. Macrophage binding to VWF under these conditions was observed in the absence of ristocetin.

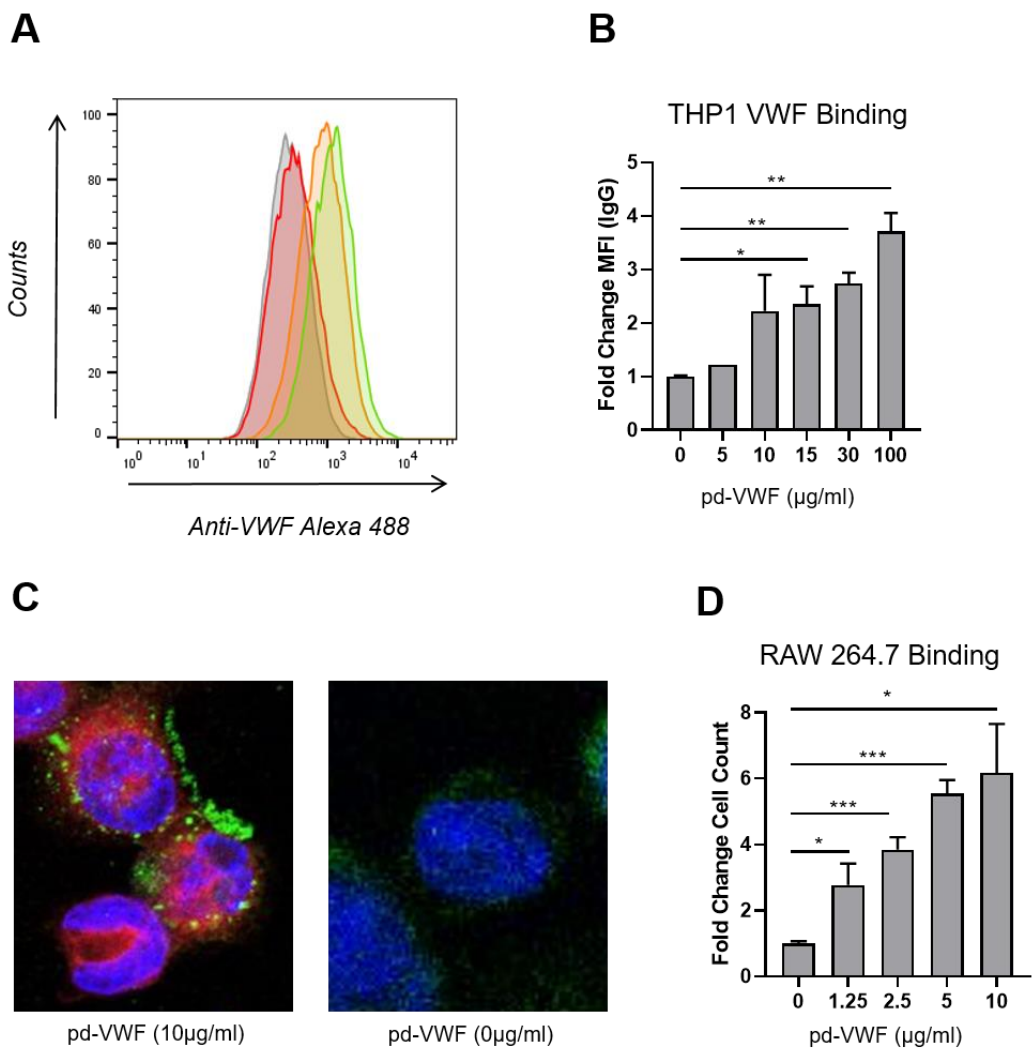

Figure 3.2: Binding of VWF to THP1 and RAW 264.7 macrophages

A: Representative histogram of pd-VWF (5µg/ml red, 15µg/ml orange and 100µg/ml green) THP1 binding following a 30min incubation at room temperature determined by flow cytometry using anti-VWF Alexa 488 antibody. **B:** Bound pd-VWF represented by fold change in mean florescence intensity (MFI) from non-VWF treated cells ±SEM. **C:** A representative image of pd-VWF (green) bound to the surface of THP1 macrophages (cell membrane red and nucleus blue) Control cells do not contain membrane stain. **D:** RAW264.7 binding was determined under static conditions, in which VWF was immobilised and bound cells were determined by high throughput imaging. Data represented by fold change cell counts from 0µg/ml VWF treated wells. Significance was determined by t-test (*p<0.05, **p<0.01).

3.3: THP1 macrophages internalise VWF

Previous studies have reported that following binding to macrophages, VWF is rapidly endocytosed and degraded. Consequently, we further investigated a time course of VWF interaction with macrophages at 37^{o}C. In keeping with previous reports, we observed that in the presence of ristocetin, pd-VWF was internalised by THP1 macrophages (Figure 3.3). Using confocal microscopy, no VWF positive staining was observed after 5 minutes incubation. In contrast, significant VWF binding to the macrophage surface was seen following 10 minutes incubation and initialization following 15 minutes. Finally, after 30 minutes, surface VWF staining was reduced (Figure 3.3 A) however, VWF was observed in early endosomes (Figure 3.3 B).

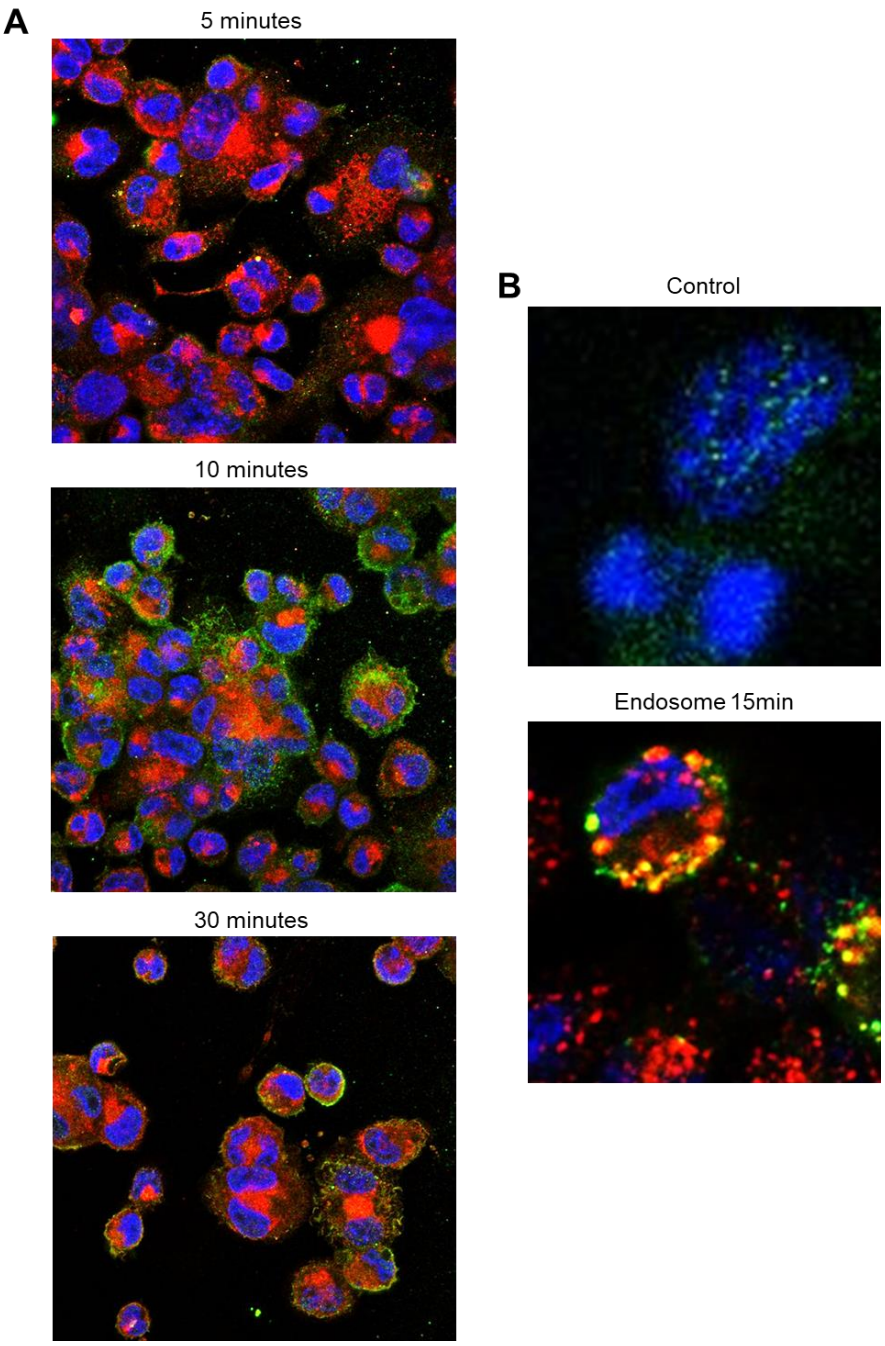

Figure 3.3: Macrophage initialisation of VWF

A: THP1 macrophages incubated with pd-VWF (300nM) for indicated times. VWF (green), lysosome associated membrane protein (LAMP) (red) and nucleus (blue). **B**: VWF (green) internalisation determined by co-localization (yellow) at with early endosome activation marker 1 (EEA1) (red). Control condition represented by VWF incubated with THP1 cells and primary antibodies with no addition of secondary fluorophores.

3.4: Recombinant VWF binds THP1 macrophages in the absence of ristocetin

To further investigate VWF interaction with macrophages, the binding of purified full-length recombinant VWF (r-VWF) produced in HEK293t cells was used. r-VWF binding to THP1 macrophages was determined in the presence or absence of ristocetin (1.5mg/ml) and detected by an anti-pentaHis antibody. (Figure 3.4 A and Figure 3.4 B). In contrast to pd-VWF, binding of r-VWF to differentiated THP1 macrophages was observed even in the absence of ristocetin. However, r-VWF binding to THP1 macrophages was also significantly enhanced in the presence of ristocetin ($p<0.05$) (Figure 3.4 A and 3.4 C).

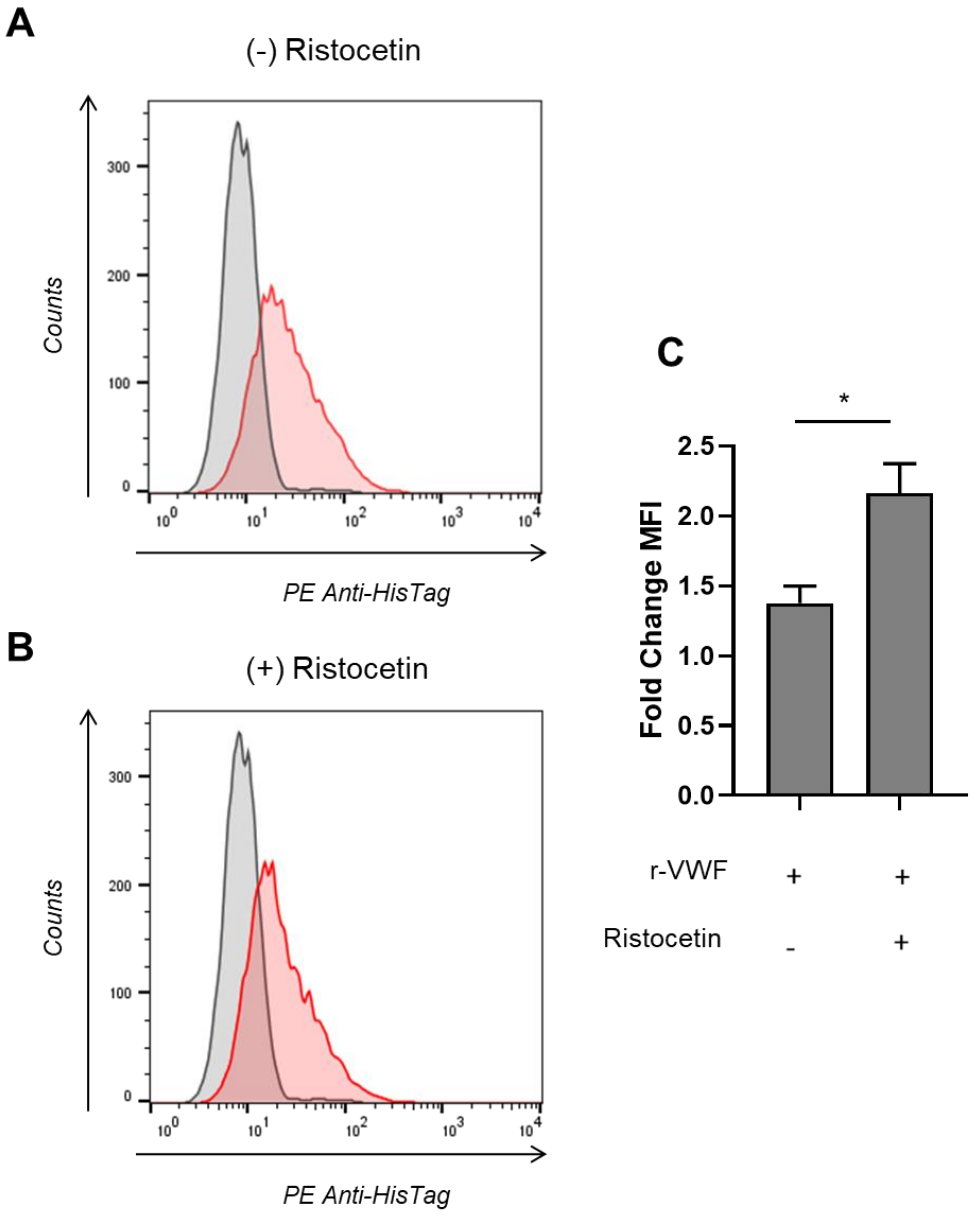

Figure 3.4: Recombinant VWF binds to macrophages without the presence of ristocetin

A and B: Representative histograms of r-VWF (300nM) binding to THP1 macrophages under static conditions in the presence or absence of ristocetin. THP1 macrophages population treated with r-VWF – red; non-treated – grey. **C:** Fold change mean florescent intensity (MFI) of THP1 bound r-VWF with and without ristocetin ±SEM. Results were calculated from three independent experiments (*p<0.05).

3.5: pd-VWF binds to primary human macrophages in the absence of ristocetin

Primary human monocytes were isolated from peripheral blood collected from healthy volunteers and differentiated into primary human monocyte-derived macrophages as previously described using 10% human serum.(201) The binding of human pd-VWF to primary human macrophages was then investigated under static conditions using both flow cytometry and confocal microscopy (Figure 3.5). Following incubation with VWF for 30 minutes at room temperature, significant binding was observed (Figures 3.5A and 3.5B).

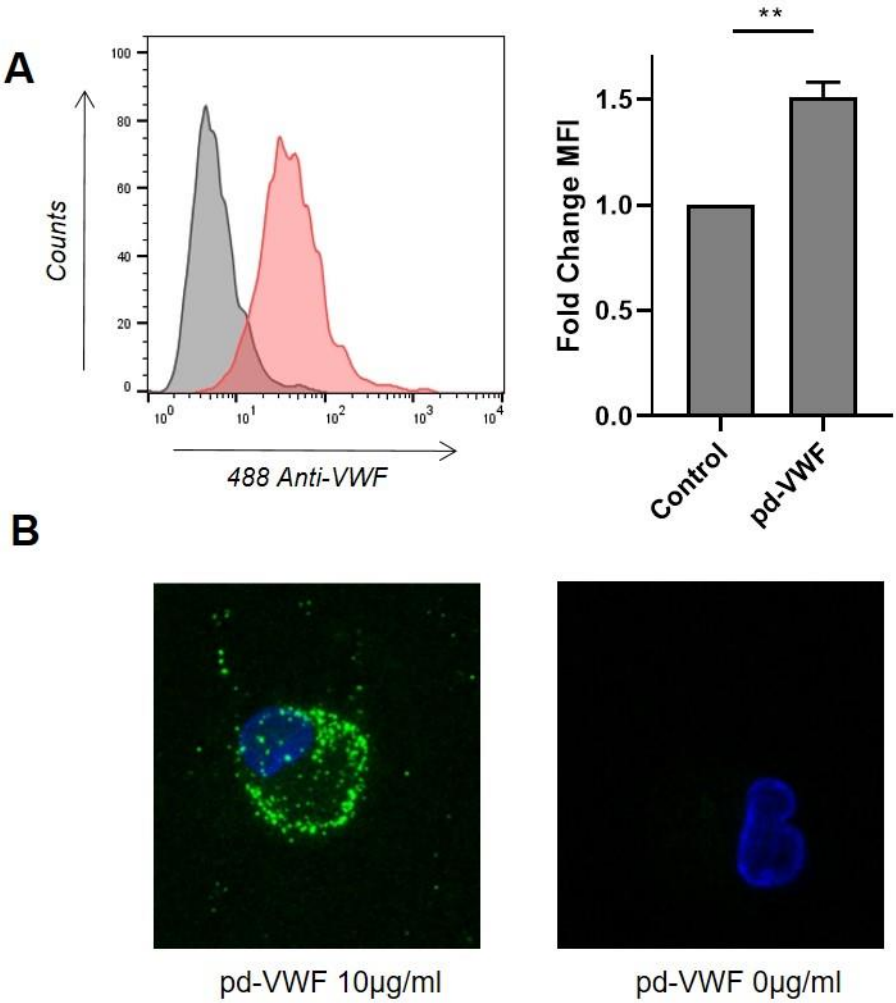

Figure 3.5: pd-VWF binds to primary human macrophages in the absence of ristocetin

A: Flow cytometry detection of pd-VWF (300nMl) bound to the surface of human primary macrophages following a 30min incubation. VWF was detected by a polyclonal anti-VWF labelled with Alexa-488 and quantified by fold change in MFI ±SEM from stained non VWF treated cells. Significance determined by t-test ($p<0.001$). Histograms are representative images of non-VWF treated macrophage red population, and VWF treated population blue. **B:** Using confocal microscopy, we detected VWF (green) bound to the surface of human primary macrophages (nucleus blue) after a 30min incubation. No positive staining for VWF could be detected in control conditions.

3.6: pd-VWF does not bind to primary monocytes

Since VWF binding to THP1 macrophages and primary human macrophages had been observed, further studies were performed to investigate whether VWF could also interact with (i) undifferentiated THP1 cells and/or (ii) primary human monocytes. Using the same flow cytometry experimental technique as before, no binding of either pd-VWF or r-VWF to either undifferentiated THP1 cells or primary human monocytes was observed even in the presence of ristocetin (Figure 3.6).

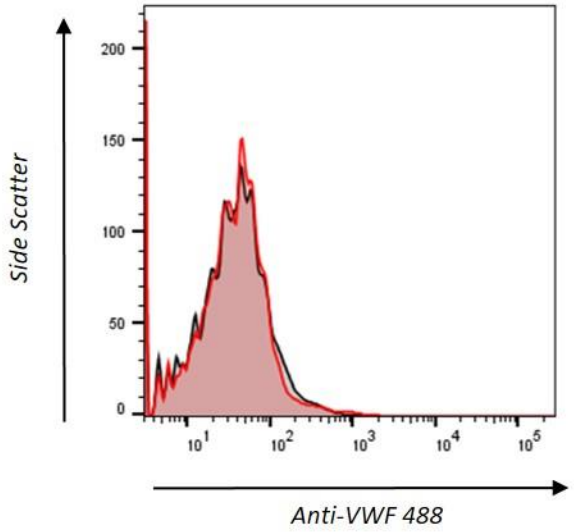

Figure 3.6: VWF does not bind to primary monocytes

Human primary monocytes displayed no binding ability to pd-VWF (300nMl). Binding to primary monocytes was detected by flow cytometry using an anti-VWF labelled Alexa 488 staining. Representative histograms: grey (polyclonal and VWF, secondary alexa 488, 300nM VWF) red (polyclonal anti VWF, secondary alexa 488 300nM VWF).

3.7: Multiple VWF domains contribute to macrophage binding

To investigate the importance of specific VWF domains in modulating macrophage binding, two r-VWF truncations (D'-A3 and A3-CK respectively) spanning the VWF monomer were expressed and purified (Figure 3.7 A). Binding of both fragments to THP1 macrophages was investigated as before using PE anti–pentahis tag. Macrophage binding was observed for both the D'-A3 (Figure 3.7B) and the A3-CK (Figure 3.7 C) truncations. In keeping with full length VWF, the binding of D'A3 fragment was significantly enhanced in the presence of ristocetin (1.5mg/ml). Together, these findings suggest that multiple regions within the VWF monomer may contribute to macrophage binding. Furthermore, the importance of ristocetin suggests that the A1A2A3 domains play a critical role in regulating VWF binding to macrophages.

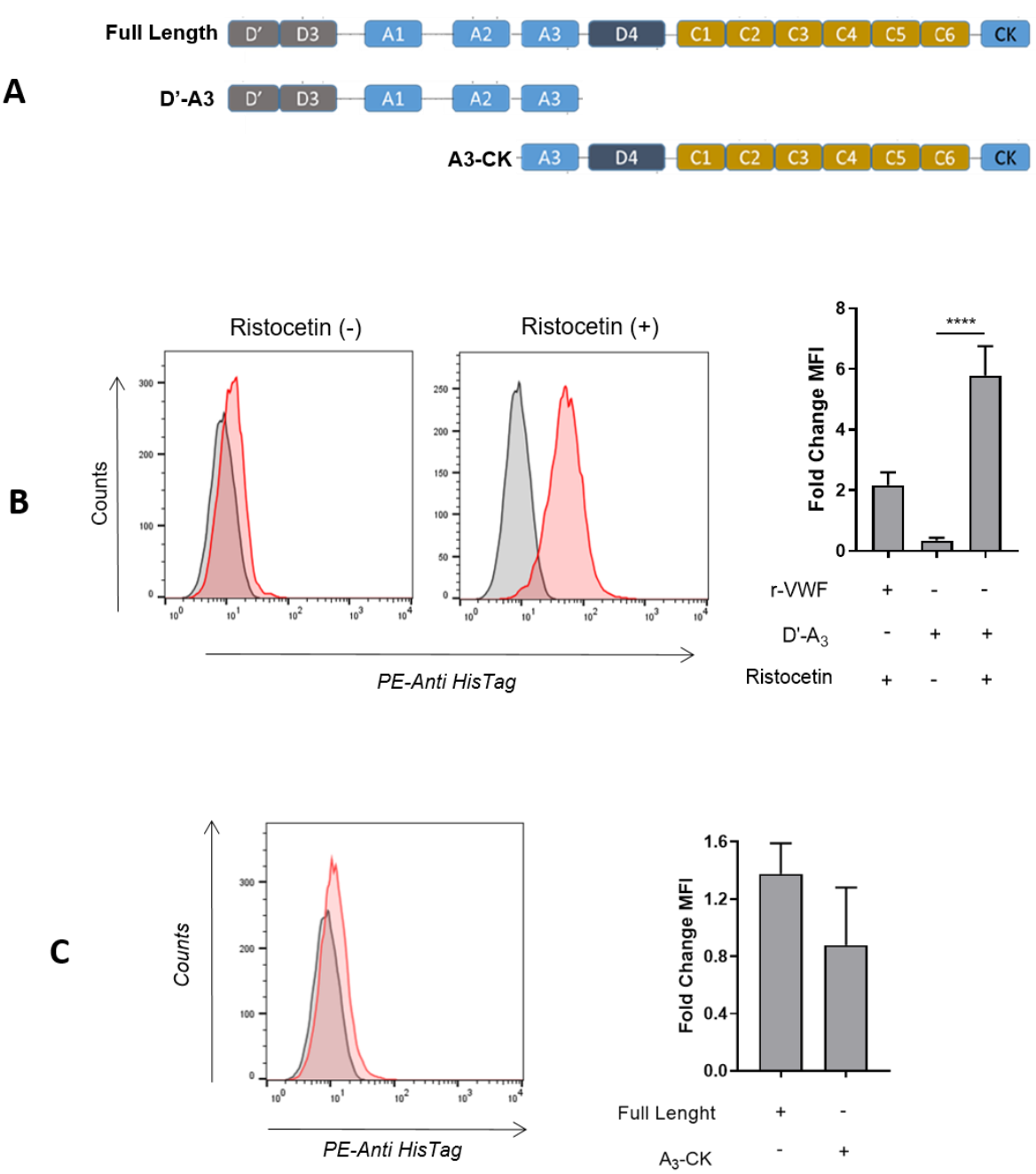

Figure 3.7: Multiple VWF domains contribute to macrophage binding

A: Schematic representation of a full length VWF monomer and the truncated fragments D'-A3 and A3-CK respectively. **B and C:** Representative histograms of non-treated macrophage population grey, and fragment treated population red following anti-histag staining. Quantification determined by fold change in MFI ±SEM. **B:** D'-A3 binds to THP1 macrophages and this binding is increased in the presence of ristocetin **C:** A3-CK (300 nM) domain binds to THP1 macrophages. Significance was determined by t-test(***p<0.001).

3.8: The A1A2A3 domains of VWF bind to THP1 macrophages

Previous studies have suggested that the A1A2A3 domains of VWF regulate its clearance by macrophages.(66,118) To investigate whether A1A2A3 could bind directly to macrophages, recombinant A1A2A3 was expressed and purified from HEK293t cells as previously described. Similar to full length VWF and the D'-A3 fragment, minimal binding of A1A2A3 to THP1 macrophages was observed in the absence of ristocetin (Figure 3.8 B). However, in the presence of ristocetin (1.5mg/ml) A1A2A3 binding was significantly enhanced. Binding of A1A2A3 to THP1 macrophages was further confirmed using confocal microscopy with ristocetin (Figure 3.8 C).

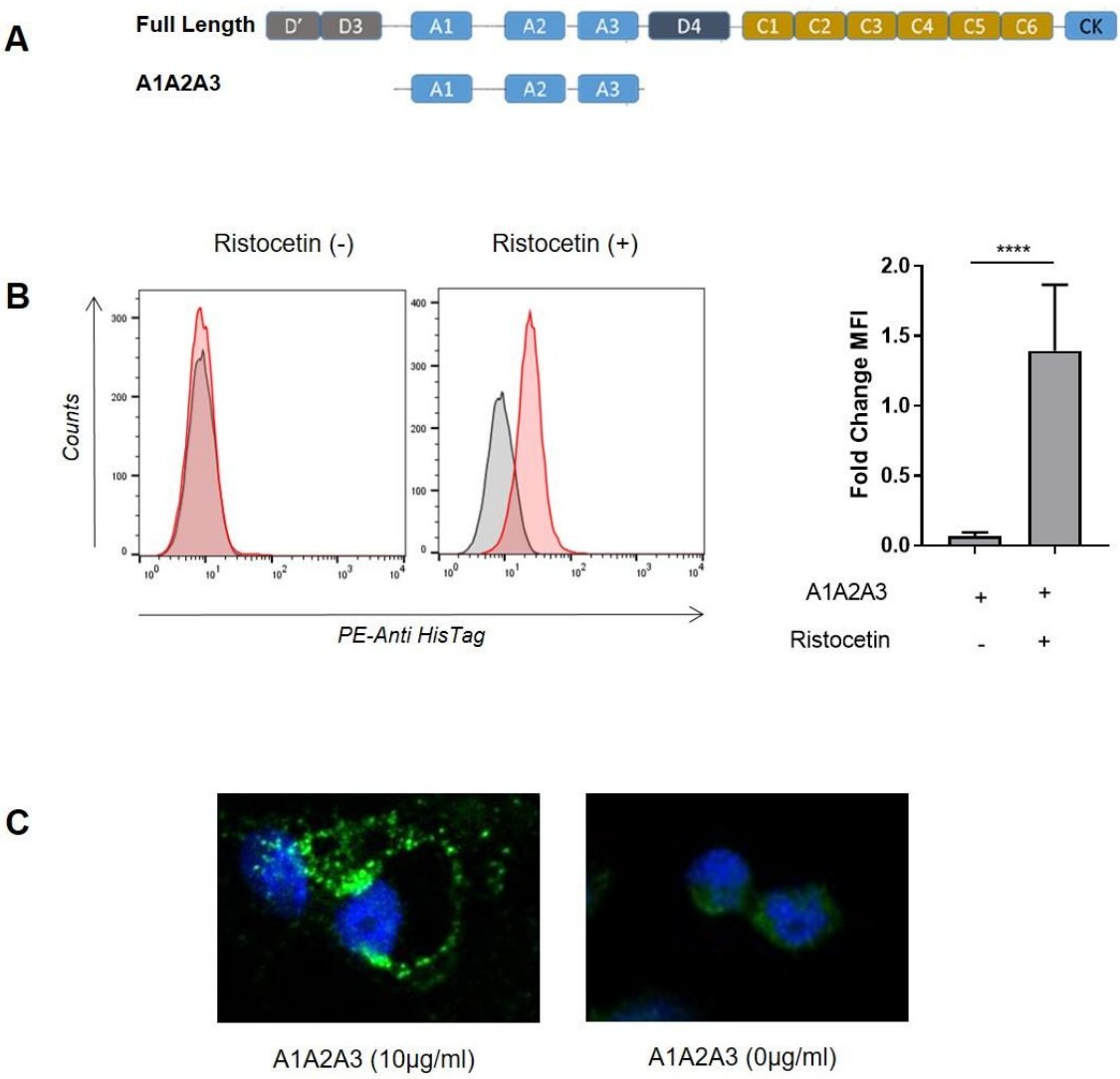

Figure 3.8: A1A2A3 domain of VWF binds to THP1 macrophages

A: Schematic representation of A1A2A3 fragment. **B:** Representative histograms of non-treated macrophage population grey and fragment treated population red following anti-histag staining. Quantification determined by fold change in MFI ± SEM. A1A2A3 (300nM) only binds to THP1 macrophages in the presence of ristocetin. The significance was determined by t-test (****p<0.001). **C:** Confocal imaging of A1A2A3 (green) THP1 macrophage binding (nucleus blue).

3.9: The A1 domain of VWF is essential for THP1 macrophage binding

To elucidate the biological mechanisms through which the A domains of VWF influence macrophage-mediated clearance, individual A1, A2 and A3 domains were expressed and purified (Figure 3.9). Binding to THP1 macrophages was then assessed for each domain as before. Importantly, the A1 domain displayed significant macrophage binding that was increased in the presence of ristocetin. In contrast, minimal binding was observed for either the A2 or A3 domains.

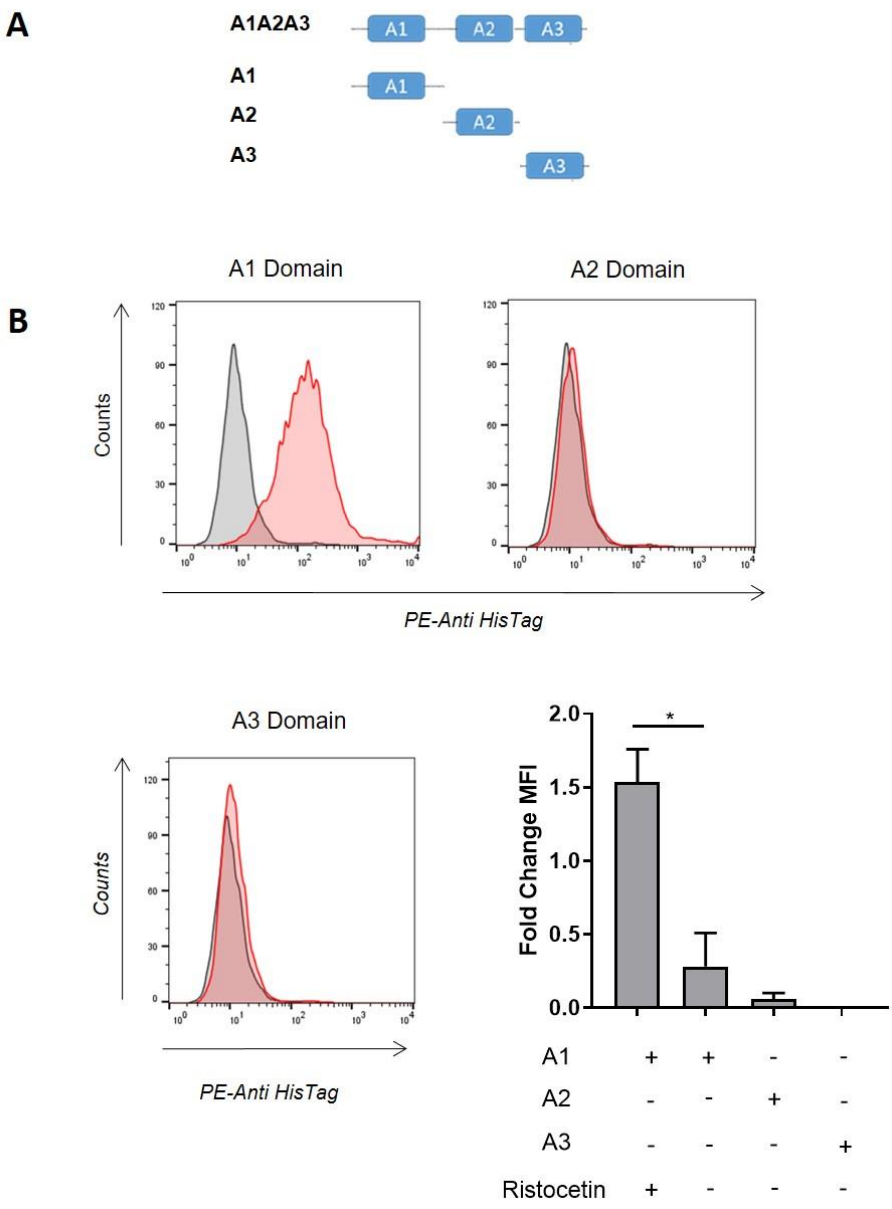

Figure 3.9: The A1 domain mediates A1A2A3 binding to THP1 macrophage

A: Schematic representation of A domain fragments. **B:** Representative histograms of non-treated macrophage population grey and fragment treated population red following anti-histag staining. A1 (300nM) domain binding was significantly enhanced following treatment with ristocetin. Minimal macrophage binding for both the A2 (300nM) and A3 (300nM) was detected as seen in bar chat. Binding was quantified by fold change MFI ± SEM from PE-anti HisTag 0nM VWF of 3 independent experiments.

3.10: The VWF A1A2A3 truncation binds to activated primary human monocytes in a dose-dependent manner

Pendu *et al*, previously reported that that monocytes activated with short term exposure to PMA (100nM) and $MnCl_2$ (1mM) for 30 minutes can bind to immobilised VWF.(113) Using this assay we further investigated the ability of activated monocytes to bind to both full length r-VWF and to the truncated VWF A1A2A3 fragment. Significant dose-dependent binding of activated human primary monocytes to both r-VWF and the A1A2A3 fragment was observed under these static experimental conditions (Figure 3.10).

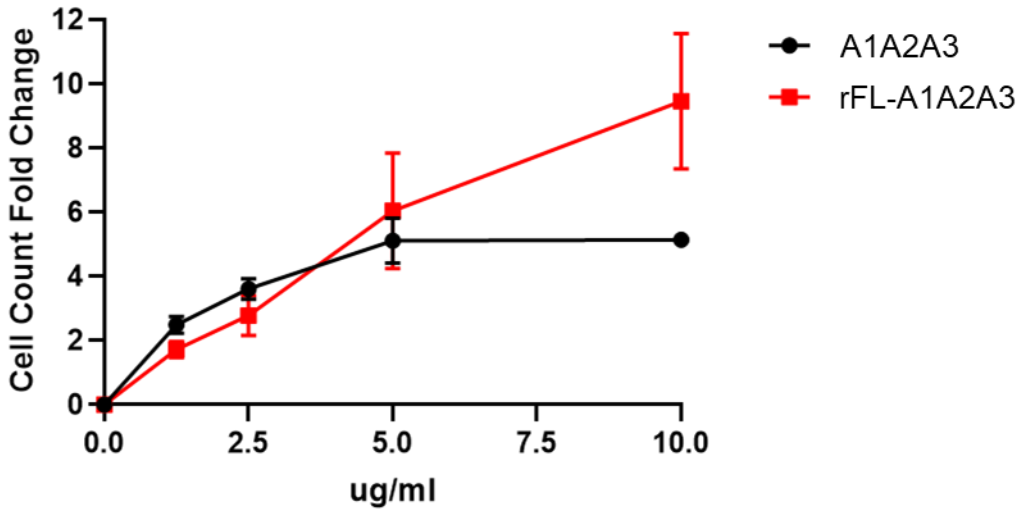

Figure 3.10: The VWF A1A2A3 truncation binds to primary human activated monocytes in a dose-dependent manner

Activated monocytes dose dependently bound to immobilised rFL-VWF (Red) and A1A2A3 (Black). VWF was coated onto a polysorp plate at the indicated concentrations. Activated primary human monocytes were incubated for 30 minutes with VWF coated plates and non-adhered cells were removed. Bound cells were determined by high throughput imaging of stained cells and quantified by fold change in cell counts from non-VWF treated wells ± SEM.

3.11: VWF glycan structures regulate its binding to primary human activated monocytes

Previous studies have demonstrated that desialylation of pd-VWF (Neu-VWF) results in significantly enhanced macrophage-mediated clearance.(119,202) Additionally, truncation of VWF N-linked glycans (PNGaseVWF) also caused a significantly reduced half-life.(202) To investigate the effects of VWF glycan determinants in regulating macrophage binding, VWF was purified from human plasma (pd-VWF). VWF was then digested enzymatically with a number of different exoglycosidase generating different VWF glycan structures. Finally lectin ELISA studies were completed to ensure glycan modification.(203) Removal of terminal N- and O- linked sialic acid and galactose significantly enhanced VWF binding to primary human macrophages (Figure 3.11 A, B and C). Additionally N-linked glycan truncation also resulted in increased VWF binding to macrophages (Figure 3.11 D).

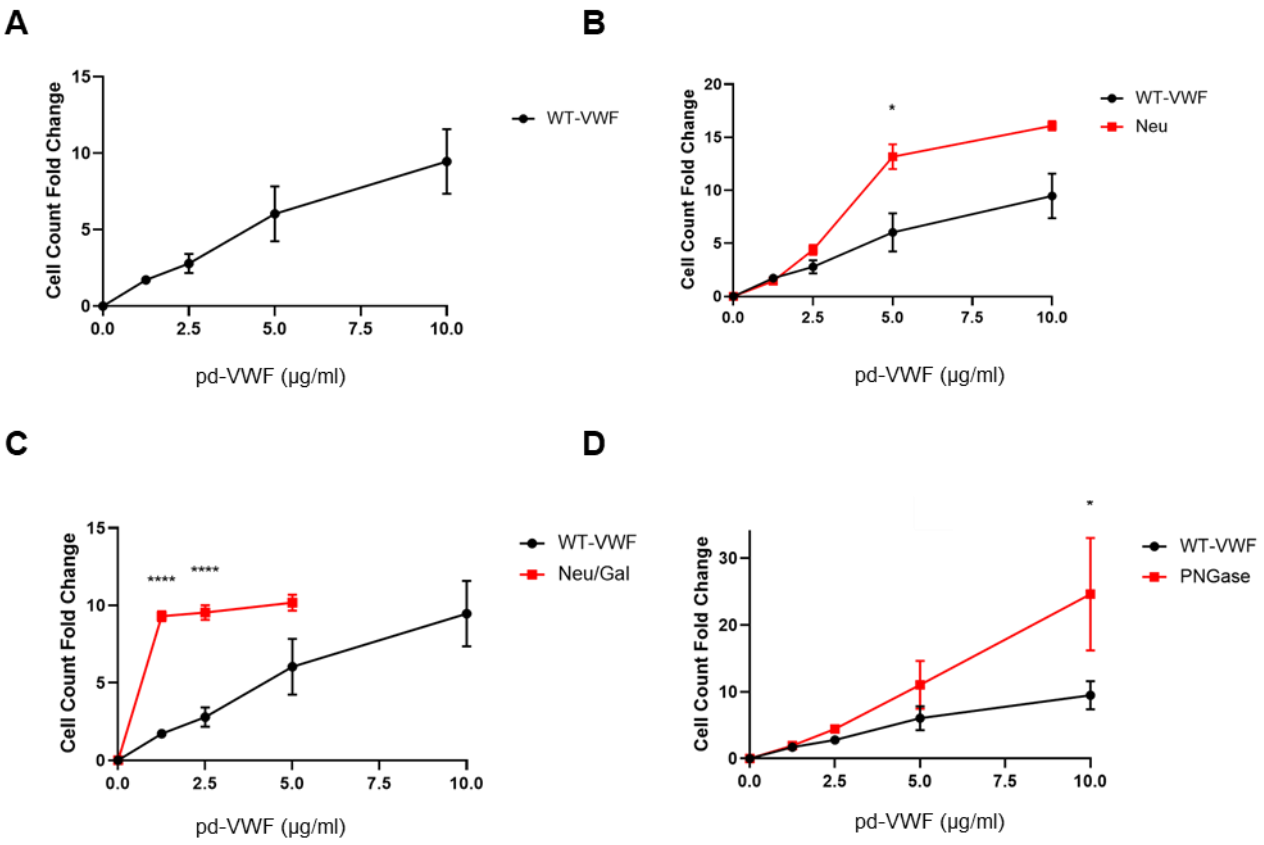

Figure 3.11: Activated primary monocytes dose dependently bind to VWF

A: PMA (100nM) activated primary monocytes dose dependently bind to immobilised pd-VWF. Activated monocyte binding is significantly enhanced following **B:** VWF desialylation (Neu-VWF), **C:** sialic acid and galactose removal (Neu/Gal) and **D:** N-Linked glycan truncation (PNGase). Activated monocyte binding was determined under static conditions, in which VWF at the indicated concentrations was immobilised onto a microtiter plate. Binding was determined by cell count fold increase from non-VWF treated wells ±SEM. Significance determined by t-test (*p<0.05,****p<0.001)

3.12: Discussion

Recent studies have defined an important role for macrophages in VWF clearance and identified several macrophage receptors that are involved in mediating VWF binding. However, different groups have reached contrasting conclusions regarding how VWF binding to macrophages is regulated. In particular, previous studies have differed with respect to the role of shear stress in regulating the VWF-macrophage interaction. To address this question, we began by using macrophages derived from the THP1 cell line stimulated with PMA for 72 hours. We found that the resultant THP1 macrophages were able to bind human pd-VWF. Critically however, reduced binding was observed in the absence of ristocetin. Conversely, in the presence of ristocetin, dose-dependent binding of pd-VWF was easily observed using both flow cytometry and confocal microscopy. If the VWF incubation with THP1 macrophages was performed at 37°C rather than on ice, we also observed that pd-VWF binding followed by endocytosis. Consequently by 30 minutes, pd-VWF was co-localised with the early endosomal marker EEA1.

Significant dose-dependent binding of human pd-VWF to murine RAW 264.7 cell line macrophages was also observed. This point is important given that many previous studies have investigated human pd-VWF clearance using *VWF*$^{-/-}$ mice, and suggests that at least some of the macrophage receptors involved in regulating VWF clearance are shared between human and murine macrophages. Besides macrophages, liver sinusoidal endothelial cells (LSECs) have also been implicated in contributing to VWF clearance.(204,205) Interestingly however, some of the

LSEC clearance receptors postulated to be important in the clearance of human VWF are not expressed on murine LSECs (e.g. CLEC4M).(206)

To further investigate the mechanisms involved in VWF interaction with macrophages, we proceeded to study pd-VWF and r-VWF interaction with primary human and murine macrophages. Interestingly, we observed that both pd-VWF and r-VWF were able to bind to primary human macrophages even in the absence of ristocetin. This finding suggests that surface receptor expression may differ between primary human monocytes compared to THP1 macrophages. Nonetheless, in the presence of ristocetin, pd-VWF binding to primary human monocytes was again markedly enhanced. In striking contrast, no VWF binding to undifferentiated primary human monocytes was seen. Collectively, these data therefore suggest that VWF binding is regulated by surface receptors that are upregulated following monocyte differentiation into macrophages. Consequently, we propose that in the normal circulation, pd-VWF and monocytes circulate together with minimal interaction. However, following tissue damage and blood vessel injury, VWF escapes from the plasma into subendothelium where it comes into contact with tissue macrophages. Macrophages express a different repertoire of surface receptors compared to undifferentiated monocytes, which may enable effective binding to VWF.(207) When VWF is released basolateral into the subendothelial it is possible that within this static environment VWF can interact with recruitment macrophages following vascular injury.

To investigate whether individual VWF domains may be important in modulating macrophage binding, we first expressed and purified two distinct VWF fragments (D'-A3 and A3-CK) that span the VWF monomer. Macrophage binding was observed for both these VWF truncations, suggesting that multiple discrete regions of the glycoprotein may contain binding sites for macrophage receptors. The ability of ristocetin to significantly enhance VWF binding to macrophages suggests that the A domains of VWF may be of particular importance in this context.(85–87) This hypothesis is consistent with previous studies from our laboratory in which we have demonstrated that a monomeric A1A2A3-VWF fragment is cleared at a similar rate to full-length multimeric VWF.(118) In addition, we have also recently shown that the N-linked glycans expressed at N1515 and N1574 within the A2 domain play a role in protecting VWF against premature *in vivo* clearance via the macrophage LRP1 receptor.(118) In this Chapter, we confirmed that an isolated A1A2A3 VWF truncation was able to bind to bind to macrophages. Similar to full length VWF, A1A2A3 binding was markedly increased in the presence of ristocetin. Furthermore, we observed that whilst the isolated A1 domain was sufficient to enable macrophage binding, no such interaction was evident for either the A2 or A3 domains respectively. Taken together, these data suggest that a critical macrophage-binding site is located within the VWF A1 domain, and that this binding site is not fully accessible in the absence of shear or ristocetin in full length VWF. Our data are consistent with subsequent publications that have reported that the isolated A1 domain can bind to purified LRP1 and SR-A1 *in vitro*.(121,122) A putative role for the A1 domain in modulating macrophage-mediated clearance

is further supported by the observation that many *VWF* mutations associated with increased clearance in patients with VWD are clustered within the A1A2A3 region.(208,209)

In conclusion, on the basis of the novel data presented in this Chapter it seems highly likely that the previously reported conflicting results regarding the basis of the VWF-macrophage interaction are due in large part to differences in the experimental approaches. In particular, differences in macrophage cell origin (primary versus cell line; human versus murine), macrophage differentiation methodology and type of VWF can all significantly influence results. Nonetheless, our findings confirm that VWF can interact with primary human macrophages under static conditions. This observation is interesting given that significant amounts of VWF are actively secreted basolaterally from endothelial cells into the subcellular space.(60,210,211) The biological function of this VWF remains unknown.

4 The role of VWF in macrophage inflammatory response

4.0: Introduction

In addition to its haemostatic function, recent studies have identified additional novel biological roles for VWF, including inhibition of angiogenesis and promotion of tumour cell apoptosis. (212–215) Furthermore, data from studies conducted in a number of different animal inflammatory disease models suggest that VWF does not merely serve as a marker of acute endothelial cell (EC) activation, but rather that it plays an active role in mediating the underlying pathophysiology.(216,217) For example, in a caecal puncture sepsis model, overall survival was significantly increased in VWF-deficient mice compared to wild type controls.(144) In addition, Petri *et al,* showed that VWF-blocking antibodies significantly attenuated neutrophil recruitment into thioglycollate-inflamed peritoneum and keratinocyte-derived chemokine (KC)-stimulated exposed cremaster muscle.(125) In both of these murine models of inflammation, VWF-modulated neutrophil extravasation was critically dependent upon the presence of platelets. Similarly, VWF-blocking antibodies were shown to again significantly reduce neutrophil recruitment in murine models of immune-complex-mediated vasculitis and irritative contact dermatitis respectively.(127) Interestingly, Hillgruber *et al*, further demonstrated that VWF-modulated neutrophil recruitment in these murine models of cutaneous inflammatory was mediated through a platelet-independent pathway.(127)

An *in vivo* model of intracranial haemorrhage (ICH) has also suggested that VWF has important pro-inflammatory properties.(183) In this ICH model, VWF infusion resulted in exacerbated blood brain barrier permeability, increased pro inflammatory cytokine secretion (including IL-1β, CCL-1, IL-6) and enhanced neutrophil recruitment. In contrast, inhibition of VWF using a specific polyclonal antibody significantly reduced ICH-associated inflammation.(183) A role for VWF in regulating cardiovascular disease and atherosclerosis has also been described. Importantly, EC activation and dysfunction resulting from dyslipidemia have been identified during the initial stages of atherosclerotic plaque development.(218,219) The high molecular weight VWF released from the activated EC then has the potential to enable platelet and/or leukocyte sequestration. Interestingly, Methia *et al,* reported that fatty streak lesions in the aorta were 40% smaller in *LDLR*$^{-/-}$*VWF*$^{-/-}$ mice compared to *LDLR*$^{-/-}$*VWF*$^{+/+}$ mice on an atherogenic diet.(163) Moreover, a significant reduction in the number of macrophages recruited into the atheromatous lesions was also observed in the VWF-deficient mice, suggesting that the protective effect of VWF deficiency on atheroma development may be macrophage-mediated.(163,168) Furthermore, again in experiments performed using murine atherosclerotic models, Gandhi *et al,* reported that *ADAMTS13*$^{-/-}$ mice demonstrated significantly increased atheromatous plaque size and enhanced macrophage recruitment compared to wild type controls.(170) These murine data are particularly interesting given that human studies have demonstrated that patients with von Willebrand disease (VWD) are protected against risk of ischemic heart disease and stroke.(161,177)

All together, these findings demonstrate that VWF influences multiple different aspects of inflammation. Critically however, the biological mechanisms underpinning the pro-inflammatory effects of VWF remain poorly understood. *In vitro* studies have confirmed that immobilized VWF can bind directly to leukocytes. Under flow conditions, this VWF-leucocyte interaction was shown to consist of initial transient rolling (mediated via VWF binding to leukocyte PSGL-1) followed by stable adhesion (mediated by VWF interaction binding to leukocyte β2-integrins).(113) As shown in the previous Chapter, we and others have shown that both pd-VWF and recombinant VWF can bind to primary human macrophages, murine BMDMs and THP1 macrophages respectively.(121,123) Importantly, VWF binding to these macrophages was seen under both shear and static conditions, and was followed by VWF internalization. Given the importance of macrophages in regulating innate immune responses, we hypothesized that VWF binding might influence macrophage biology and thereby impact upon inflammatory responses.

The large range of extracellular and intracellular receptors expressed by macrophages is discussed in section 1.2, however these receptors facilitates the macrophages ability to be a key DAMP sensor. The innate immune system not only recognises self from non-self, but in addition, macrophages sense healthy from non-healthy. Endogenous danger signals results from a variety of tissue traumas, inducing oxygen deprivation, autoimmune destruction and cell death.(220) Endogamous DAMPs included heat shock proteins and the extra-cellular matrix

protein hyaluronan which both bind to TLRs.(220) Furthermore, oxidized low-density lipoproteins acts as another endogenous DAMP by facilitating inflammasome activation.(221) The inflammasome is a complex protein structure which requires two signal activation to allow the release of IL-1β and IL-18.(221) Signal 1 is elicited from interaction with either a PAMPs or DAMP and results in the expression of inactive pro-IL-1β and pro-IL-18.(221) These immature cytokines cannot leave the cytosol until they cleaved into their active forms (IL-1β and IL-18) by caspase 1 which has become assembled into the NLRP3 inflammasome.(221)

Furthermore, to facilitate these response macrophages undergoes complex signalling pathway activation to stimulate the multiple transcription factors. In addition to NF-κB signalling is the JNK and p38 MAPKinase pathways. MAPKinase pathways involve a series and cascade of serine/threonine kinases phosphorylations leading to transcription factor activation.(222) Such transcription factors include AP-1, Ets-1 and Elk/TCF which are involved expression of many pro-inflammatory cytokines. (222)

We now postulated that VWF released following vascular damage and acute endothelial cell activation might have the potential to function as a novel damage associated molecular pattern protein in driving a pro-inflammatory response.

4.1: Purity of commercial pd-VWF preparation

In order to investigate whether VWF binding may influence macrophage function, a highly purified commercial pd-VWF preparation was used (Haematologic Technologies, FVIII free). In preliminary experiments, the purity of this pd-VWF product was assessed using SDS-PAGE under reducing conditions (Figure 4.1 A). Besides VWF, no additional bands were observed. The purity of the pd-VWF product was further studied using RAW Blue macrophages. These cells express all pattern recognition receptors (PRR) including retinoic acid-inducible gene I (RIG-I), melanoma differentiation associated protein 5 (MDA-5), toll like receptors (TLRs) and Nucleotide-binding oligomerization domain-containing protein 1/2 (NOD1/NOD2). Activation of these PRRs results in secretion of embryonic alkaline phosphatase (SEAP) that can then be quantified by metabolism of QUANTI-Blue based on 630λ absorbance. Consequently, RAW Blue macrophages were treated with either VWF (10µg/ml) or LPS (100ng/ml) for 24 hours. Cell supernatants were harvested, and SEAP expression measured. No alkaline phosphatase activity was observed in the supernatants from VWF-treated cells (Figure 4.1 B). Finally, the pd-VWF preparation was assessed for endotoxin using a gel clot Limulus amebocyte lysate (LAL) reagent assay. In contrast to the LPS positive control, VWF (10µg/ml) failed to induce gel clot formation (Appendix iii). Collectively, these findings confirm that the commercial pd-VWF product does not contain detectable endotoxin contamination.

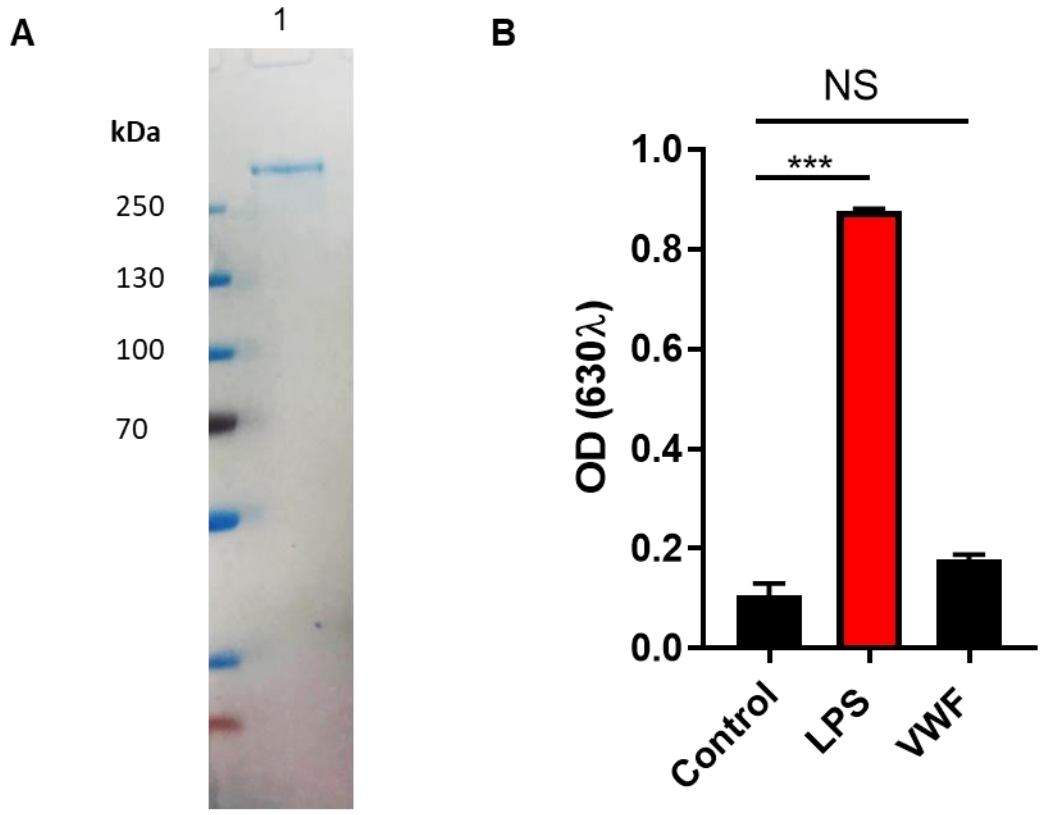

Figure 4.1: Characterisation of a high purity commercial pd-VWF

A: Commercial pd-VWF product (lane 1) was resolved using SDS-PAGE under reducing conditions and Coomassie staining. **B:** RAW Blue macrophage supernatants were harvested following treatment with VWF (10µg/ml) or LPS (100ng/ml) for 24h. Secreted alkaline phosphatase was quantified by metabolism of QUANTI-Blue based on 630λ absorbance. The significance was determined by t-test (NS, Non-Significant, ***p<0.001)

4.2: pd-VWF binding to macrophages triggers pro-inflammatory signalling

Primary human macrophages were incubated at 37^{o}C for 30 minutes with either (i) purified pd-VWF (10µg/ml) or r-VWF (Vonvendi,Takeda; 10µg/ml) or (ii) LPS (100ng/ml). Subsequently, Western blot analysis was performed to investigate effects upon specific macrophage signalling pathways of interest. In keeping with previous reports, macrophage treatment with LPS resulted in activation of pro-inflammatory intracellular signalling pathways (Figure 4.2). A: pd-VWF was associated with pro-inflammatory MAPkinase JNK and p38 activation. Additionally, the NF-κB pathway was also activated though phosphorylation of its regulatory subunit IKbα, marking it for ubiquitination.(223) B: r-VWF also induced MAPKinase p38 activation in primary human macrophages (Figure 4.2).

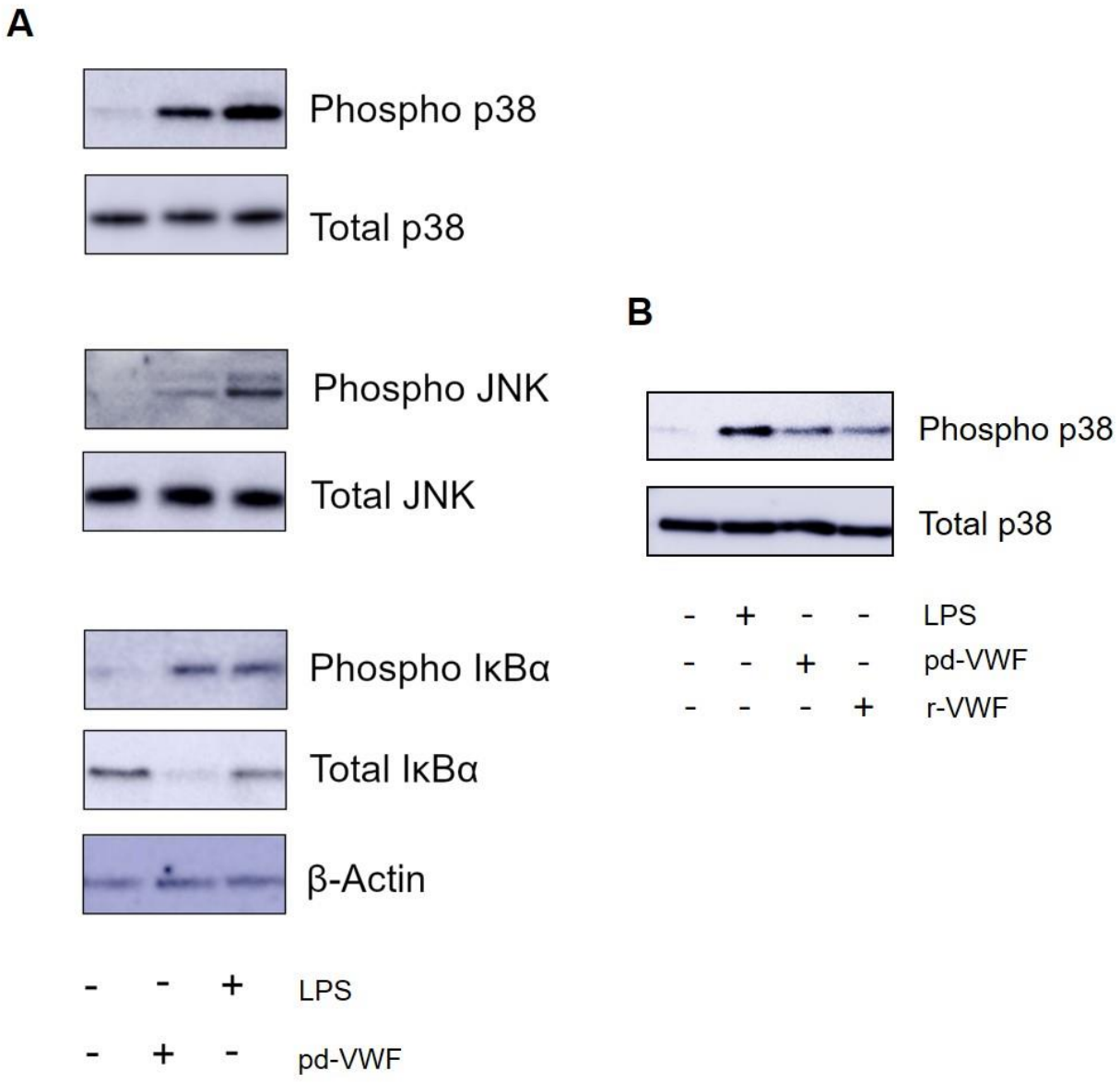

Figure 4.2: VWF triggers pro-inflammatory signalling in primary human macrophages

Western blot analysis of phosphorylated p38, JNK and IKKα in primary human macrophages following a 30 minute incubation with **A:** pd-VWF (10µg/ml) or LPS (100ng/ml) and **B:** r-VWF (10µg/ml) or LPS. Representative images from three independent experiments.

4.3: VWF binding to primary human macrophages induces pro-inflammatory cytokine expression

To further study the effects of VWF interaction on macrophage biology, primary human macrophages were incubated with either (i) purified pd-VWF (10µg/ml) or (ii) LPS (100ng/ml) for 4 hours at room temperature, and effects on pro-inflammatory cytokine mRNA expression were investigated. Consistent with the observed signalling effects observed, pd-VWF binding was associated with a significant increase in expression of pro-inflammatory cytokine *TNF-α* and *IL-6* mRNA respectively (Figure 4.3 A). In addition to increased mRNA levels, significantly increased amounts of both TNF-α and IL-6 were measured in the supernatants of macrophages exposed to either LPS or pd-VWF (Figure 4.3 B).

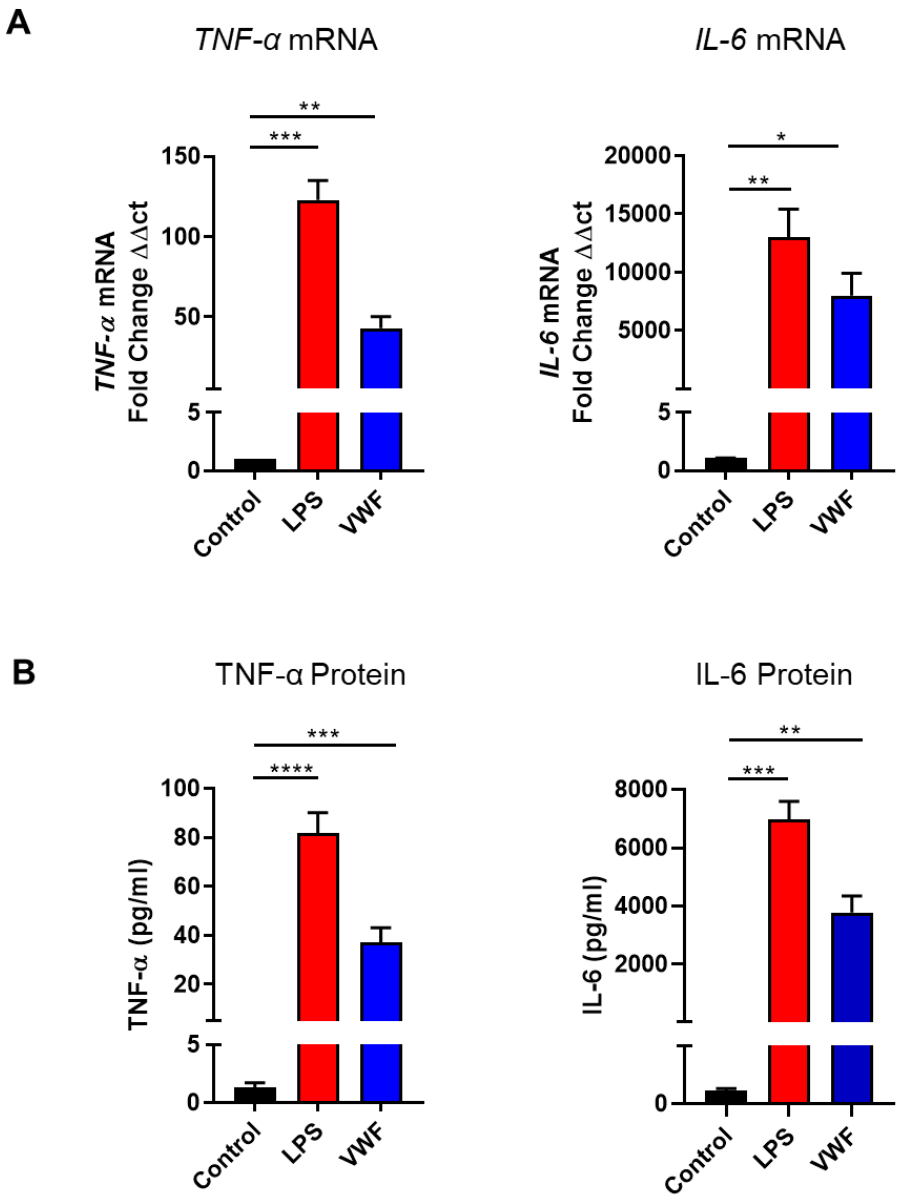

Figure 4.3: VWF binding to primary human macrophages induces expression of pro-inflammatory TNFα and IL-6 cytokines

A: TNF-α and IL-6 mRNA expression levels were assessed by quantitative RT-PCR in primary human macrophages following 4 hour treatments with cell culture media (control), pd-VWF (10µg/ml) or LPS (100ng/ml). **B:** Human macrophages were treated with pd-VWF (10µg/ml) or LPS (100ng/ml) for 24 hours, supernatants were harvested and TNF-α and IL-6 levels were measured by ELISA. The data presented represents the average of 3 independent experiments ± SEM. The significance was determined by t-test (*p<0.05, **p<0.01, ***p<0.001 and ****p<0.0001).

4.4: VWF binding to murine bone marrow derived macrophages has significant pro-inflammatory effects

On the basis of our data, it is clear that VWF binding to primary human macrophages triggers pro-inflammatory signalling and cytokine expression. To further investigate these observations, we proceeded to study the effects of VWF on murine bone marrow derived macrophages (BMDM). In keeping with the effects seen with human macrophages, VWF treatment of murine BMDM for 30 minutes was again associated with activation of pro-inflammatory signally pathways, with phosphorylation of MAPKinase p38 and JNK as well as NF-κB p65 (Figure 4.4). Furthermore, VWF stimulation of murine BMDM also induced the expression and production of pro-inflammatory cytokines TNF-α and IL-6 (Figure 4.5). Thus, the pro-inflammatory effects associated with VWF binding are consistent between both human and murine macrophages.

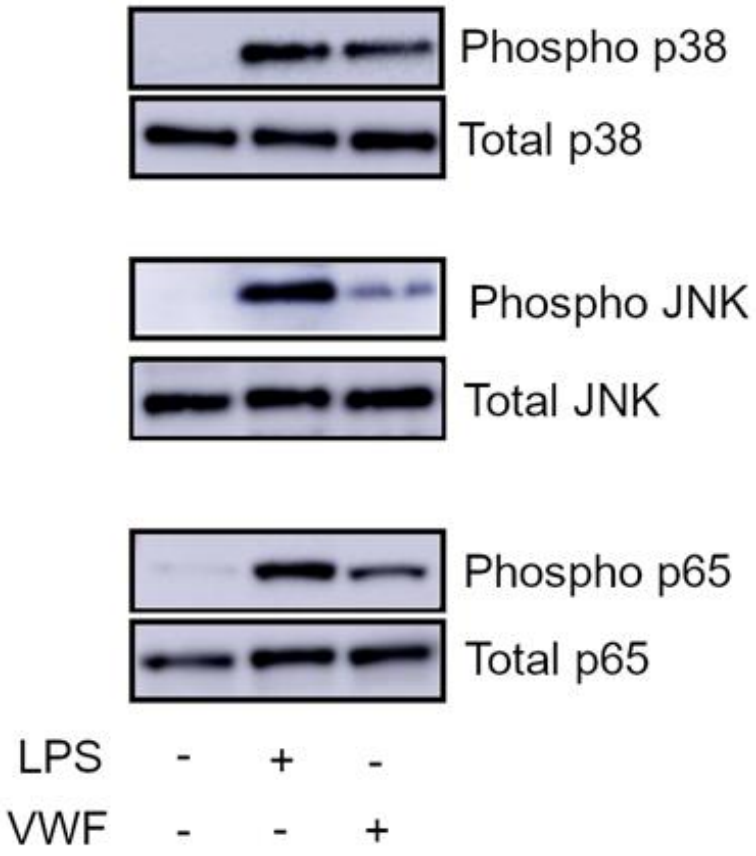

Figure 4.4: VWF triggers pro-inflammatory signalling in murine BMDM macrophages

Western blot analysis of phosphorylation of p38, JNK and p65 following incubation with pd-VWF (10 µg/ml) or LPS (100 ng/ml) for 30 minutes at 37°C. Representative images from three independent experiments.

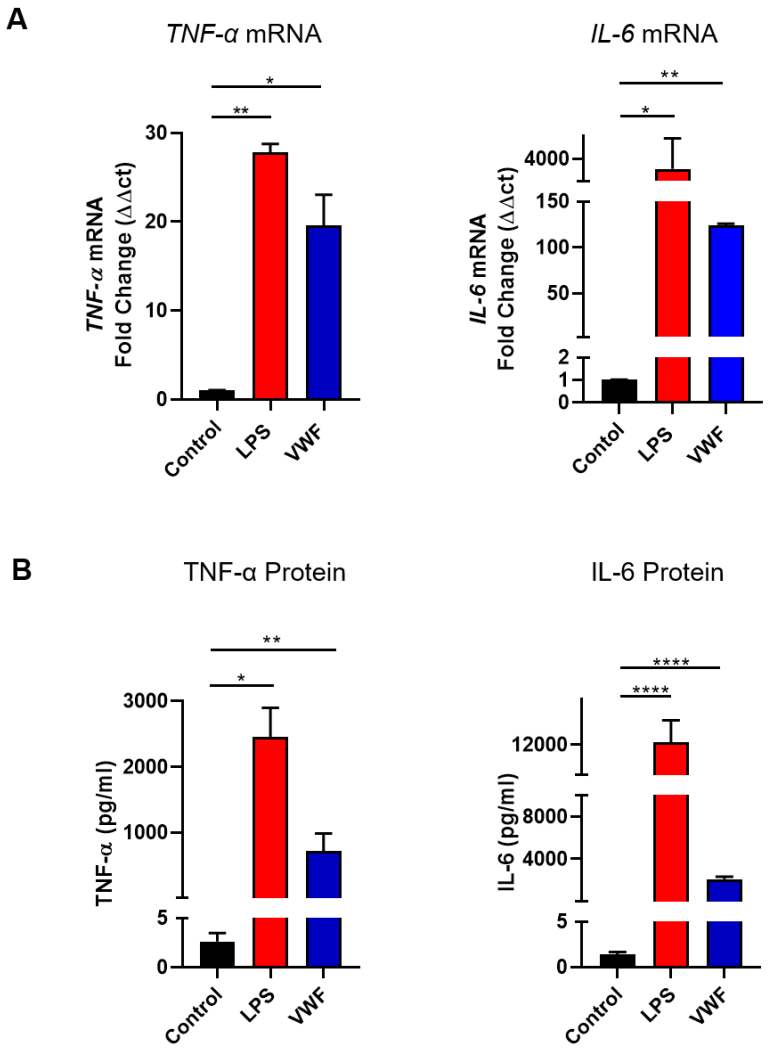

Figure 4.5: VWF binding to murine BMDM induces expression of pro-inflammatory TNFα and IL-6 cytokines

A: TNF-α and IL-6 mRNA expression levels were assessed by quantitative RT-qPCR in BMDM following 4 hour treatments with cell culture media (control), pd-VWF (10µg/ml) or LPS (100ng/ml). **B:** Murine BMDMs were treated with pd-VWF (10µg/ml) or LPS (100ng/ml) for 24 hours, supernatants were harvested and TNF-α and IL-6 levels were measured by ELISA. The data presented represents the average of 3 independent experiments ± SEM. The significance was determined by t-test (*p<0.05, **p<0.01, ***p<0.001, ****p<0.0001)

4.5: VWF treatment triggers inflammasome activation in murine BMDM

Previous studies have reported that IL-1β protein expression is associated with NLRP3 inflammasome activation in macrophages.(221) To investigate whether VWF exposure may trigger inflammasome activation, murine BMDM were treated with either pd-VWF (10µg/ml) or LPS (100ng/ml) for 4 hours. Treatment with either VWF or LPS resulted in significant *IL-1β* mRNA expression, in which the VWF dependent induction of IL-1β was similar to that of LPS (Figure 4.6 A). Similarly, both VWF and LPS exposure also resulted in increased pro-IL-1β levels (Figure 4.6 B). However, despite the increase in IL-1β gene transcription, only minimal levels of secreted IL-1β protein were seen in macrophages following treatments with VWF or the LPS positive control. Previous studies have highlighted that effective inflammasome activation requires dual signal triggering. Consistent with this hypothesis, additional stimulation with VWF and ATP (5µM) resulted in a marked increase in IL-1β secretion (Figure 4.6 C) and a concurrent decrease in pro-IL-1β levels (Figure 4.6 B).

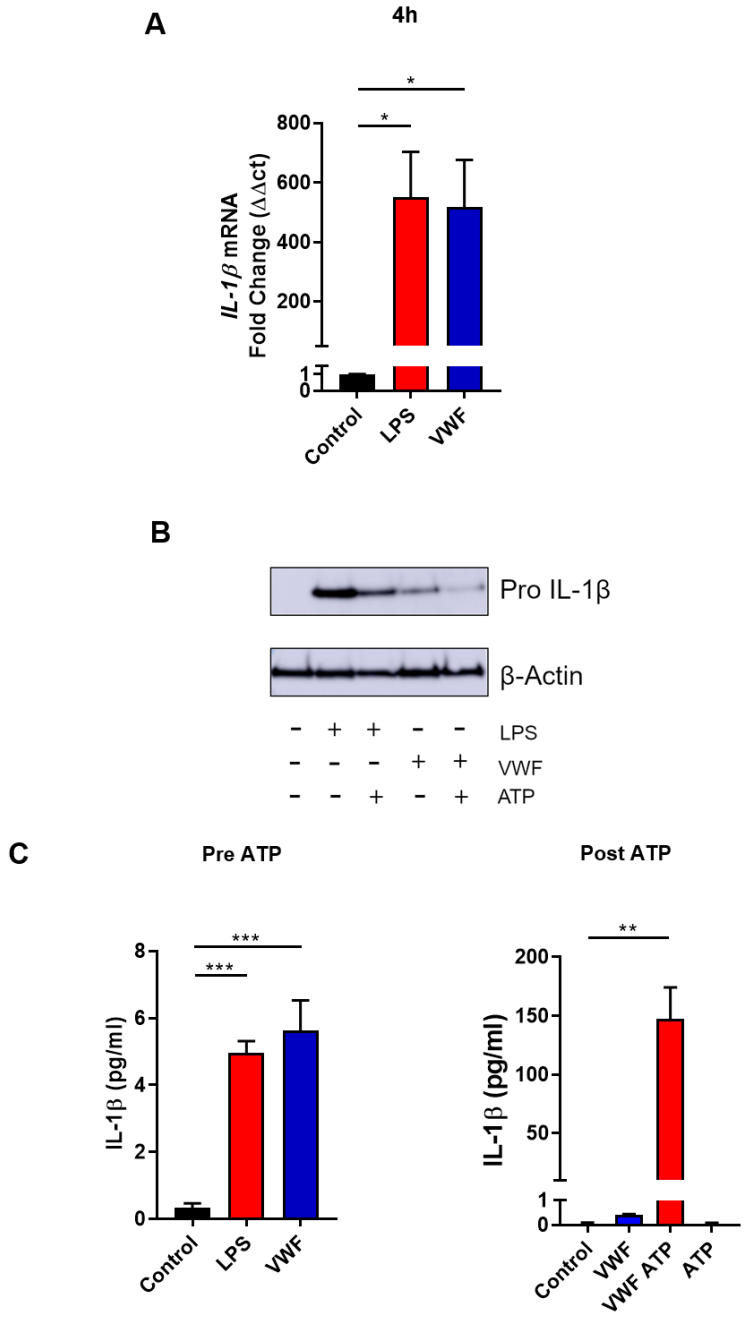

Figure 4.6: VWF treatment triggers inflammasome activation in murine BMDM

A: IL-1β mRNA expression levels were assessed by quantitative RT-PCR in BMDM following treatments with cell culture media (control), pd-VWF (10µg/ml) or LPS (100ng/ml). **B:** Murine BMDM were treated with cell culture media (control),pd-VWF (10µg/ml) or LPS (100ng/ml) and pro-IL-1β protein levels examined by Western blot analysis. **C:** Murine BMDMs were treated with pd-VWF (10µg/ml) or LPS (100ng/ml) for 4 hours, and secreted IL-1β levels measured by ELISA.

4.6: VWF triggers macrophage polarization towards an M1 phenotype

In view of the pro-inflammatory effects associated with VWF binding to macrophages, we investigated whether VWF interaction might influence macrophage polarization into M1 (classically activated or “pro-inflammatory”) or M2 (alternatively activated or “anti-inflammatory”) phenotypes using surface marker expression.(224–227) Incubation of murine BMDMs with LPS and IFN-γ resulted in approximately 75% cells adopting an M1 phenotype (positive for C11b and CD38 expression) (Figures 4.7A and 4.7B). In contrast, treatment with IL-4, IL-10 and IL-13 resulted in the majority of macrophages adopting an M2 phenotype (positive for CD11b and CD206) (Figure 4.7C). Interestingly, treatment with VWF alone was sufficient to result in more than 70% of the BMDM adopting an M1 phenotype (Figures 4.7D).

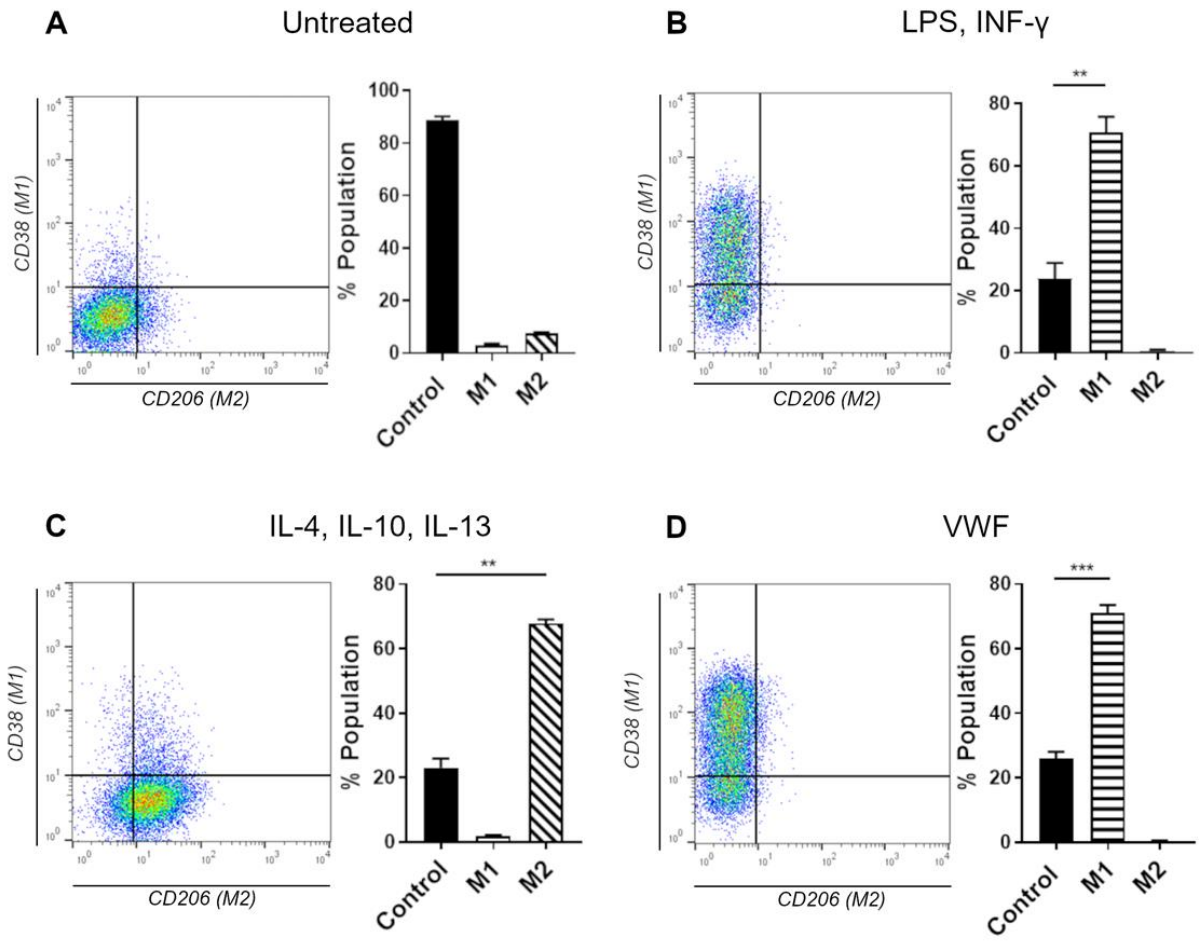

Figure 4.7: VWF triggers BMDM polarization towards an M1 phenotype

Murine BMDMs were incubated with agonist combinations including (LPS 100ng/ml and IFN- γ 20ng/ml), (IL-4 40ng/ml, IL-10 10ng/ml and IL-13 20ng/ml) or pd-VWF (10µg/ml) for 24h and then cell surface marker expression was examined by flow cytometry. CD38 and CD206 expression was determined from CD11b+ cells. **A:** Untreated BMDMs expressed no CD38 or CD206. **B:** Majority of BMDMS treated with LPS and INF-γ were CD38 positive, consistent with an M1 phenotype. **C:** In contrast, BMDMs incubated with IL-4, IL-10 and IL-13 were CD206 positive, consistent with an M2 phenotype. **D:** BMDM stimulation with pd-VWF (10µg/ml) resulted in a significant increase in expression of CD38, consistent with a pro-inflammatory M1 macrophage phenotype. The data presented represent the mean values ± SEM for three independent experiments (**$P < 0.01$, ***$P < 0.001$ ****$P < 0.0001$ respectively).

4.7: Exposure to VWF results in enhanced generation of reactive oxygen species in BMDMs

Previous studies have demonstrated that generation of reaction oxygen species (ROS) and induction of nitric oxide synthetase (iNOS) constitute hallmark features of pro-inflammatory macrophages.(228,229) To study whether VWF binding may influence ROS generation, murine BMDMs were treated with either pd-VWF (10μg/ml) or LPS (100ng/ml) for 3 hours. Cellular ROS generation was then detected using CellROX DeepRed staining by flow cytometry. CellRox is non-fluorescent while reduced, but becomes fluorescent upon ROS oxidation. Treatment with either pd-VWF or LPS resulted in a significant increase in macrophage ROS levels (Figure 4.8A). In addition, VWF treatment also resulted in a significant increase in *iNOS* mRNA expression in BMDMs (Figure 4.8B). Together, these findings further support the hypothesis that VWF binding induces significant pro-inflammatory effects in primary murine BMDMs.

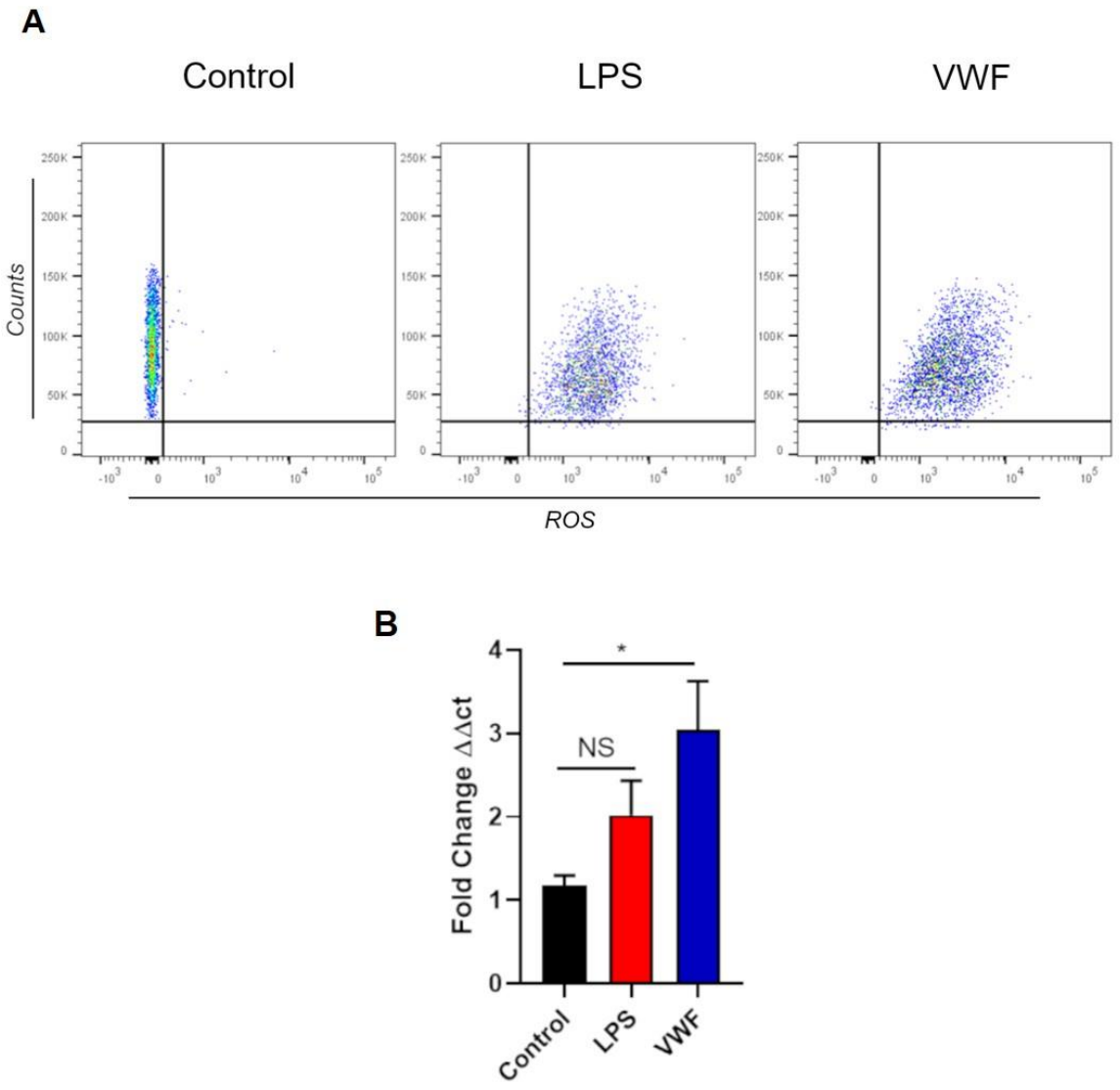

Figure 4.8 Exposure to VWF results in enhanced generation of reactive oxygen species in BMDM

A: Murine BMDM were treated with pd-VWF (10µg/ml) or LPS (100ng/ml) for 3 hours, before ROS was assayed using CellROX DeepRed staining. Flow scatter plots are a representative image of 3 independent experiments. **B:** *iNOS* mRNA expression levels were assessed by quantitative RT-PCR in BMDM following treatments with pd-VWF (10µg/ml) or LPS (100ng/ml). Data represents the average of 3 experiments ± SEM in which significance was determined by t-test (NS, Non-significant, *p<0.05).

4.8: VWF has a tolerising effect on murine BMDM

To investigate whether VWF exposure may have a tolerising effect upon macrophages, murine BMDMs were initially treated with VWF (10μg/ml) or LPS (100ng/ml) for 8 hours. Following a 16 hour rest period, the BMDM cells were then re-exposed to VWF or LPS at the same concentrations for a further 4 hour period and TNF-α expression levels assessed. Significant increased TNF-α expression was seen following initial BMDM exposure to LPS, and remained consistent at the time of LPS re-exposure (Figure 4.9). In keeping with our previous findings, initial BMDM exposure to pd-VWF also resulted in a marked increase in TNF-α expression. Importantly however, re-exposure to VWF resulted in a markedly attenuated increase in TNF-α production (Figure 4.9). These data support the hypothesis that VWF has a tolerising effect on murine BMDM.

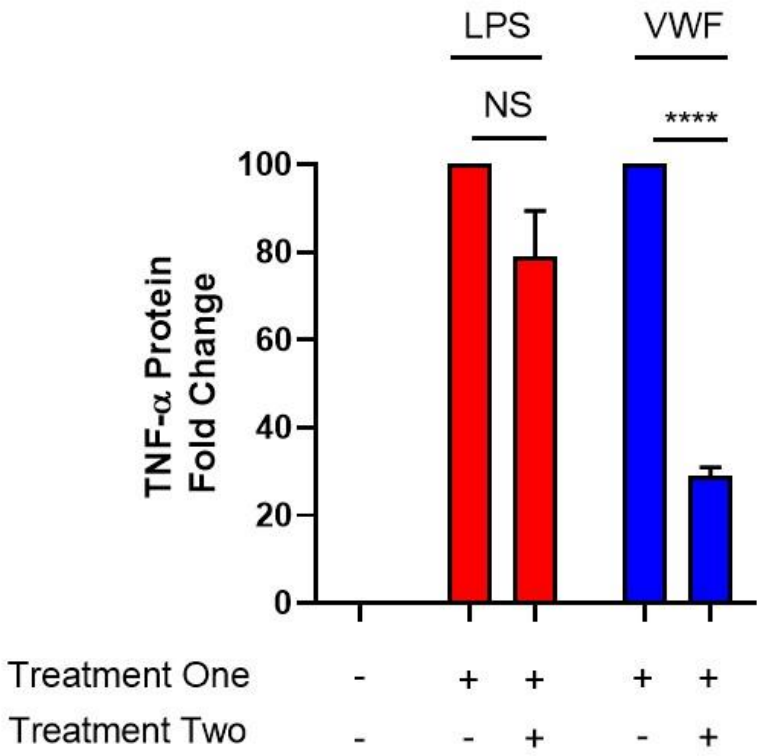

Figure 4.9 VWF has a tolerising effect on murine BMDM

Murine BMDM were re-challenged with either pd-VWF (10μg/ml) or LPS (100ng/ml) and TNF-α production was assessed by ELISA. Data is represented by the average fold change reduction in TNF-α production from initial stimulation of 3 independent experiments. Significance was determined by t-test (NS, Non-Significant, ****p<0.0001).

4.9: VWF binds to THP1 macrophages but does not promote pro-inflammatory effects

In preliminary experiments, we observed that pd-VWF could bind to differentiated THP1 monocytes in the presence of ristocetin (Figure 3.4). Given the pro-inflammatory effects associated with pd-VWF binding to both primary human macrophages and murine BMDM, we proceeded to examine whether similar effects were observed in differentiated THP1 macrophages. THP1 cells were first differentiated into macrophages with PMA treatment for 72 houres as before. Despite the pro-inflammatory signalling effects seen in primary human and murine macrophages, VWF treatment (10μg/ml for 30 minutes) of THP1 macrophages was not associated with any significant increase in phosphorylation of MAPKinase p38 and JNK or NF-κB activation (Figure 4.10 A). In contrast, pro-inflammatory signalling was seen following incubation with the LPS (100ng/ml for 30 minutes) positive control. Similarly, VWF treatment of THP1 macrophages did not alter pro-inflammatory cytokine or chemokine gene expression, (Figure 4.10 B) unlike alterations seen for human primary macrophages in sections 4.3 and 5.9.

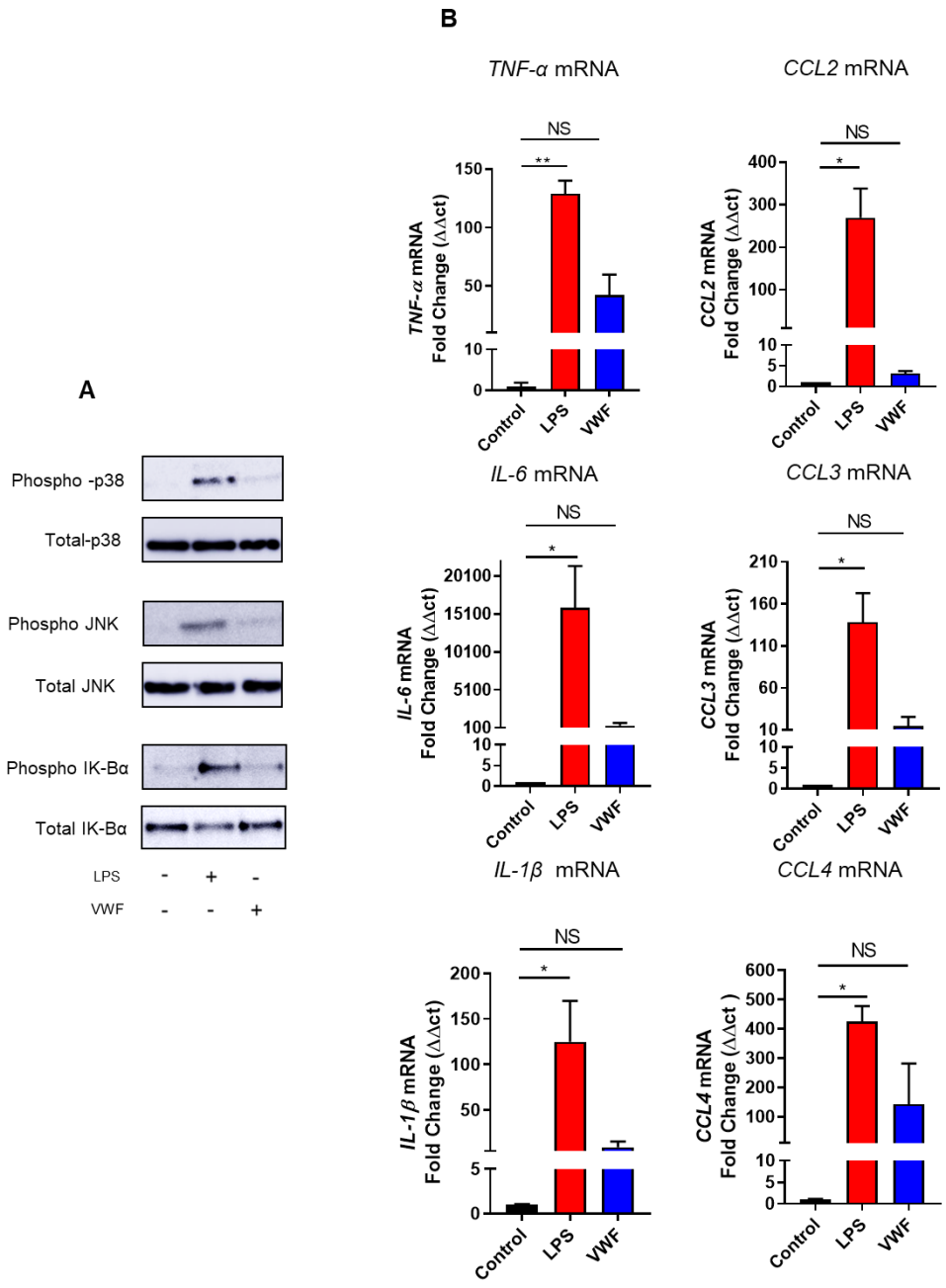

Figure 4.10: VWF binds to THP1 macrophages but does not promote pro-inflammatory effects

A: Western blot analysis of phosphorylation of p38, JNK and IkBα following incubation with pd-VWF (10 µg/ml) or LPS (100 ng/ml) for 30min. Representative images from three independent experiments. **B:** Cytokine (TNF-α, IL-6 and IL-1β) and chemokine (CCL2,3,4) mRNA expression at 4 hours and 24 hours respectively were assessed by quantitative RT-PCR following treatment with pd-VWF (10µg/ml) or LPS (100ng/ml).

4.10: Discussion

In the previous Chapter, we demonstrated binding of VWF to primary human macrophages, murine BMDMs and THP1 macrophages respectively. VWF binding was observed in both static conditions and ristocetin dependent conditions. These data are consistent with previous studies that have shown that hepatic Kupffer cells play a critical role in regulating VWF clearance.(204) Importantly, our data highlight that VWF does not simply bind to macrophages, but rather that this VWF binding also serves to trigger significant downstream signalling effects including activation of the MAPKinase pro-inflammatory pathway (with phosphorylation of p38 and JNK) and NF-κB activation.

Although VWF-induced signalling in macrophages has not previously been described, prior studies have clearly demonstrated that VWF binding to the glycoprotein (GP) Ib-IX-V receptor on platelets results in complex intracellular signalling that involves a number of different intracellular molecules including the Src family, Rac1, PI3-kinase/Akt and MAP kinases.(197,230–233) The net result of this signalling cascade induced by VWF binding to GP Ib-IX-V is to induce platelet activation, and in particular activation of the αIIbβ3 integrin receptor.(232) Additional studies will be needed to elucidate the molecular mechanisms through which VWF-binding to macrophages initiates pro-inflammatory signalling. Given the complex nature of VWF as a multimeric sialoglycoprotein, it seems likely that multiple VWF domains and various different macrophage receptors may be involved. Importantly however, a number of macrophage surface scavenger

receptors (including LRP1 and SR-A1) and C-type lectins (including MGL and Siglec-5) that have recently been reported to bind VWF, have also been shown to modulate intracellular signalling and thereby regulate inflammatory responses in both macrophages and dendritic cells.(234–240)

In keeping with the observed signalling effects, VWF binding to primary human-derived macrophages was also associated with a significant increase in pro-inflammatory cytokine expression (including TNF-α, and IL-6). Control studies excluded the presence of any endotoxin contamination of the pd-VWF product though the use of both LAL reagent and RAW.Blue reporter cell line. Furthermore, THP1 macrophages which express endotoxin-sensing receptors (TLRs and NLRs) remain unresponsive in terms of pro-inflammatory signalling activation and cytokine production when exposed to pd-VWF preparation.(241) In addition, binding of the recently licensed clinical grade recombinant VWF (Vonvendi®, Takeda) to macrophages was also associated with pro-inflammatory signalling. Together, these findings first represent the purity of the plasma derived VWF used but more importantly they also represent the first demonstration that VWF binding to macrophages directly initiates pro-inflammatory signalling, resulting in downstream pro-inflammatory cytokine production.

Macrophages possess an additional signalling mechanism in response to cell damage or infection called the NLRP3 inflammasome to generate IL-1β and IL-18. Importantly, no IL-1β is generated in response to a single inflammatory signal.(242)

For full activation, NLRP3 inflammasome activation requires a two-step process. First, NLRP3 complex expression is driven by stimulation via endogenous molecules or toll like receptor ligands though NF-Kb.(243) This initial stimulation also results in the synthesis of inactive pro-IL-1β. In response to a second stimulation step, macrophages assemble the caspase 1 containing NLRP3 inflammasome that cleaves pro-IL1β into its active form.(244) Interestingly, VWF binding to macrophages was associated with an increase in IL-1β mRNA and pro-IL-1β levels. A significant increase in IL-1β secretion (and concurrent decrease in pro-IL-1β) was only observed when VWF-treated macrophages were also subsequently exposed to ATP. Thus, consistent with the concept that VWF triggers pro-inflammatory signalling pathways and cytokine expression in macrophages, our data also show for the first time that VWF drives NLRP3 inflammasome activation.

In view of the pro-inflammatory effects associated with VWF, we also investigated whether binding to macrophages might influence macrophage polarization. Interestingly, treatment with VWF was sufficient to result in more than 70% of BMDM adopting an M1 (classically activated or “pro-inflammatory”) phenotypes. In addition, incubation of VWF with BMDM significantly enhanced production of reactive oxygen species (ROS) and iNOS expression, to levels similar to that observed with LPS. Production of ROS results from a number of sources, including mitochondrial respiration, which generates superoxide from complex I and III. ROS can also be generated through the pentose phosphate pathway from (Nicotinamide adenine dinucleotide phosphate) NADPH. These reactive chemicals

are key regulators of macrophages biology and constitute a hallmark of pro-inflammatory macrophages.(245,246)

Fundamental to initiating an inflammatory reaction is also the ability to silencing that inflammation reaction. Dampening of an immune response is paramount, as it prevents sustained deleterious cytotoxic inflammatory responses.(247,248) This regulatory process termed tolerance occurs rapidly in macrophages though epigenetic modifications that silences pro-inflammatory responses such as TNF-α cytokine production.(249) Crucially, following an initial exposure to an inflammatory agent, a subsequent re-exposure will only elicit a minor response as the macrophage has become tolerant. Here we demonstrate that VWF exposure followed by re-exposure has such a tolerizing effect. However, we noted that VWF induces changes different to LPS as VWF become much more rapidly tolerized when compared to LPS. It is possible that VWF may be induces alternative epigenetic changes within the macrophage compared to LPS.

Interestingly, although pd- and rVWF binding to primary human macrophages and murine BMDM resulted in consistent pro-inflammatory effects, minimal effects were observed in THP1 macrophages. The molecular mechanisms underpinning this difference remain unclear, but likely relate at least in part to differences in surface receptor repertoire expression on THP1 macrophages (derived from immortalised monocytic leukemia cells) as opposed to primary macrophages. Previous studies have reported that THP1 macrophages do express all putative

pattern recognition receptors and consequently have been shown to be responsive to endotoxins.(250) Thus, the fact that our VWF products fail to elicit any pro-inflammatory effects in THP1 macrophages further supports the hypothesis that VWF has direct inherent pro-inflammatory properties.

Given recent evidence that VWF contributes to the pathogenesis of a variety of different inflammatory diseases, the novel findings presented in this Chapter not only define a novel role for VWF in regulating innate immune responses, but are also of direct translational significance. Based upon our findings we propose that in the normal circulation, VWF and monocytes circulate together with minimal interaction. However, following tissue damage and blood vessel injury, VWF escapes from the plasma into subendothelium where it comes into contact with tissue macrophages. These macrophages express a different repertoire of surface receptors compared to undifferentiated monocytes, with the upregulation of specific surface receptors such as LRP1 that enables binding to VWF. VWF-binding triggers the macrophages to adopt an M1 phenotype, with consequent secretion of proinflammatory cytokines and chemokines at the site of vascular damage.

5. VWF alters macrophage immunometabolism, chemoattraction and phagocytosis

5.0: Introduction

Cells regulate their metabolic pathways in order to facilitate survival and growth. Kempner and Peschel were the first to demonstrate that macrophages increase oxygen and glucose consumption in response to inflammatory stimuli.(251) Macrophages contain a number of distinct pathways for energy production including glycolysis, the tricarboxylic acid (TCA) cycle, the pentose phosphate pathway, fatty acid synthesis and amino acid metabolic pathways.(252) In the context of immunity, glycolysis and the TCA cycle are of particular importance. Glycolysis involves the cellular uptake of glucose and its cytosolic processing to pyruvate, which produces 2 Adenosine triphosphate (ATP) compounds per molecule of glucose.(252,253) In contrast, the mitochondrial TCA cycle processes acetyl coenzyme to generate Flavin adenine dinucleotide (FADH) and NADPH. FADH and NADPH shuffle electrons to the electron transport chain that drives oxidative phosphorylation, yielding 36 ATP compounds.(252,253) A critical difference between glycolysis and the TCA cycle relates to time. Since the TCA cycle and oxidative phosphorylation require mitochondrial biogenesis, this process is relatively slow.(252,254) Conversely, although glycolysis generates significantly lower quantities of ATP, nonetheless this process can occur rapidly.(252,255,256) This rapid production of energy enables macrophages to respond to inflammatory mediators.

Alterations in macrophage metabolism are considered hallmarks of activation status and inflammatory potential. Acute PAMP stimulation rapidly elevates glycolysis by doubling glucose uptake though the enhanced synthesis of glucose transporter 1 (GLUT1).(257) Following glucose internalisation it becomes phosphorylated by hexokinase and is catabolized though anabolic pathways (glycolysis).(257,258) Additionally, acute LPS treatment also induces the phosphorylation and activation of pyruvate kinase M2 (PKM2).(259) PKM2 slows glycolysis allowing glycolytic intermediates (pyruvate and ATP) to be utilised in biosynthetic pathways.(259) Furthermore, PMK2 translocates to the nucleus and acts with HIF-1α to induce IL-1β production.(259)

Following a prolonged LPS exposure, macrophages progress into a glycolytic amplification phase resulting in profound metabolic alterations. LPS induces expression of 6-phosphofructo-2-kinase/fructose-2,6-biphosphatase 3 (PFKFB3) which converts glycolysis intermediate fructose-6-phosphate into fructose-2-6-bisphosphate.(254,260) Fructose-2-6-bisphosphate subsequently activates 6-phosphofructo-1-kinase (PFK1) the enzyme responsible for catalysing the final step of glycolysis, thus ultimately leading to its enhancement.(254,260,261) Additionally, transcription factor HIF-1α is responsible for the expression of multiple pro-glycolytic enzymes that facilitat enhanced glycolysis.(259,261–263) HIF-1α is tightly regulated by proline-hydroxylase, particularly proline-hydroxylase-3 (PHD3). PHD3 adds a hydroxyl group to proline residues 402 and 564 within HIF-1α, thus marking it for ubiquitination and subsequent degradation.(264,265) As

glycolysis persists, metabolic intermediates succinate and citrate accumulate inside macrophages which inhibiting PHD3 HIF-1α degradation leading to heightened expression of glycolytic enzymes.(258,266,267) Ultimately, prolonged LPS treatment results in the macrophages firmly adopting changes that drive glycolysis and completely disrupt oxidative respiration.

Within the macrophage, the TCA cycle and oxidative phosphorylation both occur within mitochondria. Consequently, changes in immuno-metabolism associated with macrophage activation have been shown to be associated with alterations in their mitochondrial morphology. These mitochondrial are highly dynamic organelles that can change in size and number though controlled processes of fission and fusion.(268) Fission is the formation of multiple smaller fragments from a single parent mitochondria. Fusion involves the generation of larger mitochondria from smaller individual structures.(268,269) Previous studies have reported that during periods of enhanced glycolysis there is a significant increase in mitochondrial fission (fragmentation), whilst mitochondrial fusion (elongation) is observed during periods when oxidative phosphorylation is increased.(190,270,271) Thus, LPS stimulation of macrophages results in profound mitochondrial fragmentation and concurrent loss of the elongated form as glycolysis is enhanced.

A principle macrophage effector function is the production chemokines (for example CCL2, CCL3 and CCL4) that recruit other immune cells such as monocytes

to the source of damage.(272) Chemokines are produced in large quantities at the source of inflammation, which establishes a chemokine gradient.(273) As chemokines diffuse, they bind to monocytes largely though chemokine G-protein coupled receptors, resulting in integrin activation and actin polymerisation.(274) Integrin activation and actin polymerization allows the monocyte to migration to the site of inflammation along the chemokine gradient.

In the previous two Chapters we have demonstrated that VWF binds to macrophages. Moreover, this VWF interaction serves to stimulate downstream signalling events that ultimately result in significant increases in pro-inflammatory cytokine expression and the polarisation of the majority of macrophages towards an M1 inflammatory phenotype. To further investigate the ability of VWF to modulate macrophage biology, we next proceeded to examine its effects upon (i) macrophage immune-metabolism (ii) macrophage mitochondrial morphology (iii) macrophage chemokine expression respectively.

5.1: VWF regulates macrophage metabolism and drives glycolysis

Alterations in the intracellular metabolic pathways, and in particular an increase in glycolysis, constitute a hallmark of inflammatory macrophages activated by both pathogen-associated and damage-associated signals through pattern-recognition receptor signalling.(252,255) To further investigate the hypothesis that VWF modulates macrophage functions, the effects of VWF binding on macrophage metabolism were assessed using extracellular flux analysis. Glycolysis was investigated by measuring extracellular acidification rate (ECAR) and oxidative respiration was assessed by monitoring oxygen consumption rate (OCR) using a Seahorse XF analyser. Basal rate of ECAR was assessed before addition of mitochondrial inhibitors oligo, FCCP or AA + R respectively. Oligo is an inhibitor of Complex V that decreases mitochondrial ATP generation, thereby decreasing OCR and increasing the burden on glycolysis.(184,185) FCCP, uncouples the mitochondrial membrane by collapsing the proton gradient and allowing electrons to move freely driving oxygen consumption by complex IV.(186,187) Finally AA + R: blocks complex III and I shutting down mitochondrial respiration, inducing a drop in OCR but a corresponding increase in ECAR. (188,189)

Following 3 hours stimulation with pd-VWF (10µg/ml), a significant increase in ECAR (consistent with a marked increase in glycolysis) was observed similar to that seen with LPS (100ng/ml) exposure (Figure 5.1). ECAR was consistently elevated following pd-VWF treatment throughout mitochondrial inhibition. Interestingly, after an extended 16 hour incubation, the pd-VWF-induced increase in BMDM glycolysis had returned to almost control levels, whereas ECAR remained

significantly elevated in macrophages treated with LPS over the same time course (Figure 5.2).

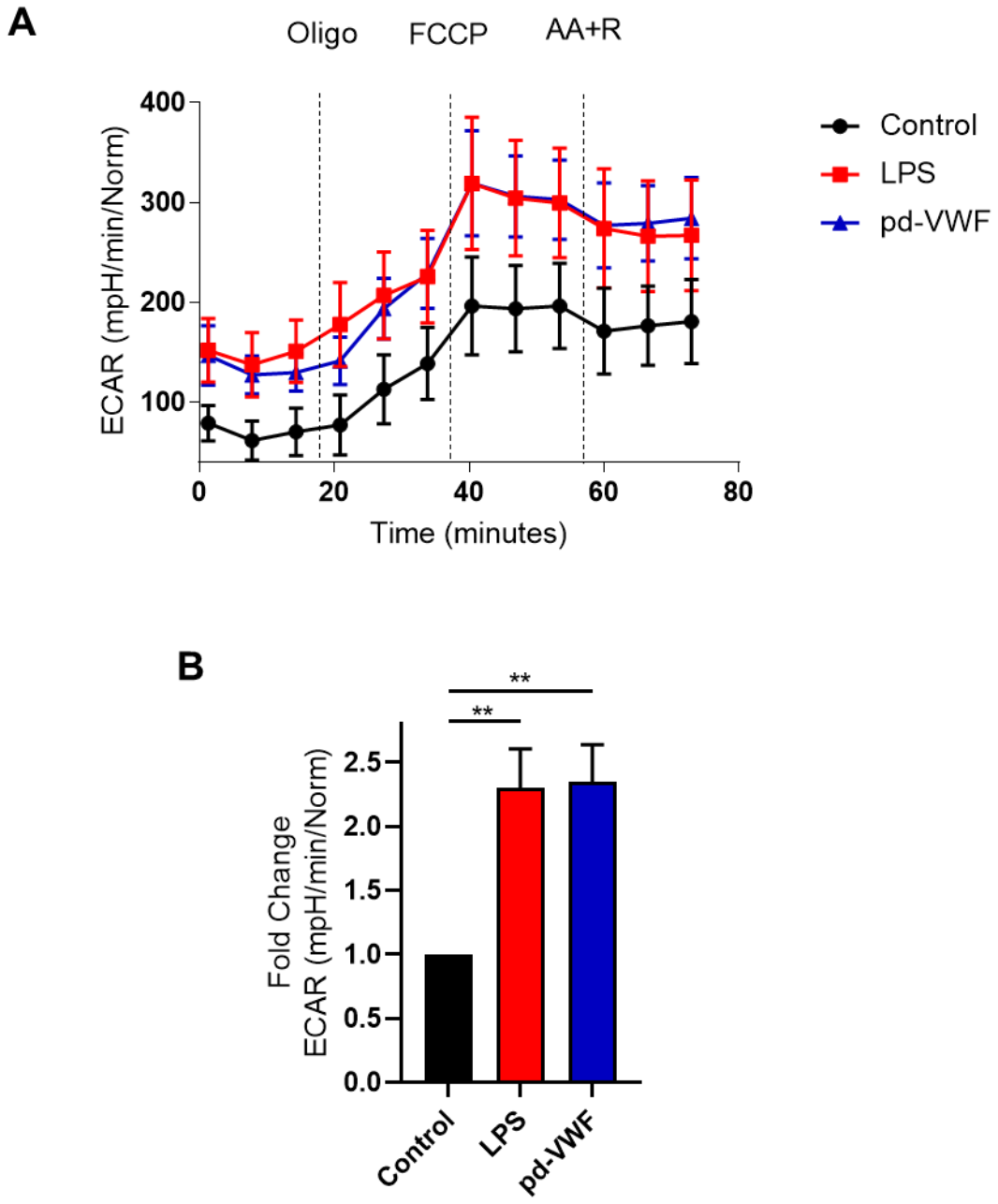

Figure 5.1: VWF regulates macrophage metabolism and drives glycolysis

Extracellular flux analysis (Seahorse XF Cell Mito Stress kit) was used to detect glycolytic dependent alterations in BMDM ECAR. Alterations in ECAR was measured following 3 hour stimulation with pd-VWF (10µg/ml), LPS (100ng/ml), or untreated controls. **A:** Representative image of BMDM ECAR following mitochondrial inhibitors. **B:** Basel ECAR from 3 independent experiments. Significance determined by t-test (**p<0.01)

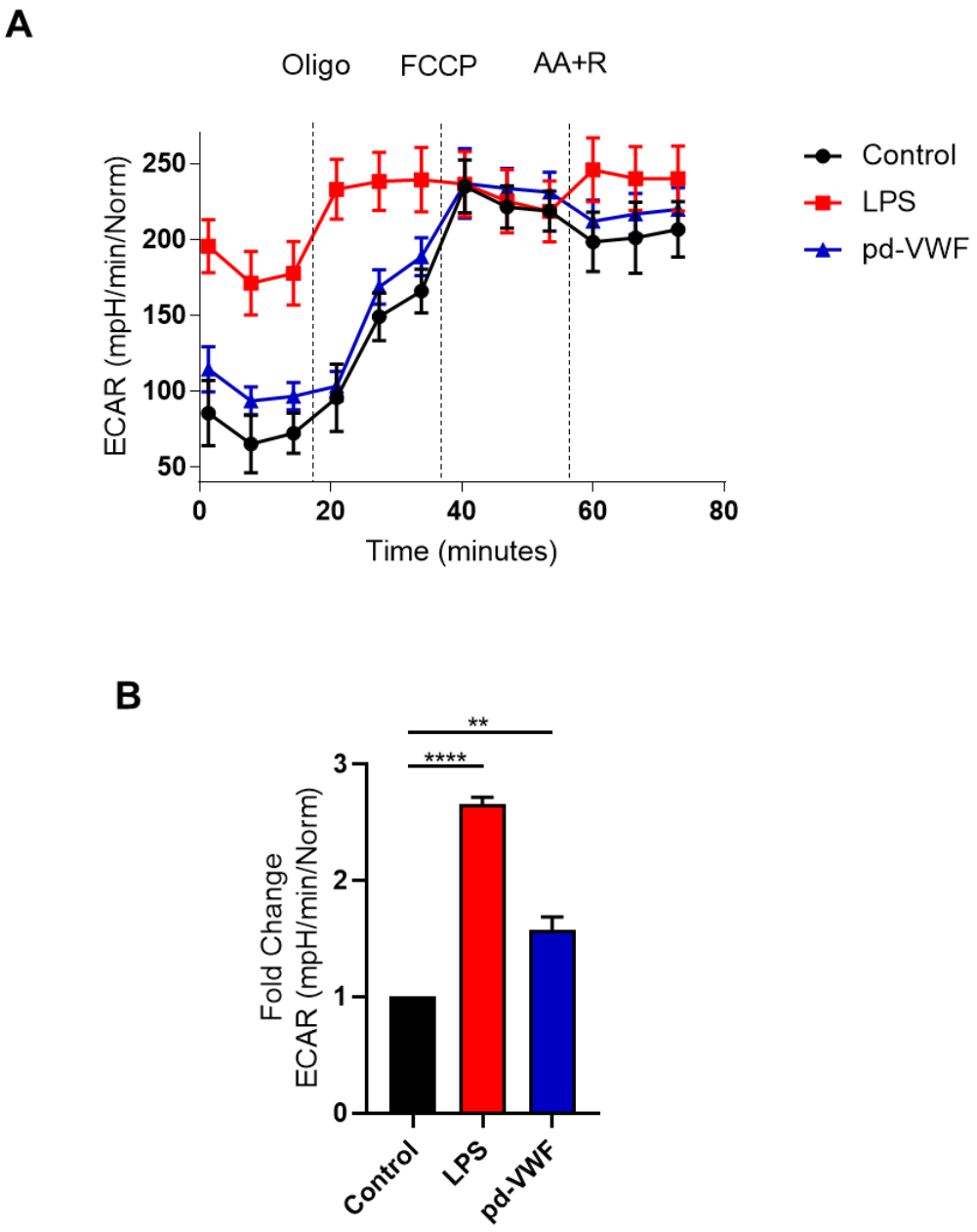

Figure 5.2: VWF regulates macrophage metabolism and drives glycolysis in a time-dependent manner

Extracellular flux analysis (Seahorse XF Cell Mito Stress kit) was used to detect glycolytic dependent alterations in BMDM ECAR. Alterations in ECAR was measured following 16 hour stimulation with pd-VWF (10µg/ml), LPS (100ng/ml), or untreated controls. **A:** Representative image of BMDM ECAR following mitochondrial inhibitors. **B:** Basel ECAR from 3 independent experiments. Significance determined by t-test (**p<0.01, ****p<0.001)

5.2: pd-VWF does not affect basal oxidative phosphorylation in BMDM

Previous studies have shown that oxidative phosphorylation represents the principal pathway for energy generation in anti-inflammatory macrophages.(275) Consequently, the effects of pd-VWF on BMDM oxidative phosphorylation in BMDMs was assessed by measuring oxygen consumption rate (OCR) using the Seahorse XF analyser. Basal rates of OCR were used to assess mitochondrial oxidative phosphorylation after incubation with LPS or pd-VWF for 3 hours and 16 hours. In contrast to its effect in promoting glycolysis, LPS or pd-VWF did not affect basal levels of mitochondrial oxidative phosphorylation after 3 hours (Figure 5.3A). However, in keeping with previous reports,(266,276) we observed that 16 hour exposure to LPS resulted in markedly reduced mitochondrial OCR (Figure 5.3B). In contrast, no such effect was observed in cells incubated with pd-VWF.

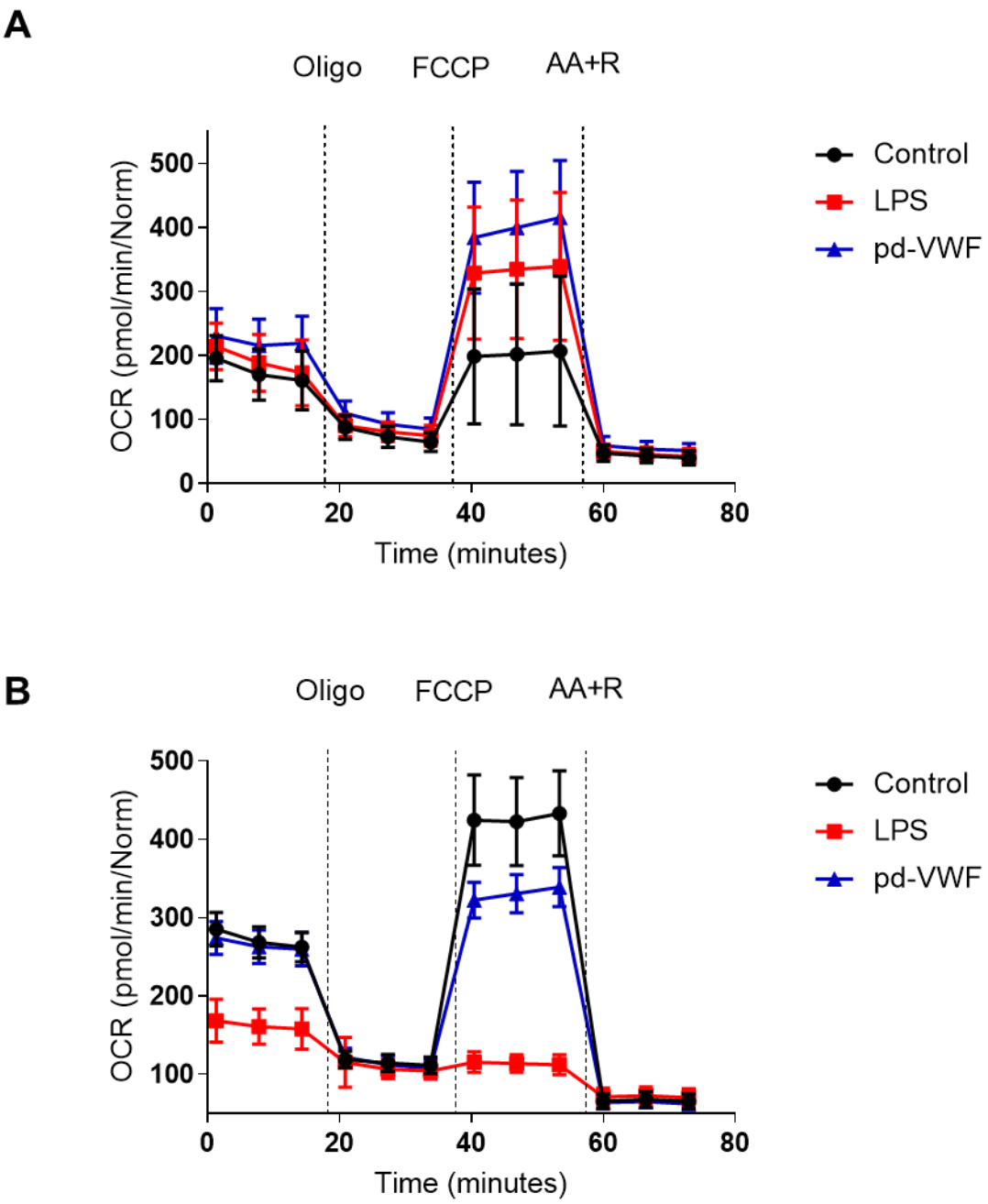

Figure 5.3: pd-VWF does not affect oxidative phosphorylation in BMDM

Extracellular flux analysis used to detect alterations in BMDM oxidative phosphorylation (OCR). Changes in OCR were measured following a **A:** 3 hour or **B:** 16 hour stimulation with pd-VWF (10µg/ml), LPS (100ng/ml), or untreated controls. Representative images of OCR are shown.

5.3: VWF alters macrophage maximum respiratory capacity and spare residual capacity

Maximum repository capacity (MRC) represent the highest capacity of the macrophage to generate energy through oxidation phosphorylation. FCCP is used to determine MRC as it uncouples the mitochondrial membrane, collapsing the proton gradient which allows electrons to move freely a drive oxygen consumption though complex IV. (186) Following a 3 hour treatment with both pd-VWF or LPS there was a significant increase in MRC (Figure 5.4A). This demonstrates that VWF or LPS can generate a more metabolically active macrophage. Interestingly however, following a 16h treatment enhanced MRC is not preserved as both LPS and VWF lead to a reduction in OCR following FCCP injection (Figure 5.4B). This reduction in MRC is most likely a result of significant glycolytic changes in macrophage metabolism following VWF or LPS treatment. Interestingly, VWF treatment is similar to control levels, and only moderately reduces MRC following a 16h treatment, unlike substantial reductions following LPS treatment. (Figure 5.4B)

Spare residual capacity (SPR) is the measurement of a macrophages ability to respond to an increased energy demand and is determined by the difference between basal respiration and maximal respirational capacity. Both oxidative phosphorylation and glycolytic SRC was elevated following a 3 hour VWF or LPS treatment (Figure 5.5A). However, following a prolonged treatment with VWF or LPS, oxidative phosphorylation MRC was reduced (Figure 5.5B). Prolonged LPS treatment dramatically reduced oxidative phosphorylation SRC to below control

levels demonstrating complete metabolic reprograming of the cell while prolonged VWF treatment also significantly reduces SRC but to levels similar to control. (Figure 5.5B)

Interestingly however, the glycolytic SRC was reduced following prolonged LPS treatment, suggesting a reduced ability the macrophage respond to an increased energy demand. This loss of SRC is most likely due to macrophage fatigue over the prolonged 16h treatment. Interestingly, in line with our other glycolytic data, no alteration in glycolytic SRC were detected following 16h VWF treatment.

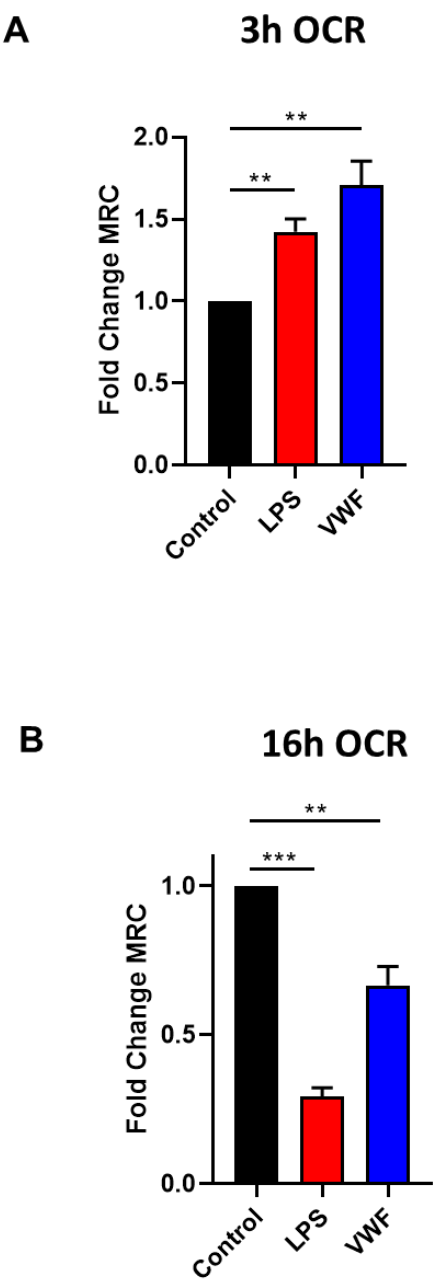

Figure 5.4: VWF and LPS treatment alters maximum respiratory capacity.

Alterations in OCR following BMDM FCCP treatment were used to determine MRC. BMDMs were pre-treated with VWF (10µg/ml), LPS (100ng/ml) or culture media (control) for **A:** 3 hours or **B:** 16 hours. Data is represented by the fold change MRC ±SEM in OCR from control conditions of 4 independent experiments. Significance determined by t-test (**p<0.01 and ***p<0.001).

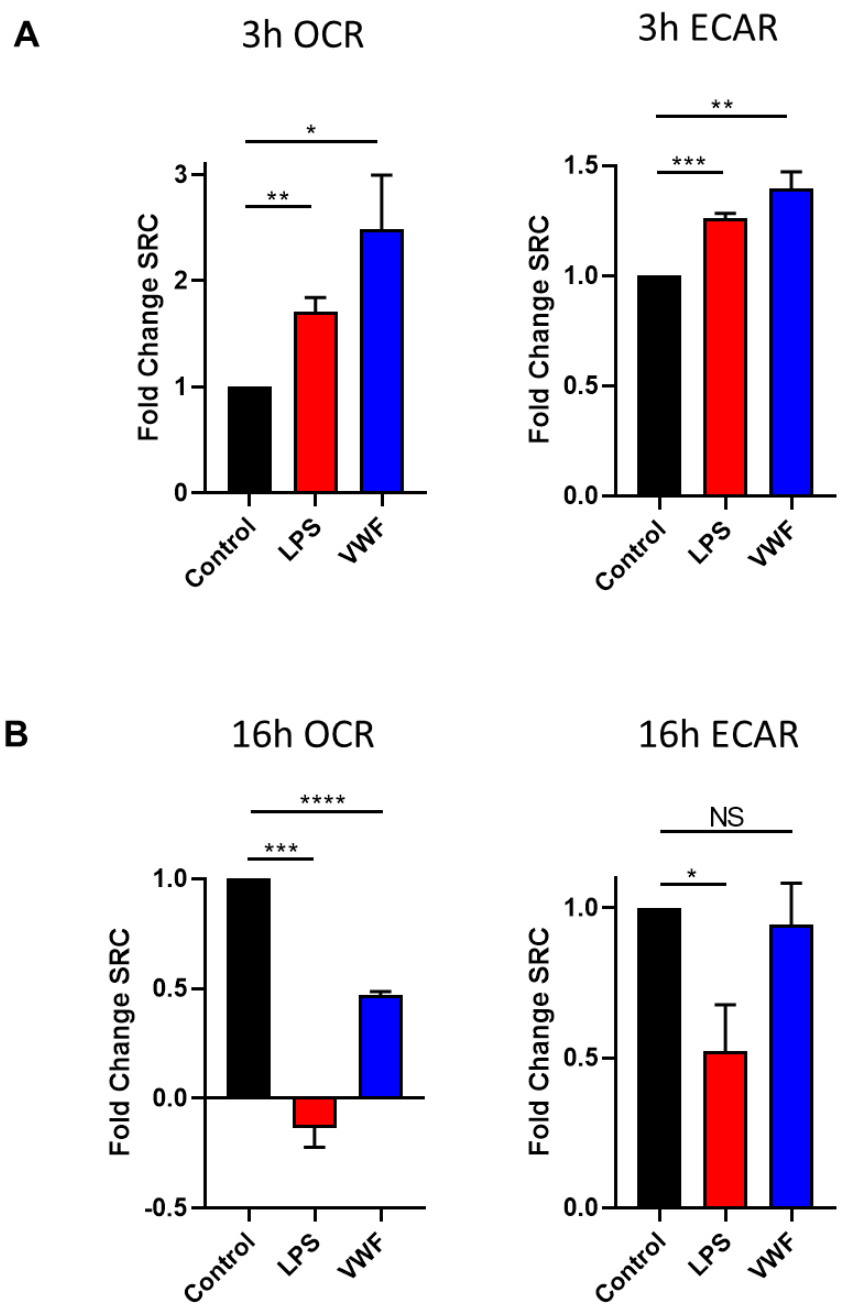

Figure 5.5:VWF and LPS alter BMDM SRC.

SRC of both OCR and ECAR was calculated by the difference between MRC and basal respiration. BMDMs were pre-treated with VWF (10µg/ml), LPS (100ng/ml) or culture media (control) **A:** 3 hours or **B:** 16 hours. Data is represented by the fold change SRC ±SEM in OCR and ECAR from control conditions of 4 independent experiments. Significance determined by t-test (*p<0.05, **p<0.01 and ***p<0.001, ****p<0.0001).

5.4: The effects of pd-VWF on macrophage energy profiles

The contrasting effects of VWF and LPS on BMDM immuno-metabolism can be summarised using energy plots (Figure 5.6).(277) Both VWF and LPS significantly enhance energetic glycolysis in BMDM following a short 3 hour exposure compared to quiescent control macrophages. This glycolytic response is a hallmark of pro-inflammatory macrophages. However, following a prolonged 16 hour treatment with LPS, BMDMs become characteristically highly glycolytic, due the complete shutdown of oxidative population. At this later time point, the VWF effects on immuno-metabolism diverge from those of LPS, with macrophage metabolism instead reverting to homeostatic aerobic oxidative phosphorylation.

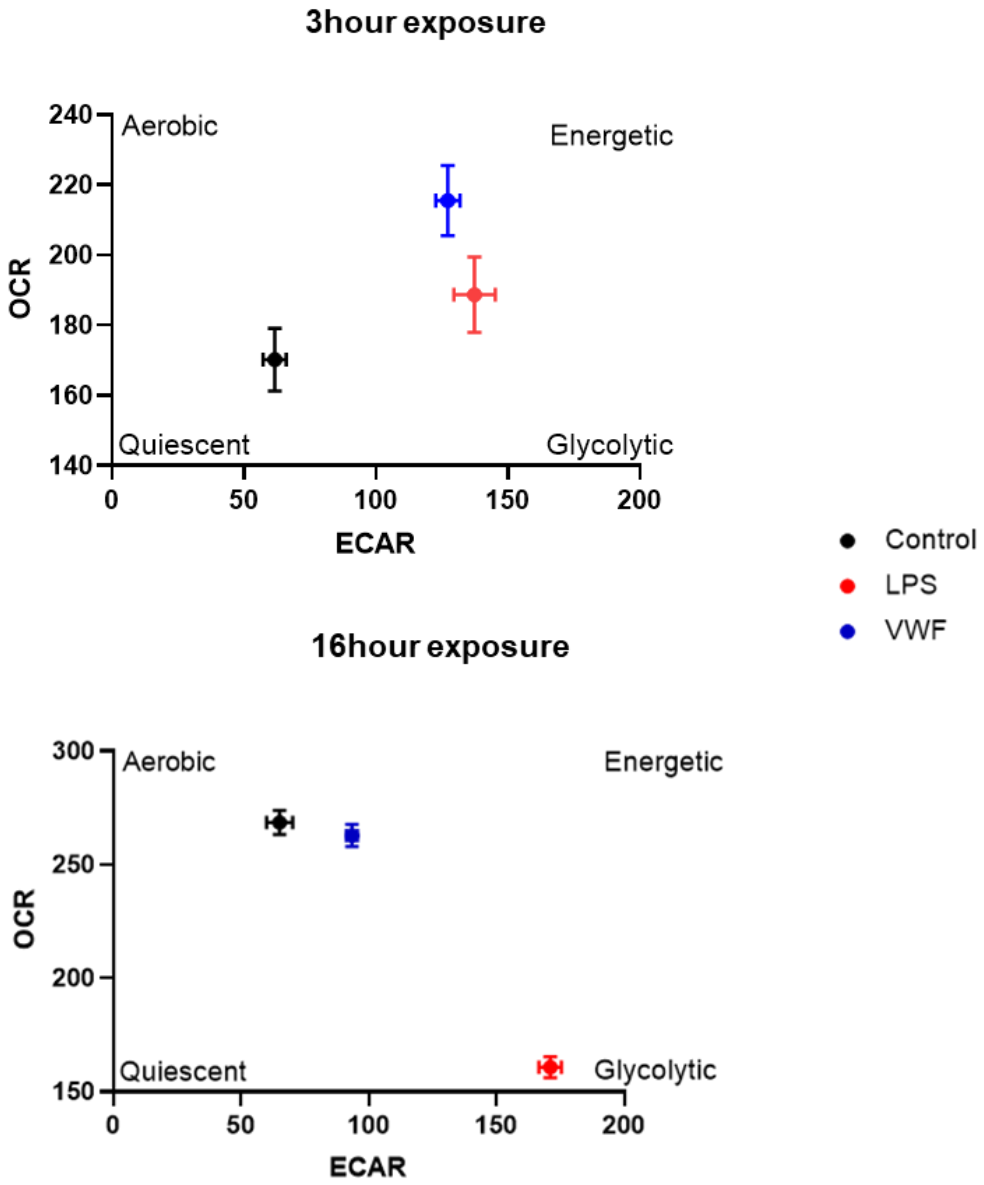

Figure 5.6: Energy plot summery of the effects of pd-VWF on BMDM metabolism

Plotting of OCR vs. ECAR ± SEM of basal respiration from 4 independent experiments.

5.5: Recombinant VWF regulates macrophage metabolism and drives glycolysis

Having observed a significant effect for pd-VWF in modulating macrophage metabolism in a time-dependent manner, we further investigated whether recombinant commercial VWF (r-VWF) used in the treatment of patients with VWD would have similar effects. Following a 3 hour stimulation with r-VWF, a significant increase in basal glycolysis was observed comparable to that previously seen with pd-VWF and LPS respectively (Figure 5.7). Furthermore, this r-VWF effect was again consistent through sequential mitochondrial inhibition. Finally, after an extended 16 hour incubation, the r-VWF-induced increase in BMDM glycolysis had resolved (Figure 5.8). Despite the similarity in glycolytic response of r-VWF and pd-VWF, there remains a quantitative difference between the two forms of VWF. This is most likely due to the large proportion of UL-VWF and high molecular weight VWF observed in recombinant preparation.(278)

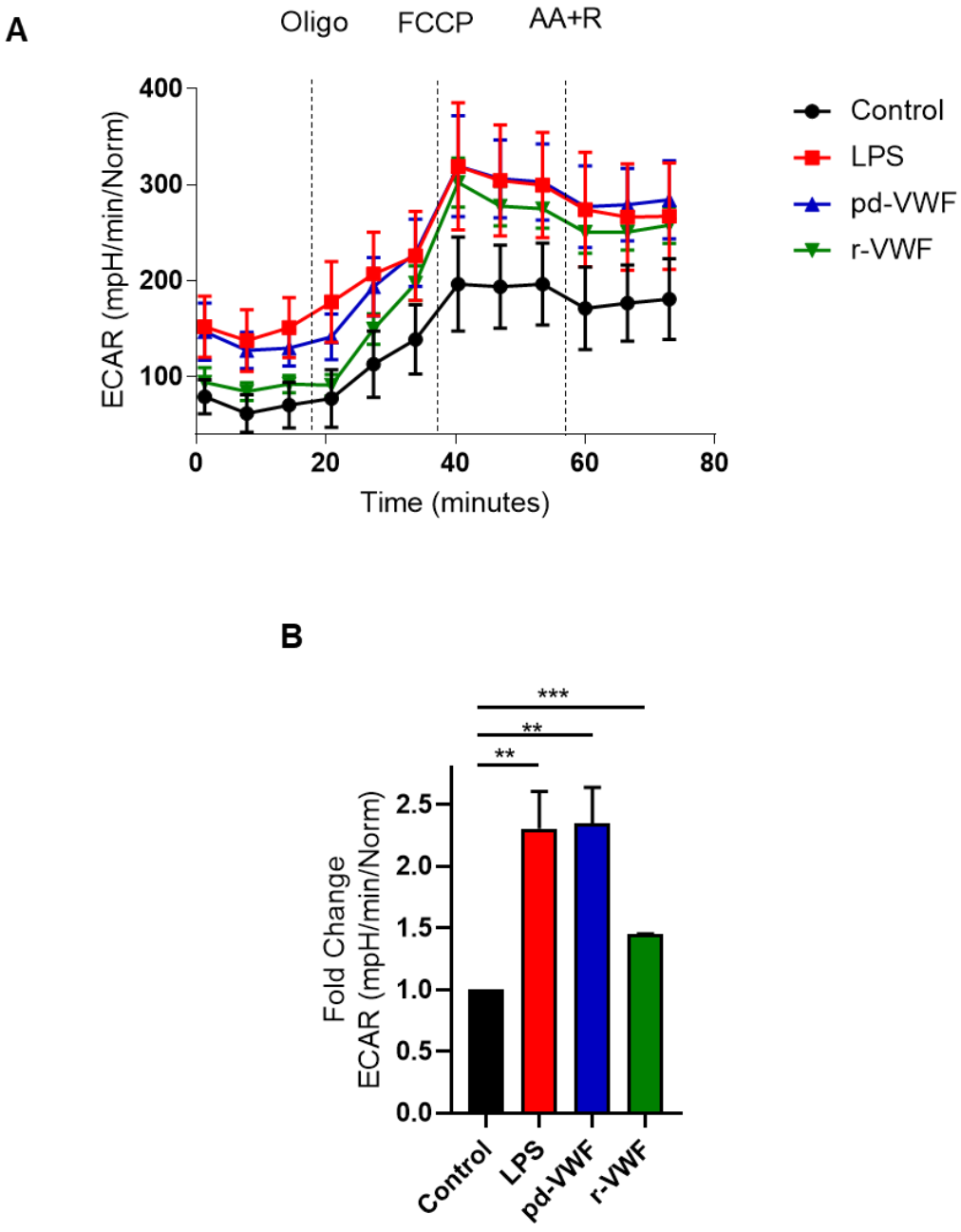

Figure 5.7: Recombinant VWF regulates macrophage metabolism and drives glycolysis

Alterations in ECAR was measured following a 3 hour stimulation with pd-VWF (10µg/ml), LPS (100ng/ml), rVWF (10µg/ml) or untreated controls. **A:** Representative image of BMDM ECAR following mitochondrial inhibitors. **B:** Basel ECAR from 3 independent experiments. Significance determined by t-test (**p<0.01, **p<0.001)

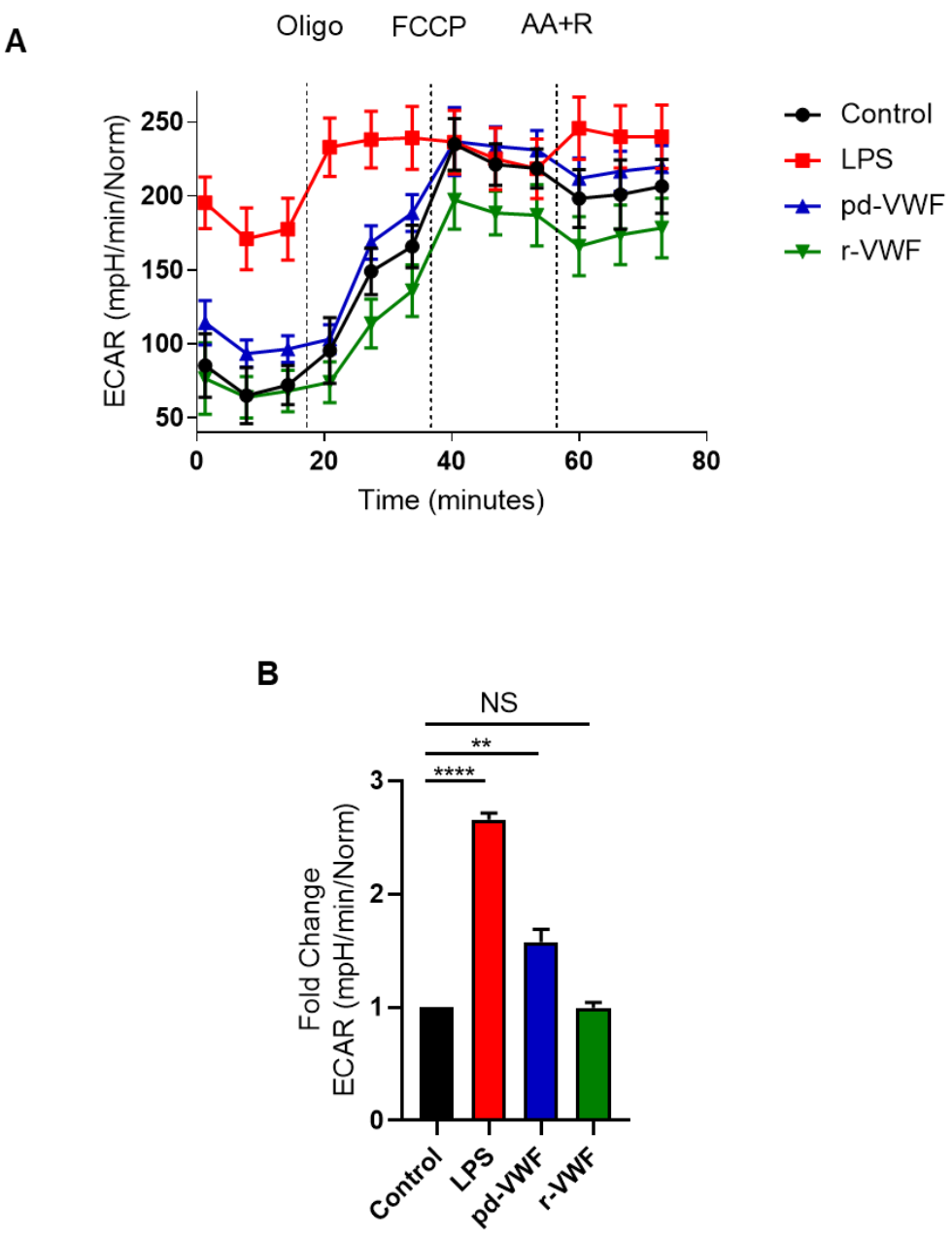

Figure 5.8: Recombinant VWF regulates macrophage metabolism and drives glycolysis in a time-dependent manner

Extracellular flux analysis (Seahorse XF Cell Mito Stress kit) was used to detect glycolytic dependent alterations in BMDM ECAR. Alterations in ECAR was measured following 16 hour stimulation with pd-VWF (10µg/ml), r-VWF (10µg/ml), LPS (100ng/ml), or untreated controls. **A:** Representative image of BMDM ECAR following mitochondrial inhibitors. **B:** Basel ECAR from 3 independent experiments. Significance determined by t-test (**p<0.01, ****p<0.0001)

5.6: Recombinant VWF does not affect oxidative phosphorylation in BMDM

The effects of r-VWF on BMDM oxidative phosphorylation in BMDMs were assessed by measuring OCR using the Seahorse XF analyser. OCR was used to assess mitochondrial oxidative phosphorylation after incubation with LPS or r-VWF for 3 hours and 16 hours. In contrast to its effect in promoting glycolysis, LPS or r-VWF did not affect basal levels of mitochondrial oxidative phosphorylation (Figure 5.9A). After a 16 hour exposure to LPS, mitochondrial OCR was markedly reduced but no such effect was observed in cells incubated with r-VWF for the same time period (Figure 5.9B).

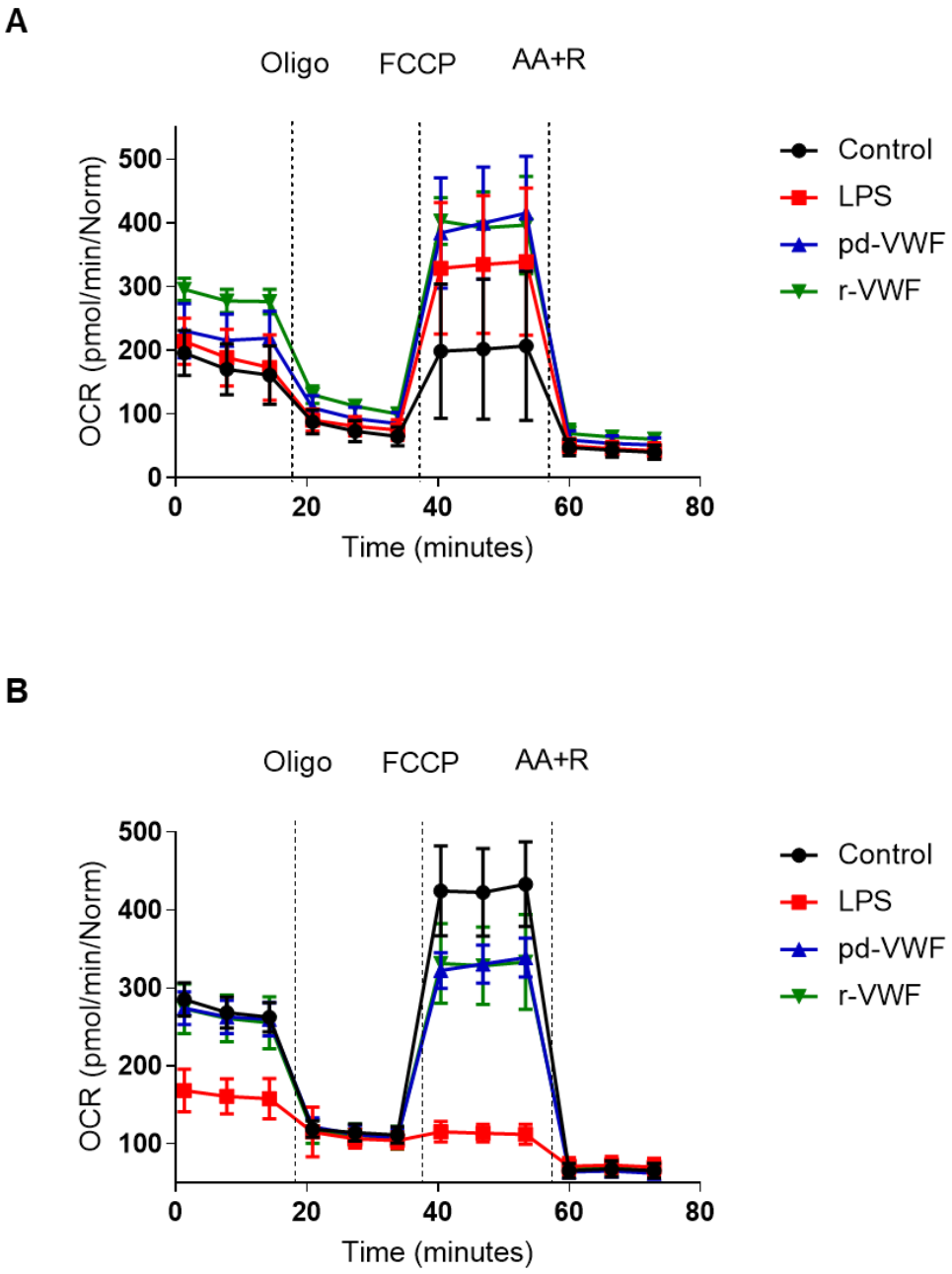

Figure 5.9: Recombinant VWF does not affect oxidative phosphorylation in BMDM

Extracellular flux analysis used to detect alterations in BMDM oxidative phosphorylation (OCR). Changes in OCR were measured following a **A:** 3 hour or **B:** 16 hour stimulation with pd-VWF (10µg/ml) r-VWF (10µg/ml), LPS (100ng/ml), or untreated controls. Representative images of OCR are shown.

5.7: Macrophage viability is not affected following VWF or LPS treatment

To confirm that the observed effects in macrophages metabolism had not resulted from altered cell viability, BMDMs were treated with pd-VWF (10µg/ml), r-VWF (10µg/ml) or LPS (100ng/ml) for 3 hours or 16 hours as before and subsequently incubated with Alamar Blue reagent at 37^{o}C. Live cell viability was assessed by measuring metabolised Alamar Blue. Absorbance was normalised to total protein content based on BCA reagent. Following a 16 hour incubation with pd-VWF or r-VWF, no significant changes in BMDM viability were apparent, however a prolonged LPS exposer resulted in a modest but significant decrease in BMDM viability. (Figure 5.10).

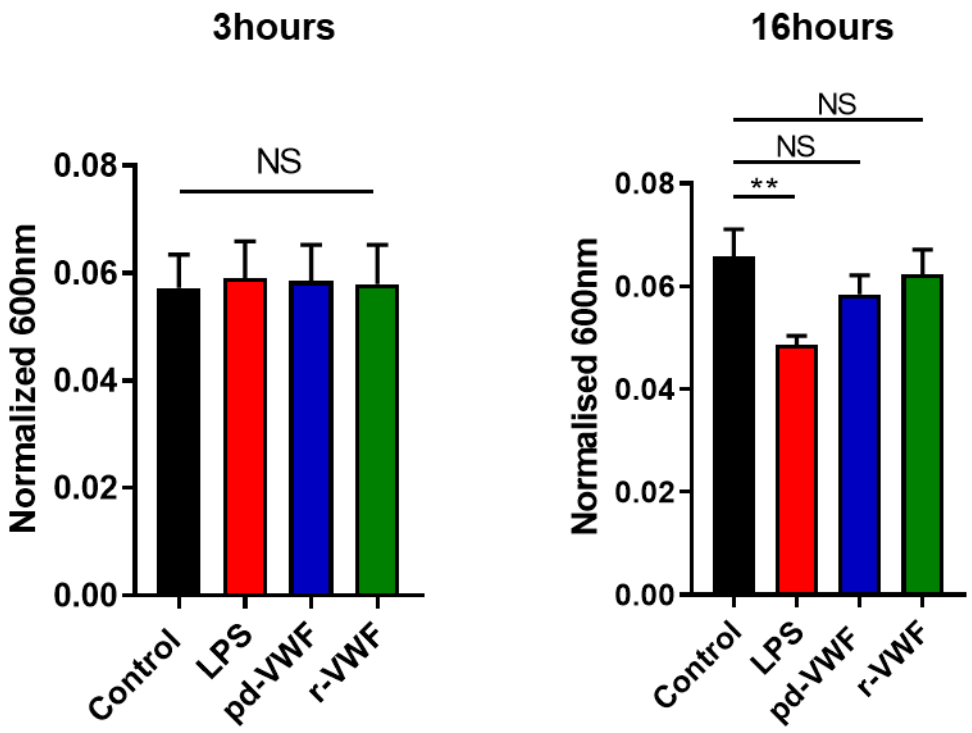

Figure 5.10: Macrophage viability is not affected following VWF or LPS treatment

BMDM were incubated with LPS (100ng/ml), pdVWF (10µg/ml) and r-VWF (10µg/ml) for the indicated times. Alamar blue metabolism was determined by absorbance at 600λ and normalised to total protein based on BCA reagent. Significance was determined by t-test (NS, non-significant, **p<0.01)

5.8: VWF influences mitochondrial morphology

Previous studies have reported that significant changes in mitochondrial morphology accompany changes in macrophage metabolic state.(190) In particular, mitochondria adopt a fragmented appearance when glycolysis levels are high, as opposed to an elongated state during periods of heightened oxidative phosphorylation.(270,271) In keeping with this hypothesis, we observed that LPS (100ng/ml) stimulation of BMDM for 3 hours resulted in fragmented mitochondrial morphology (Figure 5.11). Interestingly, treatment with pd-VWF (10μg/ml) for 3 hours was also associated with significantly higher levels of mitochondrial fragmentation (Figure 5.9).

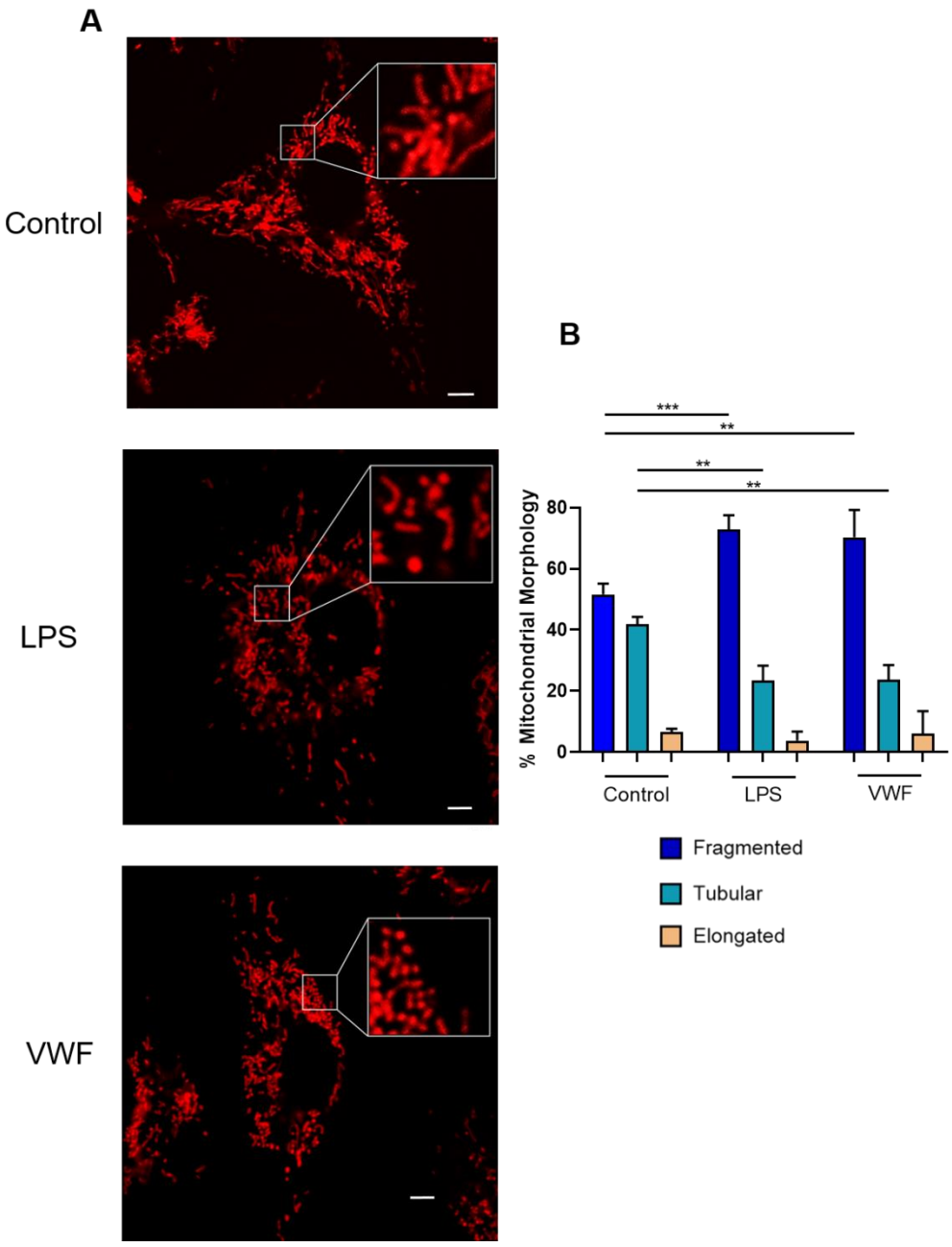

Figure 5.11: VWF influences mitochondrial morphology

A: Representative live cell image of BMDMs using scanning confocal following incubation with pd-VWF (10µg/ml) or LPS (100ng/ml) for 3 hours and mitochondria stained using MitoTracker-Red. Scale bar represents 5µm. **B:** Quantification of mitochondrial morphology ± SEM. Significance determined by one-way ANOVA (**p<0.01, *** p<0.001). A minimum of 20 images per treatment were taken and ≥ 60 mitochondria per cell were analysed per treatment. Fragmentation was classified as <1µm, tubular as 1µm – 2.9µm and elongated as >3µm.

5.9: Extended exposure to pd-VWF no longer affects macrophage architecture

In view of the fact that we previously observed that the effects of pd-VWF in regulating macrophage metabolism were time-dependent, the effects of extended duration incubation (16 hours) of pd-VWF on BMDM mitochondrial morphology were investigated. After 16 hours incubation with LPS (100ng/ml) significant mitochondrial fragmentation with concurrent loss of tubular or elongated forms was seen (Figure 5.12). In contrast however, mitochondrial morphology had normalised following 16 hours exposure to pd-VWF (10µg/ml). These findings further support the hypothesis that VWF promotes short-term marked increases in macrophage glycolysis.

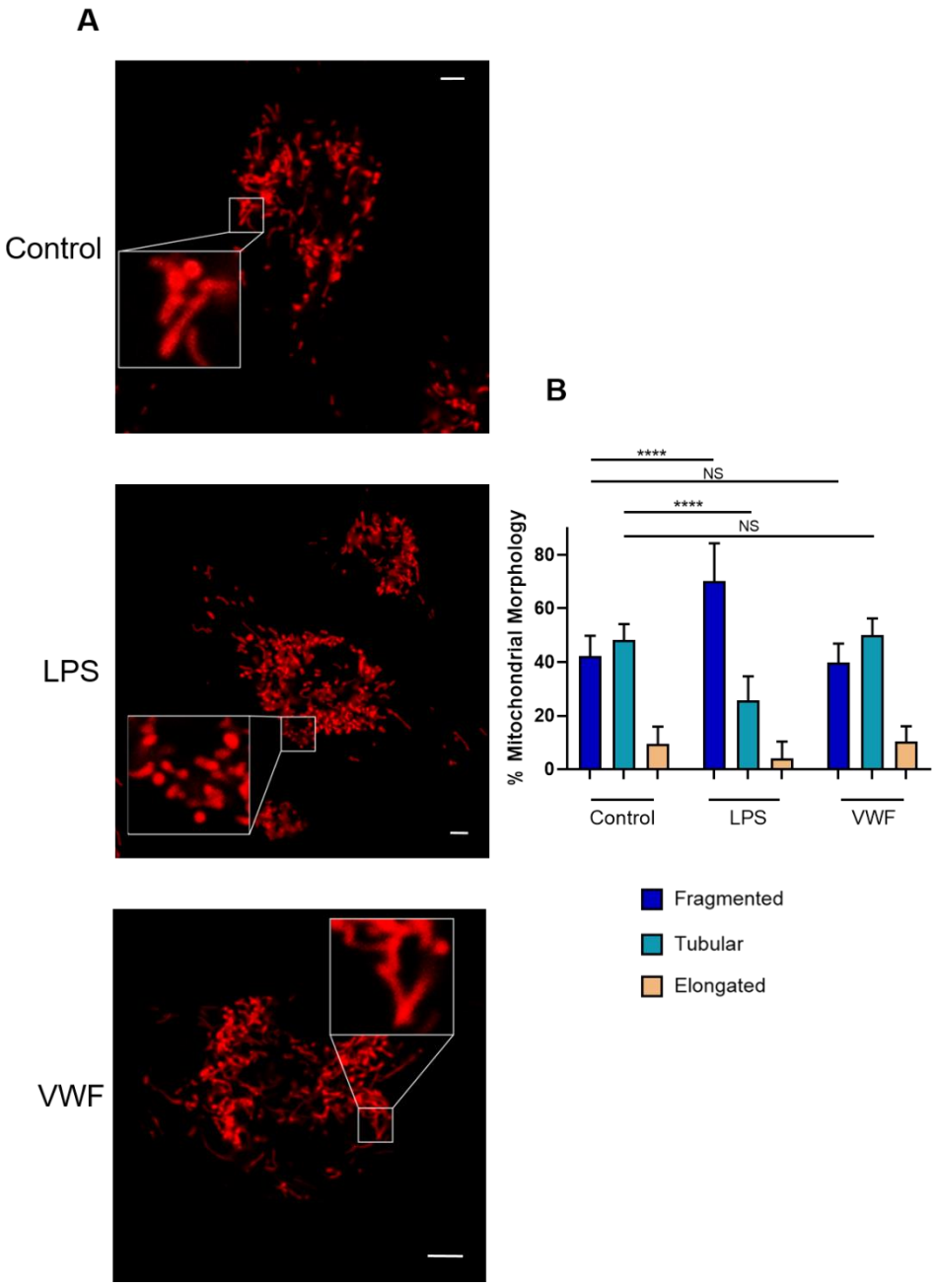

Figure 5.12: Extended exposure to pd-VWF no longer affects macrophage architecture

A: Representative live cell image of BMDMs using scanning confocal following incubation with pd-VWF (10µg/ml) or LPS (100ng/ml) for 16h and mitochondrial stained using MitoTracker-Red. **B:** Quantification of mitochondrial morphology ± SEM. Significance determined by one-way ANOVA (NS-Not Significant, **** $p<0.0001$).

5.10: VWF drives expression of pro-inflammatory chemokines

In view of the ability of VWF-binding to upregulate pro-inflammatory cytokine secretion, we investigated its effects upon macrophage chemokine expression. Chemokines are the cytokines that control cell migration in both inflammatory and homeostatic settings.(272) Numerous chemokines exist, however they can be divided into 4 families based on their initial cysteine residue location (XC, CC, CXC and CX3C).(272) When chemokines bind to their respective chemokine receptors it induces cell mobility. Importantly, following chemokine syntheses they are released into the extracellular space and bind to extracellular matrix proteins or remain in solution.(272) This local chemokines generates a concentration gradient that facilitates the direction of cell migration.(273) Pervious studies have demonstrated that antagonises a known macrophage VWF receptor (LRP1) with endogenous proteins results in the synthesis chemokines CCL2, CCL3 and CCL4.(240) Given our results thus far, we sought to investigate if VWF binding to primary human macrophages resulted in chemokine expression. Interestingly, VWF macrophage treatment was associated with a significant increase in chemokine expression of which CCL2 and CCL3 were similar to that observed with the LPS positive control (Figure 5.13).

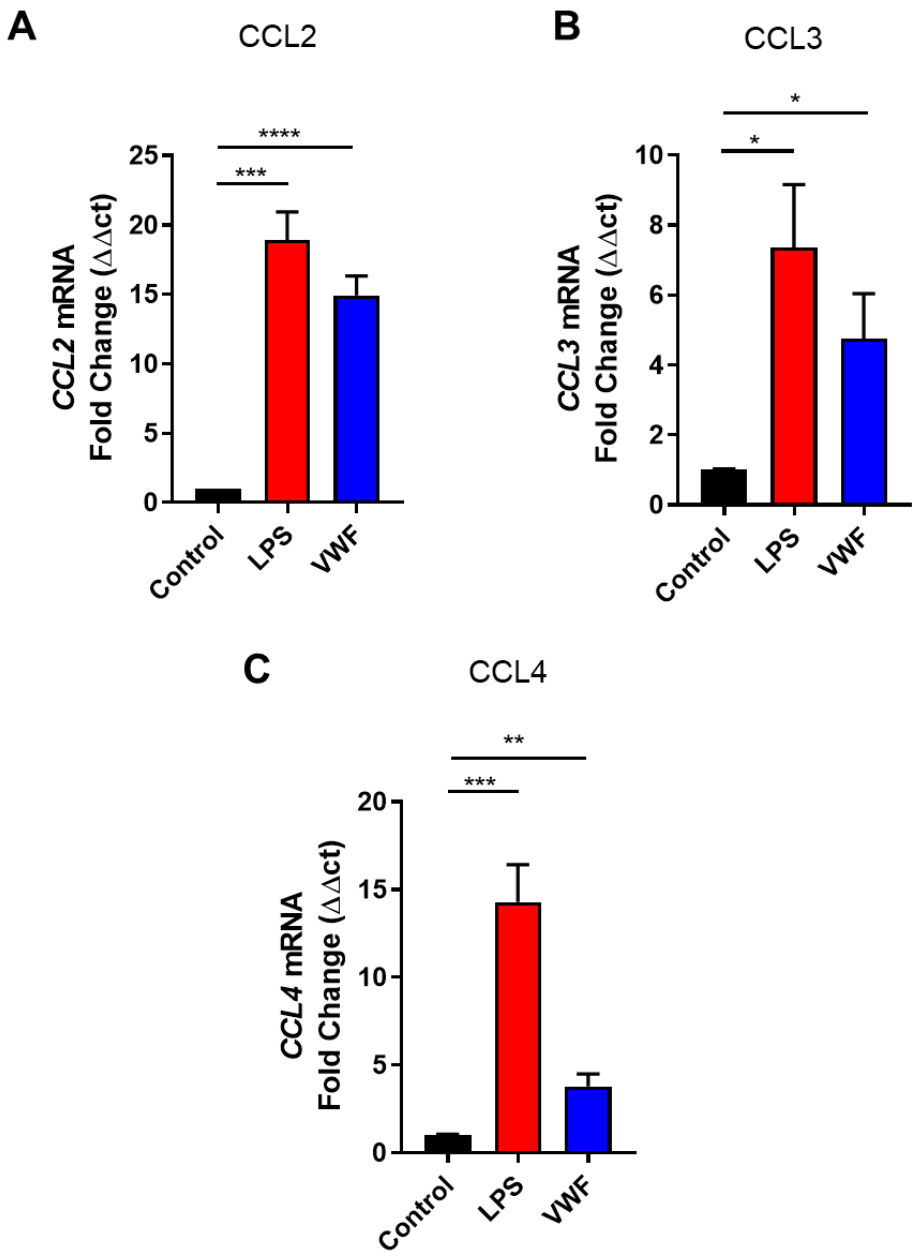

Figure 5.13: VWF induces chemokine expression

pd-VWF (10µg/ml) or LPS (100ng/ml) stimulation of primary human macrophages for 24h resulted in a significant in expression levels for a number of chemokines including **A:** CCL2 ($p<0.0001$), **B:** CCL3 ($p<0.05$) and **C:** CCL4 ($p<0.01$). All experiments were performed in triplicate, and the results presented represent the mean values ± SEM. Significance determined by t-test (*$p< 0.05$, **$p< 0.01$, ***$p< 0.001$ ****$p< 0.0001$ respectively).

5.11: VWF treatment promotes monocyte chemo-attraction

The potential functional significance of VWF-induced chemokine expression was further investigated using a transmigration chemotaxis assay with supernatants collected from primary human macrophages stimulated with either pd-VWF (10μg/ml), r-VWF (r-VWF) (10μg/ml) or LPS (100ng/ml) respectively. Chemoattraction was determined using a transwell chamber. Harvested treated macrophage supernatants were placed into the lower chamber and freshly isolated human primary monocytes were placed in the upper chamber. Monocytes were allowed to migrate to the lower chamber over a 2.5 hour period to ensure chemokine existed. Similar to LPS-treated positive controls cells, supernatants collected from macrophages stimulated with either pd-VWF or r-VWF were both effective in promoting significantly enhanced monocyte transmigration (Figure 5.14). Interestingly however, the supernatant from pd-VWF treated macrophages was significantly more effective than LPS at recruiting monocytes. Collectively, these findings demonstrate that VWF binding plays a novel role in regulating macrophage chemokine expression and thus has the potential to directly influence chemotaxis *in vivo*.

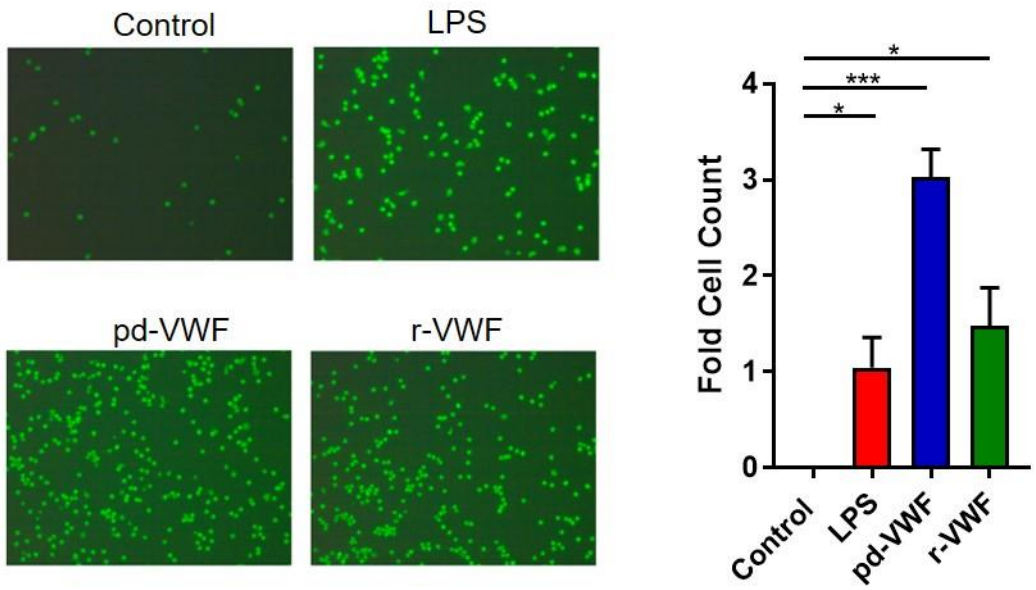

Figure 5.14: VWF treatment promotes monocyte chemoattraction

Primary human macrophages were incubated with pd-VWF (10µg/ml), r-VWF (10µg/ml) or LPS (100ng/ml) for 24 hours. Cell supernatants were collected and placed in the lower chamber of a transmigration assay. Naïve human monocytes were placed in the upper chamber and allowed to migrate for 2.5 hours. Migrated cell were ladled (cell tracker green), imaged and quantified using Image J software. Data is represented as average fold cell-count increase ± SEM. (*P < 0.05, ****P < 0.0001)

5.12: VWF has pro-inflammatory and chemo-attractive effects *in vivo*

As discussed in the previous two Chapters, *in vitro* binding of VWF to macrophages is associated with polarization towards an M1 pro-inflammatory phenotype, metabolic changes and production of pro-inflammatory cytokines and chemokines. To further investigate the potential *in vivo* significance of these observations we utilized a previously described model of chemotaxis in which pd-VWF (2mg/kg) or saline control was injected into the peritoneum of wild type mice to determine the immunogenicity of VWF. (279–281) Peritoneal lavage was then performed and cellular content analysed by flow cytometry at 3 hours and 24 hours post injection. At 3 hours, in contrast to the control mice, pd-VWF treatment was associated with a significant infiltration of both neutrophils and NK cells into the peritoneum (Figure 5.15 A and B). Moreover, VWF treatment was also associated with significant reduction in resident peritoneal macrophages (Figures 5.15 C and D). By 24 hours, no significant differences were observed between the VWF-treated and control mice with respect to peritoneal NK or macrophage levels, and only a mild increase (5.77% compared to 27.66% at 3 hour treatment) in neutrophil recruitment was remained (Figures 5.15 A, B and C). Furthermore, VWF-treatment had no effect on peritoneal T cell populations at either the 3 or 24 hour time points (Figures 5.15 E and F). Cumulatively these data, particularly the early influx of neutrophils and loss of resident macrophages (Figures 5.15 A and C), demonstrate that VWF has chemo-attractive and pro-inflammatory properties *in vivo* that are consistent with its *in vitro* effects on macrophage biology

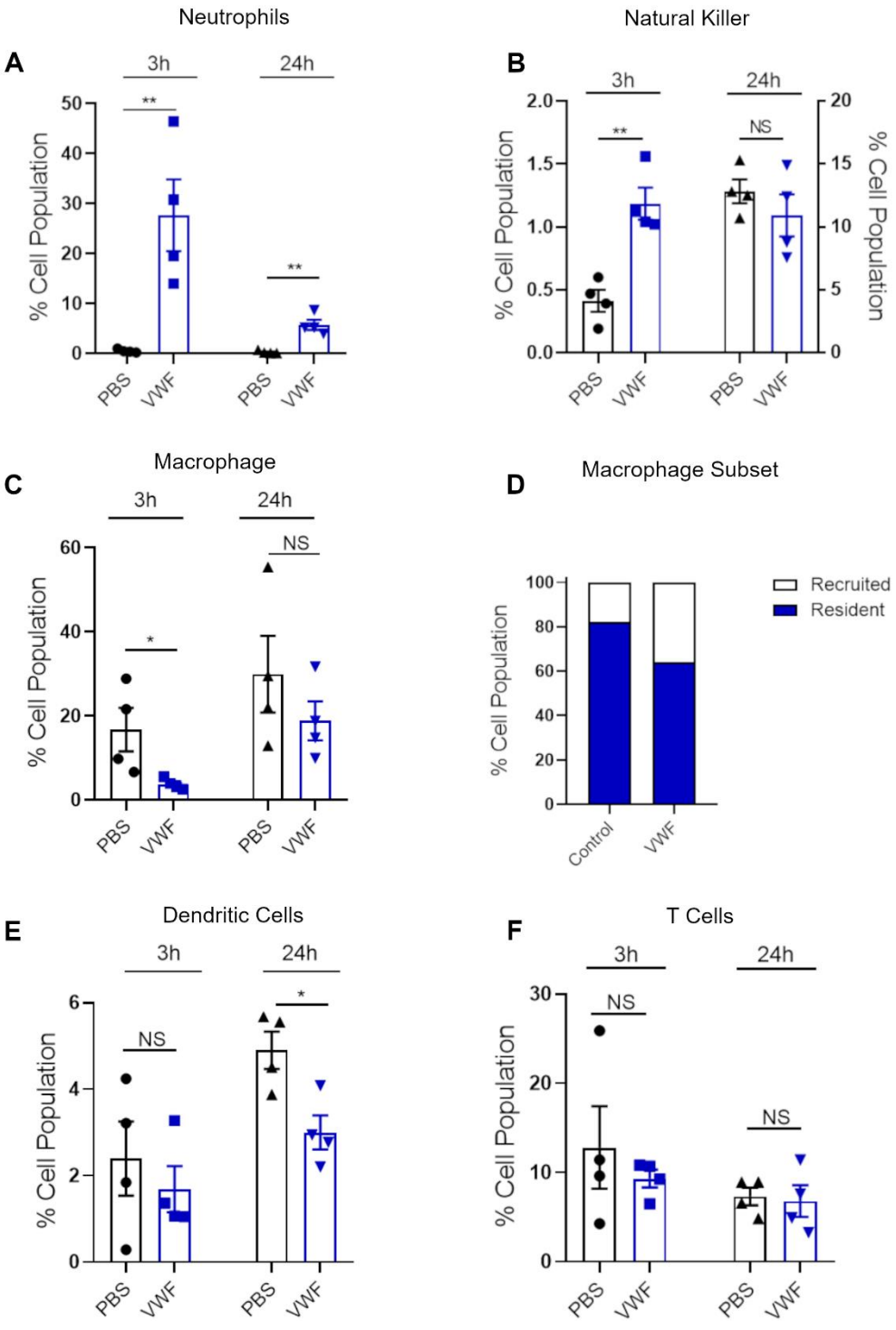

Figure 5.15: VWF has pro-inflammatory and chemo-attractive effects *in vivo*

A-F: VWF (2mg/kg) or PBS (control) were injected into the peritoneum of female WT mice. After 3 or 24 hour periods, mice were sacrificed, peritoneal lavage was performed and peritoneal cell populations quantified by flow cytometry. Data represented by percentage of cell population ± SD. 4 mice were used per group. Significance was determined by t-test (*p<0.05, **p<0.01, ***p<0.001,****p<0.0001).

5.13: VWF alters the phagocytic capacity of macrophages

Phagocytosis is a crucial immune process responsible for the clearance of invading and or self-antigens. The phagocytic capacity of macrophages has previously been reported to be dynamic in nature and thus can vary depending upon the local environment. For example, incubation with GM-CSF significantly enhances bacterial phagocytosis by macrophages. Conversely, treatment with IL-4 reduces macrophage phagocytosis capacity.(282)(283) Similarly, despite its pro-inflammatory effects, LPS has also been shown to attenuate the phagocytic ability of macrophages.(284) We have demonstrated that VWF can alter macrophage immune response and now investigate whether VWF can alter macrophage phagocytic ability.

Internalised GFP-labelled *E.Coli* were used as a marker for phagocytosis. Primary human macrophages were first treated with either pd-VWF (10µg/ml) or LPS (100ng/ml). Subsequently, the macrophages were incubated with the GFP-*E.Coli*, and intercellular florescence was determined by flow cytometry. Interestingly, a short (30-minute) pre-treatment with VWF or LPS resulted in a 50% reduction in phagocytosis capacity of primary macrophages (Figure 5.16).

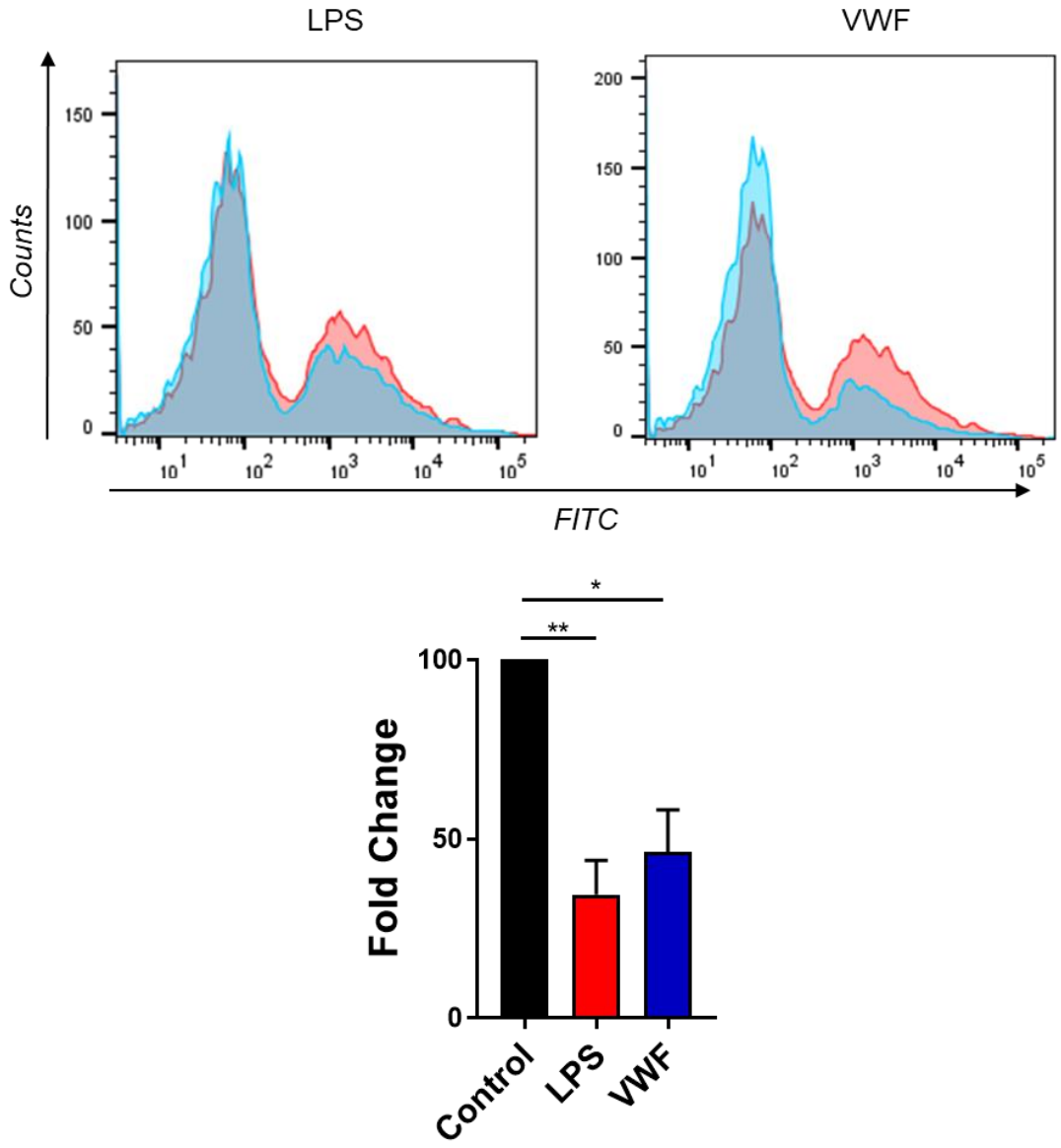

Figure 5.16: VWF attenuates macrophage phagocytosis capacity

Representative histograms of E.Coli-GFP ($2.5X10^6$) treated macrophages (1.5 hours) in which blue represents pd-VWF (10µg/ml) or LPS (100ng/ml) 30 minute pre-treatment and red population represents untreated control. Data is represented by fold reduction from untreated macrophage ± SEM. Significance determined by t-test (*p<0.05, **p<0.01).

5.14: Discussion

A 1-2hour LPS treatment rapidly elevates macrophage glycolysis/ECAR by doubling glucose uptake and metabolism though enhanced GLUT1 and hexokinase expression.(257,258) Furthermore, a 1-2 hour LPS treatment also rapidly induces expression and phosphorylation of pyruvate kinase M2, stabilizing HIF-1α.(259) In line with our results from chapter 4, IL-6 and TNF-α combined with the production of reactive oxygen species are also detected up to as early 2-4 hours post stimulation.(258,261). Beyond 4 hours of activation, macrophages progress past early glycolytic reprograming and fall into a complete glycolytic amplification phase due to profound metabolic alterations. At this time point, LPS increases the levels of glycolytic enzymes PFKFB3 and PFK1 which further drive glycolysis. (285) If exposure to inflammatory agonists continues beyond 4-6 hours the TCA cycle begins to operate as a partial anabolic system and succinate accumulates elevating HIF-1α.(266) At this point the macrophages has firmly adopted changes that drives glycolysis and diminished oxidative respiration.(266) Fascinatingly, unlike LPS, VWF cannot maintain this glycolytic effect beyond the amplification phase and distinct differences in these time dependent pathways must exist.

Both LPS and VWF rapidly (<3 hours) enhanced glycolysis (Figure 5.1, 5.2) and as expected only minor alterations in oxygen consumption rate (Figure 5.3). Macrophages undergo complete metabolic reprograming following prolonged exposure to inflammatory stimuli, adopting a heightened state of glycolysis with a concurrent reduction in oxidative phosphorylation. In line with the literature, we

demonstrated that a prolonged 16 hour LPS treatment resulted in a sustained elevation of ECAR (Figure 5.2) and a concurrent drop in oxidative phospholation (OCR) as glycolysis prevailed (Figure 5.3) as metabolic reprograming occurred. However, VWF could not exert the same effect as LPS at this longer time point (Figure 5.2) as ECAR returned to almost control levels with no reduction in OCR. This suggests that VWF has a profound ability to drive and initiate rapid glycolytic reprograming within macrophage's however, it does not lead the substantial metabolic reprograming that is observed with prolonged LPS exposure.

VWF altered one aspect of OCR, the MRC. Interestingly both VWF and LPS after a 3 hour incubation enhance MRC (Figure 5.4). However, following a 16 hour treatment VWF dependent MRC has dropped (Figure 5.4). In line with these results are the changes in SRC. SRC is a measure of macrophage bioenergetics reserve, which reveals the extent in which macrophages can respond in times of stress. Following a 3 hour incubation, VWF results in significant increase in both glycolytic and oxidative SRC (Figure 5.5), thus VWF treatment enhances the potential energy expenditure of the macrophages. All together, these novel data support the hypothesis that VWF binding is associated with a significant pro-inflammatory effect on macrophages. Furthermore, in striking contrast to LPS, the pro-inflammatory effects of VWF appear to be time-dependent in nature. The biological mechanisms underlying this time-dependent effect remain to be defined. Given that VWF is an endogenous protein perhaps it is an elegant mechanism in which VWF primes the innate immune response at sites of injury but gives way to well-established pathways of inflammation. Furthermore, our

previous studies have shown that following the binding of VWF to macrophages, it becomes internalised and degraded.(117,194,196,286) This endocytosis may clearly impact on the duration of the VWF effect in regulating cellular immuno-metabolism.

Mitochondrial are highly dynamic originals and are historically known to alter their morphology are in activated macrophages with altered metabolic state.(252,261) Changes in mitochondrial size and number are largely controlled by the processes of fission and fusion.(287) Fission is the processes of forming multiple smaller fragments from a singular parent mitochondrial while fusion is the generation of one larger mitochondria from individual structures. When macrophage glycolysis is increased, mitochondria develop a characteristic fragmented fission appearance.(190,270,271) In keeping with the concept that VWF binding has a significant pro-inflammatory effect upon macrophages, we observed that treatment with VWF for 3 hours was associated with significantly higher levels of mitochondrial fragmentation. However, once again this VWF effect had a time-dependent element, such that following 16 hours exposure to VWF, (in contrast to LPS), mitochondrial morphology had returned to normal. Cumulatively, these findings suggest that VWF binding has modulatory effects upon macrophage morphology, which in turn impact upon mitochondrial metabolism to promote a short-term marked increase in glycolysis.

In keeping with its ability to up-regulate pro-inflammatory cytokine secretion, we observed that VWF binding to macrophages was also associated with a significant

increase in expression of the chemokines CCL2, CCL3 and CCL4. Using an *in vitro* transmigration assay, we demonstrated that supernatant from VWF-stimulated macrophages was effective in promoting monocyte transmigration. In addition, we confirmed that intraperitoneal injection of VWF was associated with a significant infiltration of both neutrophils and NK cells *in vivo*. In addition, VWF was associated with a significant reduction in resident peritoneal macrophages, followed by a trending increase of recruited macrophages. Thus, VWF not only plays a key role in the initiation of haemostasis at sites of vascular injury, but also functions to prime local macrophages to initiate pro-inflammatory responses. In this local milieu, we propose that VWF functions as a damage signal that is recognized through specific macrophage pattern-recognition receptors. Importantly in this context, the pro-inflammatory effects of VWF on macrophages are time-limited such that they are lost with longer-term exposure. Thus, hepatic Kupffer cells that are involved in regulating physiological VWF circulatory clearance presumably remain unaffected due to their ongoing VWF exposure.

6. LRP1 and p38 regulate VWF inflammatory effect

6.0 Introduction

The data presented in Chapters 3,4, and 5 of this Thesis, collectively demonstrate that VWF binding to macrophages has significant pro-inflammatory effects. In this context, VWF exhibits similar properties to a number of other damage associated molecular patterns. Importantly however, in contrast to the pro-inflammatory effects observed with LPS, the effects of VWF on macrophages are time-dependent. In particular, the pro-inflammatory properties of VWF are attenuated following prolonged exposure. This finding is consistent with the observation that VWF is endocytosed and degraded by macrophages. Recent studies have described putative roles for a number of macrophage surface receptors in regulating interaction with VWF. They include scavenger receptors (e.g. SR-A1)and LRP1) as well as a number of C type lectins (e.g. MGL) and Siglecs-5.(119,121,123,124)

The SR-A1 receptor recognises a large number of diverse ligands, including endogenous proteins and microbial structures. SR-A1 contains a type A scavenger receptor cysteine-rich domain, a collagen domain, a C-type lectin domain and a cysteine-rich domain.(288),(289) Importantly, *SR-A1* knockout mice display an increased VWF propetide:antigen (VWFpp:Ag) ratio consistent with reduced clearance of endogenous murine VWF. Furthermore, it has been demonstrated that SR-A1 directly interacts with the D'D3, A1A2A3 and D4 domains of VWF.(121) These findings suggest that SR-A1 may contribute to the normal physiological clearance of VWF in mice. In addition, SR-A1 has also been implicated in regulating

immune responses. SR-A1 engages bacterial membrane structures like LPS and Lipoteichoic acid (LTA), and also acts as a co-receptor for Toll like receptors (TLRs).(290,291) In terms of its pattern recognition function, SR-A1 is important for phagocytosis of invading microbes and thus *SR-A1* knockouts have increased susceptibility to infection.(292), (293) Furthermore, SR-A1 is also important in oxidised-LDL clearance.(294,295)

The LRP1 receptor is composed of a large extracellular α-chain and a transmembrane intercellular β-chain. Importantly, the α-chain contains 4 ligand binding cysteine-rich complement type repeat regions, referred to as clusters I-IV.(296) VWF A1 domain binds to LRP1-cluster IV facilitating its clearance in a sheer dependent manner.(122) Moreover, LRP1 has a complex immune role. Genetic deletion of macrophage *LRP1* results in activation of NF-KB and JNK. Furthermore LRP1 also dimerizes with TLRs and integrins.(296–298) Given these multiple functions, it is unsurprising that recent studies have demonstrated that LRP1 signalling can trigger different inflammatory effects in response to the binding of different ligands.(240)

VWF also interacts with other macrophages receptors including Siglec-5 and MGL. The Siglec-5 receptor is composed of four immunoglobulin-like extracellular domains.(299) The extracellular domains and cytoplasmic tail are linked by a transmembrane domain.(299) Pegon *et al*, demonstrated that VWF binds to macrophage Siglec-5, and that Siglec-5 can also mediate VWF internaliseation.(124) Siglecs have been also been shown to play important roles

in immune regulation, cell adhesion and endocytic function.(300) Importantly, the Siglec 5 protein contains cytosolic immunereceptor tyrosine-based inhibitory motifs (ITIMs). Other receptors that harbour this same domain have been shown to exert anti-inflammatory effects through suppressing activation signals originating from receptors baring immunoreceptor tyrosine-based activation motifs (ITAMs).(300),(301)

Recent studies from our laboratory have identified MGL as an important receptor for the clearance of hyposialylated VWF.(119) MGL is a C-type lectin that recognises self-antigens and maintains a regulatory role, suppressing T cell response and driving immune tolerance.(302,303)

Given the fact that VWF can interact with multiple different macrophage receptors, in this Chapter we have investigated the biological mechanism(s) through which VWF binding to macrophages results in a significant pro-inflammatory effect.

6.1: Expression of LRP1 is increased in primary human macrophages compared to THP1 macrophages

Our previous studies (Chapter 2) demonstrate that VWF binds to both primary human macrophages and THP1 macrophages. VWF binding to primary macrophages was associated with significant downstream pro-inflammatory effects, including a significant increase in the expression of pro-inflammatory cytokines and chemokines. In contrast however, minimal pro-inflammatory effects were observed in THP1 macrophages. In particular there was no evidence of increased MAPKinase or NF-κB signalling. Furthermore, the expression of pro-inflammatory cytokines (TNF-α, IL-6 and IL-1β) were minimally affected following VWF treatment. Conversely, LPS treatments in both primary human macrophages and THP1 macrophages resulted in similar pro-inflammatory responses. In order to further understand the biological mechanisms underpinning the pro-inflammatory effects of VWF, we investigated expression of macrophage scavenger receptors SR-A1 and LRP1 on primary macrophages compared to THP1 macrophages. Of note, previous studies have suggested that ligand binding to both the LRP1 and SR-A1 receptors can trigger pro-inflammatory signalling.(234,238,240)

Using quantitative RT-qPCR, significantly increased levels of both LRP1 and SR-A1 were observed following differentiation of either primary human monocytes or THP1 cells into macrophages (Figure 6.1A). Interestingly, although similar levels of *SR-A1* mRNA were present in both human and primary macrophages, the levels of *LRP1* mRNA were markedly increased in primary macrophages (Figure 6.1A). Similarly, Western blot analysis preformed after 3 or 7 days of macrophage

differentiation demonstrated that LRP1 expression levels were significantly higher in primary macrophages (Figure 6.1B). Taken together, there data suggest that LRP1 rather than SR-A1 may be more important in regulating the pro-inflammatory effects of VWF on macrophages, and explain why these pro-inflammatory effects are more pronounced in primary human macrophages compared to THP1 macrophages.

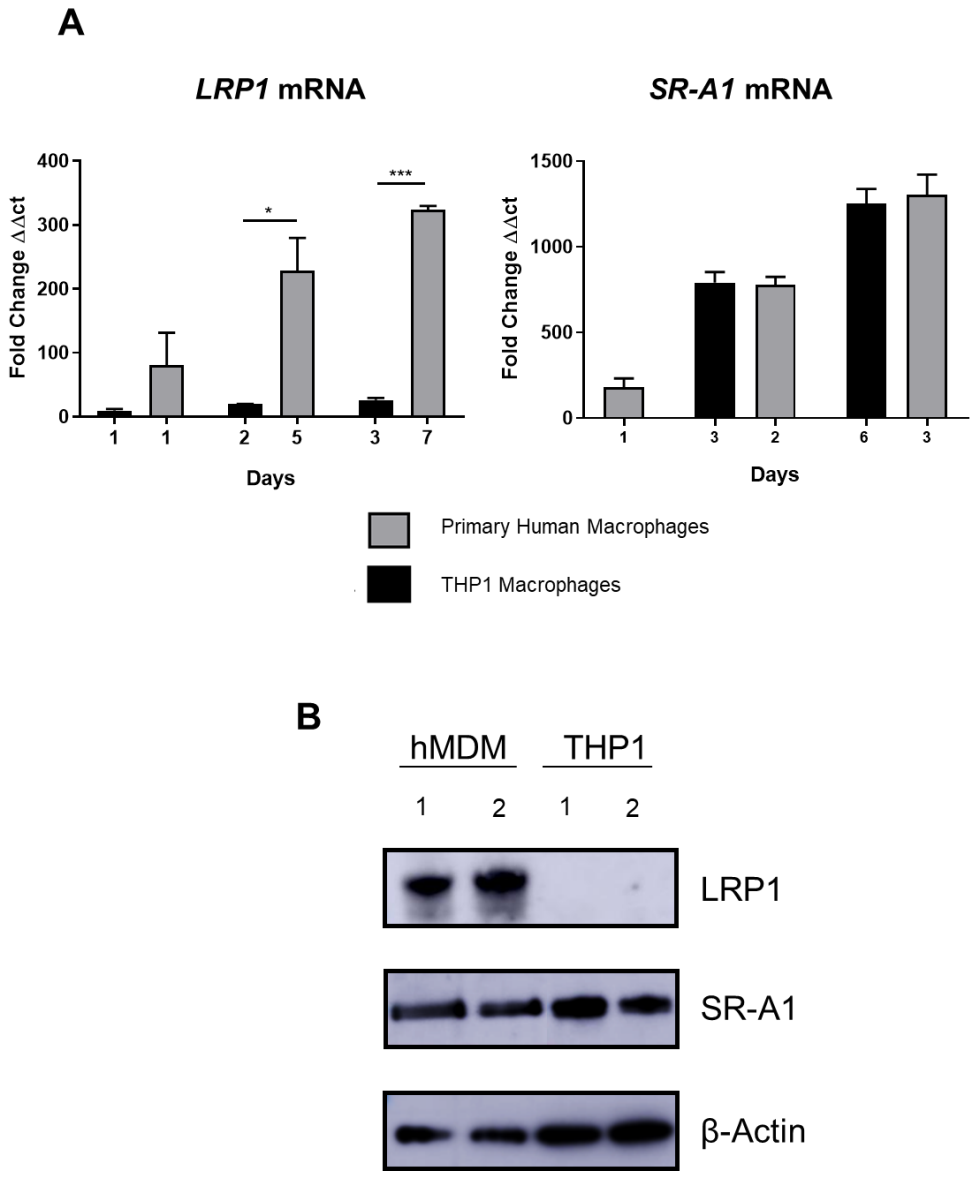

Figure 6.1: LRP1 Expression is higher in primary macrophages compared to THP1 macrophages

A: LRP1 and SR-A1 mRNA levels were assessed by RT-qPCR and are represented as mean ± SEM. Differentiation of THP1 occurs over a 3 day period and human primary macrophages over a 6-7 day period. Significance was determined by t-test (*$p<0.05$, **$p<0.001$) **B:** LRP1 and SR-A1 protein levels in primary human and THP1 macrophage lysates were assessed by Western blot. Lanes 1 and 2 are replicates of either primary human macrophages or THP1 macrophages. Total protein levels were compared by β-actin blotting.

6.2: Inhibition of LRP1 decreases VWF binding to macrophages

To further investigate a possible role for the LRP1 receptor in modulating the pro-inflammatory properties of VWF, *in vitro* binding experiments using r-VWF and primary BMDMs were repeated in the presence or absence of a monoclonal anti-LRP1 inhibitory antibody. Using flow cytometry, significantly reduced VWF binding to BMDMs was observed in the presence of this antibody (Figure 6.2). Importantly, these binding experiments were performed under static conditions (in the absence of ristocetin) are interesting given that recent studies have shown that in addition to the conformational dependent binding of the A1 domain to LRP1, a number of other domains can also modulate LRP1 interaction.(121)

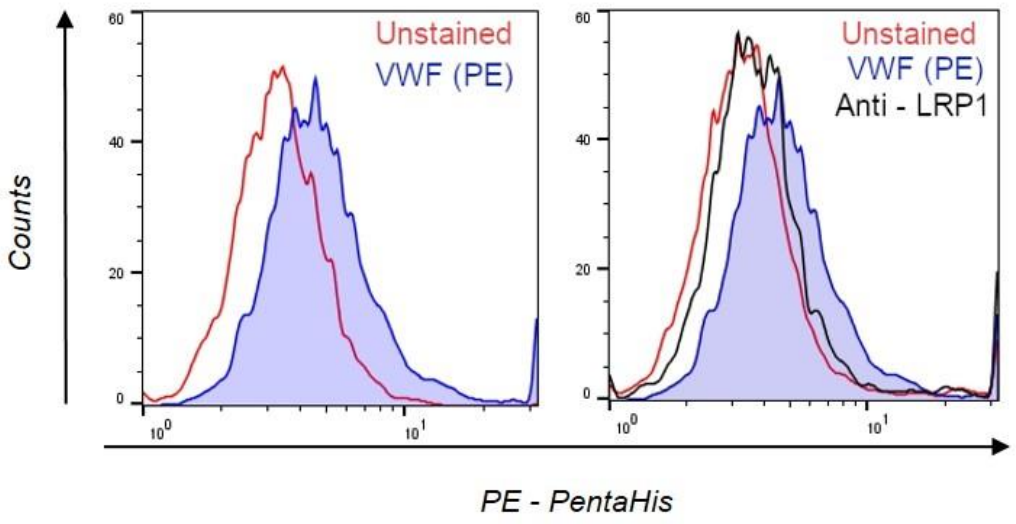

Figure 6.2: Blocking of LRP1 ablates VWF binding to macrophages

Recombinant VWF (75µg/ml) was incubated with BMDM in the presence or absence of an anti-LRP1 antibody. Binding was detected by flow cytometry as before. Representative histograms are shown. The red population represents non-VWF treated cells; the blue population shows BMDM with bound VWF detected by a PE tagged anti-pentahis; the black population shows VWF incubated in the presence of LRP1 blocking antibody.

6.3: LRP1 co-localises with VWF on the surface of macrophages in the presence or absence of ristocetin.

Previous studies have reported that LRP1 plays an important role in regulating macrophage mediated VWF clearance *in vivo*. (122,123) In addition, a number of discrete VWF domain have been implicated in modulating LRP1 binding. These include the VWF D'D3, A1 and D4 domains.(121,122) Importantly, binding of full length VWF to LRP1 was significantly enhanced in the presence of shear or ristocetin.(122) Furthermore, enhanced LRP1 binding was also reported for the type 2B VWF gain of function V1316M variant.(122) Cumulatively, these findings support the hypothesis that conformation of the VWF A1 domain impacts upon interaction with LRP1 receptor.

To further investigate the role for LRP1 in modulating VWF binding and/or triggering intercellular pro-inflammatory signalling, we performed Duolink® PLA to investigate for co-localisation of VWF and LRP1 on the surface of THP1 macrophages or BMDM in the presence or absence of ristocetin respectively. In this PLA assay, positive red florescence is observed when the proximity of two tagged proteins lies within a maximum distance of 40nm. In the presence of ristocetin (1.5mg/ml), red staining of most THP1 macrophages was observed (Figure 6.3). As before, VWF binding to macrophages was significantly reduced under static conditions in the absence of ristocetin. Nonetheless, the PLA assay demonstrated that, even in the absence of ristocetin, LRP1 was still involved in regulating VWF binding to BMDM (Figure 6.3 B). All together, this data is consistent

with the concept that domains outside of the A1 domain can support sheer independent interaction with macrophage to LRP1.

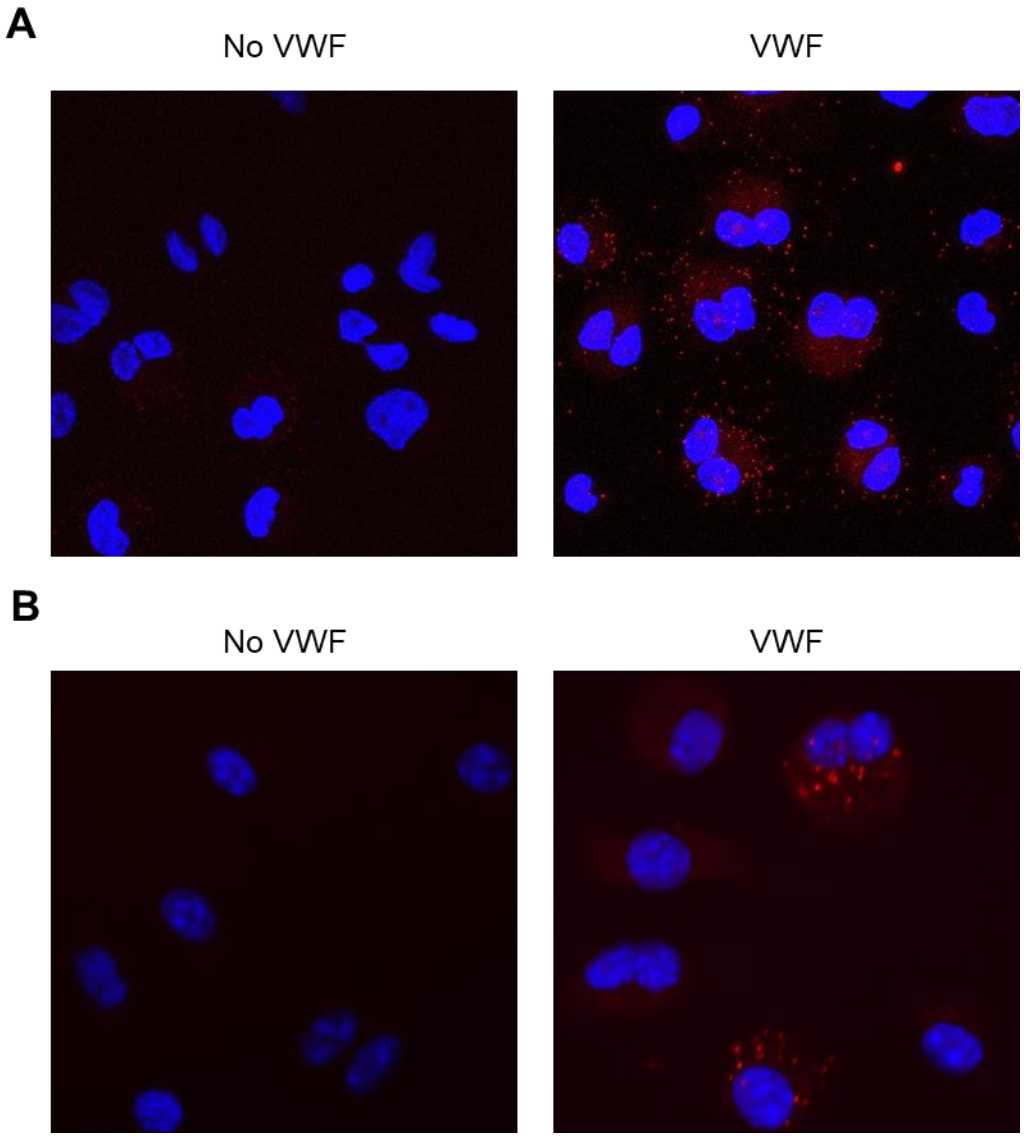

Figure 6.3: LRP1 co-localises with VWF on the surface of macrophages in the presence or absence of ristocetin

THP1 macrophages and BMDM were incubated with pd-VWF (10µg/ml) for 30minutes **A:** THP1 incubated in the presence of ristocetin (1.5mg/ml) or **B:** BMDM in the absence of ristocetin. Representative images of Duo link detection of LRP1-VWF interaction are shown. Red florescence indicated VWF-LRP1 colocalization, nucleus blue. Control: duolink staining without the presence of VWF.

6.4: Inhibition of LPR1 with receptor-associated protein (RAP) attenuates VWF signalling.

Significant evidence from previous studies has demonstrated that the LRP1 receptor plays a key role in regulating inflammatory signalling in macrophages. Thus, conditional macrophage LRP1 deletion results in profound inflammatory effects, driving production of CCL2 and CCL3, increasing migration capacity, and promoting NF-κB signaling.(304,305) The LRP1 receptor is promiscuous in nature and can bind a large range of diverse ligands. Critically, the effects of LRP1 activation in modulating the inflammatory properties of macrophages have been shown to be dependent upon specific ligand binding interactions. For example, recent studies have reported that the binding of α2-macroglobulin (α2M) and tissue-type plasminogen activator (TPA) suppress LRP1 dependent inflammatory signalling.[37] Conversely, lactoferrin binding to LRP1 significantly enhances downstream pro-inflammatory signalling with TNF-α, IL-6, CCL2 and CCL3 production through NF-κB activation.(240)

To investigate whether LRP1 binding is involved in triggering VWF pro-inflammatory signalling, primary macrophages were incubated with pd-VWF (10µg/ml) in the presence or absence of RAP (200nM) and signalling pathways were assessed as before. Receptor Associated Protein (RAP) is an endoplasmic reticulum chaperone protein for a large number low density lipoprotein receptors.(306) RAP is routinely used in VWF studs for the blocking of LRP1 and other low density lipoproteins receptors.(123,194) Interestingly, in the presence of RAP, a significant reduction in VWF induced MAPKinase p38 was activation was

seen (Figure 6.4). The RAP inhibitory effect appears to preferentially affect p38 signalling as no alterations in VWF induced JNK or NF-κB were detected.

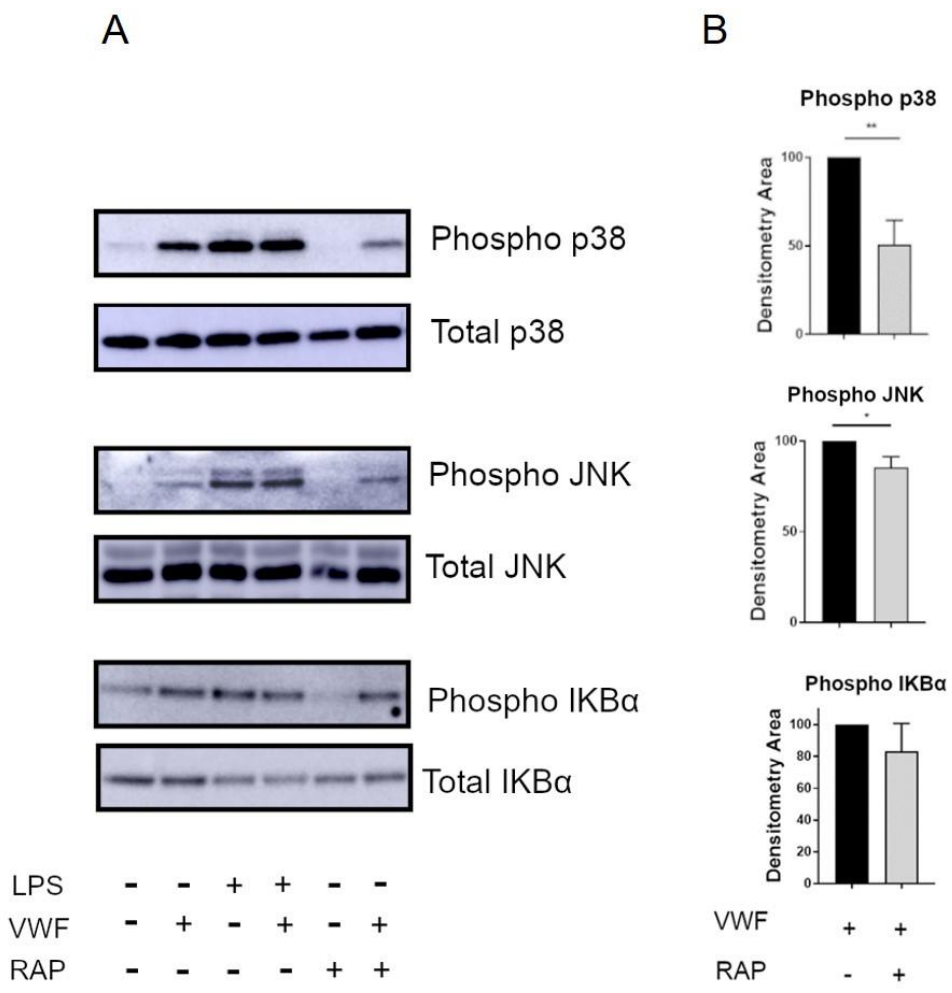

Figure 6.4: Inhabitation of LRP1 with RAP attenuates VWF dependent signalling

A: Representative Western blot of p38, JNK and IKBα signalling in human primary macrophages incubated with VWF (10µg/ml) ± LRP1 inhibitor RAP (200nM) or LPS (100ng/ml) for 30 minute. **B:** Percentage change of densitometry was determined by the average of 4 independent western blots, whereby VWF treatment alone is 100% using imageJ software. Densitometry represented by the mean percentage reduction ±SEM and significance was determined by t-test (*p<0.05, **p<0.001)

6.5: Anti-LRP1 antibody inhibits VWF dependent p38 signalling

To further investigate that the LRP1 receptor plays a role in VWF-dependent inflammatory signalling, we investigated the effects of blocking LRP1 using an inhibitory antibody. For consistency between experiments, BMDMs differentiated with M-CSF were used in order to eliminate discrepancies in donor-to-donor human monocyte derived macrophage (hMDM) differentiation. In keeping with the RAP inhibition experiments, anti-LRP1 inhibitory antibody also significantly reduced VWF-induced p38 signalling but did not alter NF-κB signalling determined by p65 (Figure 6.5). Cumulatively, these findings suggests a role for the LRP1 receptor in regulating VWF-induced p38 mediated signalling.

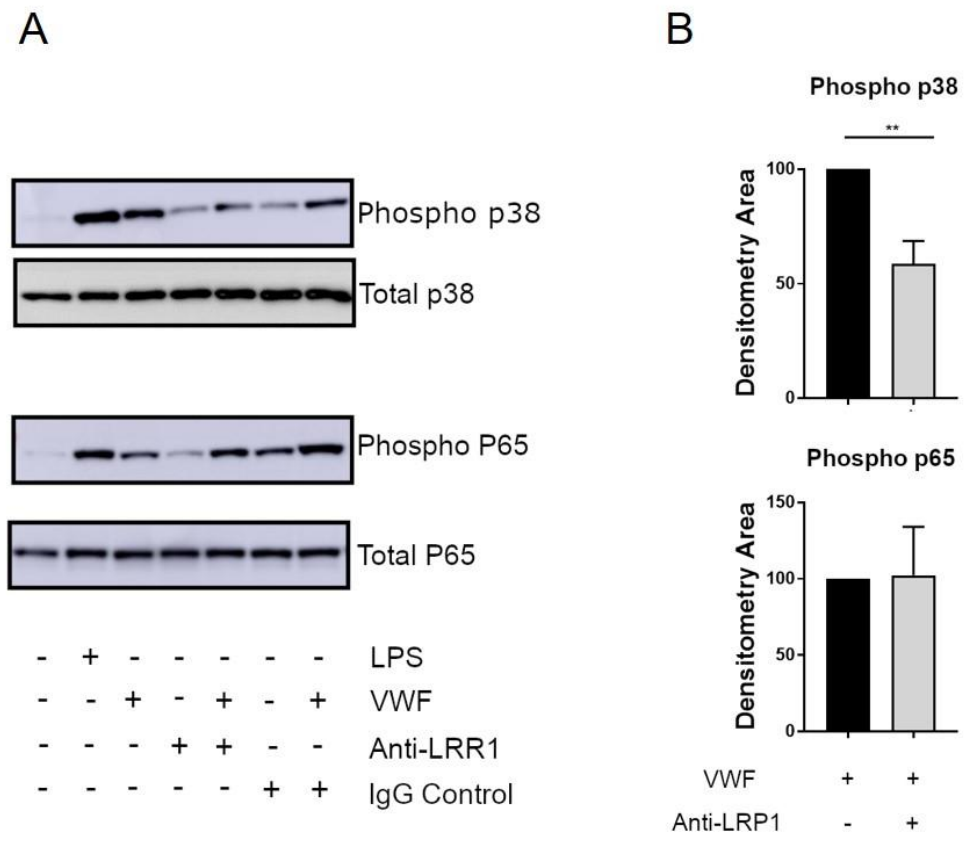

Figure 6.5: Inhibition of LRP1 with anti-LRP1 antibody attenuates VWF dependent signalling

A: Representative image of Western blot analysis from BMDM incubated with VWF (10µg/ml) ± anti-LRP1 inhibitory antibody (200nM) or LPS (100ng/ml) for 30 minute. **B:** Percentage change of densitometry was determined by the average of 4 independent western blots, whereby VWF treatment alone is 100% using imageJ software. Densitometry represented by the mean percentage reduction ±SEM and significance was determined by t-test (**p<0.01).

6.6: The role of HIF-1α in regulating the pro-inflammatory effects of VWF

We have established that VWF binding initiates a pro-inflammatory in macrophage response. In addition, this effect is triggered at least in part though the LRP1 receptor. An important component of this pro-inflammatory effect is a VWF-induced increase in macrophage glycolysis. Previous studies have demonstrated that the ability of DAMPS or PAMPS to enhance glycolysis commonly involves the activation of HIF-1α transcription factor, which subsequently induces expression of a number of key glycolytic enzymes.(259,266),(307)

To further investigate the pathways through which VWF induces time-dependent pro-inflammatory effects in macrophages, HIF-1α levels were assessed following 3 and 16 hour incubations with VWF or LPS. Following 3 hour incubations with either pd-VWF (10μg/ml) or LPS (100ng/ml), a significant increase in macrophage HIF-1α expression was observed (Figure 6.6). Interestingly, although HIF-1α levels remained elevated in BMDMs after a 16 hour LPS incubation, levels had returned almost to baseline in VWF-treated cells over this extended treatment. Thus, these time dependent effects of VWF in regulating HIF-1α expression parallel our previous observations regarding the effects of VWF on macrophage immune-metabolism.

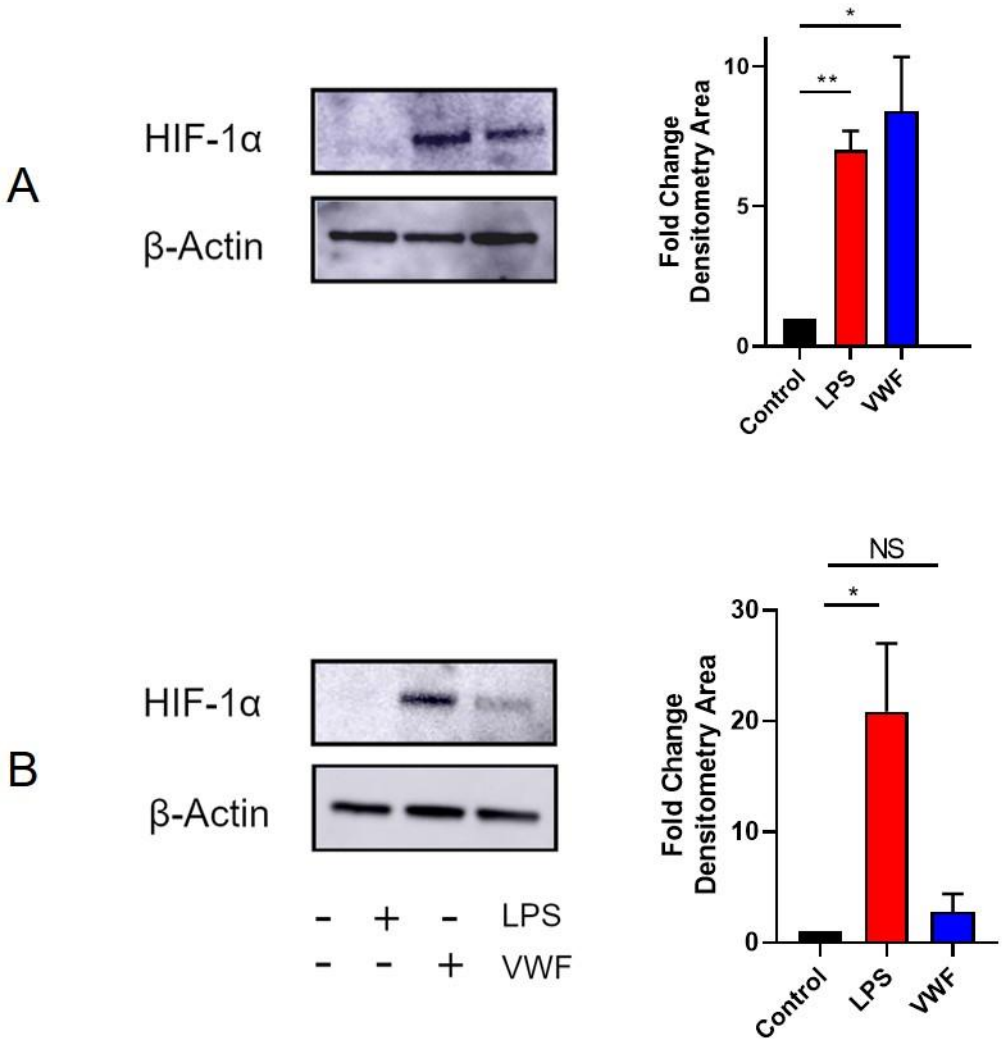

Figure 6.6: The role of HIF-1α in regulating the pro-inflammatory effects of VWF

Representative images from three independent experiments of HIF-1α activation assessed using Western blot and graphs of densitometry analysis using imageJ software. **A**: BMDMs were treated with pd-VWF (10µg/ml) or LPS (100ng/ml) for 3 hours or **B:** 16h and subsequently resolved using SDS-Page. Total protein represented by β-Actin. Densitometry area is represented by the average fold change from untreated control conditions and significance was determined by t-test (*p<0.05, **p<0.01).

6.7: VWF incubation modulates macrophage PHD3 expression levels

Within macrophages, HIF-α becomes hydroxylated in the presence of oxygen by a family of enzymes containing a proyl-hydroxylase domain (PHD). This hydroxylation marks HIF-1α for ubiquitination and thus subsequent degradation.(308) Previous studies have reported that PHD3 plays a key role in HIF-1α hydroxylation, and thereby in the regulation of macrophage immunometabolism. (264)

To further study the mechanisms though which VWF influences HIF-1α levels, macrophage PHD3 levels were assessed in BMDM following incubation with pd-VWF (10μg/ml) or LPS (100ng/ml) for 3 or 16 hours. Following 3 hours, neither VWF nor LPS had any significant effect on *PHD3* mRNA expression (Figure 6.7). However, following a 16 hour treatment with LPS, a significant increase in *PHD3* mRNA was detected. In contrast, a reduction in *PHD3* expression was observed following a 16 hour VWF incubation. Taken together, the HIF-1α and PHD3 data also highlight how the pro-inflammatory effects of VWF on macrophages differ significantly to those of LPS.

.

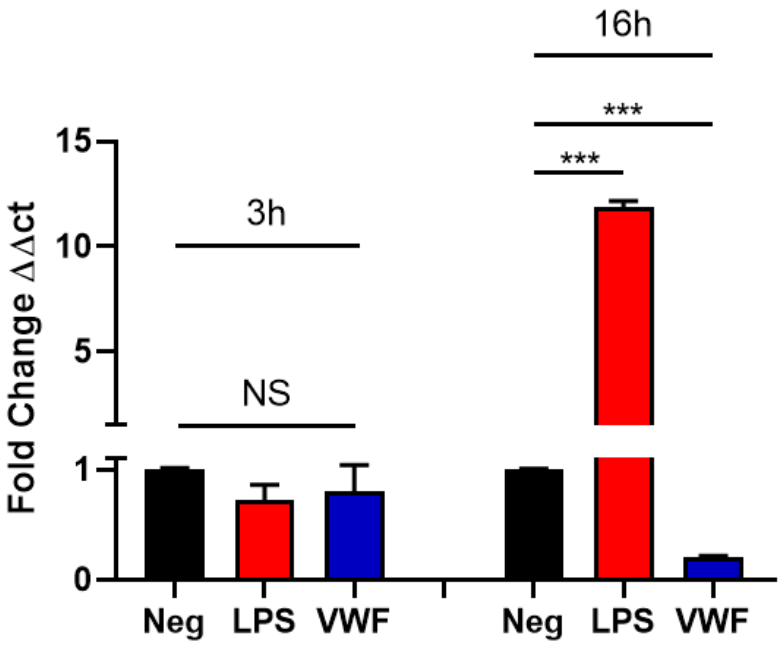

Figure 6:7: VWF incubation modulates macrophage PHD3 expression levels

BMDM were exposed to VWF (10µg/ml) or LPS (100ng/ml) for 3 hour or 16 hour and PHD3 expression was determined by RT-qPCR. Data is represented by the average fold change in gene expression from 3 independent experiments ± SEM. Significance was determined by t-test (***p<0.001, NS non significant)

6.8: VWF regulates macrophage HIF-1α levels and glycolysis via p38 MAPKinase

We have demonstrated that pd-VWF binding drives activation of p38 MAPKinase pathway in human and murine macrophages. In addition, we have further shown that this VWF dependent activation of p38 is modulated at least in part via LRP1. Importantly, previous studies have defined a role for p38 in regulating HIF-1α stabilization and thus macrophage glycolysis.(309)

Consequently, we investigated whether MAPKinase p38 might play a role in the biological mechanism through which VWF-binding promotes macrophage glycolysis. Importantly, inhibition of p38 α/β isomer with SB202190, completely ablated the ability of both LPS and VWF dependent activation of HIF-1α (Figure 6.8). In addition, p38 inhibition also significantly reduced the ability of VWF to promote macrophage glycolysis (Figure 6.9). Cumulatively these novel findings demonstrate that the early stabilization of HIF-1α and enhanced glycolysis that are observed in macrophages following VWF exposure are mediated through p38 activation.

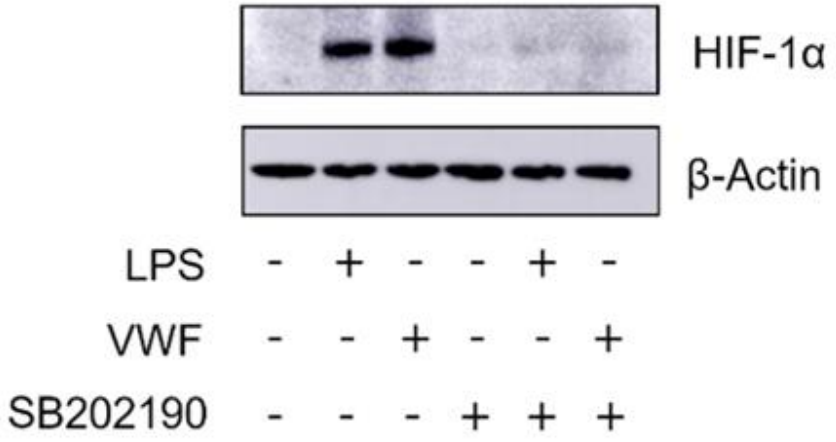

Figure 6.8: VWF regulates macrophage HIF-1α levels via p38 MAPKinase

BMDMs were treated for 3 hours with pd-VWF (10µg/ml) or LPS (100ng/ml) with or without SB202190 (50µM) 1hour pre-treatment. HIF-1α levels then examined by Western blot and total protein determined by β-actin

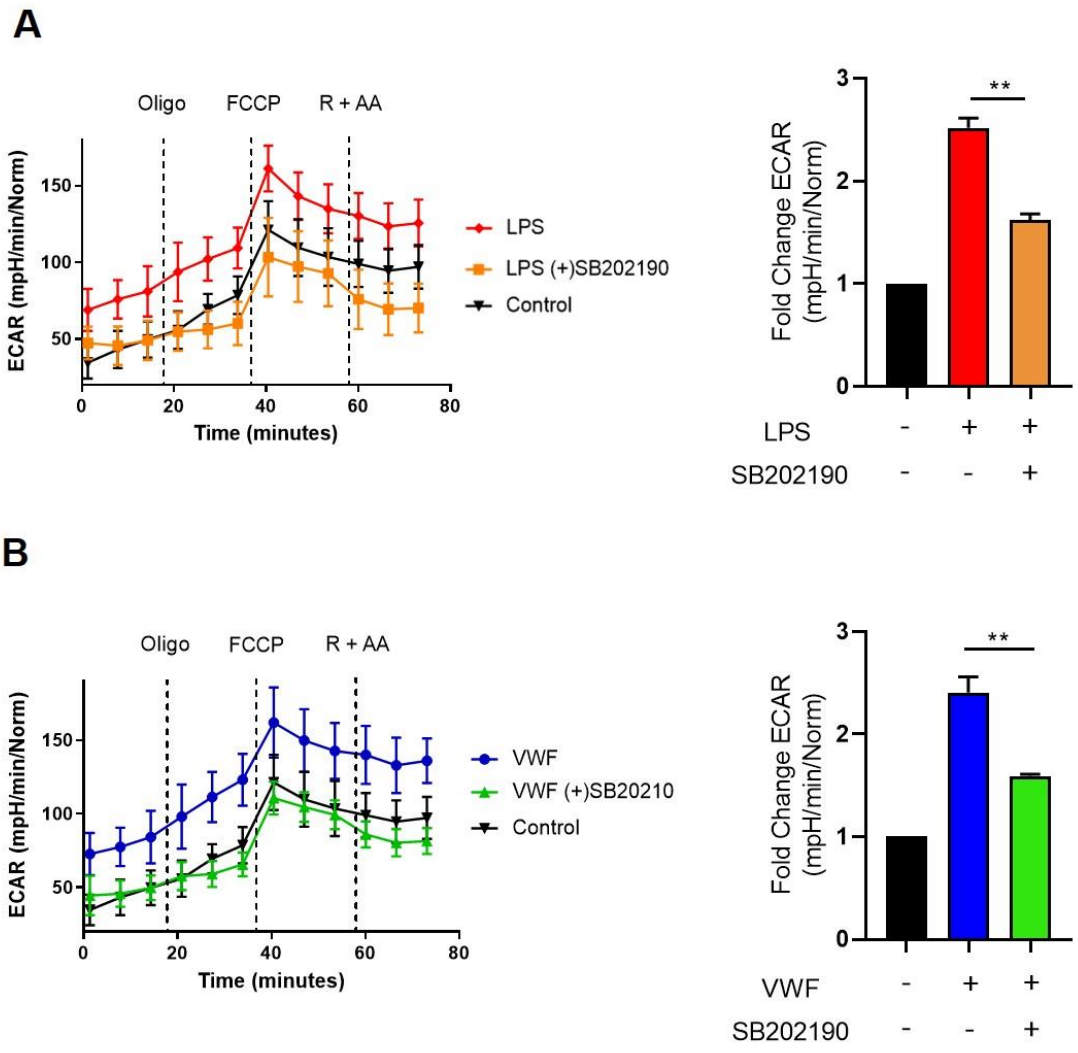

Figure 6.9: VWF regulates macrophage glycolysis via p38 MAPKinase

Representative plots of BMDM ECAR and bar charts of fold change basal ECAR following 3h treatment and with **A:** LPS (100ng/ml) or **B:** VWF (10µg/ml) with or without 1h pre-treatment of p38 inhibitor SB202190 (50µM). Fold change ECAR was determined from 3 independent experiments ± SEM. Significance was determined by t-test (**p<0.01),

6.9: Macrophage viability following SB20210 treatment

To determine that the alterations observed in BMDM glycolysis following p38 inhibition did not occur as a result of cell death, cell viability assay was assessed. Following a 4 hour incubation with SB202190 (50µM) viability of macrophages were determined by alamar blue metabolism in which living cells catabolise resazurin to fluorescent resorufin. The extent of viability was quantified by absorbance at 600nm and subsequently normalised to total protein following BCA. Importantly, no alteration in BMDM viability was observed following SB202190 treatment (Figure 6.10).

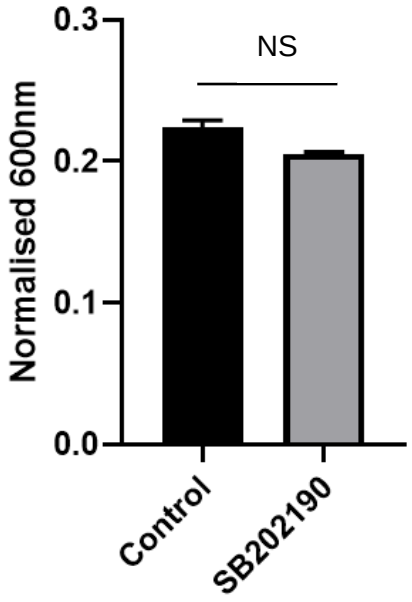

Figure 6.10: MAPKinase p38 inhibitor SB20210 does not alter macrophage viability

BMDM were incubated with or without with SB202190 (50µM) for 4 hour. Alamar blue metabolism was determined by absorbance at 600nm and normalised to total protein based on BCA reagent. (NS, not significant)

6.10: Relationship between VWF dependent HIF-α and LRP1 levels

Previous studies have reported that HIF-1α can regulate expression of the LRP1 receptor. In particular, Castellano *et al,* reported that HIF-1α can bind to the *LRP1* promoter inducing its expression. (310) As we have demonstrated that VWF both induces HIF-1α activation and in part signals through LRP1, we further investigated whether there was any correlation between the two proteins. Importantly, the LRP1-α chain is shed from the membrane following incubation with LPS.(311) Thus, to appropriately detect the levels of LRP1, we used an antibody directed to the transmembrane portion of LRP1 β chain.

Following a 3 hour incubation with VWF, HIF-1α was present and LRP1 was detected by RT-qPCR and western (Figure 6.11A+B). After a 16 hour incubation with VWF, HIF-α was inactive, and there was a decrease in *LRP1* mRNA and protein expression (Figure 6.11 B). Interestingly, these observations were again different to those observed following LPS stimulation. After a prolonged LPS treatment HIF-1α remains active but a decrease in LRP1 levels occurs. LPS stimulation also induces cleavage of the transmembrane LRP1 domain which may account for the reduced LRP1 independent of HIF-1α.

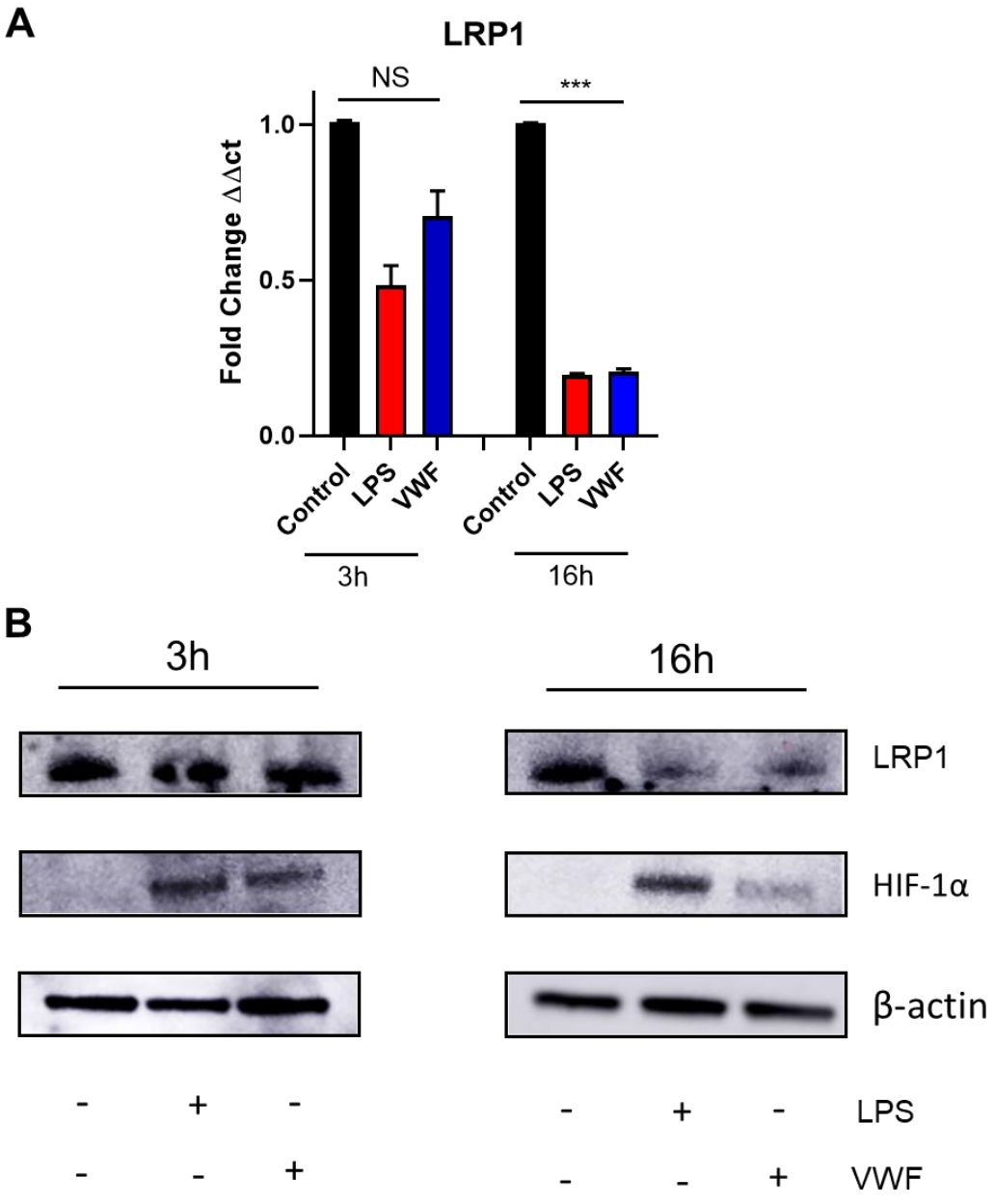

Figure 6.11: Both HIF-1α and LRP1 levels decrease following prolonged VWF exposure

BMDMs treated with VWF (10µg/ml) or LPS (100ng/ml) for indicated times. **A:** Mean LRP1 expression ±SEM determined by RT-qPCR. Significance determined by t-test (***p<0.001). **B:** Representative image of LRP1 β-chain and HIF-α western blot. Total protein determined by β-Actin.

6.11: Discussion

Through the experiments described in the earlier Chapters of this Thesis, we have shown that VWF binds to a variety of different macrophages. Furthermore, we have shown for the first time that this VWF interaction has significant effects upon macrophage biology, inducing a pro-inflammatory phenotype similar to that observed following macrophage stimulation with LPS. Interestingly however, in contrast to the effects of LPS, the pro-inflammatory effects of VWF on macrophages are time-limited. In this Chapter, we have performed a series of studies to investigate the biological mechanisms that may contribute to the pro-inflammatory effects of VWF on macrophages.

Previous studies have demonstrated that the scavenger receptors LRP1 and SRA1 play important roles in regulating macrophage-mediated VWF clearance.(121–123) In particular, both receptors have been shown to be able to modulate VWF binding on the macrophage surface and subsequent endocytosis. Importantly, a number of different studies have clearly shown that binding of a range of different ligands to both LRP1 and SR-AI can also trigger intracellular signalling sequelae in macrophages.(240,288–291,298,312) Previous reports have demonstrated that LRP1 interaction with lactoferrin or RAP induces NF-κB activation.(240) Furthermore, bone marrow derived macrophage LRP1 signalling has been associated with p38, ERK1/2, c-JUN, CREB and JNK activation resulting in production of TNF-α, IL-6 and CCL3.(234) These results highlight a potential role for LRP1 as we observed VWF dependent production in there cytokines.

Importantly, we found that LRP1 and SRA1 expression were both markedly increased following the differentiation of primary human monocytes and THP1 cells into macrophages. Overall, SR-A1 expression levels were similar in macrophages derived from either primary monocytes and THP1 macrophages. In contrast, LRP1 expression levels were significantly higher in primary human macrophages compared to THP1 macrophages. Collectively, these data are interesting given that the proinflammatory signalling effects of VWF are much more marked in primary human macrophages compared to THP1 macrophages. Consequently, we hypothesised that LRP1 might be important in modulating the pro-inflammatory effects of VWF.

We and others have previously reported that VWF can bind to LRP1 on macrophages, and that this binding is increased in the presence of shear stress.(122,202,313) This is further illustrated in this Chapter by the observation of VWF co-localisation with LRP1 on the macrophage surface even under static binding conditions. In addition, a number of discrete VWF domains have been implicated in regulating LRP1 binding.(121) Altogether, the published data suggest that the A1 domain of VWF is likely important for shear-regulated binding of VWF to LRP1 cluster IV.(122,313) Under static conditions, other VWF domains beyond the A domains (including D'-D3 and D4) are likely more important. In support of a role for LRP1 playing a role in triggering the proinflammatory effects of VWF, we observed that LRP1 inhibition using an anti-LRP1 blocking antibody significantly attenuated VWF binding to macrophages under static conditions. Moreover, inhibition of LRP1 with RAP or anti-LRP1 antibody also significantly attenuated VWF

pro-inflammatory signalling. In particular, LRP1 inhibition specifically attenuated VWF-induced MAPKinase p38 activation. Conversely. LRP1 inhibition had little effect upon VWF-induced JNK and NF-κB upregulation, suggesting that multiple different receptors and/or signalling pathways may be triggered by VWF binding to macrophages.

As previously discussed, a notable feature of the pro-inflammatory effect of VWF on macrophages is that it is time-dependent. Consequently, we were interested to investigate the molecular mechanisms underlying this phenomenon. HIF-1α is a key regulator of glycolysis whereby agonists including LPS induce its expression under normoxic conditions.(314) Subsequently, HIF-1α drives expression of multiple glycolytic enzymes.(263,266) In Chapter 5 we reported that VWF significantly induces macrophage glycolysis, and now further demonstrate that this is mediated though HIF-1α in a time-dependent manner. Thus, following a 3 hour incubation with VWF, we observed a significant activation of HIF-1α, which parallels the effects of VWF in upregulating macrophage glycolysis. However, following extended VWF incubation, the upregulation in both HIF-1α and glycolysis are no longer seen. This apparent negative regulatory effect contrasts markedly to the sustained proinflammatory effects seen with prolonged LPS treatment. Previous studies have demonstrated that HIF-1α activation is tightly regulated by a family of enzymes called prolyl hydroxylas (PHD).(315) Under normoxic conditions, HIF-1α is activated though hydroxylation at Pro-564, which becomes a target for PHD leading to HIF-1α ubiquitination and degradation.(315) When examining PHD3 following a 3 hour incubation no alterations in PHD3 were

observed. We assume that no alterations in PHD3 levels were detected at this time because HIF-1α was not activated for a sufficient period to induce a negative feedback regulation. Furthermore, following a 16 hour VWF treatment PHD3 levels are now reduced, which we assume is due prolonged HIF-1α inactivity. This is supported by the fact that following a prolonged LPS treatment, PHD3 expression has increased in order to subsequently saline the active HIF-1α.

Finally, Perrin-Cocon *et al*, have reported that p38 plays a key role in the regulation of HIF-1α dependent glycolysis.(309) Importantly, these studies demonstrated that inhibition of either HIF-1α or p38 resulted in a marked reduction in glucose consumption.(309) To investigate further the pathways involved in VWF-dependent upregulation of macrophage glycolysis, we studied the effects of binding in the presence or absence of p38 inhibition. Importantly, inhibition of p38 completely ablated VWF HIF-1α activation as well as the upregulation in glycolysis. Moreover, this effect was unrelated to any reduction in macrophage cell viability.

In conclusion, we have demonstrated for the first time that VWF binding to macrophages triggers a series of pro-inflammatory changes. The macrophage LRP1 receptor plays an important role in modulating these effects, and in particular regulates p38 activation. This induction of p38 subsequently drives HIF-1α activation, which in turn results in a marked enhancement in macrophage glycolysis, which is essential for the subsequent generation of proinflammatory cytokines and chemokines.

7. Overall Discussion

7.1 Where VWF meets macrophages

Under normal conditions, undifferentiated monocytes circulate in the blood together with multimeric VWF. We have demonstrated that VWF does not bind to unactivated monocytes. In contrast, macrophages are sequestered in tissues. Thus, with the notable exception of hepatic Kupffer cells, these macrophages are not typically exposed to VWF. However, following tissue injury, VWF escapes into the sub-endothelium where it encounters tissue-resident macrophages. Alternatively, we hypothesise that VWF will also come into contact with macrophages when both are incorporated into growing thrombi. Based on the novel data presented in this Thesis, it is clear that this interaction between VWF and recruited or tissue resident macrophages triggers a significant pro-inflammatory effect within macrophages. Under steady state conditions, Kupffer cells are the only macrophages continuously exposed to VWF. These Kupffer cells have been specifically adapted to remove circulating glycoproteins and consequently express a series of different scavenger receptors.(91),(316)(317) Importantly however, Kupffer cells are highly tolerized and thus unresponsive to pro-inflammatory stimuli. Previous studies have also reported that the functional properties of macrophages vary significantly depending upon their tissue of origin. Nevertheless, it is important to emphasise that we observed consistent cell-specific pro-inflammatory effects of VWF binding to a variety of different primary (human and murine) macrophage and immortalised macrophage cell lines. Interestingly however, macrophage

properties differed depending upon the type of stimuli used for differentiation. These differences likely explain in part some of the conflicting conclusions previously reported by other groups.

7.2 VWF "active" conformation

VWF circulates in plasma as a large multimeric glycoprotein. In addition, each VWF monomer is composed of a series of repeating domains. Consequently, it is perhaps not surprising that the functional properties of VWF are influenced by its quaternary structure and regulated by shear stress induced changes in conformation. For example, in order for VWF to bind to platelet GP1bα, shear stress must be exerted though the A1A2A3 domains to expose the buried GP1bα binding site within the A1 domain. In terms of haemostasis, this conformational change in VWF that facilitates platelet binding, is referred to as *'active'* VWF. Under static (*in vitro)* conditions, the interaction between VWF and GP1bα can be artificially induced using ristocetin, to produce an "active" VWF(318) Ristocetin has been mapped to bind to two sites within the A1 domain, the proline-rich region (Glu-700 to Asp-709, historic nomenclature) and the disulphide bond (Cys-509–Cys-695).(88,318,319) This interaction drives a conformational change within VWF allowing for GP1bα binding. Importantly however, the use of ristocetin does not fully mimic sheer dependent conformational changes in VWF as it only acts on the single A1 domain.

Our data demonstrate that the ability of VWF to interact with macrophages is both ristocetin dependent and independentt. In particular, we have shown that

macrophage-binding is enhanced for *'active'* full length VWF. Moreover, we have further demonstrated that even under static conditions (where the putative binding site in the A1 domain is concealed), full length VWF can still bind to macrophages. Furthermore, the purified A3-Ck truncation lacking the A1 domain was able to bind to macrophages under static conditions in the absence of ristocetin. In contrast, binding of the A1A2A3 truncation was dependent on conformational changes induced by ristocetin. Collectively these data suggest that multiple individual discrete regions involving several different domains within VWF also contain binding sites for macrophage receptor(s). Importantly the question of sheer dependent conformation changes in VWF is not fully investigated, as ristocetin only acts on the A domains of VWF.

7.3 The importance of time

The data presented in this thesis clearly demonstrate that VWF binding has a significant pro-inflammatory effect on macrophages. For example, we found that VWF treatment altered macrophage metabolism and triggered a rapid increase in glycolysis similar that observed following LPS exposure. Interestingly however, VWF was unable to sustain this effect. Prolonged LPS stimulation resulted in enhanced macrophage glycolysis and suppression of oxidative phosphorylation. In contrast however, following extended exposure to VWF, macrophage glycolysis and oxidative phosphorylation retuned to baseline. This data suggests that VWF may alter the rate-limiting steps that control glycolytic flux though a different mechanism to LPS. Hexokinase is a key rate limiting enzyme which controls

glycolytic capacity as it mediates the primary step in glycolysis, converting glucose to glucose-6-phosphate.(320) Phosphofructokinase and pyruvate kinase are additional rate limiting enzymes of the glycolytic pathway.(309) Phosphofructokinase coverts fructose-6-phosphate to fructose-1,6- bisphosphate and pyruvate kinase metabolises the final step of the glycolytic pathway converting phosphoenolpyruvate into pyruvate.(321,322) Perhaps VWF and LPS exert profound differences in the expression of these critical rate limiting glycolytic enzymes.

Interestingly, in vivo experiments have also observed a time-dependent pro-inflammatory effect of VWF. For example, Hillgruber et al demonstrated using two murine models of cutaneous inflammation (immune complex–mediated vasculitis and irritative contact dermatitis), that VWF-inhibition was associated with an attenuated inflammatory effect.(127) Inhibition of VWF within a 4 hour period attenuated oedema and myeloperoxidase activity within the models of cutaneous inflammation.(127) However, similar to our results, following a prolonged inflammation the inhibition of VWF could not sustain its anti-inflammatory effect. These results highlight VWF as an important potential mediator of initial response to inflammation.

7.4 Establishing a mechanism

In further studies we investigate the molecular mechanisms underlying the time-dependent pro-inflammatory properties of VWF on macrophage biology. Importantly, we have shown that VWF binding to macrophages triggers significant

downstream intracellular signalling and metabolic changes that ultimately lead to macrophages adopting an M1 phenotype. In particular, VWF binding resulted in the activation of MAPKinase p38, JNK and liberation of NF-κB. In addition to driving cytokine production, VWF binding also resulted in acute HIF-1α activation and rapid enhancement of glycolysis. Importantly however, these effects normalized with extended exposure. Our data further demonstrate that the scavenger receptor LRP1 and the MAPKinase pathway are critically involved in regulating these VWF-mediated effects.

Numerous intercellular proteins can drive an inflammatory response; however, we have determined a key role for MAPKinase p38. The p38 family is comprised of four subtypes, α,β,γ and δ, of which p38α and p38δ are abundantly expressed in macrophages.(323) p38 is phosphorylated (threonine (Thr-180) and tyrosine residue (Tyr-182).(324)) following cellular stresses and environmental factors including invading pathogens, cytokines and growth factors.(323) However the activation of p38 is tightly regulated by a number of upstream MAPkinases, inducing MAPKinase 6 and 4, which in turn drive activation of specific p38 isoforms.(325) Importantly, mutable transcription factors are phosphorylated by p38, such as myocyte enhancer factor 2, p53 and activating transcription factor 1 and 2.(326–328) Activations of these transcription factors by p38 subsequently allows the macrophage to induce an inflammatory response. We have demonstrated that inhibition of LRP1 significantly attenuated p38 signalling. Furthermore, the inhibition of p38 with SB202190 (p38α/β ATP pocket antagonist) completely ablated VWF dependent HIF-1α activation and subsequent glycolysis.

It is most likely that inhibition of p38 attenuates glycolysis as there is a loss of p38 dependent HIF-1α stability.(309) This work is in line with pervious reports that demonstrated that p38 activation drives HIF-1α stabilisation to induce hexokinase expression in dendritic cells. (309) Furthermore, Khurana et al suggest in tumour cells that the PHD3 regulator, ubiquitin ligase Siah2 is phosphorylated by p38, therefore reducing HIF-1α degradation.(329)

In summary (Figure 7.1), our data demonstrate that VWF binding to macrophage receptors triggers a number of signalling pathways resulting in changes in mitochondrial dynamics, cytokine production and metabolism. Importantly, we have defend a novel role for the LRP1 receptor and a role for p38 stabilisation of glycolytic transcription factor HIF-1α. All together, the findings presented in this thesis therefore define a novel biological role for VWF in driving inflammatory responses, and thereby establish a new link between primary haemostasis and innate immunity. Given the significant morbidity and mortality associated with inflammatory pathology, defining the roles of VWF may offer exciting opportunities to develop novel therapies to address a critical unmet clinical need. It is paramount to preserve VWF haemostatic function, but understanding the domains of VWF that mediate this inflammatory response may be a future therapeutic target for early immune response.

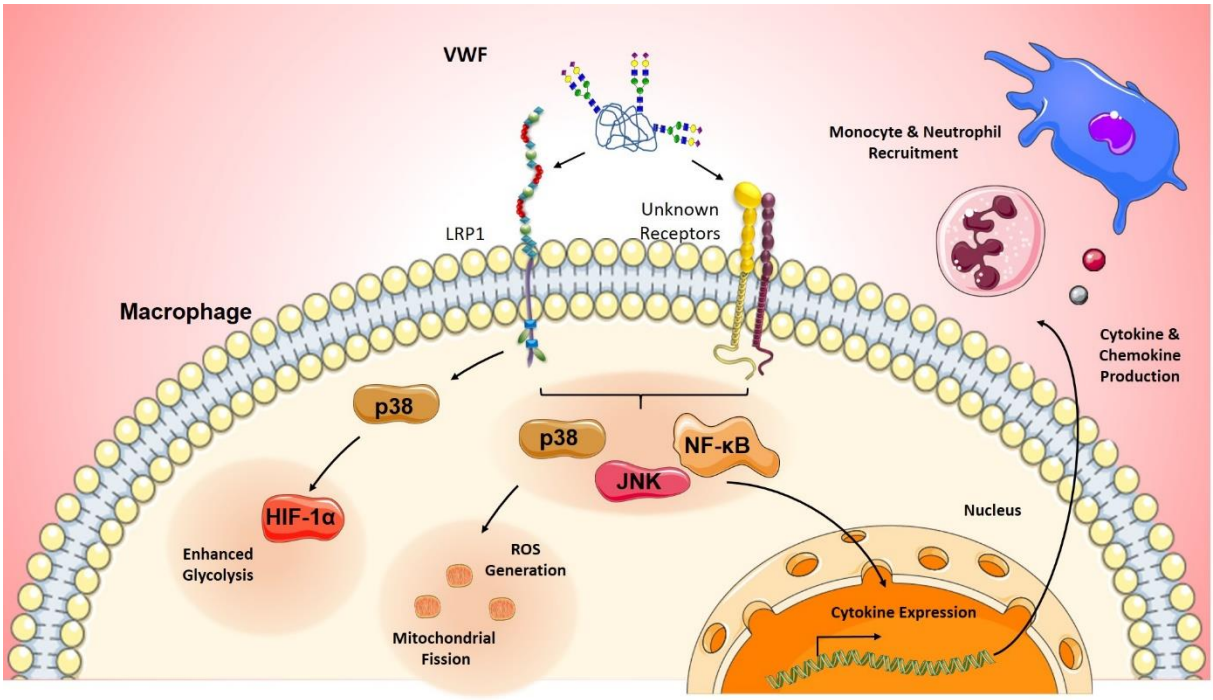

Figure 7.1: A model for VWF dependent macrophage immune response.

VWF interacts with tissue macrophages to which it can bind via a variety cell surface receptors, including LRP1. VWF binding triggers pro-inflammatory signalling within macrophages, including activation of the MAPKinase pathway (with phosphorylation of p38 and JNK) and NF-κB. VWF binding causes macrophages to adopt an M1 phenotype, and leads to enhanced expression of pro-inflammatory cytokines (including TNF-α and IL-6) chemokines (including CCL2, CCL3 and CCL4) and ROS expression. In keeping with these pro-inflammatory effects, VWF significantly effects macrophage metabolism, triggering p38 dependent HIF-1α expression to induce glycolysis.

8. Future Directions

8.1: Investigating the importance of VWF extracellular or intracellular receptor interaction

It is clear from this Thesis that VWF drives an inflammatory response. However, it remains unknown if this effect is a result of VWF extracellular receptor interaction, intercellular receptor interaction or a combination of both. We will attempt to inhibit VWF initialization to further understand how VWF drives a macrophage inflammatory response. In order to do this, cells will be pre-treated with acting polymerization inhibiters jasplakinolide or latrunculin b, and or dynamin 1 and dynamin 2 GTPase activity inhibitor Dynasore hydrate. Following inhibition of VWF internalization, similar assays completed throughout this Thesis will be preformed again to determine the role of intracellular or extracellular receptors.

8.2: Investigating the pathway of VWF internalisation

In an attempt to further understand how VWF is processed by macrophages, we will investigate its intercellular processing into endosomes and lysosome by conjugating VWF to a pH sensitive florescent probe such as pHrodo (Thermofisher Scientific). Using flow cytometry, the migration of VWF as it moves from early endosome into lysosome will be tracked over time and determined by changes in florescent intensity. Validation will be completed by confocal microscopy. Furthermore, we will investigate the importance of how mutations in VWF and or alterations in its glycosylation alter its intracellular processing.

To gain additional insight into the processing of VWF, macrophage receptor knockouts will be used and or inhibitory antibodies to determine receptor importance. These assays will also be performed with VWF mutants and glyco-variants to establish receptor hierarchy.

8.3: Identifying VWF domains and macrophage receptors that facilitate the inflammatory response

Through expression and purification of individual VWF domains, we will determine the importance of each fragment in mediating an inflammatory response. Additionally, work will be completed using macrophage receptor knockout models, CRISPR and inhibitory antibodies to elucidate and identify potential receptors of interest that interact with individual domains of interest.

8.4: Investigating in-vivo disease models to determine physiological significance

VWF has been implicated in numerous *in vivo* inflammatory pathology studies. However to date, no advances have been made in characterising a mechanism in which VWF exerts this inflammatory effect. Thus, developing a macrophage disease model in which WPB are preserved and the outcomes are independent of platelets is paramount.

Hillgruber *et al*, determined that antibody inhibition of VWF significantly attenuated cutaneous inflammation while not disturbing the VWF-platelet GP1bα axis. However, the mechanism through which VWF alters immune cell population and inflammatory effects in this disease model is not known.

We will investigate the effects of VWF using the same models of irritative contact dermatitis and immune complex–mediated vasculitis. However we will further characterise the immune response. Topical application of croton oil will be used to induce irritative contact dermatitis and subcutaneous injection of BSA following by anti-BSA antibody to induce immune complex–mediated vasculitis will be used. Following induction of cutaneous inflammation VWF will be inhibit by interventions infusion of a polyclonal anti-VWF blocking antibody. However, though tissue biopsies we will determine and characterise alterations in immune cell populations and cytokine/chemokine production. Furthermore, using data obtained from the previously sections we will also try to determine the VWF domains and receptors involved in mediating the inflammatory effect.

References

1. Kuwano A, Morimoto Y, Nagai T, Fukushima Y, Ohashi H, Hasegawa T, et al. Precise chromosomal locations of the genes for dentatorubral-pallidoluysian atrophy (DRPLA), von Willebrand factor (F8vWF) and parathyroid hormone-like hormone (PTHLH) in human chromosome 12p by deletion mapping. Hum Genet. 1996 Jan;97(1):95–8.

2. Ginsburg D, Handin RI, Bonthron DT, Donlon TA, Bruns GA, Latt SA, et al. Human von Willebrand factor (vWF): isolation of complementary DNA (cDNA) clones and chromosomal localization. Science. 1985 Jun 21;228(4706):1401–6.

3. Mancuso DJ, Tuley EA, Westfield LA, Worrall NK, Shelton-Inloes BB, Sorace JM, et al. Structure of the gene for human von Willebrand factor. J Biol Chem. 1989 Nov 25;264(33):19514–27.

4. Bonthron DT, Handin RI, Kaufman RJ, Wasley LC, Orr EC, Mitsock LM, et al. Structure of pre-pro-von Willebrand factor and its expression in heterologous cells. Nature. 1986 Nov;324(6094):270.

5. Mancuso DJ, Tuley EA, Westfield LA, Lester-Mancuso TL, Le Beau MM, Sorace JM, et al. Human von Willebrand factor gene and pseudogene: structural analysis and differentiation by polymerase chain reaction. Biochemistry. 1991 Jan 8;30(1):253–69.

6. Tannenbaum SH, Rick ME, Shafer B, Gralnick HR. Subendothelial matrix of cultured endothelial cells contains fully processed high molecular weight von Willebrand factor. J Lab Clin Med. 1989 Mar;113(3):372–8.

7. Nachman R, Levine R, Jaffe EA. Synthesis of factor VIII antigen by cultured guinea pig megakaryocytes. J Clin Invest. 1977 Oct;60(4):914–21.

8. Pusztaszeri MP, Seelentag W, Bosman FT. Immunohistochemical Expression of Endothelial Markers CD31, CD34, von Willebrand Factor, and Fli-1 in Normal Human Tissues. J Histochem Cytochem. 2006 Apr 1;54(4):385–95.

9. Yamamoto K, de Waard V, Fearns C, Loskutoff DJ. Tissue distribution and regulation of murine von Willebrand factor gene expression in vivo. Blood. 1998 Oct 15;92(8):2791–801.

10. Pannekoek H, Voorberg J. Molecular cloning, expression and assembly of multimeric von Willebrand factor. Baillieres Clin Haematol. 1989 Oct;2(4):879–96.

11. Zhou Y-F, Eng ET, Zhu J, Lu C, Walz T, Springer TA. Sequence and structure relationships within von Willebrand factor. Blood. 2012 Jul 12;120(2):449–58.

12. Huizinga EG, Tsuji S, Romijn RAP, Schiphorst ME, de Groot PG, Sixma JJ, et al. Structures of glycoprotein Ibalpha and its complex with von Willebrand factor A1 domain. Science. 2002 Aug 16;297(5584):1176–9.

13. Rastegar-Lari G, Villoutreix BO, Ribba A-S, Legendre P, Meyer D, Baruch D. Two Clusters of Charged Residues Located in the Electropositive Face of the Von Willebrand Factor A1 Domain Are Essential for Heparin Binding †. Biochemistry. 41:6668–78.

14. Pareti FI, Niiya K, McPherson JM, Ruggeri ZM. Isolation and characterization of two domains of human von Willebrand factor that interact with fibrillar collagen types I and III. J Biol Chem. 1987 Oct 5;262(28):13835–41.

15. Nishida N, Sumikawa H, Sakakura M, Shimba N, Takahashi H, Terasawa H, et al. Collagen-binding mode of vWF-A3 domain determined by a transferred cross-saturation experiment. Nat Struct Biol. 2003 Jan;10(1):53–8.

16. Brondijk THC, Bihan D, Farndale RW, Huizinga EG. Implications for collagen I chain registry from the structure of the collagen von Willebrand factor A3 domain complex. Proc Natl Acad Sci U S A. 2012 Apr 3;109(14):5253–8.

17. Hoylaerts MF, Yamamoto H, Nuyts K, Vreys I, Deckmyn H, Vermylen J. von Willebrand factor binds to native collagen VI primarily via its A1 domain. Biochem J. 1997 May 15;324 (Pt 1):185–91.

18. Zhang Q, Zhou Y-F, Zhang C-Z, Zhang X, Lu C, Springer TA. Structural specializations of A2, a force-sensing domain in the ultralarge vascular protein von Willebrand factor. Proc Natl Acad Sci U S A. 2009 Jun 9;106(23):9226–31.

19. Zhou M, Dong X, Baldauf C, Chen H, Zhou Y, Springer TA, et al. A novel calcium-binding site of von Willebrand factor A2 domain regulates its cleavage by ADAMTS13. Blood. 2011 Apr 28;117(17):4623–31.

20. Foster PA, Fulcher CA, Marti T, Titani K, Zimmerman TS. A major factor VIII binding domain resides within the amino-terminal 272 amino acid residues of von Willebrand factor. J Biol Chem. 1987 Jun 25;262(18):8443–6.

21. Katsumi A, Tuley EA, Bodó I, Sadler JE. Localization of disulfide bonds in the cystine knot domain of human von Willebrand factor. J Biol Chem. 2000 Aug 18;275(33):25585–94.

22. Shapiro SE, Nowak AA, Wooding C, Birdsey G, Laffan MA, McKinnon T a. J. The von Willebrand factor predicted unpaired cysteines are essential for secretion. J Thromb Haemost JTH. 2014 Feb;12(2):246–54.

23. Mayadas TN, Wagner DD. In vitro multimerization of von Willebrand factor is triggered by low pH. Importance of the propolypeptide and free sulfhydryls. J Biol Chem. 1989 Aug 15;264(23):13497–503.

24. Wagner DD. Cell biology of von Willebrand factor. Annu Rev Cell Biol. 1990;6:217–46.

25. Huang R-H, Wang Y, Roth R, Yu X, Purvis AR, Heuser JE, et al. Assembly of Weibel-Palade body-like tubules from N-terminal domains of von Willebrand factor. Proc Natl Acad Sci U S A. 2008 Jan 15;105(2):482–7.

26. Vischer UM, Wagner DD. von Willebrand factor proteolytic processing and multimerization precede the formation of Weibel-Palade bodies. Blood. 1994 Jun 15;83(12):3536–44.

27. Zhou Y-F, Eng ET, Nishida N, Lu C, Walz T, Springer TA. A pH-regulated dimeric bouquet in the structure of von Willebrand factor. EMBO J. 2011 Oct 5;30(19):4098–111.

28. Fowler WE, Fretto LJ, Hamilton KK, Erickson HP, McKee PA. Substructure of human von Willebrand factor. J Clin Invest. 1985 Oct 1;76(4):1491–500.

29. Haberichter SL, Fahs SA, Montgomery RR. von Willebrand factor storage and multimerization: 2 independent intracellular processes. Blood. 2000 Sep 1;96(5):1808–15.

30. Kornfeld R, Kornfeld S. Assembly of asparagine-linked oligosaccharides. Annu Rev Biochem. 1985;54:631–64.

31. Weerapana E, Imperiali B. Asparagine-linked protein glycosylation: from eukaryotic to prokaryotic systems. Glycobiology. 2006 Jun;16(6):91R-101R.

32. Samor B, Michalski JC, Debray H, Mazurier C, Goudemand M, Van Halbeek H, et al. Primary structure of a new tetraantennary glycan of the N-acetyllactosaminic type isolated from human factor VIII/von Willebrand factor. Eur J Biochem. 1986 Jul 15;158(2):295–8.

33. Canis K, McKinnon TAJ, Nowak A, Haslam SM, Panico M, Morris HR, et al. Mapping the N-glycome of human von Willebrand factor. Biochem J. 2012 Oct 15;447(2):217–28.

34. Schwarz F, Aebi M. Mechanisms and principles of N-linked protein glycosylation. Curr Opin Struct Biol. 2011 Oct 1;21(5):576–82.

35. Solecka BA, Weise C, Laffan MA, Kannicht C. Site-specific analysis of von Willebrand factor O-glycosylation. J Thromb Haemost. 2016;14(4):733–46.

36. Canis K, Mckinnon T a. J, Nowak A, Panico M, Morris HR, Laffan M, et al. The plasma von Willebrand factor O-glycome comprises a surprising variety of structures including ABH antigens and disialosyl motifs. J Thromb Haemost. 2010 Jan 1;8(1):137–45.

37. Van den Steen P, Rudd PM, Dwek RA, Opdenakker G. Concepts and principles of O-linked glycosylation. Crit Rev Biochem Mol Biol. 1998;33(3):151–208.

38. Samor B, Michalski J-C, Mazurier C, Goudemand M, De Waard P, Vliegenthart JFG, et al. Primary structure of the majorO-glycosidically linked carbohydrate unit of human von Willebrand factor. Glycoconj J. 1989 Sep 1;6(3):263–70.

39. Matsui T, Titani K, Mizuochi T. Structures of the asparagine-linked oligosaccharide chains of human von Willebrand factor. Occurrence of blood group A, B, and H(O) structures. J Biol Chem. 1992 May 5;267(13):8723–31.

40. Valentijn KM, Eikenboom J. Weibel–Palade bodies: a window to von Willebrand disease. J Thromb Haemost. 2013;11(4):581–92.

41. Lenting PJ, Christophe OD, Denis CV. von Willebrand factor biosynthesis, secretion, and clearance: connecting the far ends. Blood. 2015 Mar 26;125(13):2019–28.

42. Ferraro F, Kriston-Vizi J, Metcalf DJ, Martin-Martin B, Freeman J, Burden JJ, et al. A two-tier Golgi-based control of organelle size underpins the functional plasticity of endothelial cells. Dev Cell. 2014 May 12;29(3):292–304.

43. Wagner DD, Saffaripour S, Bonfanti R, Sadler JE, Cramer EM, Chapman B, et al. Induction of specific storage organelles by von Willebrand factor propolypeptide. Cell. 1991 Jan 25;64(2):403–13.

44. Denis CV, André P, Saffaripour S, Wagner DD. Defect in regulated secretion of P-selectin affects leukocyte recruitment in von Willebrand factor-deficient mice. Proc Natl Acad Sci. 2001 Mar 27;98(7):4072–7.

45. Fiedler U, Reiss Y, Scharpfenecker M, Grunow V, Koidl S, Thurston G, et al. Angiopoietin-2 sensitizes endothelial cells to TNF-α and has a crucial role in the induction of inflammation. Nat Med. 2006 Feb;12(2):235–9.

46. van Breevoort D, van Agtmaal EL, Dragt BS, Gebbinck JK, Dienava-Verdoold I, Kragt A, et al. Proteomic screen identifies IGFBP7 as a novel component of endothelial cell-specific Weibel-Palade bodies. J Proteome Res. 2012 May 4;11(5):2925–36.

47. Zannettino ACW, Holding CA, Diamond P, Atkins GJ, Kostakis P, Farrugia A, et al. Osteoprotegerin (OPG) is localized to the Weibel-Palade bodies of human vascular endothelial cells and is physically associated with von Willebrand factor. J Cell Physiol. 2005 Aug;204(2):714–23.

48. Bonfanti R, Furie BC, Furie B, Wagner DD. PADGEM (GMP140) is a component of Weibel-Palade bodies of human endothelial cells. Blood. 1989 Apr;73(5):1109–12.

49. Wolff B, Burns AR, Middleton J, Rot A. Endothelial Cell "Memory" of Inflammatory Stimulation: Human Venular Endothelial Cells Store Interleukin 8 in Weibel-Palade Bodies. J Exp Med. 1998 Nov 2;188(9):1757–62.

50. Jacquemin M, Neyrinck A, Hermanns MI, Lavend'homme R, Rega F, Saint-Remy J-M, et al. FVIII production by human lung microvascular endothelial cells. Blood. 2006 Jul 15;108(2):515–7.

51. Cramer EM, Meyer D, Menn R le, Breton-Gorius J. Eccentric localization of von Willebrand factor in an internal structure of platelet alpha-granule resembling that of Weibel-Palade bodies. Blood. 1985 Sep 1;66(3):710–3.

52. Nightingale T, Cutler D. The secretion of von Willebrand factor from endothelial cells; an increasingly complicated story. J Thromb Haemost JTH. 2013 Jun;11 Suppl 1:192–201.

53. van den Biggelaar M, Hernández-Fernaud JR, van den Eshof BL, Neilson LJ, Meijer AB, Mertens K, et al. Quantitative phosphoproteomics unveils temporal dynamics of thrombin signaling in human endothelial cells. Blood. 2014 Mar 20;123(12):e22-36.

54. Giblin JP, Hewlett LJ, Hannah MJ. Basal secretion of von Willebrand factor from human endothelial cells. Blood. 2008 Aug 15;112(4):957–64.

55. Romani de Wit T, Rondaij MG, Hordijk PL, Voorberg J, van Mourik JA. Real-time imaging of the dynamics and secretory behavior of Weibel-Palade bodies. Arterioscler Thromb Vasc Biol. 2003 May 1;23(5):755–61.

56. Steyer JA, Horstmann H, Almers W. Transport, docking and exocytosis of single secretory granules in live chromaffin cells. Nature. 1997 Jul 31;388(6641):474–8.

57. Rudolf R, Salm T, Rustom A, Gerdes HH. Dynamics of immature secretory granules: role of cytoskeletal elements during transport, cortical restriction, and F-actin-dependent tethering. Mol Biol Cell. 2001 May;12(5):1353–65.

58. Dong J, Moake JL, Nolasco L, Bernardo A, Arceneaux W, Shrimpton CN, et al. ADAMTS-13 rapidly cleaves newly secreted ultralarge von Willebrand factor multimers on the endothelial surface under flowing conditions. Blood. 2002 Dec 1;100(12):4033–9.

59. André P, Denis CV, Ware J, Saffaripour S, Hynes RO, Ruggeri ZM, et al. Platelets adhere to and translocate on von Willebrand factor presented by endothelium in stimulated veins. Blood. 2000 Nov 15;96(10):3322–8.

60. van Buul-Wortelboer MF, Brinkman H-JM, Reinders JH, van Aken WG, van Mourik JA. Polar secretion of von Willebrand factor by endothelial cells. Biochim Biophys Acta BBA - Mol Cell Res. 1989 May 10;1011(2):129–33.

61. Sporn LA, Marder VJ, Wagner DD. Inducible secretion of large, biologically potent von Willebrand factor multimers. Cell. 1986 Jul 18;46(2):185–90.

62. Silva ML da, Cutler DF. von Willebrand factor multimerization and the polarity of secretory pathways in endothelial cells. Blood. 2016 Jul 14;128(2):277–85.

63. Bierings R, Voorberg J. Up or out: polarity of VWF release. Blood. 2016 Jul 14;128(2):154–5.

64. Savage B, Sixma JJ, Ruggeri ZM. Functional self-association of von Willebrand factor during platelet adhesion under flow. Proc Natl Acad Sci U S A. 2002 Jan 8;99(1):425–30.

65. Ulrichts H, Vanhoorelbeke K, Girma JP, Lenting PJ, Vauterin S, Deckmyn H. The von Willebrand factor self-association is modulated by a multiple domain interaction. J Thromb Haemost JTH. 2005 Mar;3(3):552–61.

66. Martin C, Morales LD, Cruz MA. Purified A2 domain of von Willebrand factor binds to the active conformation of von Willebrand factor and blocks the interaction with platelet glycoprotein Ibα. J Thromb Haemost. 2007;5(7):1363–70.

67. Auton M, Sowa KE, Smith SM, Sedlák E, Vijayan KV, Cruz MA. Destabilization of the A1 Domain in von Willebrand Factor Dissociates the A1A2A3 Tri-domain and Provokes Spontaneous Binding to Glycoprotein Ibα and Platelet Activation under Shear Stress. J Biol Chem. 2010 Jul 23;285(30):22831–9.

68. Siediecki CA, Lestini BJ, Kottke-Marchant KK, Eppell SJ, Wilson DL, Marchant RE. Shear-dependent changes in the three-dimensional structure of human von Willebrand factor. Blood. 1996 Oct 15;88(8):2939–50.

69. Shankaran H, Alexandridis P, Neelamegham S. Aspects of hydrodynamic shear regulating shear-induced platelet activation and self-association of von Willebrand factor in suspension. Blood. 2003 Apr 1;101(7):2637–45.

70. Blenner MA, Dong X, Springer TA. Structural Basis of Regulation of von Willebrand Factor Binding to Glycoprotein Ib. J Biol Chem. 2014 Feb 28;289(9):5565–79.

71. Fullard JF. The role of the platelet glycoprotein IIb/IIIa in thrombosis and haemostasis. Curr Pharm Des. 2004;10(14):1567–76.

72. Von Willebrand's Disease. N Engl J Med. 2017 Feb 16;376(7):701–2.

73. Zheng X, Chung D, Takayama TK, Majerus EM, Sadler JE, Fujikawa K. Structure of von Willebrand factor-cleaving protease (ADAMTS13), a metalloprotease involved in thrombotic thrombocytopenic purpura. J Biol Chem. 2001 Nov 2;276(44):41059–63.

74. Zhou W, Inada M, Lee T-P, Benten D, Lyubsky S, Bouhassira EE, et al. ADAMTS13 is expressed in hepatic stellate cells. Lab Investig J Tech Methods Pathol. 2005 Jun;85(6):780–8.

75. Tsai HM. Physiologic cleavage of von Willebrand factor by a plasma protease is dependent on its conformation and requires calcium ion. Blood. 1996 May 15;87(10):4235–44.

76. Ai J, Smith P, Wang S, Zhang P, Zheng XL. The proximal carboxyl-terminal domains of ADAMTS13 determine substrate specificity and are all required for cleavage of von Willebrand factor. J Biol Chem. 2005 Aug 19;280(33):29428–34.

77. Furlan M, Robles R, Lämmle B. Partial purification and characterization of a protease from human plasma cleaving von Willebrand factor to fragments produced by in vivo proteolysis. Blood. 1996 May 15;87(10):4223–34.

78. Zheng XL. ADAMTS13 and von Willebrand factor in thrombotic thrombocytopenic purpura. Annu Rev Med. 2015;66:211–25.

79. Interlandi G, Ling M, Tu AY, Chung DW, Thomas WE. Structural Basis of Type 2A von Willebrand Disease Investigated by Molecular Dynamics Simulations and

Experiments. PLoS ONE [Internet]. 2012 Oct 23 [cited 2019 Jul 19];7(10). Available from: https://www.ncbi.nlm.nih.gov/pmc/articles/PMC3479114/

80. Vlot AJ, Koppelman SJ, van den Berg MH, Bouma BN, Sixma JJ. The affinity and stoichiometry of binding of human factor VIII to von Willebrand factor. Blood. 1995 Jun 1;85(11):3150–7.

81. Weiss HJ, Sussman II, Hoyer LW. Stabilization of factor VIII in plasma by the von Willebrand factor. Studies on posttransfusion and dissociated factor VIII and in patients with von Willebrand's disease. J Clin Invest. 1977 Aug;60(2):390–404.

82. Yee A, Gildersleeve RD, Gu S, Kretz CA, McGee BM, Carr KM, et al. A von Willebrand factor fragment containing the D'D3 domains is sufficient to stabilize coagulation factor VIII in mice. Blood. 2014 Jul 17;124(3):445–52.

83. Casonato A, Galletta E, Sarolo L, Daidone V. Type 2N von Willebrand disease: Characterization and diagnostic difficulties. Haemoph Off J World Fed Hemoph. 2018 Jan;24(1):134–40.

84. Zhang X, Halvorsen K, Zhang C-Z, Wong WP, Springer TA. Mechanoenzymatic Cleavage of the Ultralarge Vascular Protein von Willebrand Factor. Science. 2009 Jun 5;324(5932):1330–4.

85. Ginsburg D, Sadler JE. von Willebrand disease: a database of point mutations, insertions, and deletions. For the Consortium on von Willebrand Factor Mutations and Polymorphisms, and the Subcommittee on von Willebrand Factor of the Scientific and Standardization Committee of the International Society on Thrombosis and Haemostasis. Thromb Haemost. 1993 Feb 1;69(2):177–84.

86. Miura S, Sakurai Y, Takatsuka H, Yoshioka A, Matsumoto M, Yagi H, et al. Total inhibition of high shear stress induced platelet aggregation by homodimeric von Willebrand factor A1-loop fragments. Br J Haematol. 1999 Jun;105(4):1092–100.

87. Mohri H, Fujimura Y, Shima M, Yoshioka A, Houghten RA, Ruggeri ZM, et al. Structure of the von Willebrand factor domain interacting with glycoprotein Ib. J Biol Chem. 1988 Dec 5;263(34):17901–4.

88. Girma JP, Takahashi Y, Yoshioka A, Diaz J, Meyer D. Ristocetin and Botrocetin Involve Two Distinct Domains of von Willebrand Factor for Binding to Platelet Membrane Glycoprotein Ib. Thromb Haemost. 1990 Oct;64(2):326–32.

89. Bianchi ME. DAMPs, PAMPs and alarmins: all we need to know about danger. J Leukoc Biol. 2007;81(1):1–5.

90. Lawrence T, Natoli G. Transcriptional regulation of macrophage polarization: enabling diversity with identity. Nat Rev Immunol. 2011 Oct 25;11(11):750–61.

91. Gordon S, Plüddemann A. Tissue macrophages: heterogeneity and functions. BMC Biol [Internet]. 2017 Jun 29 [cited 2019 Jun 19];15. Available from: https://www.ncbi.nlm.nih.gov/pmc/articles/PMC5492929/

92. Shapouri-Moghaddam A, Mohammadian S, Vazini H, Taghadosi M, Esmaeili S-A, Mardani F, et al. Macrophage plasticity, polarization, and function in health and disease. J Cell Physiol. 2018;233(9):6425–40.

93. Arango Duque G, Descoteaux A. Macrophage Cytokines: Involvement in Immunity and Infectious Diseases. Front Immunol [Internet]. 2014 Oct 7 [cited 2019 Oct 18];5. Available from: https://www.ncbi.nlm.nih.gov/pmc/articles/PMC4188125/

94. Deng Z, Shi F, Zhou Z, Sun F, Sun M-H, Sun Q, et al. M1 macrophage mediated increased reactive oxygen species (ROS) influence wound healing via the MAPK signaling in vitro and in vivo. Toxicol Appl Pharmacol. 2019 Mar 1;366:83–95.

95. Arnold CE, Gordon P, Barker RN, Wilson HM. The activation status of human macrophages presenting antigen determines the efficiency of Th17 responses. Immunobiology. 2015 Jan 1;220(1):10–9.

96. Stunault MI, Bories G, Guinamard RR, Ivanov S. Metabolism Plays a Key Role during Macrophage Activation [Internet]. Mediators of Inflammation. 2018 [cited 2019 Oct 18]. Available from: https://www.hindawi.com/journals/mi/2018/2426138/

97. Martinez FO, Helming L, Gordon S. Alternative Activation of Macrophages: An Immunologic Functional Perspective. Annu Rev Immunol. 2009;27(1):451–83.

98. Billack B. Macrophage Activation: Role of Toll-like Receptors, Nitric Oxide, and Nuclear Factor kappa B. Am J Pharm Educ [Internet]. 2006 Oct 15 [cited 2019 Oct 18];70(5). Available from: https://www.ncbi.nlm.nih.gov/pmc/articles/PMC1637021/

99. Osorio F, Reis e Sousa C. Myeloid C-type lectin receptors in pathogen recognition and host defense. Immunity. 2011 May 27;34(5):651–64.

100. Elinav E, Strowig T, Henao-Mejia J, Flavell RA. Regulation of the antimicrobial response by NLR proteins. Immunity. 2011 May 27;34(5):665–79.

101. Loo Y-M, Gale M. Immune signaling by RIG-I-like receptors. Immunity. 2011 May 27;34(5):680–92.

102. Kawai T, Akira S. The role of pattern-recognition receptors in innate immunity: update on Toll-like receptors. Nat Immunol. 2010 May;11(5):373–84.

103. Kerrigan AM, Brown GD. Syk-coupled C-type lectin receptors that mediate cellular activation via single tyrosine based activation motifs. Immunol Rev. 2010 Mar;234(1):335–52.

104. Kanneganti T-D, Lamkanfi M, Núñez G. Intracellular NOD-like Receptors in Host Defense and Disease. Immunity. 2007 Oct 26;27(4):549–59.

105. Coulombe F, Divangahi M, Veyrier F, de Léséleuc L, Gleason JL, Yang Y, et al. Increased NOD2-mediated recognition of N-glycolyl muramyl dipeptide. J Exp Med. 2009 Aug 3;206(8):1709–16.

106. Davis BK, Wen H, Ting JP-Y. The Inflammasome NLRs in Immunity, Inflammation, and Associated Diseases. Annu Rev Immunol. 2011;29:707–35.

107. Wynn TA, Chawla A, Pollard JW. Macrophage biology in development, homeostasis and disease. Nature. 2013 Apr 25;496(7446):445–55.

108. Murray PJ, Wynn TA. Protective and pathogenic functions of macrophage subsets. Nat Rev Immunol. 2011 Nov;11(11):723.

109. Mahon BP, Ryan MS, Griffin F, Mills KH. Interleukin-12 is produced by macrophages in response to live or killed Bordetella pertussis and enhances the efficacy of an acellular pertussis vaccine by promoting induction of Th1 cells. Infect Immun. 1996 Dec;64(12):5295–301.

110. Morrison PJ, Ballantyne SJ, Kullberg MC. Interleukin-23 and T helper 17-type responses in intestinal inflammation: from cytokines to T-cell plasticity. Immunology. 2011 Aug;133(4):397–408.

111. Van Dyken SJ, Locksley RM. INTERLEUKIN-4- AND INTERLEUKIN-13-MEDIATED ALTERNATIVELY ACTIVATED MACROPHAGES: ROLES IN HOMEOSTASIS AND DISEASE. Annu Rev Immunol. 2013 Mar 21;31:317–43.

112. Zhang L, Wang C-C. Inflammatory response of macrophages in infection. Hepatobiliary Pancreat Dis Int. 2014 Apr 15;13(2):138–52.

113. Pendu R, Terraube V, Christophe OD, Gahmberg CG, Groot PG de, Lenting PJ, et al. P-selectin glycoprotein ligand 1 and β2-integrins cooperate in the adhesion of leukocytes to von Willebrand factor. Blood. 2006 Dec 1;108(12):3746–52.

114. Koivunen E, Ranta T-M, Annila A, Taube S, Uppala A, Jokinen M, et al. Inhibition of β2Integrin–Mediated Leukocyte Cell Adhesion by Leucine–Leucine–Glycine Motif–Containing Peptides. J Cell Biol. 2001 May 28;153(5):905–16.

115. Isobe T, Hisaoka T, Shimizu A, Okuno M, Aimoto S, Takada Y, et al. Propolypeptide of von Willebrand Factor Is a Novel Ligand for Very Late Antigen-4 Integrin. J Biol Chem. 1997 Mar 28;272(13):8447–53.

116. Takahashi H, Isobe T, Horibe S, Takagi J, Yokosaki Y, Sheppard D, et al. Tissue Transglutaminase, Coagulation Factor XIII, and the Pro-polypeptide of von Willebrand Factor Are All Ligands for the Integrins α9β1 and α4β1. J Biol Chem. 2000 Aug 4;275(31):23589–95.

117. Schooten CJ van, Shahbazi S, Groot E, Oortwijn BD, Berg HM van den, Denis CV, et al. Macrophages contribute to the cellular uptake of von Willebrand factor and factor VIII in vivo. Blood. 2008 Sep 1;112(5):1704–12.

118. Chion A, O'Sullivan JM, Drakeford C, Bergsson G, Dalton N, Aguila S, et al. N-linked glycans within the A2 domain of von Willebrand factor modulate macrophage-mediated clearance. Blood. 2016 Oct 13;128(15):1959–68.

119. Ward SE, O'Sullivan JM, Drakeford C, Aguila S, Jondle CN, Sharma J, et al. A novel role for the macrophage galactose-type lectin receptor in mediating von Willebrand factor clearance. Blood. 2018 Feb 22;131(8):911–6.

120. Casari C, Du V, Wu Y-P, Kauskot A, de Groot PG, Christophe OD, et al. Accelerated uptake of VWF/platelet complexes in macrophages contributes to VWD type 2B-associated thrombocytopenia. Blood. 2013 Oct 17;122(16):2893–902.

121. Wohner N, Muczynski V, Mohamadi A, Legendre P, Aymé G, Christophe OD, et al. Macrophage scavenger-receptor SR-AI contributes to the clearance of von Willebrand factor. Haematologica. 2018 Jan 11;haematol.2017.175216.

122. Wohner N, Legendre P, Casari C, Christophe OD, Lenting PJ, Denis CV. Shear stress-independent binding of von Willebrand factor-type 2B mutants p.R1306Q & p.V1316M to LRP1 explains their increased clearance. J Thromb Haemost. 2015 May 1;13(5):815–20.

123. Rastegarlari G, Pegon JN, Casari C, Odouard S, Navarrete A-M, Saint-Lu N, et al. Macrophage LRP1 contributes to the clearance of von Willebrand factor. Blood. 2012 Mar 1;119(9):2126–34.

124. Pegon JN, Kurdi M, Casari C, Odouard S, Denis CV, Christophe OD, et al. Factor VIII and von Willebrand factor are ligands for the carbohydrate-receptor Siglec-5. Haematologica. 2012 Dec;97(12):1855–63.

125. Petri B, Broermann A, Li H, Khandoga AG, Zarbock A, Krombach F, et al. von Willebrand factor promotes leukocyte extravasation. Blood. 2010 Nov 25;116(22):4712–9.

126. Suidan GL, Brill A, Meyer SFD, Voorhees JR, Cifuni SM, Cabral JE, et al. Endothelial Von Willebrand Factor Promotes Blood–Brain Barrier Flexibility and Provides Protection From Hypoxia and Seizures in MiceSignificance. Arterioscler Thromb Vasc Biol. 2013 Sep 1;33(9):2112–20.

127. Hillgruber C, Steingräber AK, Pöppelmann B, Denis CV, Ware J, Vestweber D, et al. Blocking Von Willebrand Factor for Treatment of Cutaneous Inflammation. J Invest Dermatol. 2014 Jan 1;134(1):77–86.

128. Brinkmann V, Reichard U, Goosmann C, Fauler B, Uhlemann Y, Weiss DS, et al. Neutrophil extracellular traps kill bacteria. Science. 2004 Mar 5;303(5663):1532–5.

129. Fuchs TA, Abed U, Goosmann C, Hurwitz R, Schulze I, Wahn V, et al. Novel cell death program leads to neutrophil extracellular traps. J Cell Biol. 2007 Jan 15;176(2):231–41.

130. Grässle S, Huck V, Pappelbaum KI, Gorzelanny C, Aponte-Santamaría C, Baldauf C, et al. von Willebrand Factor Directly Interacts With DNA From Neutrophil Extracellular Traps. Arterioscler Thromb Vasc Biol. 2014 Jul 1;34(7):1382–9.

131. Fuchs TA, Brill A, Duerschmied D, Schatzberg D, Monestier M, Myers DD, et al. Extracellular DNA traps promote thrombosis. Proc Natl Acad Sci U S A. 2010 Sep 7;107(36):15880–5.

132. Brill A, Fuchs TA, Savchenko AS, Thomas GM, Martinod K, De Meyer SF, et al. Neutrophil extracellular traps promote deep vein thrombosis in mice. J Thromb Haemost. 2012 Jan;10(1):136–44.

133. Hoshiba Y, Hatakeyama K, Tanabe T, Asada Y, Goto S. Co-localization of von Willebrand factor with platelet thrombi, tissue factor and platelets with fibrin, and consistent presence of inflammatory cells in coronary thrombi obtained by an aspiration device from patients with acute myocardial infarction. J Thromb Haemost. 2006 Jan 1;4(1):114–20.

134. Yamashita A, Sumi T, Goto S, Hoshiba Y, Nishihira K, Kawamoto R, et al. Detection of von Willebrand Factor and Tissue Factor in Platelets-Fibrin Rich Coronary Thrombi in Acute Myocardial Infarction. Am J Cardiol. 2006 Jan 1;97(1):26–8.

135. Staessens S, Denorme F, François O, Desender L, Dewaele T, Vanacker P, et al. Structural analysis of ischemic stroke thrombi: histological indications for therapy resistance. Haematologica. 2019 May 2;haematol.2019.219881.

136. Savchenko AS, Borissoff JI, Martinod K, De Meyer SF, Gallant M, Erpenbeck L, et al. VWF-mediated leukocyte recruitment with chromatin decondensation by PAD4 increases myocardial ischemia/reperfusion injury in mice. Blood. 2014 Jan 2;123(1):141–8.

137. Pappelbaum KI, Gorzelanny C, Grässle S, Suckau J, Laschke MW, Bischoff M, et al. Ultralarge von Willebrand Factor Fibers Mediate Luminal Staphylococcus aureus Adhesion to an Intact Endothelial Cell Layer Under Shear StressClinical Perspective. Circulation. 2013 Jul 2;128(1):50–9.

138. O'Seaghdha M, van Schooten CJ, Kerrigan SW, Emsley J, Silverman GJ, Cox D, et al. Staphylococcus aureus protein A binding to von Willebrand factor A1 domain is mediated by conserved IgG binding regions. FEBS J. 2006 Nov 1;273(21):4831–41.

139. Sarma JV, Ward PA. The complement system. Cell Tissue Res. 2011 Jan;343(1):227–35.

140. Kölm R, Schaller M, Roumenina LT, Niemiec I, Kremer Hovinga JA, Khanicheh E, et al. Von Willebrand Factor Interacts with Surface-Bound C1q and Induces Platelet Rolling. J Immunol Baltim Md 1950. 2016 Oct 3;

141. Seya T, Nakamura K, Masaki T, Ichihara-Itoh C, Matsumoto M, Nagasawa S. Human factor H and C4b-binding protein serve as factor I-cofactors both encompassing inactivation of C3b and C4b. Mol Immunol. 1995 Apr 1;32(5):355–60.

142. Feng S, Liang X, Kroll MH, Chung DW, Afshar-Kharghan V. von Willebrand factor is a cofactor in complement regulation. Blood. 2015 Feb 5;125(6):1034–7.

143. Lerolle N, DUNOIS-LARDé C, Badirou I, Motto DG, Hill G, Bruneval P, et al. von Willebrand factor is a major determinant of ADAMTS-13 decrease during mouse sepsis induced by cecum ligation and puncture. J Thromb Haemost. 2009 May 1;7(5):843–50.

144. Kasuda S, Matsui H, Ono S, Matsunari Y, Nishio K, Shima M, et al. Relevant role of von Willebrand factor in neutrophil recruitment in a mouse sepsis model involving cecal ligation and puncture. Haematologica. 2016 Feb 1;101(2):e52–4.

145. Newton CRJC, Krishna S. Severe Falciparum Malaria in Children: Current Understanding of Pathophysiology and Supportive Treatment. Pharmacol Ther. 1998 Jul 1;79(1):1–53.

146. Hadad N, Tuval L, Elgazar-Carmom V, Levy R, Levy R. Endothelial ICAM-1 Protein Induction Is Regulated by Cytosolic Phospholipase A2α via Both NF-κB and CREB Transcription Factors. J Immunol. 2011 Feb 1;186(3):1816–27.

147. Turner GD, Ly VC, Nguyen TH, Tran TH, Nguyen HP, Bethell D, et al. Systemic endothelial activation occurs in both mild and severe malaria. Correlating dermal microvascular endothelial cell phenotype and soluble cell adhesion molecules with disease severity. Am J Pathol. 1998 Jun;152(6):1477–87.

148. Larkin D, Laat B de, Jenkins PV, Bunn J, Craig AG, Terraube V, et al. Severe Plasmodium falciparum Malaria Is Associated with Circulating Ultra-Large von Willebrand Multimers and ADAMTS13 Inhibition. PLOS Pathog. 2009 Mar 20;5(3):e1000349.

149. de Mast Q, Groot E, Lenting PJ, de Groot PG, McCall M, Sauerwein RW, et al. Thrombocytopenia and release of activated von Willebrand Factor during early Plasmodium falciparum malaria. J Infect Dis. 2007 Aug 15;196(4):622–8.

150. Hollestelle MJ, Donkor C, Mantey EA, Chakravorty SJ, Craig A, Akoto AO, et al. von Willebrand factor propeptide in malaria: evidence of acute endothelial cell activation. Br J Haematol. 2006;133(5):562–9.

151. O'Regan N, Gegenbauer K, O'Sullivan JM, Maleki S, Brophy TM, Dalton N, et al. A novel role for von Willebrand factor in the pathogenesis of experimental cerebral malaria. Blood. 2016 Mar 3;127(9):1192–201.

152. de Mast Q, de Groot PG, van Heerde WL, Roestenberg M, van Velzen JF, Verbruggen B, et al. Thrombocytopenia in early malaria is associated with GP1b shedding in absence of systemic platelet activation and consumptive coagulopathy. Br J Haematol. 2010 Dec;151(5):495–503.

153. Brown H, Hien TT, Day N, Mai NT, Chuong LV, Chau TT, et al. Evidence of blood-brain barrier dysfunction in human cerebral malaria. Neuropathol Appl Neurobiol. 1999 Aug;25(4):331–40.

154. Brown H, Rogerson S, Taylor T, Tembo M, Mwenechanya J, Molyneux M, et al. Blood-brain barrier function in cerebral malaria in Malawian children. Am J Trop Med Hyg. 2001 Apr;64(3–4):207–13.

155. Thumwood CM, Hunt NH, Clark IA, Cowden WB. Breakdown of the blood-brain barrier in murine cerebral malaria. Parasitology. 1988 Jun;96 (Pt 3):579–89.

156. Kraisin S, Verhenne S, Pham T-T, Martinod K, Tersteeg C, Vandeputte N, et al. von Willebrand factor in experimental malaria-associated acute respiratory distress syndrome. J Thromb Haemost [Internet]. [cited 2019 Jun 5];0(ja). Available from: https://onlinelibrary.wiley.com/doi/abs/10.1111/jth.14485

157. Sonneveld MAH, Cheng JM, Oemrawsingh RM, de Maat MPM, Kardys I, Garcia-Garcia HM, et al. Von Willebrand factor in relation to coronary plaque characteristics and cardiovascular outcome. Results of the ATHEROREMO-IVUS study. Thromb Haemost. 2015 Mar;113(3):577–84.

158. Whincup PH, Danesh J, Walker M, Lennon L, Thomson A, Appleby P, et al. von Willebrand factor and coronary heart disease: prospective study and meta-analysis. Eur Heart J. 2002 Nov;23(22):1764–70.

159. Sonneveld MAH, de Maat MPM, Leebeek FWG. Von Willebrand factor and ADAMTS13 in arterial thrombosis: a systematic review and meta-analysis. Blood Rev. 2014 Jul;28(4):167–78.

160. Montoro-García S, Shantsila E, Lip GYH. Potential value of targeting von Willebrand factor in atherosclerotic cardiovascular disease. Expert Opin Ther Targets. 2014 Jan;18(1):43–53.

161. Seaman CD, George KM, Ragni M, Folsom AR. Association of von Willebrand factor deficiency with prevalent cardiovascular disease and asymptomatic carotid atherosclerosis: The Atherosclerosis Risk in Communities Study. Thromb Res. 2016 Aug;144:236–8.

162. van Galen KPM, Tuinenburg A, Smeets EM, Schutgens REG. Von Willebrand factor deficiency and atherosclerosis. Blood Rev. 2012 Sep;26(5):189–96.

163. Methia N, André P, Denis CV, Economopoulos M, Wagner DD. Localized reduction of atherosclerosis in von Willebrand factor-deficient mice. Blood. 2001 Sep 1;98(5):1424–8.

164. Libby P. Inflammation in atherosclerosis. Nature. 2002 Dec 19;420(6917):868–74.

165. Weber C, Zernecke A, Libby P. The multifaceted contributions of leukocyte subsets to atherosclerosis: lessons from mouse models. Nat Rev Immunol. 2008 Oct;8(10):802–15.

166. Bobryshev YV, Lord RS. Ultrastructural recognition of cells with dendritic cell morphology in human aortic intima. Contacting interactions of Vascular Dendritic Cells in athero-resistant and athero-prone areas of the normal aorta. Arch Histol Cytol. 1995 Aug;58(3):307–22.

167. Brown MS, Goldstein JL, Krieger M, Ho YK, Anderson RG. Reversible accumulation of cholesteryl esters in macrophages incubated with acetylated lipoproteins. J Cell Biol. 1979 Sep 1;82(3):597–613.

168. Babaev VR, Bobryshev YV, Sukhova GK, Kasantseva IA. Monocyte/macrophage accumulation and smooth muscle cell phenotypes in early atherosclerotic lesions of human aorta. Atherosclerosis. 1993 May;100(2):237–48.

169. Weber C, Noels H. Atherosclerosis: current pathogenesis and therapeutic options. Nat Med. 2011 Nov;17(11):1410–22.

170. Gandhi C, Ahmad A, Wilson KM, Chauhan AK. ADAMTS13 modulates atherosclerotic plaque progression in mice via a VWF-dependent mechanism. J Thromb Haemost JTH. 2014 Feb;12(2):255–60.

171. Jin R, Yang G, Li G. Inflammatory mechanisms in ischemic stroke: role of inflammatory cells. J Leukoc Biol. 2010 May;87(5):779–89.

172. Fu Y, Liu Q, Anrather J, Shi F-D. Immune interventions in stroke. Nat Rev Neurol. 2015 Sep;11(9):524–35.

173. Laridan E, Denorme F, Desender L, François O, Andersson T, Deckmyn H, et al. Neutrophil extracellular traps in ischemic stroke thrombi. Ann Neurol. 2017;82(2):223–32.

174. Enzmann G, Kargaran S, Engelhardt B. Ischemia–reperfusion injury in stroke: impact of the brain barriers and brain immune privilege on neutrophil function. Ther Adv Neurol Disord [Internet]. 2018 Aug 27 [cited 2019 Jul 19];11. Available from: https://www.ncbi.nlm.nih.gov/pmc/articles/PMC6111395/

175. Bath PM, Blann A, Smith N, Butterworth RJ. Von Willebrand factor, P-selectin and fibrinogen levels in patients with acute ischaemic and haemorrhagic stroke, and their relationship with stroke sub-type and functional outcome. Platelets. 1998;9(3–4):155–9.

176. van Schie MC, de Maat MPM, Isaacs A, van Duijn CM, Deckers JW, Dippel DWJ, et al. Variation in the von Willebrand factor gene is associated with von Willebrand factor levels and with the risk for cardiovascular disease. Blood. 2011 Jan 27;117(4):1393–9.

177. Folsom AR, Wu KK, Shahar E, Davis CE. Association of hemostatic variables with prevalent cardiovascular disease and asymptomatic carotid artery atherosclerosis. The Atherosclerosis Risk in Communities (ARIC) Study Investigators. Arterioscler Thromb J Vasc Biol. 1993 Dec;13(12):1829–36.

178. Kleinschnitz C, Meyer SFD, Schwarz T, Austinat M, Vanhoorelbeke K, Nieswandt B, et al. Deficiency of von Willebrand factor protects mice from ischemic stroke. Blood. 2009 Apr 9;113(15):3600–3.

179. De Meyer SF, Schwarz T, Deckmyn H, Denis CV, Nieswandt B, Stoll G, et al. Binding of von Willebrand factor to collagen and glycoprotein Ibalpha, but not to glycoprotein IIb/IIIa, contributes to ischemic stroke in mice--brief report. Arterioscler Thromb Vasc Biol. 2010 Oct;30(10):1949–51.

180. Verhenne S, Denorme F, Libbrecht S, Vandenbulcke A, Pareyn I, Deckmyn H, et al. Platelet-derived VWF is not essential for normal thrombosis and hemostasis but fosters ischemic stroke injury in mice. Blood. 2015 Oct 1;126(14):1715–22.

181. Fujioka M, Hayakawa K, Mishima K, Kunizawa A, Irie K, Higuchi S, et al. ADAMTS13 gene deletion aggravates ischemic brain damage: a possible neuroprotective role of ADAMTS13 by ameliorating postischemic hypoperfusion. Blood. 2010 Feb 25;115(8):1650–3.

182. Zhao B-Q, Chauhan AK, Canault M, Patten IS, Yang JJ, Dockal M, et al. von Willebrand factor–cleaving protease ADAMTS13 reduces ischemic brain injury in experimental stroke. Blood. 2009 Oct 8;114(15):3329–34.

183. Zhu X, Cao Y, Wei L, Cai P, Xu H, Luo H, et al. von Willebrand factor contributes to poor outcome in a mouse model of intracerebral haemorrhage. Sci Rep. 2016 Oct 26;6:35901.

184. Devenish RJ, Prescott M, Boyle GM, Nagley P. The Oligomycin Axis of Mitochondrial ATP Synthase: OSCP and the Proton Channel. J Bioenerg Biomembr. 2000 Oct 1;32(5):507–15.

185. Capaldi RA, Aggeler R, Turina P, Wilkens S. Coupling between catalytic sites and the proton channel in F1F0-type ATPases. Trends Biochem Sci. 1994 Jul 1;19(7):284–9.

186. Yuan XJ, Sugiyama T, Goldman WF, Rubin LJ, Blaustein MP. A mitochondrial uncoupler increases KCa currents but decreases KV currents in pulmonary artery myocytes. Am J Physiol. 1996 Jan;270(1 Pt 1):C321-331.

187. Ting HP, Wilson DF, Chance B. Effects of uncouplers of oxidative phosphorylation on the specific conductance of bimolecular lipid membranes. Arch Biochem Biophys. 1970 Nov;141(1):141–6.

188. Chance B, Williams GR. The respiratory chain and oxidative phosphorylation. Adv Enzymol Relat Subj Biochem. 1956;17:65–134.

189. Hollingworth RM, Ahammadsahib KI, Gadelhak G, McLaughlin JL. New inhibitors of complex I of the mitochondrial electron transport chain with activity as pesticides. Biochem Soc Trans. 1994 Feb;22(1):230–3.

190. Park J, Choi H, Min J-S, Park S-J, Kim J-H, Park H-J, et al. Mitochondrial dynamics modulate the expression of pro-inflammatory mediators in microglial cells. Mitochondrial Dyn Modul Expr -Inflamm Mediat Microglial Cells. 2013;127(2):221–32.

191. Lenting PJ, Westein E, Terraube V, Ribba A-S, Huizinga EG, Meyer D, et al. An Experimental Model to Study the in Vivo Survival of von Willebrand Factor BASIC ASPECTS AND APPLICATION TO THE R1205H MUTATION. J Biol Chem. 2004 Mar 26;279(13):12102–9.

192. McRae E, Rawley O, Nel H, McGrath RT, Bergsson G, Chan A, et al. A Critical Role for N- and O-Linked Carbohydrates In Modulating Von Willebrand Factor Clearance In Vivo. Blood. 2011 Nov 18;118(21):382–382.

193. Groeneveld D, Vlijmen B van, Cheung KL, Wiegers R, Reitsma P, Eikenboom J. Liver and spleen macrophage depletion increases the plasma half-life of von Willebrand factor. J Thromb Haemost [Internet]. 2011 Jul 1 [cited 2019 May 27];9. Available from: insights.ovid.com

194. Chion A, O'Sullivan JM, Drakeford C, Bergsson G, Dalton N, Aguila S, et al. N-linked glycans within the A2 domain of von Willebrand factor modulate macrophage-mediated clearance. Blood. 2016 Oct 13;128(15):1959–68.

195. Gézsi A, Budde U, Deák I, Nagy E, Mohl A, Schlammadinger Á, et al. Accelerated clearance alone explains ultralarge multimers in VWD Vicenza. J Thromb Haemost JTH [Internet]. 2010 Jun [cited 2019 May 27];8(6). Available from: https://www.ncbi.nlm.nih.gov/pmc/articles/PMC3863617/

196. Castro-Núñez L, Dienava-Verdoold I, Herczenik E, Mertens K, Meijer AB. Shear stress is required for the endocytic uptake of the factor VIII-von Willebrand factor complex by macrophages. J Thromb Haemost. 2012 Sep 1;10(9):1929–37.

197. Casari C, Paul DS, Susen S, Lavenu-Bombled C, Harroche A, Piatt R, et al. Protein kinase C signaling dysfunction in von Willebrand disease (p.V1316M) type 2B platelets. Blood Adv. 2018 26;2(12):1417–28.

198. Ruggeri ZM, Pareti FI, Mannucci PM, Ciavarella N, Zimmerman TS. Heightened interaction between platelets and factor VIII/von Willebrand factor in a new subtype of von Willebrand's disease. N Engl J Med. 1980 May 8;302(19):1047–51.

199. De Marco L, Mazzucato M, De Roia D, Casonato A, Federici AB, Girolami A, et al. Distinct abnormalities in the interaction of purified types IIA and IIB von Willebrand factor with the two platelet binding sites, glycoprotein complexes Ib-IX and IIb-IIIa. J Clin Invest. 1990 Sep;86(3):785–92.

200. Daigneault M, Preston JA, Marriott HM, Whyte MKB, Dockrell DH. The Identification of Markers of Macrophage Differentiation in PMA-Stimulated THP-1 Cells and Monocyte-Derived Macrophages. PLOS ONE. 2010 Jan 13;5(1):e8668.

201. Gantner F, Kupferschmidt R, Schudt C, Wendel A, Hatzelmann A. In vitro differentiation of human monocytes to macrophages: change of PDE profile and its relationship to suppression of tumour necrosis factor-alpha release by PDE inhibitors. Br J Pharmacol. 1997 May;121(2):221–31.

202. O'Sullivan JM, Aguila S, McRae E, Ward SE, Rawley O, Fallon PG, et al. N-linked glycan truncation causes enhanced clearance of plasma-derived von Willebrand factor. J Thromb Haemost. 2016;14(12):2446–57.

203. Aguila S, Lavin M, Dalton N, Patmore S, Chion A, Trahan GD, et al. Increased galactose expression and enhanced clearance in patients with low von Willebrand factor. Blood. 2019 Apr 4;133(14):1585–96.

204. Swystun LL, Lai JD, Notley C, Georgescu I, Paine AS, Mewburn J, et al. The endothelial cell receptor stabilin-2 regulates VWF-FVIII complex half-life and immunogenicity. J Clin Invest. 2018 Aug 31;128(9):4057–73.

205. Swystun LL, Notley C, Georgescu I, Lai JD, Nesbitt K, James PD, et al. The endothelial lectin clearance receptor CLEC4M binds and internalizes factor VIII in a VWF-dependent and independent manner. J Thromb Haemost. 2019;17(4):681–94.

206. Rydz N, Swystun LL, Notley C, Paterson AD, Riches JJ, Sponagle K, et al. The C-type lectin receptor CLEC4M binds, internalizes, and clears von Willebrand factor and contributes to the variation in plasma von Willebrand factor levels. Blood. 2013 Jun 27;121(26):5228–37.

207. Lehtonen A, Ahlfors H, Veckman V, Miettinen M, Lahesmaa R, Julkunen I. Gene expression profiling during differentiation of human monocytes to macrophages or dendritic cells. J Leukoc Biol. 2007;82(3):710–20.

208. Bellissimo DB, Christopherson PA, Flood VH, Gill JC, Friedman KD, Haberichter SL, et al. VWF mutations and new sequence variations identified in healthy controls are more frequent in the African-American population. Blood. 2012 Mar 1;119(9):2135–40.

209. Hassenpflug WA, Budde U, Obser T, Angerhaus D, Drewke E, Schneppenheim S, et al. Impact of mutations in the von Willebrand factor A2 domain on ADAMTS13-dependent proteolysis. Blood. 2006 Mar 15;107(6):2339–45.

210. Silva ML da, Cutler DF. von Willebrand factor multimerization and the polarity of secretory pathways in endothelial cells. Blood. 2016 Jul 14;128(2):277–85.

211. Hakkert BC, Rentenaar JM, Mourik JAV. Monocytes enhance endothelial von Willebrand factor release and prostacyclin production with different kinetics and dependency on intercellular contact between these two cell types. Br J Haematol. 1992;80(4):495–503.

212. Yang A, Wang M, Wang Y, Cai W, Li Q, Zhao T, et al. Cancer cell-derived von Willebrand factor enhanced metastasis of gastric adenocarcinoma. Oncogenesis. 2018 Jan 24;7(1):12.

213. Bauer AT, Suckau J, Frank K, Desch A, Goertz L, Wagner AH, et al. von Willebrand factor fibers promote cancer-associated platelet aggregation in malignant melanoma of mice and humans. Blood. 2015 May 14;125(20):3153–63.

214. Starke RD, Ferraro F, Paschalaki KE, Dryden NH, McKinnon TAJ, Sutton RE, et al. Endothelial von Willebrand factor regulates angiogenesis. Blood. 2011 Jan 20;117(3):1071–80.

215. Mochizuki S, Soejima K, Shimoda M, Abe H, Sasaki A, Okano HJ, et al. Effect of ADAM28 on carcinoma cell metastasis by cleavage of von Willebrand factor. J Natl Cancer Inst. 2012 Jun 20;104(12):906–22.

216. Reinhart K, Bayer O, Brunkhorst F, Meisner M. Markers of endothelial damage in organ dysfunction and sepsis. Crit Care Med. 2002 May;30(5 Suppl):S302-312.

217. Paulus P, Carla Jennewein, Zacharowski K. Biomarkers of endothelial dysfunction: can they help us deciphering systemic inflammation and sepsis? Biomarkers. 2011 Jul 1;16(sup1):S11–21.

218. Vanhoutte PM. Endothelial dysfunction and atherosclerosis. Eur Heart J. 1997 Nov 1;18(suppl_E):19–29.

219. Cai Jianming, Hatsukami Thomas S., Ferguson Marina S., Kerwin William S., Saam Tobias, Chu Baocheng, et al. In Vivo Quantitative Measurement of Intact Fibrous Cap and Lipid-Rich Necrotic Core Size in Atherosclerotic Carotid Plaque. Circulation. 2005 Nov 29;112(22):3437–44.

220. Zhang X, Mosser D. Macrophage activation by endogenous danger signals. J Pathol. 2008 Jan;214(2):161–78.

221. Swanson KV, Deng M, Ting JP-Y. The NLRP3 inflammasome: molecular activation and regulation to therapeutics. Nat Rev Immunol. 2019 Aug;19(8):477–89.

222. Lloberas J, Valverde-Estrella L, Tur J, Vico T, Celada A. Mitogen-Activated Protein Kinases and Mitogen Kinase Phosphatase 1: A Critical Interplay in Macrophage Biology. Front Mol Biosci [Internet]. 2016 Jun 28 [cited 2019 Oct 24];3. Available from: https://www.ncbi.nlm.nih.gov/pmc/articles/PMC4923182/

223. Oeckinghaus A, Ghosh S. The NF-κB Family of Transcription Factors and Its Regulation. Cold Spring Harb Perspect Biol [Internet]. 2009 Oct [cited 2019 Oct 25];1(4). Available from: https://www.ncbi.nlm.nih.gov/pmc/articles/PMC2773619/

224. Gensel JC, Kopper TJ, Zhang B, Orr MB, Bailey WM. Predictive screening of M1 and M2 macrophages reveals the immunomodulatory effectiveness of post spinal cord injury azithromycin treatment. Sci Rep. 2017 Jan 6;7:40144.

225. Jablonski KA, Amici SA, Webb LM, Ruiz-Rosado J de D, Popovich PG, Partida-Sanchez S, et al. Novel Markers to Delineate Murine M1 and M2 Macrophages. PLOS ONE. 2015 Dec 23;10(12):e0145342.

226. Nawaz A, Aminuddin A, Kado T, Takikawa A, Yamamoto S, Tsuneyama K, et al. CD206 + M2-like macrophages regulate systemic glucose metabolism by inhibiting proliferation of adipocyte progenitors. Nat Commun. 2017 Aug 18;8(1):286.

227. Amici SA, Young NA, Narvaez-Miranda J, Jablonski KA, Arcos J, Rosas L, et al. CD38 Is Robustly Induced in Human Macrophages and Monocytes in Inflammatory Conditions. Front Immunol [Internet]. 2018 Jul 10 [cited 2019 Apr 1];9. Available from: https://www.ncbi.nlm.nih.gov/pmc/articles/PMC6048227/

228. Xu Q, Choksi S, Qu J, Jang J, Choe M, Banfi B, et al. NADPH Oxidases Are Essential for Macrophage Differentiation. J Biol Chem. 2016 16;291(38):20030–41.

229. Cruz CM, Rinna A, Forman HJ, Ventura ALM, Persechini PM, Ojcius DM. ATP Activates a Reactive Oxygen Species-dependent Oxidative Stress Response and Secretion of Proinflammatory Cytokines in Macrophages. J Biol Chem. 2007 Feb 2;282(5):2871–9.

230. Yin H, Liu J, Li Z, Berndt MC, Lowell CA, Du X. Src family tyrosine kinase Lyn mediates VWF/GPIb-IX-induced platelet activation via the cGMP signaling pathway. Blood. 2008 Aug 15;112(4):1139–46.

231. Wu Y, Asazuma N, Satoh K, Yatomi Y, Takafuta T, Berndt MC, et al. Interaction between von Willebrand factor and glycoprotein Ib activates Src kinase in human platelets: role of phosphoinositide 3-kinase. Blood. 2003 May 1;101(9):3469–76.

232. Delaney MK, Liu J, Zheng Y, Berndt MC, Du X. A Role for Rac1 in Glycoprotein Ib-IX-mediated Signal Transduction and Integrin Activation. Arterioscler Thromb Vasc Biol. 2012 Nov;32(11):2761–8.

233. Canobbio I, Reineri S, Sinigaglia F, Balduini C, Torti M. A role for p38 MAP kinase in platelet activation by von Willebrand factor. Thromb Haemost. 2004 Jan;91(1):102–10.

234. Mantuano E, Azmoon P, Brifault C, Banki MA, Gilder AS, Campana WM, et al. Tissue-type Plasminogen Activator Regulates Macrophage Activation and Innate Immunity. Blood. 2017 Jan 1;blood-2017-04-780205.

235. Taylor DR, Hooper NM. The low-density lipoprotein receptor-related protein 1 (LRP1) mediates the endocytosis of the cellular prion protein. Biochem J. 2007 Feb 15;402(1):17–23.

236. Napoletano C, Zizzari IG, Rughetti A, Rahimi H, Irimura T, Clausen H, et al. Targeting of macrophage galactose-type C-type lectin (MGL) induces DC signaling and activation. Eur J Immunol. 2012 Apr;42(4):936–45.

237. Muratoglu SC, Mikhailenko I, Newton C, Migliorini M, Strickland DK. Low Density Lipoprotein Receptor-related Protein 1 (LRP1) Forms a Signaling Complex with Platelet-derived Growth Factor Receptor-β in Endosomes and Regulates Activation of the MAPK Pathway. J Biol Chem. 2010 May 7;285(19):14308–17.

238. Hsu H-Y, Chiu S-L, Wen M-H, Chen K-Y, Hua K-F. Ligands of Macrophage Scavenger Receptor Induce Cytokine Expression via Differential Modulation of Protein Kinase Signaling Pathways. J Biol Chem. 2001 Aug 3;276(31):28719–30.

239. Hsu H-Y, Hajjar DP, Khan KMF, Falcone DJ. Ligand Binding to Macrophage Scavenger Receptor-A Induces Urokinase-type Plasminogen Activator Expression by a Protein Kinase-dependent Signaling Pathway. J Biol Chem. 1998 Jan 9;273(2):1240–6.

240. Mantuano E, Brifault C, Lam MS, Azmoon P, Gilder AS, Gonias SL. LDL receptor-related protein-1 regulates NFκB and microRNA-155 in macrophages to control the inflammatory response. Proc Natl Acad Sci. 2016 Feb 2;113(5):1369–74.

241. Jiang M-X, Hong X, Liao B-B, Shi S-Z, Lai X-F, Zheng H-Y, et al. Expression profiling of TRIM protein family in THP1-derived macrophages following TLR stimulation. Sci Rep. 2017 17;7:42781.

242. He Y, Hara H, Núñez G. Mechanism and regulation of NLRP3 inflammasome activation. Trends Biochem Sci. 2016 Dec;41(12):1012–21.

243. Bauernfeind FG, Horvath G, Stutz A, Alnemri ES, MacDonald K, Speert D, et al. Cutting edge: NF-kappaB activating pattern recognition and cytokine receptors license NLRP3 inflammasome activation by regulating NLRP3 expression. J Immunol Baltim Md 1950. 2009 Jul 15;183(2):787–91.

244. Martinon F, Mayor A, Tschopp J. The Inflammasomes: Guardians of the Body. Annu Rev Immunol. 2009;27(1):229–65.

245. Takada Y, Mukhopadhyay A, Kundu GC, Mahabeleshwar GH, Singh S, Aggarwal BB. Hydrogen peroxide activates NF-kappa B through tyrosine phosphorylation of I kappa B alpha and serine phosphorylation of p65: evidence for the involvement of I kappa B alpha kinase and Syk protein-tyrosine kinase. J Biol Chem. 2003 Jun 27;278(26):24233–41.

246. Kamata H, Honda S-I, Maeda S, Chang L, Hirata H, Karin M. Reactive oxygen species promote TNFalpha-induced death and sustained JNK activation by inhibiting MAP kinase phosphatases. Cell. 2005 Mar 11;120(5):649–61.

247. West MA, Heagy W. Endotoxin tolerance: a review. Crit Care Med. 2002 Jan;30(1 Suppl):S64-73.

248. Mages J, Dietrich H, Lang R. A genome-wide analysis of LPS tolerance in macrophages. Immunobiology. 2008 Jan 18;212(9):723–37.

249. El Gazzar M, Yoza BK, Chen X, Garcia BA, Young NL, McCall CE. Chromatin-specific remodeling by HMGB1 and linker histone H1 silences proinflammatory genes during endotoxin tolerance. Mol Cell Biol. 2009 Apr;29(7):1959–71.

250. Zarember KA, Godowski PJ. Tissue Expression of Human Toll-Like Receptors and Differential Regulation of Toll-Like Receptor mRNAs in Leukocytes in Response to Microbes, Their Products, and Cytokines. J Immunol. 2002 Jan 15;168(2):554–61.

251. Pesche K. Stoffwechsel der entzuendung. Ztschr F Klin Med. 1930;(114):439–55.

252. O'Neill LAJ, Kishton RJ, Rathmell J. A guide to immunometabolism for immunologists. Nat Rev Immunol. 2016 Sep;16(9):553–65.

253. Diskin C, Pålsson-McDermott EM. Metabolic Modulation in Macrophage Effector Function. Front Immunol [Internet]. 2018 Feb 19 [cited 2019 Jun 3];9. Available from: https://www.ncbi.nlm.nih.gov/pmc/articles/PMC5827535/

254. Rodríguez-Prados J-C, Través PG, Cuenca J, Rico D, Aragonés J, Martín-Sanz P, et al. Substrate fate in activated macrophages: a comparison between innate,

classic, and alternative activation. J Immunol Baltim Md 1950. 2010 Jul 1;185(1):605–14.

255. Krawczyk CM, Holowka T, Sun J, Blagih J, Amiel E, DeBerardinis RJ, et al. Toll-like receptor–induced changes in glycolytic metabolism regulate dendritic cell activation. Blood. 2010 Jun 10;115(23):4742–9.

256. Donnelly RP, Loftus RM, Keating SE, Liou KT, Biron CA, Gardiner CM, et al. mTORC1-dependent metabolic reprogramming is a prerequisite for NK cell effector function. J Immunol Baltim Md 1950. 2014 Nov 1;193(9):4477–84.

257. Fukuzumi M, Shinomiya H, Shimizu Y, Ohishi K, Utsumi S. Endotoxin-induced enhancement of glucose influx into murine peritoneal macrophages via GLUT1. Infect Immun. 1996 Jan;64(1):108–12.

258. Haschemi A, Kosma P, Gille L, Evans CR, Burant CF, Starkl P, et al. The Sedoheptulose Kinase CARKL Directs Macrophage Polarization through Control of Glucose Metabolism. Cell Metab. 2012 Jun 6;15(6):813–26.

259. Palsson-McDermott EM, Curtis AM, Goel G, Lauterbach MAR, Sheedy FJ, Gleeson LE, et al. Pyruvate Kinase M2 Regulates Hif-1α Activity and IL-1β Induction and Is a Critical Determinant of the Warburg Effect in LPS-Activated Macrophages. Cell Metab. 2015 Jan 6;21(1):65–80.

260. Ruiz-García A, Monsalve E, Novellasdemunt L, Navarro-Sabaté A, Manzano A, Rivero S, et al. Cooperation of adenosine with macrophage Toll-4 receptor agonists leads to increased glycolytic flux through the enhanced expression of PFKFB3 gene. J Biol Chem. 2011 Jun 3;286(22):19247–58.

261. Nagy C, Haschemi A. Time and Demand are Two Critical Dimensions of Immunometabolism: The Process of Macrophage Activation and the Pentose Phosphate Pathway. Front Immunol [Internet]. 2015 [cited 2019 Feb 11];6. Available from: https://www.frontiersin.org/articles/10.3389/fimmu.2015.00164/full

262. Luo W, Hu H, Chang R, Zhong J, Knabel M, O'Meally R, et al. Pyruvate kinase M2 is a PHD3-stimulated coactivator for hypoxia-inducible factor 1. Cell. 2011 May 27;145(5):732–44.

263. Marín-Hernández A, Gallardo-Pérez JC, Ralph SJ, Rodríguez-Enríquez S, Moreno-Sánchez R. Mini Rev Med Chem. 2009 Aug;9(9):1084–101.

264. Walmsley SR, Chilvers ER, Thompson AA, Vaughan K, Marriott HM, Parker LC, et al. Prolyl hydroxylase 3 (PHD3) is essential for hypoxic regulation of neutrophilic inflammation in humans and mice. J Clin Invest. 2011 Mar 1;121(3):1053–63.

265. Palazon A, Goldrath A, Nizet V, Johnson RS. HIF Transcription Factors, Inflammation, and Immunity. Immunity. 2014 Oct 16;41(4):518–28.

266. Tannahill GM, Curtis AM, Adamik J, Palsson-McDermott EM, McGettrick AF, Goel G, et al. Succinate is an inflammatory signal that induces IL-1β through HIF-1α. Nature. 2013 Apr;496(7444):238–42.

267. Selak MA, Armour SM, MacKenzie ED, Boulahbel H, Watson DG, Mansfield KD, et al. Succinate links TCA cycle dysfunction to oncogenesis by inhibiting HIF-alpha prolyl hydroxylase. Cancer Cell. 2005 Jan;7(1):77–85.

268. Scott I, Youle RJ. Mitochondrial fission and fusion. Essays Biochem. 2010;47:85–98.

269. Lewis MR, Lewis WH. Mitochondria in Tissue Culture. Science. 1914 Feb 27;39(1000):330–3.

270. Gao Z, Li Y, Wang F, Huang T, Fan K, Zhang Y, et al. Mitochondrial dynamics controls anti-tumour innate immunity by regulating CHIP-IRF1 axis stability. Nat Commun. 2017 Nov 27;8(1):1805.

271. Escoll P, Song O-R, Viana F, Steiner B, Lagache T, Olivo-Marin J-C, et al. Legionella pneumophila Modulates Mitochondrial Dynamics to Trigger Metabolic Repurposing of Infected Macrophages. Cell Host Microbe. 2017 Sep 13;22(3):302-316.e7.

272. Sokol CL, Luster AD. The Chemokine System in Innate Immunity. Cold Spring Harb Perspect Biol. 2015 Jan 29;a016303.

273. Borroni EM, Bonecchi R. Shaping the gradient by nonchemotactic chemokine receptors. Cell Adhes Migr. 2009;3(2):146–7.

274. Murdoch C, Finn A. Chemokine receptors and their role in inflammation and infectious diseases. Blood. 2000 May 15;95(10):3032–43.

275. Jha AK, Huang SC-C, Sergushichev A, Lampropoulou V, Ivanova Y, Loginicheva E, et al. Network Integration of Parallel Metabolic and Transcriptional Data Reveals Metabolic Modules that Regulate Macrophage Polarization. Immunity. 2015 Mar 17;42(3):419–30.

276. Ip WKE, Hoshi N, Shouval DS, Snapper S, Medzhitov R. Anti-inflammatory effect of IL-10 mediated by metabolic reprogramming of macrophages. Science. 2017 May 5;356(6337):513–9.

277. Van den Bossche J, Baardman J, Otto NA, van der Velden S, Neele AE, van den Berg SM, et al. Mitochondrial Dysfunction Prevents Repolarization of Inflammatory Macrophages. Cell Rep. 2016 Oct 11;17(3):684–96.

278. Peyvandi F, Kouides P, Turecek PL, Dow E, Berntorp E. Evolution of replacement therapy for von Willebrand disease: From plasma fraction to recombinant von Willebrand factor. Blood Rev. 2019 Nov 1;38:100572.

279. Miyazaki S, Ishikawa F, Fujikawa T, Nagata S, Yamaguchi K. Intraperitoneal Injection of Lipopolysaccharide Induces Dynamic Migration of Gr-1high

Polymorphonuclear Neutrophils in the Murine Abdominal Cavity. Clin Diagn Lab Immunol. 2004 May;11(3):452–7.

280. Lund ME, O'Brien BA, Hutchinson AT, Robinson MW, Simpson AM, Dalton JP, et al. Secreted Proteins from the Helminth Fasciola hepatica Inhibit the Initiation of Autoreactive T Cell Responses and Prevent Diabetes in the NOD Mouse. PLoS ONE [Internet]. 2014 Jan 21 [cited 2019 Apr 3];9(1). Available from: https://www.ncbi.nlm.nih.gov/pmc/articles/PMC3897667/

281. Jenkins SJ, Ruckerl D, Thomas GD, Hewitson JP, Duncan S, Brombacher F, et al. IL-4 directly signals tissue-resident macrophages to proliferate beyond homeostatic levels controlled by CSF-1. J Exp Med. 2013 Oct 21;210(11):2477–91.

282. Fleischmann J, Golde DW, Weisbart RH, Gasson JC. Granulocyte-macrophage colony-stimulating factor enhances phagocytosis of bacteria by human neutrophils. Blood. 1986 Sep 1;68(3):708–11.

283. Varin A, Mukhopadhyay S, Herbein G, Gordon S. Alternative activation of macrophages by IL-4 impairs phagocytosis of pathogens but potentiates microbial-induced signalling and cytokine secretion. Blood. 2010 Jan 14;115(2):353–62.

284. Feng X, Deng T, Zhang Y, Su S, Wei C, Han D. Lipopolysaccharide inhibits macrophage phagocytosis of apoptotic neutrophils by regulating the production of tumour necrosis factor α and growth arrest-specific gene 6. Immunology. 2011 Feb;132(2):287–95.

285. Jurica MS, Mesecar A, Heath PJ, Shi W, Nowak T, Stoddard BL. The allosteric regulation of pyruvate kinase by fructose-1,6-bisphosphate. Structure. 1998 Feb 15;6(2):195–210.

286. Wohner N, Muczynski V, Mohamadi A, Legendre P, Aymé G, Christophe OD, et al. Macrophage scavenger-receptor SR-AI contributes to the clearance of von Willebrand factor. Haematologica. 2018 Jan 11;haematol.2017.175216.

287. Suen D-F, Norris KL, Youle RJ. Mitochondrial dynamics and apoptosis. Genes Dev. 2008 Jun 15;22(12):1577–90.

288. Canton J, Neculai D, Grinstein S. Scavenger receptors in homeostasis and immunity. Nat Rev Immunol. 2013 Sep;13(9):621–34.

289. Zani IA, Stephen SL, Mughal NA, Russell D, Homer-Vanniasinkam S, Wheatcroft SB, et al. Scavenger Receptor Structure and Function in Health and Disease. Cells. 2015 Jun;4(2):178–201.

290. Areschoug T, Gordon S. Scavenger receptors: role in innate immunity and microbial pathogenesis. Cell Microbiol. 2009;11(8):1160–9.

291. Hampton RY, Golenbock DT, Penman M, Krieger M, Raetz CR. Recognition and plasma clearance of endotoxin by scavenger receptors. Nature. 1991 Jul 25;352(6333):342–4.

292. Peiser L, Makepeace K, Plüddemann A, Savino S, Wright JC, Pizza M, et al. Identification of Neisseria meningitidis nonlipopolysaccharide ligands for class A macrophage scavenger receptor by using a novel assay. Infect Immun. 2006 Sep;74(9):5191–9.

293. Suzuki H, Kurihara Y, Takeya M, Kamada N, Kataoka M, Jishage K, et al. A role for macrophage scavenger receptors in atherosclerosis and susceptibility to infection. Nature. 1997 Mar 20;386(6622):292–6.

294. Suzuki H, Kurihara Y, Takeya M, Kamada N, Kataoka M, Jishage K, et al. A role for macrophage scavenger receptors in atherosclerosis and susceptibility to infection. Nature. 1997 Mar;386(6622):292.

295. Manning-Tobin JJ, Moore KJ, Seimon TA, Bell SA, Sharuk M, Alvarez-Leite JI, et al. Loss of SR-A and CD36 activity reduces atherosclerotic lesion complexity without abrogating foam cell formation in hyperlipidemic mice. Arterioscler Thromb Vasc Biol. 2009 Jan;29(1):19–26.

296. Lillis AP, Van Duyn LB, Murphy-Ullrich JE, Strickland DK. The low density lipoprotein receptor-related protein 1: Unique tissue-specific functions revealed by selective gene knockout studies. Physiol Rev. 2008 Jul;88(3):887–918.

297. Luo L, Wall AA, Tong SJ, Hung Y, Xiao Z, Tarique AA, et al. TLR Crosstalk Activates LRP1 to Recruit Rab8a and PI3Kγ for Suppression of Inflammatory Responses. Cell Rep. 2018 Sep 11;24(11):3033–44.

298. Yang L, Liu C-C, Zheng H, Kanekiyo T, Atagi Y, Jia L, et al. LRP1 modulates the microglial immune response via regulation of JNK and NF-κB signaling pathways. J Neuroinflammation [Internet]. 2016 Dec 8;13. Available from: https://www.ncbi.nlm.nih.gov/pmc/articles/PMC5146875/

299. Cornish AL, Freeman S, Forbes G, Ni J, Zhang M, Cepeda M, et al. Characterization of siglec-5, a novel glycoprotein expressed on myeloid cells related to CD33. Blood. 1998 Sep 15;92(6):2123–32.

300. Crocker PR, Paulson JC, Varki A. Siglecs and their roles in the immune system. Nat Rev Immunol. 2007 Apr;7(4):255–66.

301. Crocker PR. Siglecs in innate immunity. Curr Opin Pharmacol. 2005 Aug 1;5(4):431–7.

302. van Vliet SJ, van Liempt E, Saeland E, Aarnoudse CA, Appelmelk B, Irimura T, et al. Carbohydrate profiling reveals a distinctive role for the C-type lectin MGL in the recognition of helminth parasites and tumor antigens by dendritic cells. Int Immunol. 2005 May;17(5):661–9.

303. van Vliet SJ, Gringhuis SI, Geijtenbeek TBH, van Kooyk Y. Regulation of effector T cells by antigen-presenting cells via interaction of the C-type lectin MGL with CD45. Nat Immunol. 2006 Nov;7(11):1200–8.

304. Staudt ND, Jo M, Hu J, Bristow JM, Pizzo DP, Gaultier A, et al. Myeloid cell receptor LRP1/CD91 regulates monocyte recruitment and angiogenesis in tumors. Cancer Res. 2013 Jul 1;73(13):3902–12.

305. Gaultier A, Arandjelovic S, Niessen S, Overton CD, Linton MF, Fazio S, et al. Regulation of tumor necrosis factor receptor-1 and the IKK-NF-kappaB pathway by LDL receptor-related protein explains the antiinflammatory activity of this receptor. Blood. 2008 Jun 1;111(11):5316–25.

306. Lee D, Walsh JD, Migliorini M, Yu P, Cai T, Schwieters CD, et al. The structure of receptor-associated protein (RAP). Protein Sci Publ Protein Soc. 2007 Aug;16(8):1628–40.

307. Del Rey MJ, Valín Á, Usategui A, García-Herrero CM, Sánchez-Aragó M, Cuezva JM, et al. Hif-1α Knockdown Reduces Glycolytic Metabolism and Induces Cell Death of Human Synovial Fibroblasts Under Normoxic Conditions. Sci Rep [Internet]. 2017 Jun 16 [cited 2019 May 8];7. Available from: https://www.ncbi.nlm.nih.gov/pmc/articles/PMC5473902/

308. Kaelin WG, Ratcliffe PJ. Oxygen sensing by metazoans: the central role of the HIF hydroxylase pathway. Mol Cell. 2008 May 23;30(4):393–402.

309. Perrin-Cocon L, Aublin-Gex A, Diaz O, Ramière C, Peri F, André P, et al. Toll-like Receptor 4–Induced Glycolytic Burst in Human Monocyte-Derived Dendritic Cells Results from p38-Dependent Stabilization of HIF-1α and Increased Hexokinase II Expression. J Immunol. 2018 Jul 23;ji1701522.

310. Castellano J, Aledo R, Sendra J, Costales P, Juan-Babot O, Badimon L, et al. Hypoxia stimulates low-density lipoprotein receptor-related protein-1 expression through hypoxia-inducible factor-1α in human vascular smooth muscle cells. Arterioscler Thromb Vasc Biol. 2011 Jun;31(6):1411–20.

311. Gorovoy M, Gaultier A, Campana WM, Firestein GS, Gonias SL. Inflammatory mediators promote production of shed LRP1/CD91, which regulates cell signaling and cytokine expression by macrophages. J Leukoc Biol. 2010 Oct 1;88(4):769–78.

312. Luo L, Wall AA, Tong SJ, Hung Y, Xiao Z, Tarique AA, et al. TLR Crosstalk Activates LRP1 to Recruit Rab8a and PI3Kγ for Suppression of Inflammatory Responses. Cell Rep. 2018 Sep 11;24(11):3033–44.

313. Chion A, O'Sullivan J, Bergsson G, Keyes S, Rawley O, Fallon P, et al. N-Linked Glycans within the A1A2A3 Domains of VWF Play a Critical Role in Modulating Macrophage-Mediated Clearance. Blood. 2014 Dec 6;124(21):469–469.

314. Westra J, Brouwer E, van Roosmalen IA, Doornbos-van der Meer B, van Leeuwen MA, Posthumus MD, et al. Expression and regulation of HIF-1alpha in macrophages under inflammatory conditions; significant reduction of VEGF by CaMKII inhibitor. BMC Musculoskelet Disord. 2010 Mar 30;11:61.

315. Yu F, White SB, Zhao Q, Lee FS. HIF-1α binding to VHL is regulated by stimulus-sensitive proline hydroxylation. Proc Natl Acad Sci. 2001 Aug 14;98(17):9630–5.

316. Martinez-Pomares L. The mannose receptor. J Leukoc Biol. 2012 Dec;92(6):1177–86.

317. Lepay DA, Steinman RM, Nathan CF, Murray HW, Cohn ZA. Liver macrophages in murine listeriosis. Cell-mediated immunity is correlated with an influx of macrophages capable of generating reactive oxygen intermediates. J Exp Med. 1985 Jun 1;161(6):1503–12.

318. Dong J-F, Berndt MC, Schade A, McIntire LV, Andrews RK, López JA. Ristocetin-dependent, but not botrocetin-dependent, binding of von Willebrand factor to the platelet glycoprotein Ib-IX-V complex correlates with shear-dependent interactions. Blood. 2001 Jan 1;97(1):162–8.

319. De Luca M, Facey DA, Favaloro EJ, Hertzberg MS, Whisstock JC, McNally T, et al. Structure and function of the von Willebrand factor A1 domain: analysis with monoclonal antibodies reveals distinct binding sites involved in recognition of the platelet membrane glycoprotein Ib-IX-V complex and ristocetin-dependent activation. Blood. 2000 Jan 1;95(1):164–72.

320. Kelly B, O'Neill LA. Metabolic reprogramming in macrophages and dendritic cells in innate immunity. Cell Res. 2015 Jul;25(7):771–84.

321. Wegener G, Krause U. Different modes of activating phosphofructokinase, a key regulatory enzyme of glycolysis, in working vertebrate muscle. Biochem Soc Trans. 2002 Apr;30(2):264–70.

322. Gupta V, Bamezai RN. Human pyruvate kinase M2: A multifunctional protein. Protein Sci Publ Protein Soc. 2010 Nov;19(11):2031–44.

323. Yang Y, Kim SC, Yu T, Yi Y-S, Rhee MH, Sung G-H, et al. Functional Roles of p38 Mitogen-Activated Protein Kinase in Macrophage-Mediated Inflammatory Responses. Mediators Inflamm [Internet]. 2014 [cited 2019 Oct 31];2014. Available from: https://www.ncbi.nlm.nih.gov/pmc/articles/PMC3977509/

324. Wang Z, Harkins PC, Ulevitch RJ, Han J, Cobb MH, Goldsmith EJ. The structure of mitogen-activated protein kinase p38 at 2.1-Å resolution. Proc Natl Acad Sci. 1997 Mar 18;94(6):2327–32.

325. Keesler GA, Bray J, Hunt J, Johnson DA, Gleason T, Yao Z, et al. Purification and activation of recombinant p38 isoforms alpha, beta, gamma, and delta. Protein Expr Purif. 1998 Nov;14(2):221–8.

326. Huang C, Ma WY, Maxiner A, Sun Y, Dong Z. p38 kinase mediates UV-induced phosphorylation of p53 protein at serine 389. J Biol Chem. 1999 Apr 30;274(18):12229–35.

327. Zhao M, New L, Kravchenko VV, Kato Y, Gram H, di Padova F, et al. Regulation of the MEF2 family of transcription factors by p38. Mol Cell Biol. 1999 Jan;19(1):21–30.

328. Han J, Jiang Y, Li Z, Kravchenko VV, Ulevitch RJ. Activation of the transcription factor MEF2C by the MAP kinase p38 in inflammation. Nature. 1997 Mar 20;386(6622):296–9.

329. Khurana A, Nakayama K, Williams S, Davis RJ, Mustelin T, Ronai Z. Regulation of the Ring Finger E3 Ligase Siah2 by p38 MAPK. J Biol Chem. 2006 Nov 17;281(46):35316–26.

Appendix i: Abstracts submitted for oral communications

Haematology Association of Ireland, Annual Meeting 2018

A novel role for von Willebrand factor promoting pro-inflammatory responses in macrophages

Clive Drakeford, Sonia Aguila, Alain Chion, Eamon Breen, Mariana Cervantes, Frederick J Sheedy, James S O'Donnell

Introduction
von Willebrand factor (VWF) is a large multimeric glycoprotein that plays a critical role in normal haemostasis by tethering platelets to exposed sub-endothelial collagen at sites of vascular injury. Importantly, recent studies have also demonstrated that VWF can bind directly to innate immune cells including macrophages and neutrophils. Furthermore, emerging data suggest that VWF is implicated in modulating the pathogenesis underlying *in vivo* inflammation in models of cutaneous inflammation, malaria and sepsis. However, the molecular mechanisms through which VWF functions to modulate inflammatory responses remains unknown. In this study, we investigated the hypothesis that VWF binding influences macrophages biology.

Methodology
Human CD14High monocytes were isolated from healthy donors and differentiated into macrophages with 10% human serum. Primary bone marrow-derived macrophages were isolated from murine bone marrow and cultured with MCSF. THP1 monocytes were differentiated to macrophages with PMA for 72h. Binding of full length VWF and fragments (D'-D3, A1A2A3, A1, A2, A3, D'-A3 and A3-CK) to THP1 was assessed by flow cytometry. After treatment with purified full length VWF, macrophage mRNA and cell lysates were harvested. Cytokines were measured by ELISA from supernatant. Macrophage physiological changes in metabolism and phagocytosis were assessed using Seahorse technology and phagocytosis capacity of fluorescent bacteria.

Results
In keeping with previous studies, we observed that macrophages derived from the THP1 bound to VWF in a dose- and time-dependent manner. Assessment of the VWF fragments revealed significant binding to the constructs A1A2A3, A1 and D'-A3. Incubation of full-length VWF with primary macrophages significantly induced pro-inflammatory signalling and activation. In particular, interaction with VWF resulted in phosphorylation of the MAP-kinase pathway, P-p38 and P-JNK, in both human and murine primary macrophages. Moreover, VWF interaction with macrophages also lead to activation of the NF-kB pathway. Thus, VWF led to enhanced mRNA expression for a panel of pro-inflammatory cytokines (including TNF-α, IL-1β, IL-6, CCL2/3/4). Moreover, it increased the secretion levels of TNF-α and IL-1β in the cell culture supernatant. Given the observed increase in chemokine expression, we assessed VWF chemoattractant ability. To this end, VWF significantly induced monocyte transmigration. Previous studies have demonstrated that the scavenger receptor Low Density Receptor-Related Protein 1 (LRP1) plays a key role in macrophage-mediated VWF clearance. Interestingly, LRP1 inhibition with RAP or a monoclonal antibody anti-LRP1 markedly attenuated the pro-inflammatory signalling of VWF in primary macrophages. Finally, we found that VWF increases the maximal respiratory capacity and glycolysis of macrophages while also reducing its phagocytosis capacity. This demonstrates that VWF alters macrophage inflammatory function.

Conclusion

Collectively, our findings demonstrate that macrophages do not merely play a central role in regulating clearance of VWF *in vivo*. Rather, our findings support the hypostasis that VWF interaction with macrophages also plays a direct role in macrophages activation modulating multiple aspects of its biology. Given that VWF deposition is responsible for triggering recruitment of both platelets and mononuclear leucocytes at sites of vascular injury, we now propose an additional novel role for VWF in coupling primary haemostasis and innate immunity by priming a pro-inflammatory macrophage phenotype.

A novel role for von Willebrand factor promoting pro-inflammatory responses in macrophages

Clive Drakeford, Sonia Aguila, Alain Chion, Eamon Breen, Mariana Cervantes, Frederick J Sheedy, James S O'Donnell

Introduction

von Willebrand factor (VWF) is a large multimeric glycoprotein that plays a critical role in normal haemostasis by tethering platelets to exposed sub-endothelial collagen at sites of vascular injury. Importantly, recent studies have also demonstrated that VWF can bind directly to innate immune cells including macrophages and neutrophils. Furthermore, emerging data suggest that VWF is implicated in modulating the pathogenesis underlying *in vivo* inflammation in models of cutaneous inflammation, malaria and sepsis. However, the molecular mechanisms through which VWF functions to modulate inflammatory responses remains unknown. In this study, we investigated the hypothesis that VWF binding influences macrophages biology.

Methodology

Human CD14High monocytes were isolated from blood from healthy donors and differentiated into macrophages in 10% human serum for 7 days. In addition, primary bone marrow-derived macrophages were isolated from murine bone marrow and cultured with MCSF for 7 days. Finally, THP1 monocytes were differentiated to macrophages with PMA for 72h. Binding of full length VWF and fragments (D'-D3, A1A2A3, A1, A2, A3, D'-A3 and A3-CK) to THP1 was assessed by flow cytometry. After treatment with purified full length VWF, macrophage mRNA and cell lysates were harvested for RT-qPCR and western blot. Cytokines were measured by ELISA from supernatant. Macrophage physiological changes in metabolism and phagocytosis were assessed using Seahorse technology and phagocytosis capacity of fluorescent bacteria.

Results

In keeping with previous studies, we observed that macrophages derived from the THP1 bound to VWF in a dose- and time-dependent manner. Assessment of the VWF fragments revealed significant binding to the constructs A1A2A3, A1 and D'-A3. Incubation of full-length VWF with primary macrophages significantly induced pro-inflammatory signalling and activation. In particular, interaction with VWF resulted in phosphorylation of the MAP-kinase pathway, P-p38 and P-JNK, in both human and murine primary macrophages. Moreover, VWF interaction with macrophages also lead to activation of the NF-kB pathway. Thus, VWF led to enhanced mRNA expression for a panel of pro-inflammatory cytokines (including TNF-α, IL-1β, IL-6, CCL2/3/4). Moreover, it increased the secretion levels of TNF-α and IL-1β in the cell culture supernatant. Previous studies have demonstrated that the scavenger receptor Low Density Receptor-Related Protein 1 (LRP1) plays a key role in macrophage-mediated VWF clearance. Interestingly, LRP1 inhibition with RAP or a monoclonal antibody anti-LRP1 markedly attenuated but did not completely ablate the pro-inflammatory signalling of VWF on primary macrophages. Finally, we found that VWF increases the maximal respiratory capacity and glycolysis of macrophages while also reducing its phagocytosis capacity. This demonstrates that VWF alters macrophage inflammatory function.

Conclusion

Collectively, our findings demonstrate that macrophages do not merely play a central role in regulating clearance of VWF *in vivo*. Rather, our findings support the hypostasis that VWF interaction with macrophages also plays a direct role in macrophages activation modulating multiple aspects of its biology. Given that VWF deposition is responsible for triggering recruitment

of both platelets and mononuclear leucocytes at sites of vascular injury, we now propose an additional novel role for VWF in coupling primary haemostasis and innate immunity by priming a pro-inflammatory macrophage phenotype.

The binding of VWF augments macrophage TLR (2/4) signalling – an emerging role for VWF in macrophage biology and vascular haemostasis.

Clive Drakeford, Frederick J Sheedy, Sharee Basdeo, Alain Chion, Sonia Aguila, Joseph Keane and James O'Donnell

Background

Von Willebrand Factor (VWF) is a large glycoprotein with a crucial haemostatic function in tethering platelets to damaged endothelium. However recent studies have identified novel roles for VWF binding leukocytes and assisting their transmigration at sites of injury. Toll like receptors (TLR) are a class of proteins on sentinel cells involved in the innate immune response. TLRs are responsible for recognition of a number of pathogen or damage associated molecular patterns. In this study we investigated the ability of VWF to bind monocytes, and its subsequent effect on monocyte biology mediated by TLR activation.

Methods

The binding and endocytosis of VWF by THP1 (human monocytic cell line) or primary monocytes-macrophages was analysed by high content analysis and confocal microscopy. The immunomodulatory effect of VWF on macrophage activation was assessed by treating macrophages with VWF prior to the addition of TLR agonists. Concentrations of TNF-α present in the supernatants were determined by ELISA. Classically phorbol ester (PMA) differentiated THP1 macrophages treated as above and lysed after 30 minutes post-treatment. Lysates were analysed by SDS-PAGE gel and probed for phospho-p38 and phospho-JNK using polyclonal antibodies.

Results

Our results demonstrate that macrophages can efficiently bind and internalise labelled VWF and it co-localises with positive early endosomes marker 1. Furthermore macrophages bound with VWF and subsequently treated with TLR ligands, had a significant increase in pro inflammatory cytokine TNFα production specifically in response to TLR4 or TLR1/2 activation with LPS and PAM3, respectively. VWF did not however affect the production of TNF-α by macrophages treated with TLR 2/6, 3, 7/8 agonists. Importantly VWF alone had no significant effect on TNFα secretion. Upstream of TNF production is the activation of pro inflammatory transcription factors which are regulated by the MAP kinase pathways. Immunoblotting analysis reveals that VWF treatment augments the signalling of TLRs 2 and 4 through MAP kinase phospho-JNK and phospho-p38. These results indicate that macrophages/monocytes can bind VWF and this can specifically augment TLR signalling through TLRs 1:2 and TLR4.

Discussion

Our data confirm the ability of monocytes to bind VWF and critically for the first time show that VWF can synergise with TLR4 and TLR2 to enhance pro-inflammatory cytokine production. Crucially these specific bacteria sensing TLRs 2 and 4 also implicated in vascular injury and inflammation, can non-conically utilise the adapter protein Mal to trigger MAP kinase and PI3-kinase signalling. Furthermore, Mal dependent signalling works in a low ligand concentrations, VWF may be acting as a Mal sensitizer for a TLR-2 and 4 agonists, potently explaining why we did not observe an affect from VWF alone. These novel findings indicate that VWF may have a role in propagating inflammation during vascular injury. Thus, VWF may potentially be a therapeutic target in cardiovascular disease given its function in both immunology and haemostasis.

Appendix ii

Negative Control

Positive Control

VWF

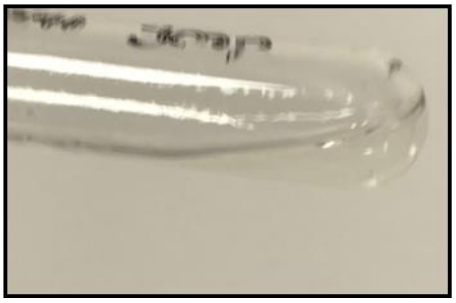

Plasma derived VWF is negative for endotoxin contamination

The Limulus Amebocyte Lysate (LAL) gel clot assay is a qualitative test for Gram-negative bacterial endotoxin. In the presence of endotoxin (0.25EU/ml), gelation occurs; in the absence of endotoxin, gelation does not occur. Negative control, cell culture grade PBS does not result in gel clot formation, positive control, (LPS 0.25EU/ml) results in gel clot formation and VWF (10µg/ml) does not result in gel clot formation.

Appendix iii Publications

VON WILLEBRAND FACTOR REGULATES MACROPHAGE METABOLISM TO PROMOTE A PRO-INFLAMMATORY PHENOTYPE

Clive Drakeford[1]*, Sonia Aguila[1]*, Alain Chion[1], Eamon Breen[2], Mariana P. Cervantes[3], Annie M. Curtis[3], Joe Keane[2], Padraic Fallon[4,5], Roger J.S. Preston[1,5], Jamie M. O'Sullivan[1], Ross Murphy[6], Frederick J. Sheedy[7] and James S. O'Donnell[1,5,8]

[1] Haemostasis Research Group, Irish Centre for Vascular Biology, Royal College of Surgeons in Ireland.

[2] Department of Clinical Medicine, Trinity Translational Medicine Institute, Trinity College Dublin, Dublin, Ireland.

[3] Department of Molecular and Cellular Therapeutics and Tissue Engineering Research Group (TERG), Royal College of Surgeons in Ireland, Dublin 2, Ireland

[4] School of Medicine, Trinity Biomedical Sciences Institute, Trinity College Dublin, Dublin 2, Ireland.

[5] National Children's Research Centre, Our Lady's Children's Hospital, Dublin, Ireland.

[6] Department of Cardiology, St James's Hospital, Dublin, Ireland.

[7] School of Biochemistry and Immunology, Trinity Biomedical Sciences Institute, Trinity College Dublin, Ireland

[8] National Coagulation Centre, St James's Hospital, Dublin, Ireland.

Running Title:	**VWF regulates macrophage metabolism**
Text word count:	**4337**
Abstract word count:	**145**
Figure count:	**8**
Reference count:	**67**

Editorial correspondence should be addressed to:
Prof. James O'Donnell,
Irish Centre for Vascular Biology,
Royal College of Surgeons in Ireland,
Ardilaun House, 111 St. Stephen's Green, Dublin 2, Ireland.
Tel +353 (1) 416 2141; Fax +353 (1) 410 3570;
e-mail jamesodonnell@rcsi.ie

KEY POINTS

[1] VWF binding to macrophages triggers direct downstream MAPkinase signalling leading to NF-κB activation and production of pro-inflammatory cytokines and chemokines.

[2] VWF binding also promotes macrophage pro-inflammatory M1 polarization and shifts macrophage metabolism towards glycolysis.

ABSTRACT

The plasma multimeric glycoprotein von Willebrand factor (VWF) plays a critical role in primary haemostasis by tethering platelets to exposed collagen at sites of vascular injury. Recent studies have identified additional biological roles for VWF, and in particular suggest that VWF may play an important role in regulating inflammatory responses. Critically however, the molecular mechanisms through which VWF exerts its immuno-modulatory effects remains poorly understood. In this study, we report for the first time that VWF binding to macrophages triggers direct downstream MAPkinase signalling leading to NF-κB activation and production of pro-inflammatory cytokines and chemokines. In keeping with these observations, VWF binding also promotes macrophage M1 polarization and shifts macrophage metabolism towards glycolysis. Cumulatively, our findings define an entirely novel biological role for VWF in modulating macrophage function, and thereby establish a novel link between primary haemostasis and innate immunity.

KEYWORDS

– von Willebrand factor; Von Willebrand disease; Macrophage; Inflammation; Mitochondria.

INTRODUCTION

von Willebrand factor (VWF) is a large sialoglycoprotein that circulates in normal plasma as a series of heterogeneous multimers.[1,2] For many years, the importance of plasma VWF in maintaining normal hemostasis has been recognized.[3,4] VWF binds to exposed subendothelial collagen at sites of vascular injury.[5] Subsequently, shear stress-induced unwinding of globular VWF results in exposure of the platelet glycoprotein Ibα (GPIbα) binding site within the A1 domain.[5,6] Consequently, tethered and unwound VWF can recruit platelets to the site of injury, leading to formation of the primary platelet plug. In addition, VWF also binds with high affinity to procoagulant factor VIII, thereby protecting it against proteolysis and premature clearance.[7]

In addition to its hemostatic function, recent studies have identified additional novel biological roles for VWF, including inhibition of angiogenesis and promotion of tumor cell apoptosis.[8-10] Furthermore, accumulating evidence suggests that VWF plays important roles in enhancing inflammatory responses.[11-18] Acute activation of endothelial cells (EC) triggers secretion of high molecular weight multimeric (HMWM) VWF stored within Weibel Palade bodies (WPB).[1] Consequently, it is perhaps unsurprising that elevated plasma VWF levels have been reported in association with different types of sepsis, as well as a number of other vascular pathologies.[11] Indeed plasma VWF:Ag and VWF propeptide (VWFpp) levels have both been proposed as useful biomarkers that correlate with severity and/or clinical outcomes in a number of different disease settings, including cerebral malaria, sickle cell disease, systemic inflammatory response syndrome and a variety of different cancers (e.g. colorectal, hepatocellular and lung).[9,19-23]

Importantly, data from studies conducted in a number of different animal inflammatory disease models suggest that VWF does not merely serve as a marker of acute EC activation, but rather that it plays an active role in mediating the underlying pathophysiology.[13-16,19] For example, in a caecal puncture sepsis model, overall survival was significantly increased in

VWF-deficient mice compared to wild type controls.[15] In addition, Petri *et al* showed that VWF-blocking antibodies significantly attenuated neutrophil recruitment into thioglycollate-inflamed peritoneum and keratinocyte-derived chemokine (KC)-stimulated exposed cremaster muscle.[14] In both of these murine models of inflammation, VWF-modulated neutrophil extravasation was critically dependent upon the presence of platelets. Similarly, VWF-blocking antibodies were shown to again significantly reduce neutrophil recruitment in murine models of immune-complex-mediated vasculitis and irritative contact dermatitis respectively.[13] Interestingly, Hillgruber *et al* further demonstrated that VWF-modulated neutrophil recruitment in these murine models of cutaneous inflammatory was mediated through a platelet-independent pathway.[13]

All together, these findings demonstrate that VWF influences multiple different aspects of inflammation. Critically however, the molecular mechanisms through which VWF exerts its pro-inflammatory effects remain poorly understood. Recent studies have reported that VWF can bind to macrophages, following which it is rapidly endocytosed.[24-26] Moreover, hepatic Kupffer cells have been shown to play a key role in regulating the circulatory half-life of plasma VWF.[24,27] A number of specific macrophage receptors have been implicated in regulating VWF binding, including the low density lipoprotein receptor-related protein-1 (LRP1), the scavenger receptor class A member 1 (SR-A1), macrophage galactose-type lectin (MGL) and Siglec-5.[26-30] Given the importance of macrophages in regulating innate immune responses, we hypothesized that VWF binding might influence macrophage biology and thereby impact upon inflammatory responses. We report a novel biological role for VWF in directing pro-inflammatory macrophage responses, and thereby define a previously unrecognized link between primary hemostasis and innate immunity.

MATERIALS AND METHODS

Reagents

Human plasma derived von Willebrand factor-Factor VIII free (VWF) (Haematology Technologies Inc.), Recombinant von Willebrand factor, VonVendi® (r-VWF) (Takeda), Ultra pure lipopolyssacharide (LPS) (Sigma), INFγ (Life technologies, Gibco), IL-4 (Life technologies, Gibco), IL-10 (Life technologies, Gibco), IL-13 (Life technologies, Gibco). Recombinant mouse M-CSF (rm M-CSF) (R&D System), Cell Tracker green CMFDA Dye (Thermofisher), Seahorse XF Cell Mito Stress Cell Kit (Agilent), Primary antibodies human anti-p38, P-p38, JNK, P-JNK, IKBα, P-IKBα, p65, P-p65, HIF-1α and β-actin (Cell Signalling technologies), Alexa Fluor 488 conjugate (Molecular Probes, Thermofisher Scientific).

Cell culture

Peripheral blood mononuclear cells (PBMC) were isolated from health donor buffy coats following histopaque (Sigma) gradient separation. Anti-CD14 beads (Miltenyi Biotec) were used to isolate monocytes. Isolated monocytes were differentiated into macrophages for 7-10 days in the RPMI media supplemented with 10% human serum (Sigma), Penicillin-Streptomycin 100µg/ml (Life technologies, Gibco). Murine PBMC were isolated from the bone marrow from 8-12 weeks old C57/B6JB mice. PBMC were incubated for 7 days in RPMI supplemented with 10% fetal bovine serum (Life Technologies, Gibco), 25ng/ml rmM-CSF and Penicillin-Streptomycin 100ug/ml. THP1 monocytes were differentiated into macrophages in the presence of 100µM PMA (Sigma) for 3 days.

Western blotting

Cells were lysed in RIPA Buffer (ThermoFisher) supplemented with protease (Merck) and phosphatase (Sigma) inhibitors and normalised using BCA Protein Assay Kit (Pierce,

ThermoFisher). Samples were resolved by SDS-PAGE. Primary antibodies were incubated overnight at 4^0C and subsequently incubated with 1/1000 IgG-HRP antibodies. Blots were developed using chemiluminescence staining (ECL, Pierce, Thermofisher).

mRNA isolation and qRT-PCR

Total mRNA was isolated using Trizol (Sigma). cDNA was synthesised using RevertAid reverse transcriptase (ThermoFisher) and RT-qPCR was performed in triplicates with Go Taq qPCR master mix (Promega) using Life Technologies 7500 Real Time PCR System. The mRNA level was normalized to β-actin. To determine the activation of PHD3 and iNOS cell lysates and RNA were isolated from human primary macrophages after 24h treatment of VWF or LPS. Primer sequences are listed in Supplementary Table 1.

Cytokine analysis

Human primary macrophage IL-1β, TNFα and IL-6 cytokines were quantified by ELISA (Invitrogen) following a 4h or 24h treatment with either 10 μg/ml of VWF or 100 μg/ml of LPS in RPMI supplemented with 1mM $CaCl_2$. Human primary macrophage inflammasome activation was detected after 24h incubation with VWF or LPS. Cells were subsequently incubated with ATP 150mM for 1h in serum free RPMI and pro-IL1β was determined by western blot (goat anti-pro-IL-1β CST).

VWF binding to human and murine macrophages

Flow Cytometry: Human monocyte derived macrophages were incubated with plasma derived or recombinant VWF (10μg/ml) of in RPMI + 1mM CaCl for 30 min on ice. Fc receptors were blocked using a Fc-gamma receptor inhibitor (Thermofisher). Bound VWF was detected using polyclonal rabbit anti-human VWF (Dako, Agilent) for 30 min followed by anti-rabbit Alexa-

488 (Thermofisher) for 30 min. Bound recombinant VWF was detected using a PE-labelled Anti-His Tag antibody (BioLegand).

Confocal microscopy. Monocytes were differentiated on glass coverslips (Nunc, Lab-Tek). Macrophages were incubated with 20 μg/ml of VWF at room temperature in RPMI supplemented with CaCl 1mM for 30 min. Cells were blocked with Fc-gamma receptor inhibitor (ThermoFisher) and 3% BSA and incubated with anti-VWF and anti-rabbit Alexa 488. THP1 cells were differentiated and incubated with anti-VWF antibody and anti-early endosomal antigen 1 (EEA1) antibody (Santa-Cruz). Cell membrane was labelled with cell mask deep red (Molecular probes, Thermofisher Scientific) cells were mounted with mounting media and in-situ DAPI stain (Sigma).

Role of VWF in Macrophage Polarization

Murine - Bone marrow derived macrophages (BMDM) were cultured with M-CSF (25ng/ml) for 24 hours. Additionally LPS (100ng/ml) and INFγ (20ng/ml) were added to generate a M1 polarized phenotype. IL-4 (40ng/ml), IL-13 (20ng/ml) and IL-10 (10ng/ml) was added to generate M2 polarized macrophages. Alternatively, VWF (10μg/ml) in RPMI with 1mM $CaCl_2$ was used. Cells were examined for surface marker expression by flow cytometry. M1 macrophages were dual positive for CD11b (BioLegend) and CD38 (BioLegend). M2 were dual positive for CD11b and CD206 (BioLegend). Cellular reactive oxygen spices (ROS) generation was detected using CellROX DeepRed staining (ThermoFisher). BMDM were incubated with VWF or LPS for 24h and analysed by flow cytometry after exclusion of dead cells by Live-Dead FITC (ThermoFisher).

Measurement of VWF-mediated monocyte chemotaxis and transmigration

BMDM were stimulated with VWF (10µg/ml) or LPS (100ng/ml) in RPMI supplemented with $CaCl_2$ (1mM) and M-CSF (25ng/ml) for 24h. Supernatants were harvested and placed in the lower chamber and isolated human naive monocytes placed in the top chamber. Monocytes were allowed to migrate to the lower chamber for 2.5h. Migrated cells were stained using Cell Tracker green (ThermoFisher) for 30 min. Cell counts were quantified using ImageJ software and represented as fold change from control.

Effects of VWF on macrophage metabolism

Following BMDM differentiation, cells were seeded into Seahorse XF96 culture plates (Agilent) at a density of $5x10^5$ well and were stimulated with LPS (100ng/ml) or VWF (10µg/ml) for 3h or 16h in RPMI supplemented with 1mM $CaCl_2$. Following treatment BMDM were incubated with Seahorse phenol red-free base media in a CO_2 free incubator as per manufacturer's instructions (Agilent). To determine extracellular acidification and the oxygen consumption rate (ECAR & OCR), Seahorse Mito Stress Kit (Agilent) was used according to manufacturer's instructions. BMDMs were treated with mitochondrial complex V inhibitor oligomycin (Oligio), mitochondrial membrane uncoupling agent carbonyl cyanide p-trifluoromethoxyphenylhydrazone (FCCP) and finally complex I and III inhibitors rotenone and antimycin A (R+AA) all as previously described.[31,32] Mitochondrial morphology was determined using a Leica SP8 scanning confocal microscopy under live cell imaging. BMDM were seeded onto 4 well culture dishes (Ibidi) at $1x10^5$ cells /well. Cells were stained with MitoTracker™ Red (Molecular Probes, Thermo fisher) and 20 images were taken per treatment. Images were analysed for mitochondrial morphology using Fiji ImageJ software. On average 60 mitochondrias were measured per cell. Mitochondrial fragmentation was considered <1µm, and elongated >3µm.[33,34]

Role of VWF administration on peritoneal immune cell recruitment

All in vivo experiments were performed in accordance with the Health Product Regulatory Authority, Ireland as previously described. In brief, female mice were injected intraperitoneally with VWF (2mg/kg) or PBS. Mice were subsequently sacrificed after 3h and 24 hr. Peritoneal lavage was performed using 5ml of ice cold PBS + 2% FBS. Cell populations were analysed by flow cytometry from the lavage fluid (Ly-6G$^+$ neutrophils; F4/80$^+$ macrophages; CD45RB$^+$ B-Cells; CD3$^+$ T-Cells; CD11c$^+$ dendritic cells (DC) and CD122$^+$ natural killer (NK) cells). Antibodies were sourced from Biolegend. Cell populations were quantified by CyAn ADP platform (Dako, Agilent) and Flowjo software.

Data Presentation and Statistical Analysis

All experimental data and statistical analysis were performed using the GraphPad Prism program (Graphpad Prism version 5.0 for Windows; GraphPad Software, Inc. San Diego, CA). Data were expressed as mean values ± standard error of the mean (SEM). To assess statistical differences, data were analysed using Student's unpaired 2-tailed t test. For all statistical tests, P values <0.05 were considered significant.

RESULTS

VWF binding to macrophages triggers pro-inflammatory signaling

Recent studies have reported shear-dependent binding of VWF to macrophages.[35,36] In preliminary studies, we observed that purified plasma-derived (pd)-VWF can also bind to primary human macrophages and THP-1 derived macrophages under static conditions (Figures 1A and 1B). Moreover, this static binding was followed by VWF endocytosis (Figure 1C). Flow cytometry studies confirmed that pd-VWF and recombinant VWF both bound to human macrophages (Figures 1D, 1E and 1F). In contrast, no VWF binding to undifferentiated primary human monocytes or THP1 cells was observed (Supplementary Figure 1). Importantly, we further observed that pd-VWF binding was associated with pro-inflammatory intracellular signaling in both primary human macrophages (Figure 1G) and in murine bone marrow derived macrophages (BMDMs) (Figure 1H). In particular, VWF induced activation of the MAPKinase pro-inflammatory signaling pathway with phosphorylation of p38 and JNK. In addition, VWF binding also activated NF-κB with phosphorylation of its regulatory subunit IKBα (Figures 1G and 1H).

In keeping with these observed signaling effects, VWF binding to primary human-derived macrophages was associated with a significant increase in pro-inflammatory cytokine expression (including TNF-α, and IL-6) (Figures 2A and 2B). IL-1β protein expression associated with NLRP3 inflammasome activation has been reported to require dual signal triggering.[37] Interestingly, although VWF binding to macrophages was associated with an increase in IL-1β mRNA and pro-IL-1β levels (Figures 2C and 2D), a significant increase in IL-1β secretion (and concurrent decrease in pro-IL-1β) levels was only observed when VWF-treated macrophages were also subsequently exposed to ATP (Figures 2C and 2D). Control studies excluded endotoxin contamination of the pd-VWF product and that binding of the recently licensed clinical grade recombinant VWF (Vonvendi®, Takeda) to macrophages was

also associated with proinflammatory signaling (Supplementary Figures 2A and 2B). Together, these findings represent the first demonstration that VWF binding to macrophages directly initiates pro-inflammatory signaling, resulting in downstream pro-inflammatory cytokine production.

VWF induces chemokine expression and promotes monocyte chemotaxis

In view of the ability of VWF-binding to upregulate pro-inflammatory cytokine secretion, we investigated its effects upon macrophage chemokine expression. VWF binding to primary human macrophages was associated with a significant increase in chemokine expression (including CCL2, CCL3 and CCL4) similar to that observed with the LPS positive control (Figures 3A, 3B and 3C). The potential functional significance of this VWF-induced chemokine expression was further investigated using a transmigration chemotaxis assay with supernatants collected from primary human macrophages stimulated with either pd-VWF, commercial recombinant VWF or LPS respectively. Similar to LPS-treated positive controls cells, supernatants collected from macrophages stimulated with either pd-VWF or recombinant VWF were both effective in promoting significantly enhanced monocyte transmigration (Figure 3D and Supplementary Figure 2C). Interestingly however, the supernatant from both the pd- and recombinant VWF-treated macrophages was significantly more effective than LPS at recruiting monocytes (Figure 3E and Supplementary Figure 2C). Collectively, these findings demonstrate that VWF binding plays a novel role in regulating macrophage chemokine expression and thus has the potential to directly influence chemotaxis in vivo.

VWF triggers macrophage polarization towards an M1 phenotype

In view of the pro-inflammatory effects associated with pd- and recombinant VWF binding to macrophages, we investigated whether VWF interaction might influence macrophage polarization into M1 (classically activated or "pro-inflammatory") or M2 (alternatively activated or "anti-inflammatory") phenotypes. Incubation of murine BMDMs with LPS and IFN-γ resulted in approximately 75% cells adopting an M1 phenotype (positive for C11b and CD38 expression) (Figures 4A and 4B). In contrast, treatment with IL-4, IL-10 and IL-13 resulted in the majority of macrophages adopting an M2 phenotype (positive for CD11b and CD206) (Figure 4C). Interestingly, treatment with VWF alone was sufficient to result in more than 70% of the BMDM adopting an M1 phenotype (Figures 4D). Previous studies have demonstrated that generation of reaction oxygen species (ROS) and induction of nitric oxide synthetase (iNOS) constitute a hallmark feature of M1 macrophages.[38,39] We observed that VWF treatment of BMDM was associated with a significant increase in both iNOS expression (Figure 4E) and ROS production (Figure 4F). Together, these findings further support the hypothesis that VWF binding induces significant pro-inflammatory effects in both primary human macrophages and murine BMDMs.

VWF regulates macrophage metabolism and drives glycolysis

Alterations in the intracellular metabolic pathways, and in particular an increase in glycolysis, constitute a hallmark of inflammatory macrophages activated by both pathogen-associated and damage-associated signals through pattern-recognition receptor signaling.[40,41] To further investigate the hypothesis that VWF modulates macrophage function, the effects of VWF-binding on macrophage metabolism were assessed using extracellular flux analysis. Basal rates of glycolysis and oxidative phosphorylation were assessed using a Seahorse XF analyzer which measures extracellular acidification (ECAR) and cellular oxygen consumption rate (OCR) as

readouts of glycolysis and mitochondrial respiration respectively. Basal rates of ECAR and OCR were assessed before and after the addition of mitochondrial inhibitors (including oligomycin, FCCP or Antimycin A and rotenone (AA + R) respectively) as previously described.[32] Following 3 hours stimulation with pd-VWF, a significant increase in ECAR (consistent with a marked increase in glycolysis) was observed in basal glycolysis (ECAR readings prior to addition of Oligo) similar in magnitude to that observed with LPS exposure (Figures 5A and 5B). Interestingly, after an extended 16-hour incubation, the pd-VWF-induced increase in BMDM glycolysis had resolved, whereas ECAR remained significantly elevated in macrophages treated with LPS over the same time course (Figures 5C and 5D).

OCR was used to assess mitochondrial oxidative phosphorylation after incubation with LPS or pd-VWF for 3 hours and 16 hours. In contrast to its effect in promoting glycolysis, LPS or pd-VWF did not affect basal levels of mitochondrial oxidative phosphorylation (Figure 5E). However, in keeping with previous reports,[40,41] we observed that 16 hour exposure to LPS resulted in markedly reduced mitochondrial OCR (Figure 5G). No such effect was observed in cells incubated with pd-VWF. Importantly, similar effects on macrophage metabolism were also observed when macrophages were treated with commercial recombinant VWF in place of pd-VWF (Supplementary Figures 2D and 2E). In addition, the effects of VWF on macrophage metabolism were not attributable to altered BMDM cell viability after stimulation (Supplementary Figure 3).

VWF influences mitochondrial morphology and up-regulates HIF-1α expression

Previous studies have reported that significant changes in mitochondrial morphology accompany changes in macrophage metabolic state.[42] In particular, mitochondria adopt a fragmented appearance when glycolysis levels are high, as opposed to an elongated state during periods of heightened oxidative phosphorylation.[33,34,42] In keeping with this hypothesis, we observed that LPS stimulation of macrophages for either 3 or 16 hours resulted in fragmented mitochondrial morphology (Figures 6A and 6B). Interestingly, treatment with VWF for 3 hours was also associated with significantly higher levels of mitochondrial fragmentation. However, in contrast to LPS, mitochondrial morphology had returned to normal following 16 hours exposure to VWF. These findings further support the hypothesis that VWF binding has significant modulatory effects upon macrophage morphology which will impact on mitochondrial metabolism and in particular demonstrate that VWF promotes short-term marked increases in macrophage glycolysis.

The ability of LPS to promote macrophage glycolysis, even with prolonged exposure, has been attributed at least in part to an upregulation in HIF-1α expression.[43,44] To investigate potential mechanisms through which VWF promotes macrophage glycolysis in a time-dependent manner, HIF-1α expression following 3- and 16-hour incubations with VWF or LPS respectively was assessed. After 3-hour incubations with either VWF or LPS, a significant increase in macrophage HIF-1α expression levels was observed (Figure 6C). Interestingly, although HIF-1α expression remained elevated in BMDMs after a 16-hour incubation with LPS, levels were reduced in the VWF-treated cells following this extended treatment (Figure 6C). Furthermore, we observed similar time-dependent effects of LPS and VWF on expression of macrophage PHD3 which is a key negative regulator of HIF-1α expression (Figure 6D).[45]

VWF has pro-inflammatory and chemo-attractive effects in vivo

In vitro binding of VWF to macrophages is associated with polarization towards an M1 pro-inflammatory phenotype, metabolic changes and production of pro-inflammatory cytokines and chemokines. To further investigate the potential in vivo significance of these observations we utilized a previously described model of chemotaxis in which VWF or saline control were injected into the peritoneum of wild type mice.[46-48] Peritoneal lavage was then performed and cellular content analyzed by flow cytometry. At 3 hours, in contrast to the control mice, VWF treatment was associated with a significant infiltration of both neutrophils and NK cells into the peritoneum (Figure 7A and 7B). Moreover, VWF treatment was also associated with significant reduction in resident peritoneal macrophages (Figures 7C and 7D). By 24 hours, no significant differences were observed between the VWF-treated and control mice with respect to peritoneal NK or macrophage levels, and only a mild increase in neutrophil recruitment was remained (Figures 7A, 7B and 7C). Furthermore, VWF-treatment had no effect on peritoneal T cell populations at either the 3- or 24-hour time points (Figures 7E and 7F). Cumulatively these data, particularly the early influx of neutrophils and loss of resident macrophages (Figures 7A and 7C, followed by the later invasion of recruited macrophages (Figures 7C and 7D) demonstrate that VWF has chemo-attractive and pro-inflammatory properties in vivo that are consistent with its in vitro effects on macrophage biology.

DISCUSSION

Accumulating recent data has demonstrated that VWF not only regulates primary hemostasis, but also has direct effects upon inflammatory responses.[11,13-17] These pro-inflammatory properties of VWF have been observed in a variety of different murine inflammatory disease models and have been independently validated using experiments with either VWF-blocking antibodies or in $VWF^{-/-}$ mice.[13-15] Critically however, the biological mechanisms underpinning the immuno-modulatory effects of VWF remain poorly understood. In vitro studies have confirmed that immobilized VWF can bind directly to leukocytes.[36,49] Under flow conditions, this VWF-leucocyte interaction was shown to consist of initial transient rolling (mediated via VWF binding to leukocyte PSGL-1) followed by stable adhesion (mediated by VWF interaction binding to leukocyte β2-integrins).[36] In keeping with previous studies demonstrating a role for liver Kupffer cells in regulating VWF clearance,[24,27] we observed binding of both pd-VWF and recombinant VWF to primary human macrophages, murine BMDMs and THP-1 macrophages respectively. Importantly, VWF binding to these macrophages was seen under both shear and static conditions, and was followed by VWF internalization. In contrast, no significant VWF binding to undifferentiated primary monocytes was seen. Interestingly, under static conditions, binding of pd-VWF to macrophages was significantly enhanced compared to that of recombinant VWF. Further studies will be required to define the mechanisms underlying the reduced binding of recombinant VWF, but it may be in part attributable to the fact that the recombinant VWF therapy is hypersialylated and enriched in high molecular weight multimers compared to pd-VWF.

Importantly, our data highlight that VWF does not simply bind to macrophages, but rather that this VWF binding also serves to trigger significant downstream signaling effects including activation of the MAPKinase pro-inflammatory pathway (with phosphorylation of p38 and JNK) leading to NF-κB activation. Although VWF-induced signaling macrophages has not

previously been described, prior studies have clearly demonstrated that VWF binding to the glycoprotein (GP) Ib-IX-V receptor on platelets results in complex intracellular signaling that involves a number of different intracellular molecules including the Src family, Rac1, PI3-kinase/Akt and MAP kinases.[50-52] The net result of this signaling cascade induced by VWF binding to GP Ib-IX-V is to induce platelet activation, and in particular activation of the αIIbβ3 integrin receptor.[53] Additional studies will be needed to elucidate the molecular mechanisms through which VWF-binding to macrophages initiates pro-inflammatory signaling. Given the complex nature of VWF as a multimeric sialoglycoprotein, it seems likely that multiple VWF domains and various different macrophage receptors may be involved.[27] Importantly however, a number of macrophage surface scavenger receptors (including LRP1 and SR-A1) and C-type lectins (including MGL and Siglec-5) that have recently been reported to bind VWF, have also been shown to modulate intracellular signaling and thereby regulate inflammatory responses in both macrophages and dendritic cells.[54-57]

In keeping with the pro-inflammatory signaling associated with VWF binding to primary human macrophages or murine BMDMs, we observed that binding was also associated with significant increases in (i) proinflammatory cytokine expression (ii) chemokine expression (iii) iNOS expression and ROS production. Furthermore, VWF binding induced the majority of macrophages to adopt an M1 inflammatory phenotype. Unsurprisingly, given these major effects on macrophage biology, using extracellular flux analysis we observed that VWF also had significant effects upon macrophage metabolism. Incubation with either pd- or recombinant VWF resulted in a marked initial increase in macrophage glycolysis. Interestingly however, in contrast to the sustained increase in glycolysis and suppression of oxidative phosphorylation observed with prolonged LPS stimulation, the VWF effects on macrophage metabolism were time-limited. Similarly, a significant increase in macrophage HIF-1α expression levels (which are known to play an important role in promoting macrophage glycolysis[43,44]) was observed

following a 3-hour incubation with VWF, but had normalized by 16-hours. Our data further demonstrate that the MAPKinase pathway is critically involved in regulating VWF-dependent glycolysis. Collectively, these data support the hypothesis that VWF binding has significant but short-term pro-inflammatory effects on macrophage biology.

Given recent evidence that VWF contributes to the pathogenesis of a variety of different inflammatory diseases,[11] our data not only define a novel role for VWF in regulating innate immune responses, but are also of direct translational significance. Based upon our findings we propose that in the normal circulation, VWF and monocytes circulate together with minimal interaction. However, following tissue damage and blood vessel injury, VWF escapes from the plasma into subendothelium where it comes into contact with tissue macrophages (Figure 8). These macrophages express a different repertoire of surface receptors compared to undifferentiated monocytes, with the upregulation of specific surface receptors such as LRP1 that enables binding to VWF. VWF-binding triggers the macrophages to adopt an M1 phenotype, with consequent secretion of proinflammatory cytokines and chemokines at the site of vascular damage. Thus, VWF is not only playing a key role in initiating primary hemostasis and platelet plug formation at the site of blood vessel injury, it is also priming macrophages in the vicinity to promote a pro-inflammatory response. Importantly in this context, the pro-inflammatory effects of VWF on macrophages are time-limited such that they are lost with longer-term exposure. Thus, hepatic Kupffer cells that are involved in regulating physiological VWF circulatory clearance presumably remain unaffected due to their ongoing VWF exposure.[27]

Previous studies suggest that the proinflammatory effects of VWF-binding on macrophage biology may have additional implications beyond sites of vascular injury. For example, Methia *et al* reported that fatty streak lesions in the aorta were 40% smaller in $LDLR^{-/-}VWF^{-/-}$ mice compared to $LDLR^{-/-}VWF^{+/+}$ mice on an atherogenic diet.[58] Moreover, a significant reduction

in the number of macrophages recruited into the atheromatous lesions was also observed in the VWF-deficient mice, suggesting that the protective effect of VWF deficiency on atheroma development may be macrophage-mediated.[58] These murine data are particularly interesting given that human studies have demonstrated that patients with von Willebrand disease (VWD) are protected against risk of ischemic heart disease and stroke.[59-61] Furthermore, ABO blood group has also been shown to constitute a risk factor for cardiovascular disease, with significantly reduced cardiovascular risk in group O compared to non-O (A, B or AB) individuals. Of note, plasma VWF levels are 20-30% lower in blood group O compared to non-O subjects.[62-64]

In conclusion, recent studies have described the complex cross-talk that exists in vivo between hemostasis and inflammation, and developed the concept of immuno-thrombosis.[65-67] Our data define a novel biological role and mechanism for VWF in driving inflammatory responses, and thereby establish a new link between primary hemostasis and innate immunity. Thus, VWF not only plays a key role in the initiation of hemostasis at sites of vascular injury, but also functions to prime local macrophages to initiate pro-inflammatory responses. In this local milieu, we propose that VWF functions as a damage signal that is recognized through specific macrophage pattern-recognition receptors. In addition, our findings also provide novel insights into the effects of VWF binding on macrophage biology that may help to explain the accumulating evidence that VWF is involved in the pathogenesis of a number of different murine inflammatory disease models. Given the significant morbidity and mortality associated with inflammatory pathology, defining the roles of VWF in this context may offer exciting opportunities to develop novel therapies to target these pathways and address a critical unmet clinical need.

ACKNOWLEDGEMENTS:

This work was supported through a project grant from the Royal City of Dublin Hospital Trust (Project grant 181).

AUTHORSHIP

Contribution:

C.D., S.A., M.L., A.C., E.B., and M.P.C. performed experiments;

C.D., S.A., A.M.C., J.K., P.F., R.J.P., J.M.O'S, R.M., F.J.S. and J.S.O'D. designed the research and analyzed the data; All authors were involved in writing and reviewing the paper.

Conflict-of-interest disclosure:

J.S.O'D has served on the speaker's bureau for Baxter, Bayer, Novo Nordisk, Boehringer Ingelheim, Leo Pharma, Takeda and Octapharma. He has also served on the advisory boards of Baxter, Bayer, Octapharma CSL Behring, Daiichi Sankyo, Boehringer Ingelheim, Takeda and Pfizer. J.S.O.D has also received research grant funding awards from Baxter, Bayer, Pfizer, Shire, Takeda and Novo Nordisk.

FIGURE LEGENDS

Figure 1: VWF binds to macrophages and triggers inflammatory signalling

(A) Binding of plasma-derived VWF (pd-VWF) to primary human macrophages and **(B)** THP1 macrophages was assessed in vitro using confocal microscopy as detailed in Materials and Methods (VWF staining in green; nuclear DAPI staining in blue; cell membrane staining in red). **(C)** VWF internalization was assessed using THP1 macrophages, using anti-VWF, DAPI and anti-EEA1 (early endosomes antigen 1) in red and co-localization in yellow. pd-VWF or recombinant VWF (300-600 μM) were incubated with macrophages for 30 minutes at 37°C and cells analyzed by flow cytometry. Representative histograms are presented where red represents control cells not treated with VWF and blue cells treated with VWF. **(D)** pd-VWF and **(E)** recombinant VWF binding to primary human macrophages; **(F)** recombinant VWF binding to THP1 macrophages. Western blot analysis of phosphorylation of p38, JNK, IKKα and p65 in **(G)** primary human and **(H)** primary murine macrophages incubated with VWF (10 μg/ml) or LPS (100 ng/ml) for 30min.

Figure 2: VWF binding leads to pro-inflammatory cytokine expression

(A) pd-VWF (10μg/ml) or LPS (100ng/ml) incubation with primary human macrophages significantly induced TNF-α expression ($p<0.01$) and secretion ($p<0.01$) after 4h incubation. **(B)** Furthermore, pd-VWF significantly enhanced IL-6 expression ($p<0.05$) and secretion ($p<0.01$) to similar levels as LPS induction. **(C and D)** Incubation with both VWF and LPS was associated with a significant increase in macrophage IL1β mRNA and Pro IL-1β levels ($p<0.05$). When VWF-treated macrophages were subsequently exposed to ATP (5mM for 1h), a significant increase in IL1β was observed ($p<0.01$). All experiments were performed in triplicate, and the results presented represent the mean values ± standard error of the mean, unless otherwise stated. $*P < 0.05$, $**P < 0.01$, $***P < 0.001$ respectively.

Figure 3: VWF induces chemokine expression and promotes monocyte chemotaxis

pd-VWF (10μg/ml) or LPS (100ng/ml) stimulation of primary human macrophages for 24h resulted in a significant in expression levels for a number of chemokines including **(A)** CCL2 ($p<0.0001$), **(B)** CCL3 ($p<0.05$) and **(C)** CCL4 ($p<0.01$). All results All experiments were performed in triplicate, and the results presented represent the mean values ± standard error of the mean. $*P < 0.05$, $**P < 0.01$, $***P < 0.001$ $****P < 0.0001$ respectively.

(D, E) Primary human macrophages were incubated with pd-VWF (10μg/ml) or LPS (100ng/ml) for 24 hours. Cell supernatants were then collected and placed in the lower chamber of a transmigration assay. Naïve human monocytes were placed in the upper chamber and allowed to migrate for 2.5 hours. Migrated cell numbers were assessed using Image J software. Data is represented as average fold cell-count increase of three independent experiments represented by mean values ± standard error of the mean. *$P < 0.05$, **$P < 0.01$, ***$P < 0.001$ ****$P < 0.0001$ respectively.

Figure 4: VWF triggers M1 macrophage phenotype

(A-D) Murine BMDMs were incubated in the presence or absence of a variety of different agonist combinations including (LPS 100ng/ml and IFN- γ 20ng/ml), (IL-4 40ng/ml, IL-10 10ng/ml and IL-13 20ng/ml) or pd-VWF (10μg/ml) for 24h and then cell surface marker expression was examined by flow cytometry. **(A)** Untreated control BMDMs expressed no CD38 or CD206. **(B)** The majority of BMDMS treated with LPS and INF-γ were CD38 positive, consistent with an M1 phenotype. **(C)** In contrast, the majority of BMDMs incubated with IL-4, IL-10 and IL-13 (20ng/ml) were CD206 positive, consistent with an M2 phenotype. **(D)** BMDM stimulation with pd-VWF (10μg/ml) resulted in a significant increase in expression of CD38, consistent with a pro-inflammatory M1 macrophage phenotype. Consistent with this M1 phenotype, VWF treatment also resulted in a significant increase in iNOS expression in BMDM ($p<0.05$) **(E),** together with a marked increase in generation of reactive oxygen species (ROS) **(F)**. The data presented represent the mean values ± standard error of the mean for three independent experiments *$P < 0.05$, **$P < 0.01$, ***$P < 0.001$ ****$P < 0.0001$ respectively.

Figure 5: VWF regulates macrophages metabolism and drives glycolysis

Extracellular flux analysis (Seahorse XF Cell Mito Stress kit) was used to assess the effects of VWF-binding upon macrophage metabolism. Extracellular acidification (ECAR) measured to study the effects on glycolysis following stimulation with VWF (10μg/ml) (blue), LPS (100ng/ml) (red), or untreated controls (black) for 3 hours **(A** and **B)** and 16 hours **(C and D)** respectively. Similarly, cellular oxygen consumption rate (OCR) was assayed to study the effects on BMDM oxidative phosphorylation after 3 hour **(E and F)** and 16 hour **(G and H)** incubations. The effects of VWF and LPS on BMDM glycolysis and oxidative phosphorylation were studied in the presence or absence of specific mitochondrial inhibitors. Plots are representative images collected from three independent assays.

Figure 6: VWF influences mitochondrial morphology and up-regulates HIF-1α expression.

(A-B) Murine BMDMs were incubated in the presence or absence of VWF (10μg/ml) or LPS (100ng/ml) for 3 hours or 16 hours and mitochondrial morphology assessed using scanning confocal live cell imaging as detailed in the Materials and Methods. A minimum of 20 images including ≥ 60 mitochondria per cell were analysed per treatment. Following 3 hour stimulation with either VWF or LPS, a significant increase in mitochondrial fragmentation consistent with an increase in glycolysis was observed ($p<0.01$ and $p<0.001$ respectively). Although a significant increase in mitochondrial fragmentation was still observed following a 16 hour incubation with LPS ($p<0.01$), it was no longer observed in BMDM treated with VWF (NS = not significant). **(C-D)** BMDM were treated with either VWF (10μg/ml) or LPS (100ng/ml) for 3 hours or 16 hours, and then HIF-1α or PHD3 expression were assessed using Western blotting or Qrt-PCR respectively. $*P < 0.05$, $**P < 0.01$, $***P < 0.001$ $****P < 0.0001$ respectively.

Figure 7: VWF has pro-inflammatory and chemo-attractive effects in vivo

(A-F) VWF (2mg/kg) or PBS (control) were injected into the peritoneum of female WT mice. After 3 or 24 hour periods, mice were sacrificed, peritoneal lavage was performed and peritoneal cell populations quantified by flow cytometry. Data represented by percentage of cell population ±SD from four independent mice. Significance was determined by t-test in which *p<0.05, **p<0.01, ***p<0.001,****p<0.0001.

Figure 8: Model of VWF-induced macrophages activation

Following vascular injury, the plasma sialoglycoprotein VWF comes into contact with tissue macrophages to which it can bind via a variety of different scavenger (eg. LRP1 and SR-A1) and/or lectin (eg. MGL and Siglec-5) cell surface receptors. VWF binding to macrophages is followed by rapid VWF internalization. VWF binding also triggers pro-inflammatory signalling within macrophages, including activation of the MAPKinase pathway (with phosphorylation of p38 and JNK) and NF-κB activation. VWF binding causes macrophages to adopt an M1 phenotype, and leads to enhanced expression of pro-inflammatory cytokines (including TNF-α and IL-6) and chemokines (including CCL2, CCL3 and CCL4). Furthermore, there is also an increase in iNOS and ROS expression. In keeping with these pro-inflammatory effects, VWF binding also has significant effects upon macrophage metabolism, triggering an increase in HIF-1α expression levels and a marked increase in glycolysis. Thus, VWF not only plays a key role in initiation of primary hemostasis at sites of vascular injury, but also serves as a damage signal to prime local tissue macrophages to initiate pro-inflammatory responses.

REFERENCES

1. Lenting PJ, Christophe OD, Denis CV. von Willebrand factor biosynthesis, secretion, and clearance: connecting the far ends. *Blood*. 2015;125(13):2019-2028.
2. Leebeek FWG, Eikenboom JCJ. Von Willebrand's Disease. *N Engl J Med*. 2017;376(7):701-702.
3. Lillicrap D. von Willebrand disease: advances in pathogenetic understanding, diagnosis, and therapy. *Hematology Am Soc Hematol Educ Program*. 2013;2013:254-260.
4. Laffan MA, Lester W, O'Donnell JS, et al. The diagnosis and management of von Willebrand disease: a United Kingdom Haemophilia Centre Doctors Organization guideline approved by the British Committee for Standards in Haematology. *Br J Haematol*. 2014;167(4):453-465.
5. Bockenstedt P, Greenberg JM, Handin RI. Structural basis of von Willebrand factor binding to platelet glycoprotein Ib and collagen. Effects of disulfide reduction and limited proteolysis of polymeric von Willebrand factor. *J Clin Invest*. 1986;77(3):743-749.
6. Moake JL, Turner NA, Stathopoulos NA, Nolasco LH, Hellums JD. Involvement of large plasma von Willebrand factor (vWF) multimers and unusually large vWF forms derived from endothelial cells in shear stress-induced platelet aggregation. *J Clin Invest*. 1986;78(6):1456-1461.
7. Terraube V, O'Donnell JS, Jenkins PV. Factor VIII and von Willebrand factor interaction: biological, clinical and therapeutic importance. *Haemophilia*. 2010;16(1):3-13.
8. Starke RD, Ferraro F, Paschalaki KE, et al. Endothelial von Willebrand factor regulates angiogenesis. *Blood*. 2011;117(3):1071-1080.
9. O'Sullivan JM, Preston RJS, Robson T, O'Donnell JS. Emerging Roles for von Willebrand Factor in Cancer Cell Biology. *Semin Thromb Hemost*. 2018;44(2):159-166.
10. Lenting PJ, Casari C, Christophe OD, Denis CV. von Willebrand factor: the old, the new and the unknown. *J Thromb Haemost*. 2012;10(12):2428-2437.
11. Kawecki C, Lenting PJ, Denis CV. von Willebrand factor and inflammation. *J Thromb Haemost*. 2017;15(7):1285-1294.
12. Gragnano F, Sperlongano S, Golia E, et al. The Role of von Willebrand Factor in Vascular Inflammation: From Pathogenesis to Targeted Therapy. *Mediators Inflamm*. 2017;2017:5620314.
13. Hillgruber C, Steingraber AK, Poppelmann B, et al. Blocking von Willebrand factor for treatment of cutaneous inflammation. *J Invest Dermatol*. 2014;134(1):77-86.
14. Petri B, Broermann A, Li H, et al. von Willebrand factor promotes leukocyte extravasation. *Blood*. 2010;116(22):4712-4719.
15. Lerolle N, Dunois-Larde C, Badirou I, et al. von Willebrand factor is a major determinant of ADAMTS-13 decrease during mouse sepsis induced by cecum ligation and puncture. *J Thromb Haemost*. 2009;7(5):843-850.
16. Adam F, Casari C, Prevost N, et al. A genetically-engineered von Willebrand disease type 2B mouse model displays defects in hemostasis and inflammation. *Sci Rep*. 2016;6:26306.
17. Ayme G, Adam F, Legendre P, et al. A Novel Single-Domain Antibody Against von Willebrand Factor A1 Domain Resolves Leukocyte Recruitment and Vascular Leakage During Inflammation-Brief Report. *Arterioscler Thromb Vasc Biol*. 2017;37(9):1736-1740.
18. Kasuda S, Matsui H, Ono S, et al. Relevant role of von Willebrand factor in neutrophil recruitment in a mouse sepsis model involving cecal ligation and puncture. *Haematologica*. 2016;101(2):e52-54.
19. O'Regan N, Gegenbauer K, O'Sullivan JM, et al. A novel role for von Willebrand factor in the pathogenesis of experimental cerebral malaria. *Blood*. 2016;127(9):1192-1201.
20. O'Sullivan JM, Preston RJ, O'Regan N, O'Donnell JS. Emerging roles for hemostatic dysfunction in malaria pathogenesis. *Blood*. 2016;127(19):2281-2288.

21. Reinhart K, Bayer O, Brunkhorst F, Meisner M. Markers of endothelial damage in organ dysfunction and sepsis. *Crit Care Med*. 2002;30(5 Suppl):S302-312.
22. Paulus P, Jennewein C, Zacharowski K. Biomarkers of endothelial dysfunction: can they help us deciphering systemic inflammation and sepsis? *Biomarkers*. 2011;16 Suppl 1:S11-21.
23. Hyseni A, Kemperman H, de Lange DW, Kesecioglu J, de Groot PG, Roest M. Active von Willebrand factor predicts 28-day mortality in patients with systemic inflammatory response syndrome. *Blood*. 2014;123(14):2153-2156.
24. van Schooten CJ, Shahbazi S, Groot E, et al. Macrophages contribute to the cellular uptake of von Willebrand factor and factor VIII in vivo. *Blood*. 2008;112(5):1704-1712.
25. Chion A, O'Sullivan JM, Drakeford C, et al. N-linked glycans within the A2 domain of von Willebrand factor modulate macrophage-mediated clearance. *Blood*. 2016;128(15):1959-1968.
26. Rastegar-Lari G, Villoutreix BO, Ribba AS, Legendre P, Meyer D, Baruch D. Two clusters of charged residues located in the electropositive face of the von Willebrand factor A1 domain are essential for heparin binding. *Biochemistry*. 2002;41(21):6668-6678.
27. O'Sullivan JM, Ward S, Lavin M, O'Donnell JS. von Willebrand factor clearance - biological mechanisms and clinical significance. *Br J Haematol*. 2018;183(2):185-195.
28. Ward SE, O'Sullivan JM, Drakeford C, et al. A novel role for the macrophage galactose-type lectin receptor in mediating von Willebrand factor clearance. *Blood*. 2018;131(8):911-916.
29. Pegon JN, Kurdi M, Casari C, et al. Factor VIII and von Willebrand factor are ligands for the carbohydrate-receptor Siglec-5. *Haematologica*. 2012;97(12):1855-1863.
30. Wohner N, Muczynski V, Mohamadi A, et al. Macrophage scavenger receptor SR-AI contributes to the clearance of von Willebrand factor. *Haematologica*. 2018;103(4):728-737.
31. Capaldi RA, Aggeler R, Turina P, Wilkens S. Coupling between catalytic sites and the proton channel in F1F0-type ATPases. *Trends Biochem Sci*. 1994;19(7):284-289.
32. Shirai T, Nazarewicz RR, Wallis BB, et al. The glycolytic enzyme PKM2 bridges metabolic and inflammatory dysfunction in coronary artery disease. *J Exp Med*. 2016;213(3):337-354.
33. Gao Z, Li Y, Wang F, et al. Mitochondrial dynamics controls anti-tumour innate immunity by regulating CHIP-IRF1 axis stability. *Nat Commun*. 2017;8(1):1805.
34. Escoll P, Song OR, Viana F, et al. Legionella pneumophila Modulates Mitochondrial Dynamics to Trigger Metabolic Repurposing of Infected Macrophages. *Cell Host Microbe*. 2017;22(3):302-316 e307.
35. Castro-Nunez L, Dienava-Verdoold I, Herczenik E, Mertens K, Meijer AB. Shear stress is required for the endocytic uptake of the factor VIII-von Willebrand factor complex by macrophages. *J Thromb Haemost*. 2012;10(9):1929-1937.
36. Pendu R, Terraube V, Christophe OD, et al. P-selectin glycoprotein ligand 1 and beta2-integrins cooperate in the adhesion of leukocytes to von Willebrand factor. *Blood*. 2006;108(12):3746-3752.
37. He Y, Hara H, Nunez G. Mechanism and Regulation of NLRP3 Inflammasome Activation. *Trends Biochem Sci*. 2016;41(12):1012-1021.
38. Weisser SB, McLarren KW, Kuroda E, Sly LM. Generation and characterization of murine alternatively activated macrophages. *Methods Mol Biol*. 2013;946:225-239.
39. West AP, Brodsky IE, Rahner C, et al. TLR signalling augments macrophage bactericidal activity through mitochondrial ROS. *Nature*. 2011;472(7344):476-480.
40. O'Neill LA, Kishton RJ, Rathmell J. A guide to immunometabolism for immunologists. *Nat Rev Immunol*. 2016;16(9):553-565.

41. Nagy C, Haschemi A. Time and Demand are Two Critical Dimensions of Immunometabolism: The Process of Macrophage Activation and the Pentose Phosphate Pathway. *Front Immunol*. 2015;6:164.
42. Park J, Choi H, Min JS, et al. Mitochondrial dynamics modulate the expression of pro-inflammatory mediators in microglial cells. *J Neurochem*. 2013;127(2):221-232.
43. Tannahill GM, Curtis AM, Adamik J, et al. Succinate is an inflammatory signal that induces IL-1beta through HIF-1alpha. *Nature*. 2013;496(7444):238-242.
44. Palsson-McDermott EM, Curtis AM, Goel G, et al. Pyruvate Kinase M2 Regulates Hif-1alpha Activity and IL-1beta Induction and Is a Critical Determinant of the Warburg Effect in LPS-Activated Macrophages. *Cell Metab*. 2015;21(2):347.
45. Walmsley SR, Chilvers ER, Thompson AA, et al. Prolyl hydroxylase 3 (PHD3) is essential for hypoxic regulation of neutrophilic inflammation in humans and mice. *J Clin Invest*. 2011;121(3):1053-1063.
46. Miyazaki S, Ishikawa F, Fujikawa T, Nagata S, Yamaguchi K. Intraperitoneal injection of lipopolysaccharide induces dynamic migration of Gr-1high polymorphonuclear neutrophils in the murine abdominal cavity. *Clin Diagn Lab Immunol*. 2004;11(3):452-457.
47. Lund ME, O'Brien BA, Hutchinson AT, et al. Secreted proteins from the helminth Fasciola hepatica inhibit the initiation of autoreactive T cell responses and prevent diabetes in the NOD mouse. *PLoS One*. 2014;9(1):e86289.
48. Jenkins SJ, Ruckerl D, Thomas GD, et al. IL-4 directly signals tissue-resident macrophages to proliferate beyond homeostatic levels controlled by CSF-1. *J Exp Med*. 2013;210(11):2477-2491.
49. Koivunen E, Ranta TM, Annila A, et al. Inhibition of beta(2) integrin-mediated leukocyte cell adhesion by leucine-leucine-glycine motif-containing peptides. *J Cell Biol*. 2001;153(5):905-916.
50. Canobbio I, Reineri S, Sinigaglia F, Balduini C, Torti M. A role for p38 MAP kinase in platelet activation by von Willebrand factor. *Thromb Haemost*. 2004;91(1):102-110.
51. Delaney MK, Liu J, Zheng Y, Berndt MC, Du X. The role of Rac1 in glycoprotein Ib-IX-mediated signal transduction and integrin activation. *Arterioscler Thromb Vasc Biol*. 2012;32(11):2761-2768.
52. Yin H, Liu J, Li Z, Berndt MC, Lowell CA, Du X. Src family tyrosine kinase Lyn mediates VWF/GPIb-IX-induced platelet activation via the cGMP signaling pathway. *Blood*. 2008;112(4):1139-1146.
53. Bryckaert M, Rosa JP, Denis CV, Lenting PJ. Of von Willebrand factor and platelets. *Cell Mol Life Sci*. 2015;72(2):307-326.
54. Mantuano E, Azmoon P, Brifault C, et al. Tissue-type plasminogen activator regulates macrophage activation and innate immunity. *Blood*. 2017;130(11):1364-1374.
55. Mantuano E, Brifault C, Lam MS, Azmoon P, Gilder AS, Gonias SL. LDL receptor-related protein-1 regulates NFkappaB and microRNA-155 in macrophages to control the inflammatory response. *Proc Natl Acad Sci U S A*. 2016;113(5):1369-1374.
56. Hsu HY, Hajjar DP, Khan KM, Falcone DJ. Ligand binding to macrophage scavenger receptor-A induces urokinase-type plasminogen activator expression by a protein kinase-dependent signaling pathway. *J Biol Chem*. 1998;273(2):1240-1246.
57. Napoletano C, Zizzari IG, Rughetti A, et al. Targeting of macrophage galactose-type C-type lectin (MGL) induces DC signaling and activation. *Eur J Immunol*. 2012;42(4):936-945.
58. Methia N, Andre P, Denis CV, Economopoulos M, Wagner DD. Localized reduction of atherosclerosis in von Willebrand factor-deficient mice. *Blood*. 2001;98(5):1424-1428.
59. Sonneveld MA, de Maat MP, Leebeek FW. Von Willebrand factor and ADAMTS13 in arterial thrombosis: a systematic review and meta-analysis. *Blood Rev*. 2014;28(4):167-178.

60. Sanders YV, Eikenboom J, de Wee EM, et al. Reduced prevalence of arterial thrombosis in von Willebrand disease. *J Thromb Haemost*. 2013;11(5):845-854.
61. van Schie MC, de Maat MP, Isaacs A, et al. Variation in the von Willebrand factor gene is associated with von Willebrand factor levels and with the risk for cardiovascular disease. *Blood*. 2011;117(4):1393-1399.
62. Preston RJ, Rawley O, Gleeson EM, O'Donnell JS. Elucidating the role of carbohydrate determinants in regulating hemostasis: insights and opportunities. *Blood*. 2013;121(19):3801-3810.
63. Jenkins PV, O'Donnell JS. ABO blood group determines plasma von Willebrand factor levels: a biologic function after all? *Transfusion*. 2006;46(10):1836-1844.
64. Gill JC, Endres-Brooks J, Bauer PJ, Marks WJ, Jr., Montgomery RR. The effect of ABO blood group on the diagnosis of von Willebrand disease. *Blood*. 1987;69(6):1691-1695.
65. Levi M, van der Poll T. Inflammation and coagulation. *Crit Care Med*. 2010;38(2 Suppl):S26-34.
66. Gleeson EM, O'Donnell JS, Preston RJ. The endothelial cell protein C receptor: cell surface conductor of cytoprotective coagulation factor signaling. *Cell Mol Life Sci*. 2012;69(5):717-726.
67. Esmon CT. The interactions between inflammation and coagulation. *Br J Haematol*. 2005;131(4):417-430.

SUPPLEMENTARY FIGURE LEGENDS

Supplementary Figure 1

Binding of plasma-derived VWF (pd-VWF) to undifferentiated primary human monocytes was assessed in vitro using by flow cytometry. A representative histogram is presented where red represents control cells not treated with VWF and blue cells treated with VWF. In contrast to macrophages, no VWF binding to primary monocytes was observed.

Supplementary Figure 2

(A) Commercial purified pd-VWF was tested for contaminating endotoxin using macrophage a RAW-Blue cell line (InvivoGen). RAW-Blue cells were incubated with pd-VWF (10µg/ml) or LPS (100ng/ml) overnight. Secreted embryonic alkaline phosphatase (SEAP) was quantified using QUANTI-Blue (InvivoGen).

(B) Western blot analysis of phosphorylation of MAPKinase p38 in primary human macrophages incubated with recombinant clinical grade VWF (10 µg/ml) compared to either pd-VWF (10 µg/ml) or LPS (100 ng/ml) for 30min.

(C) Primary human macrophages were incubated with recombinant VWF(10µg/ml), pd-VWF (10µg/ml) or LPS (100ng/ml) for 24 hours. Cell supernatants were then collected and placed in the lower chamber of a transmigration assay. Naïve human monocytes were placed in the upper chamber and allowed to migrate for 2.5 hours. Representative images of migrated cell tracker green ladled primary monocytes.

(D) Extracellular flux analysis (Seahorse XF Cell Mito Stress kit) was used to assess the effects of recombinant VWF binding upon macrophage metabolism. Extracellular acidification (ECAR) measured to study the effects on glycolysis following stimulation with rVWF (10µg/ml) (green), pd-VWF (10µg/ml) (blue), LPS (100ng/ml) (red), or untreated controls (black) for 3 hours and 16 hours respectively. Similarly, cellular oxygen consumption rate (OCR) was assayed to study the effects on BMDM oxidative phosphorylation after 3 hour and 16 hour incubations. The effects of VWF and LPS on BMDM glycolysis and oxidative phosphorylation were studied in the presence or absence of specific mitochondrial inhibitors as before. Plots are representative images collected from three independent assays. Bar charts are a pool of 4 independent experiments. The significance was determined by t-test in which *$p<0.05$, **$p<0.01$, ***$p<0.001$, ****$p<0.0001$.

Supplementary Figure 3

BMDM viability was assessed after incubations with rVWF (10µg/ml) (green), pd-VWF (10µg/ml) (blue), LPS (100ng/ml) (red), or untreated controls (black) for 3 hours and 16 hours respectively. Cell viability was determined using Alamar Blue metabolism (absorbance λ = 600nm) normalised to total protein.

Figure 1

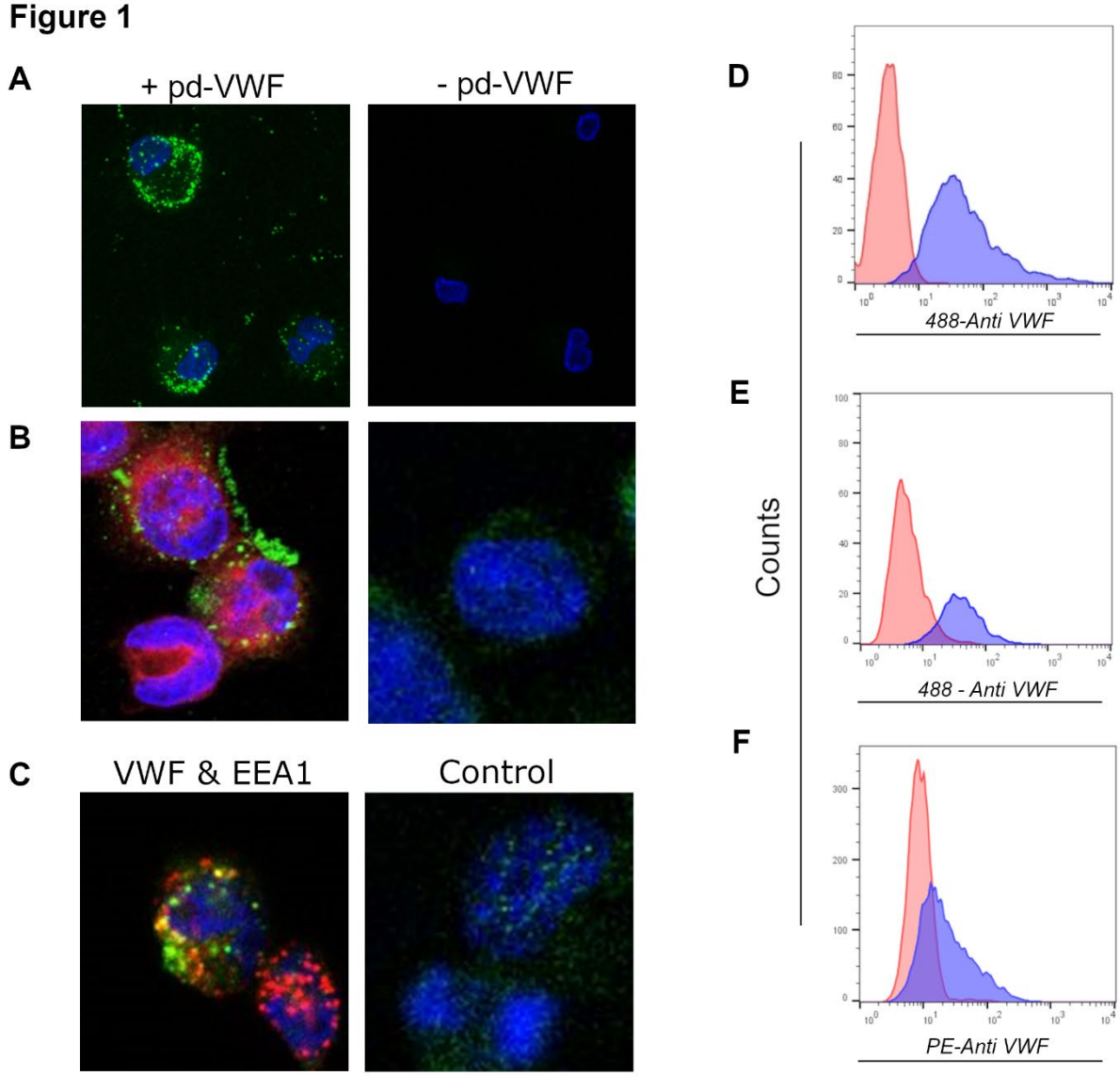
A
+ pd-VWF
- pd-VWF
B
C
VWF & EEA1
Control
D
488-Anti VWF
E
Counts
488 - Anti VWF
F
PE-Anti VWF
G
Phospho p38
Total p38
Phospho JNK
Total JNK
Phospho IκBα
Total IκBα
β-Actin
- - + LPS
- + - VWF
H
Phospho p38
Total p38
Phospho JNK
Total JNK
Phospho p65
Total p65
- + - LPS
- - + VWF

Figure 2

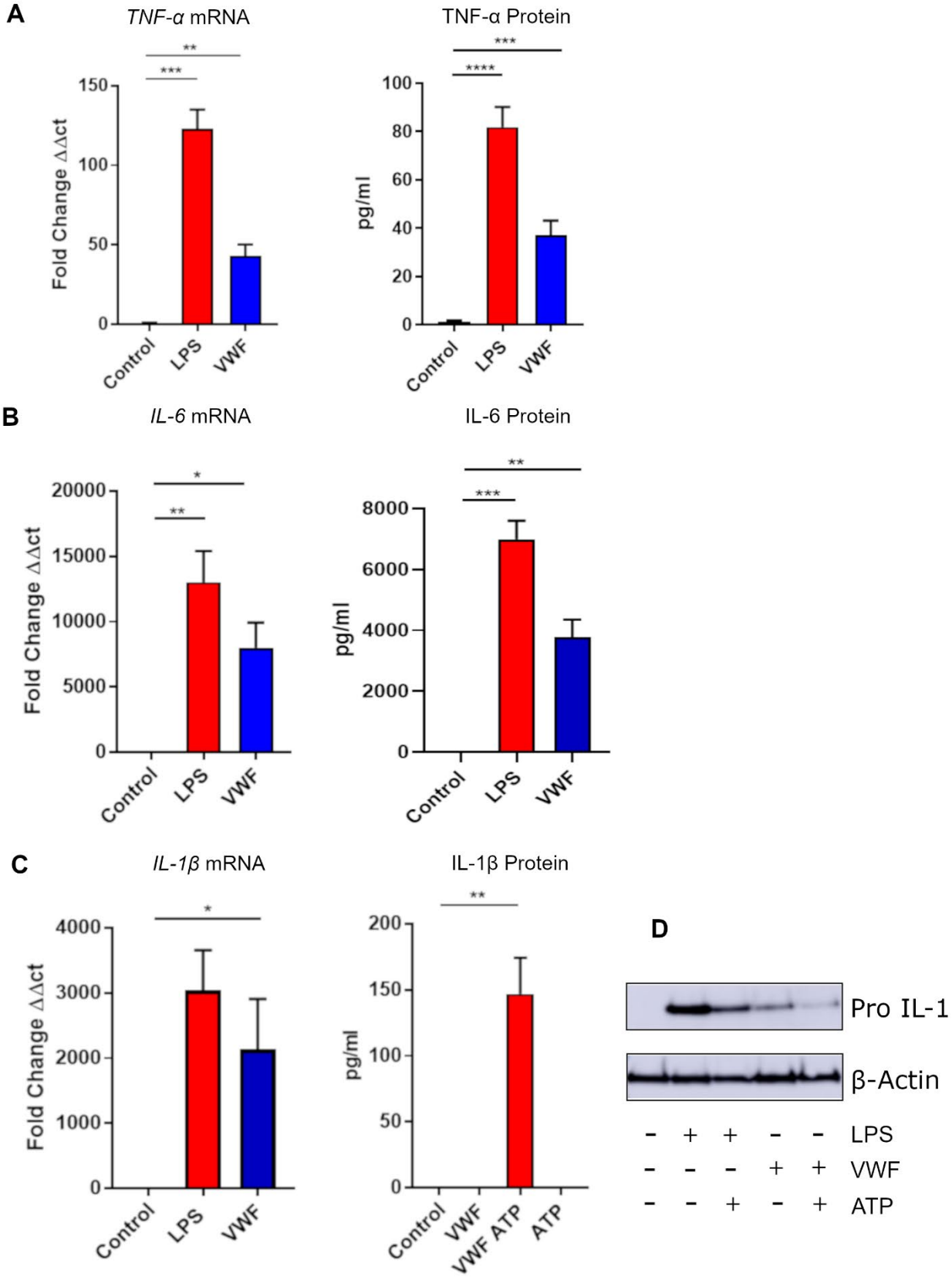
A
TNF-α mRNA
Fold Change ΔΔct
150
100
50
0
**
***
Control
LPS
VWF
TNF-α Protein
pg/ml
100
80
60
40
20
0
***
****
Control
LPS
VWF
B
IL-6 mRNA
Fold Change ΔΔct
20000
15000
10000
5000
0
*
**
Control
LPS
VWF
IL-6 Protein
pg/ml
8000
6000
4000
2000
0
**
***
Control
LPS
VWF
C
IL-1β mRNA
Fold Change ΔΔct
4000
3000
2000
1000
0
*
Control
LPS
VWF
IL-1β Protein
pg/ml
200
150
100
50
0
**
Control
VWF
VWF ATP
ATP
D
Pro IL-1
β-Actin
- + + - - LPS
- - - + + VWF
- - + - + ATP

Figure 3

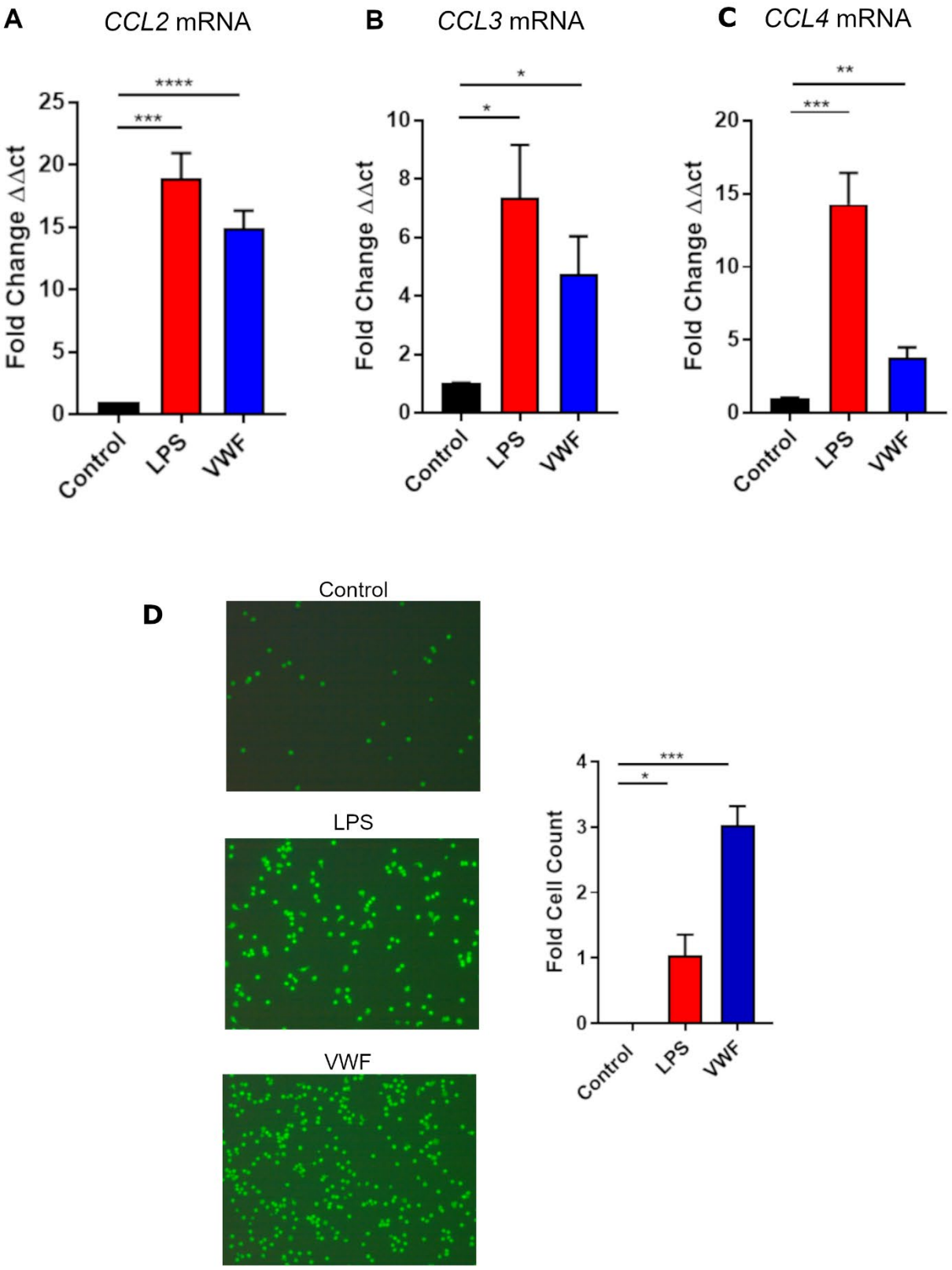
A
CCL2 mRNA
Fold Change ΔΔct
25
20
15
10
5
0
****
***
Control
LPS
VWF
B
CCL3 mRNA
Fold Change ΔΔct
10
8
6
4
2
0
*
*
Control
LPS
VWF
C
CCL4 mRNA
Fold Change ΔΔct
20
15
10
5
0
**
***
Control
LPS
VWF
D
Control
LPS
VWF
Fold Cell Count
4
3
2
1
0
***
*
Control
LPS
VWF

Figure 4

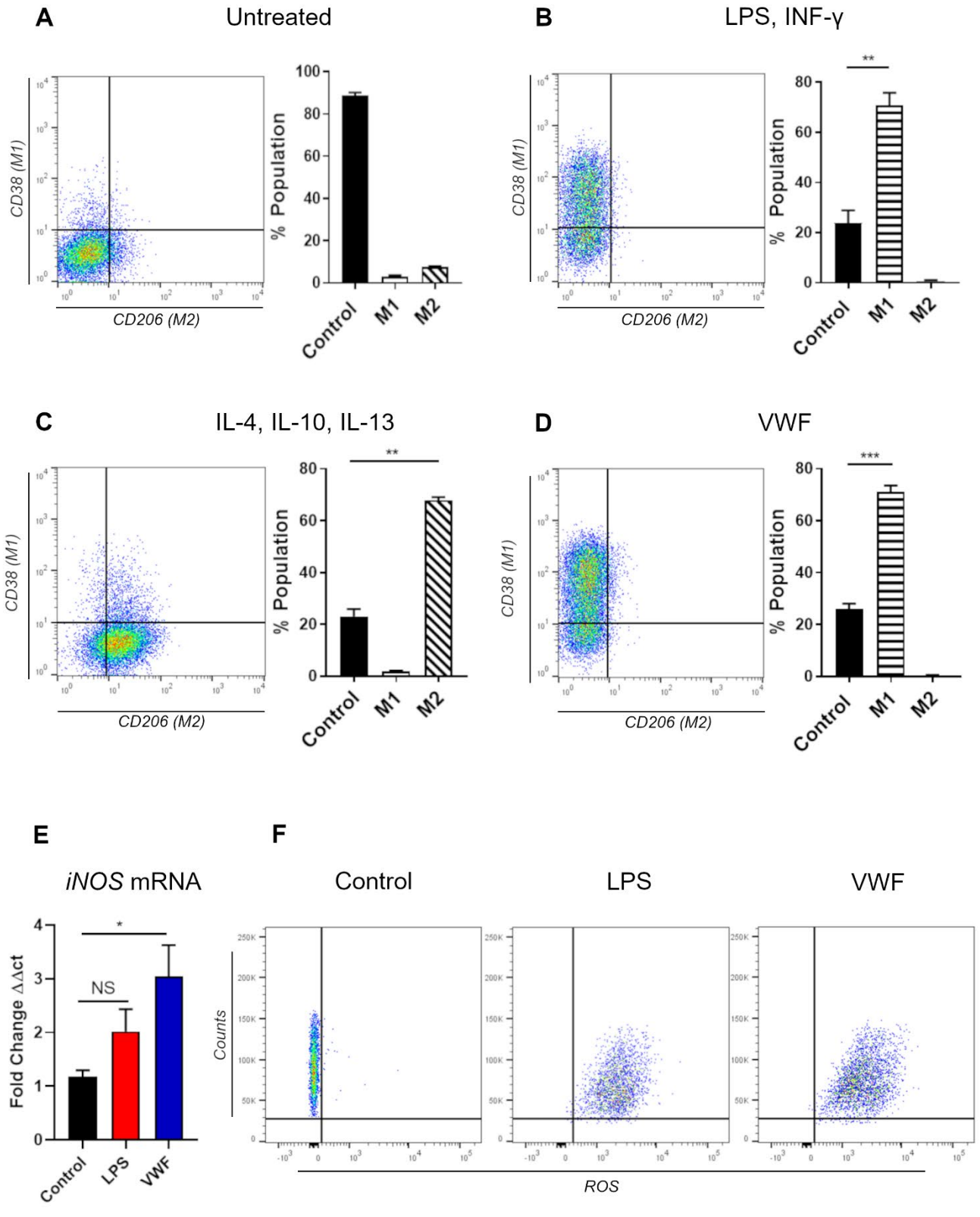
A
Untreated
CD38 (M1)
CD206 (M2)
% Population
Control
M1
M2
B
LPS, INF-γ
**
C
IL-4, IL-10, IL-13
**
D
VWF
***
E
iNOS mRNA
Fold Change ΔΔct
*
NS
Control
LPS
VWF
F
Control
LPS
VWF
Counts
ROS

Figure 5

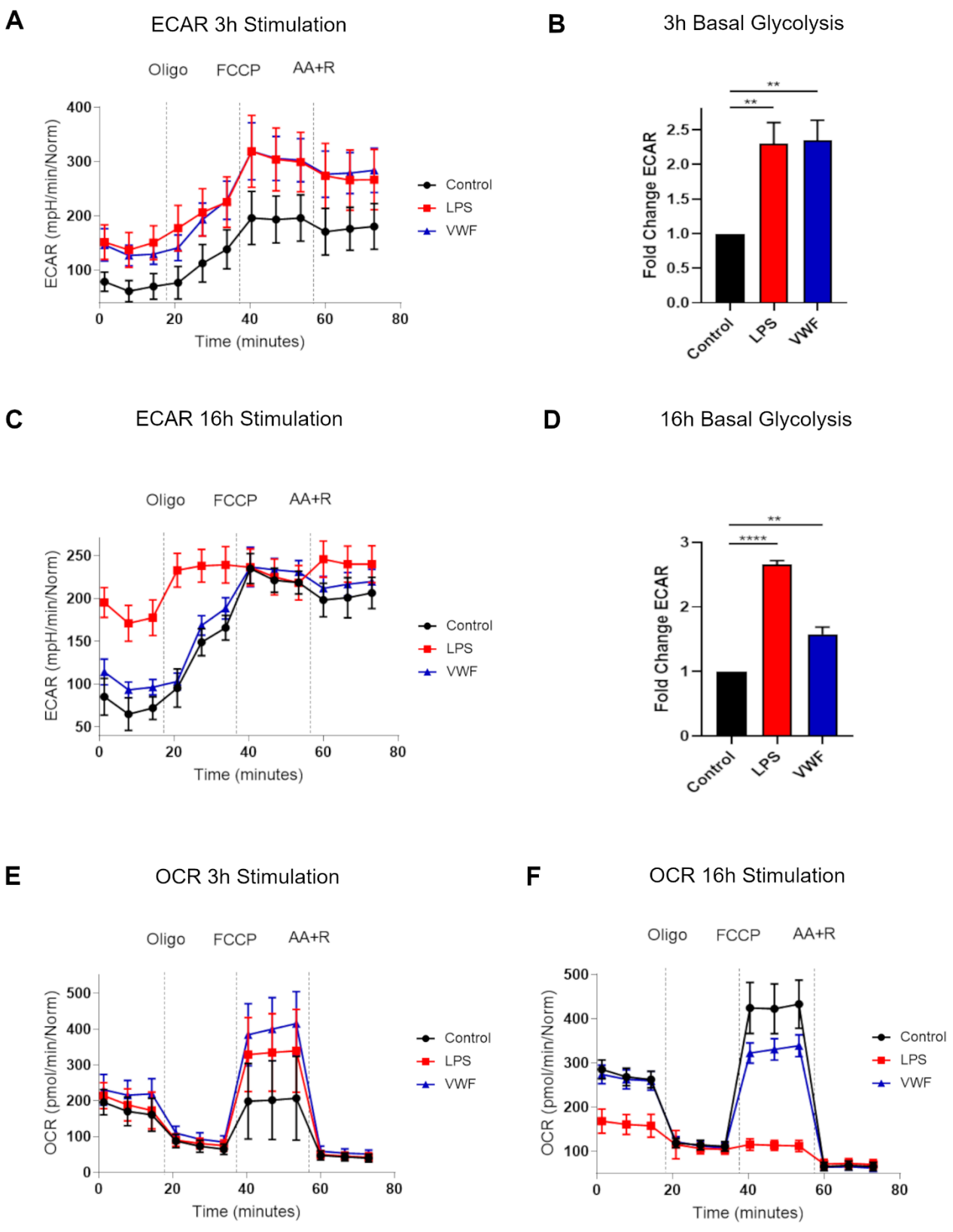
A
ECAR 3h Stimulation
Oligo
FCCP
AA+R
ECAR (mpH/min/Norm)
Time (minutes)
Control
LPS
VWF
B
3h Basal Glycolysis
Fold Change ECAR
**
**
Control
LPS
VWF
C
ECAR 16h Stimulation
Oligo
FCCP
AA+R
ECAR (mpH/min/Norm)
Time (minutes)
Control
LPS
VWF
D
16h Basal Glycolysis
Fold Change ECAR
**
****
Control
LPS
VWF
E
OCR 3h Stimulation
Oligo
FCCP
AA+R
OCR (pmol/min/Norm)
Time (minutes)
Control
LPS
VWF
F
OCR 16h Stimulation
Oligo
FCCP
AA+R
OCR (pmol/min/Norm)
Time (minutes)
Control
LPS
VWF

Figure 6

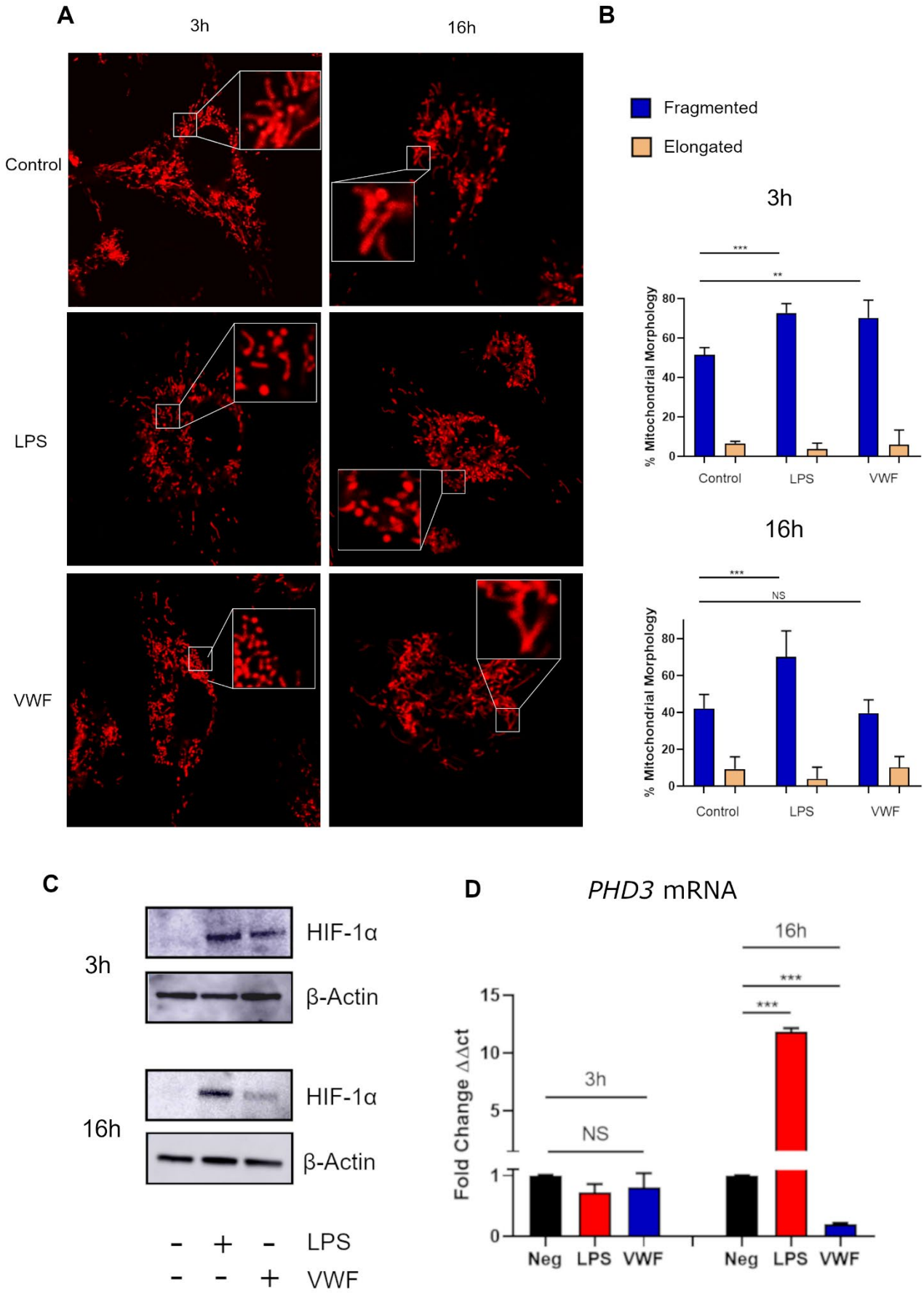
A
3h
16h
Control
LPS
VWF
B
Fragmented
Elongated
3h
% Mitochondrial Morphology
***
**
Control
LPS
VWF
16h
% Mitochondrial Morphology
***
NS
Control
LPS
VWF
C
3h
HIF-1α
β-Actin
16h
HIF-1α
β-Actin
- + - LPS
- - + VWF
D
PHD3 mRNA
Fold Change ΔΔct
3h
NS
16h
***
***
Neg
LPS
VWF
Neg
LPS
VWF

Figure 7

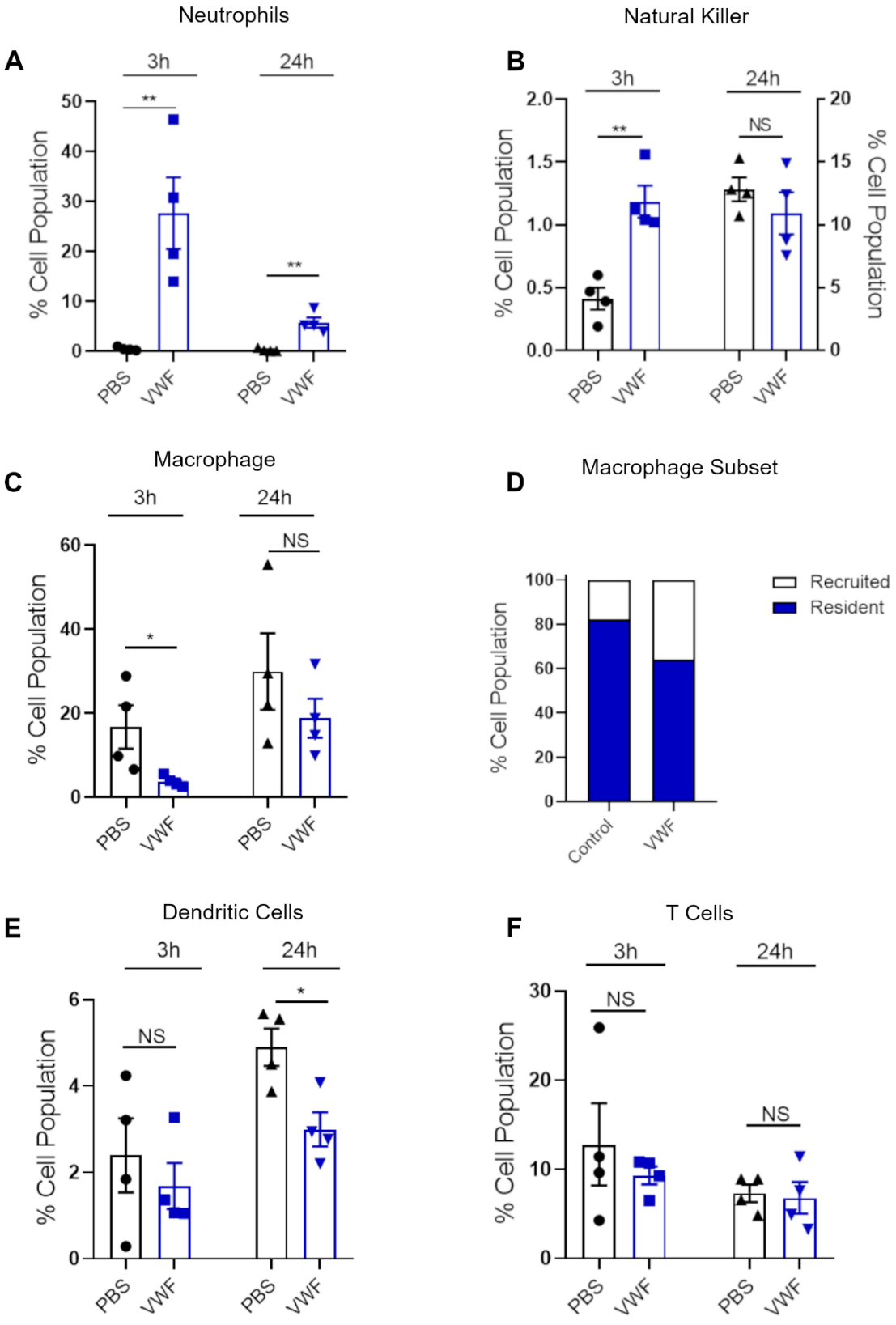
A
Neutrophils
3h
24h
**
**
% Cell Population
50
40
30
20
10
0
PBS
VWF
PBS
VWF
B
Natural Killer
3h
24h
**
NS
% Cell Population
2.0
1.5
1.0
0.5
0.0
20
15
10
5
0
% Cell Population
PBS
VWF
PBS
VWF
C
Macrophage
3h
24h
NS
*
% Cell Population
60
40
20
0
PBS
VWF
PBS
VWF
D
Macrophage Subset
Recruited
Resident
% Cell Population
100
80
60
40
20
0
Control
VWF
E
Dendritic Cells
3h
24h
NS
*
% Cell Population
6
4
2
0
PBS
VWF
PBS
VWF
F
T Cells
3h
24h
NS
NS
% Cell Population
30
20
10
0
PBS
VWF
PBS
VWF

Supplementary Figure 1

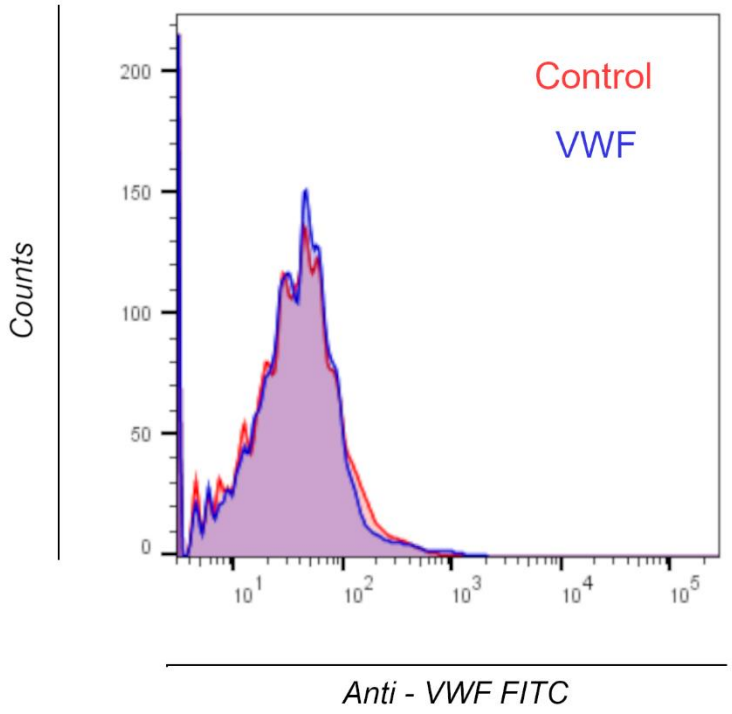

Supplementary Figure 2

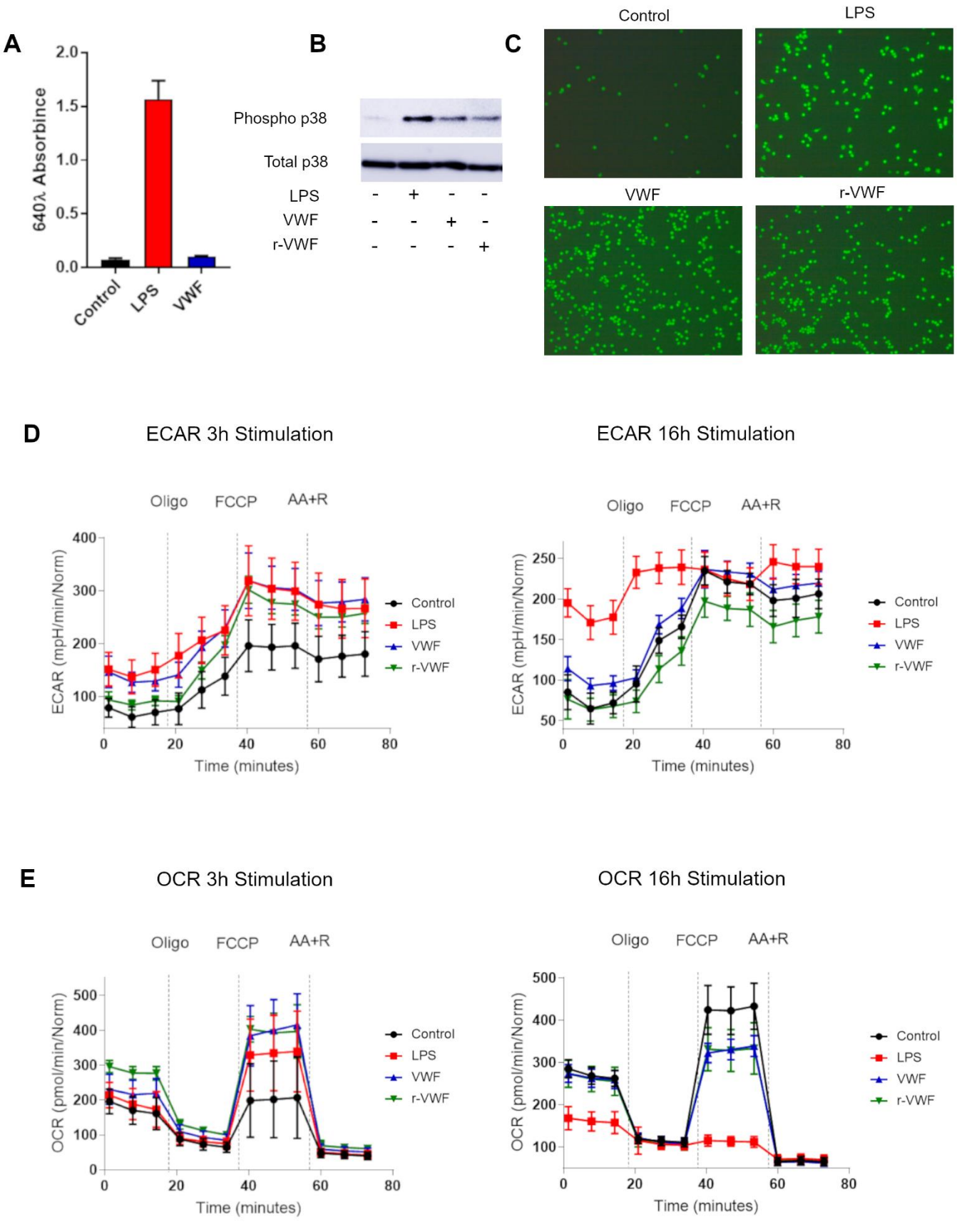

Supplementary Figure 3

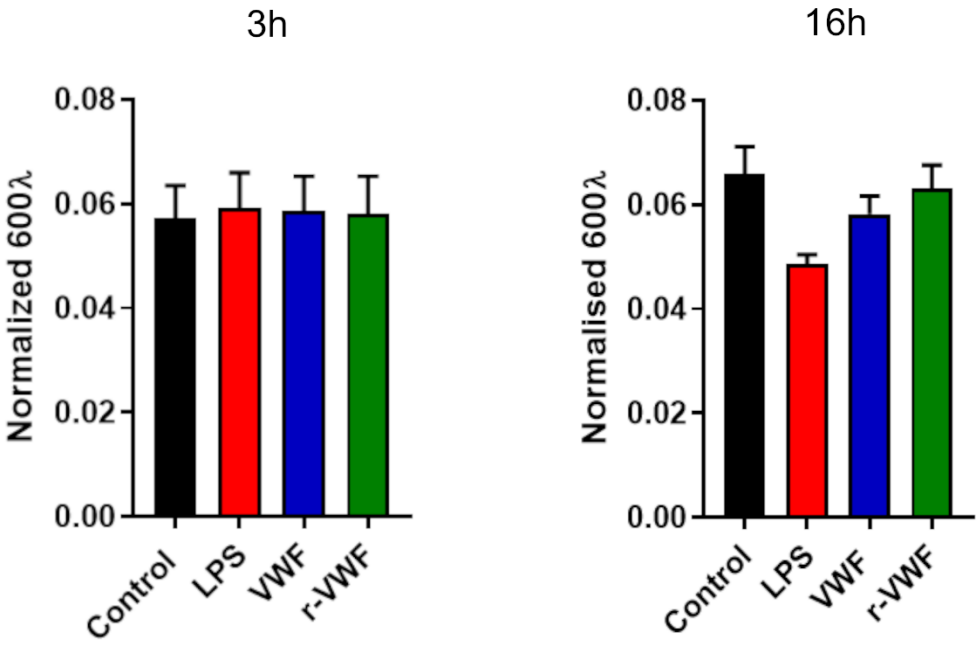

Supplementary Figure 4

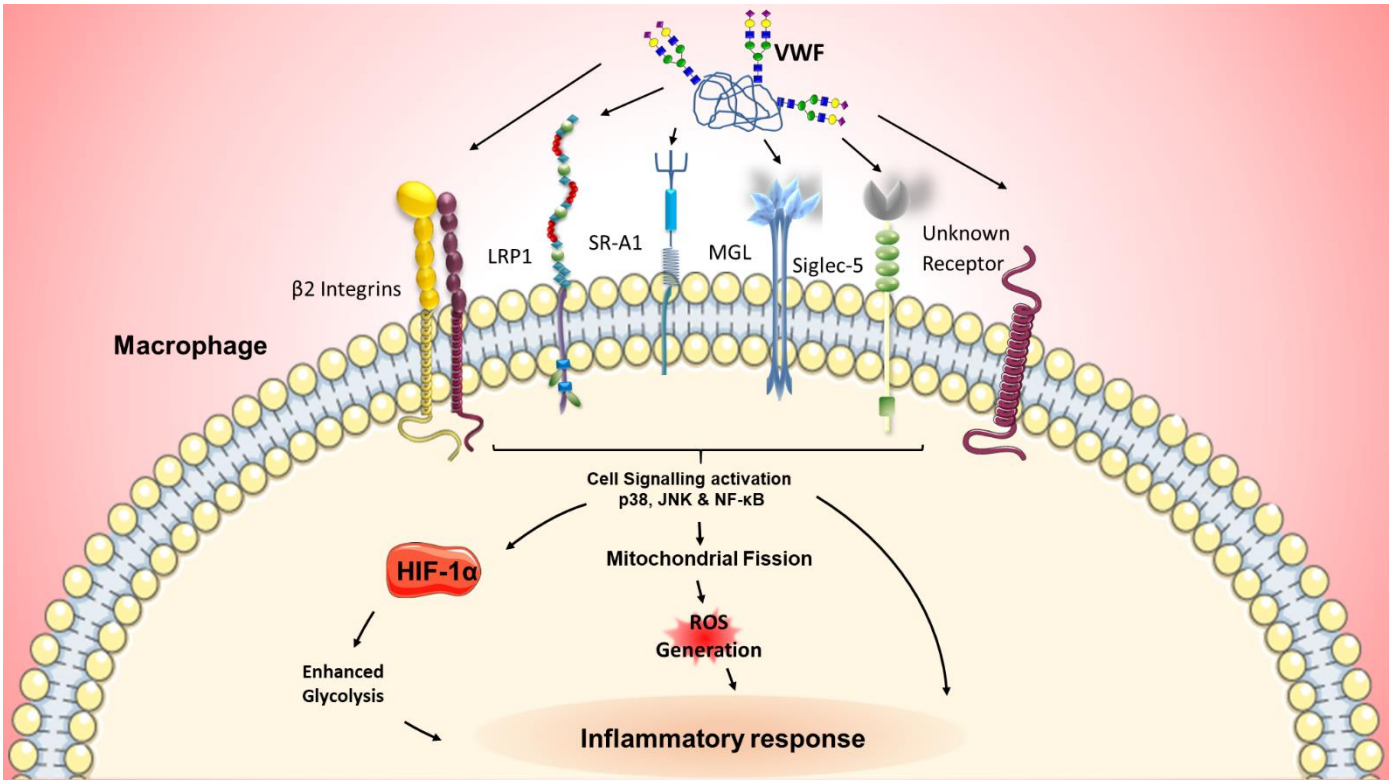

Supplementary Table 1

Human

Gene	Forward Primer	Reverse Primer
IL-1β	CTAAACAGATGAAGTGCTCC	GGTCATTCTCCTGGAAGG
IL-6	GCAGAAAAAGGCAAAGAATC	CTACATTTGCCGAAGAGC
TNFα	AGGCAGTCAGATCATCTTC	TTATCTCTCAGCTCCAGC
CCL2	AGACTAACCCAGAAACATCC	ATTGATTGCATCTGGCTG
CCL3	GCAACCAGTTCTCTGCATCA	TGGCTGCTCGTCTCAAAGTA
CCL4	GCTTTTCTTACACTGCGAGGA	CCAGGATTCACTGGGATCAG
β-Actin	GACGACATGGAGAAAATCTG	ATGATCTGGGTCATCTTCTC
NOS2	GCTCTACACCTCCAATGTGACC	CTGCCGAGATTTGAGCCTCATG

Murine

Gene	Forward Primer	Reverse Primer
β-actin	TGCTGTCCCTGTATGCCTCT	TTGATGTCACGCACGATTTC
TNFα	ACGTCGTAGCAAACCACCAA	GAGAACCTGGGAGTAGACAAGG
IL-6	ATGAAGTTCCTCTCTGCAAGAGACT	CACTAGGTTTGCCGAGTAGATCTC
PHD3	CAACTTCCTCCTGTCCCTCA	CCTGGATAGCAAGCCACCA

blood®

Brief Report

THROMBOSIS AND HEMOSTASIS

A novel role for the macrophage galactose-type lectin receptor in mediating von Willebrand factor clearance

Soracha E. Ward,[1,*] Jamie M. O'Sullivan,[1,*] Clive Drakeford,[1] Sonia Aguila,[1] Christopher N. Jondle,[2] Jyotika Sharma,[2] Padraic G. Fallon,[3] Teresa M. Brophy,[1] Roger J. S. Preston,[1] Paul Smyth,[4] Orla Sheils,[4] Alain Chion,[1] and James S. O'Donnell[1,5]

[1]Irish Centre for Vascular Biology, Molecular and Cellular Therapeutics, Royal College of Surgeons in Ireland, Dublin, Ireland; [2]Department of Basic Biomedical Sciences, University of North Dakota School of Medicine and Health Sciences, Grand Forks, ND; [3]Inflammation and Immunity Research Group, Trinity Translational Medicine Institute, and [4]Department of Histopathology, Trinity Translational Medicine Institute, Trinity College Dublin, St. James's Hospital, Dublin, Ireland; and [5]National Centre for Coagulation Disorders, St. James's Hospital, Dublin, Ireland

KEY POINTS

- VWF sialylation modulates in vivo clearance through Ashwell-Morrell independent pathways.
- VWF binding to MGL plays a novel role in facilitating VWF clearance.

Previous studies have shown that loss of terminal sialic acid causes enhanced von Willebrand factor (VWF) clearance through the Ashwell-Morrell receptor (AMR). In this study, we investigated (1) the specific importance of *N*- vs *O*-linked sialic acid in protecting against VWF clearance and (2) whether additional receptors contribute to the reduced half-life of hyposialylated VWF. α2-3-linked sialic acid accounts for <20% of total sialic acid and is predominantly expressed on VWF *O*-glycans. Nevertheless, specific digestion with α2-3 neuraminidase (α2-3Neu-VWF) was sufficient to cause markedly enhanced VWF clearance. Interestingly, in vivo clearance experiments in dual *VWF*$^{-/-}$/*Asgr1*$^{-/-}$ mice demonstrated enhanced clearance of α2-3Neu-VWF even in the absence of the AMR. The macrophage galactose-type lectin (MGL) is a C-type lectin that binds to glycoproteins expressing terminal *N*-acetylgalactosamine or galactose residues. Importantly, the markedly enhanced clearance of hyposialylated VWF in *VWF*$^{-/-}$/*Asgr1*$^{-/-}$ mice was significantly attenuated in the presence of an anti-MGL inhibitory antibody. Furthermore, dose-dependent binding of human VWF to purified recombinant human MGL was confirmed using surface plasmon resonance. Additionally, plasma VWF:Ag levels were significantly elevated in *MGL1*$^{-/-}$ mice compared with controls. Collectively, these findings identify MGL as a novel macrophage receptor for VWF that significantly contributes to the clearance of both wild-type and hyposialylated VWF. (*Blood*. 2018;131(8):911-916)

Introduction

Although substantial progress has been achieved in understanding von Willebrand factor (VWF) structure and function, the biological mechanisms underpinning VWF clearance from the plasma remain poorly understood.[1] Nevertheless, studies have demonstrated that enhanced VWF clearance plays an important role in the etiology of both type 1 and type 2 von Willebrand disease (VWD).[1,2] During biosynthesis, VWF undergoes complex posttranslational modification, including significant *N*- and *O*-linked glycosylation. Mass spectrometry studies have shown that sialylated biantennary complex-type chains constitute the commonest *N*-linked glycans expressed on VWF, whereas a disialylated core 1 tetrasaccharide structure (known as the T antigen) accounts for 70% of the total *O*-glycan population.[3,4] Thus, the majority of *N*- and *O*-linked glycans of human VWF are capped by negatively charged sialic acid residues.[5] In keeping with other plasma glycoproteins, terminal sialic acid expression plays an important role in protecting VWF against clearance.[6,7] Consequently, enzymatic removal of terminal sialylation from VWF has been associated with a markedly reduced plasma half-life in vivo.[8] Similarly, genetic inactivation of ST3GalIV sialyltransferase in a transgenic mouse model causes enhanced VWF clearance.[9] Several studies have reported significantly reduced VWF sialylation levels in patients with type 1 VWD.[7,9] Furthermore, van Schooten et al reported an inverse correlation between aberrant sialylation of T antigen and plasma VWF:Ag levels, suggesting that *O*-linked sialylation on VWF may be of particular importance.[7]

Current evidence suggests that the enhanced clearance of hyposialylated VWF occurs via the Ashwell-Morrell receptor (AMR).[10] This C-type lectin is expressed on hepatocytes and is composed of 2 transmembrane protein subunits (Asgpr-1 and Asgpr-2). Grewal et al previously demonstrated that plasma VWF clearance is significantly attenuated in *Asgr-1* knockout mice.[10] Nevertheless, important questions regarding the biological mechanisms through which VWF sialylation regulates its clearance in vivo remain unclear. In particular, the relative importance of *N*-linked vs *O*-linked sialylation in regulating physiological and/or pathological clearance of VWF has not been defined. In addition to the AMR, a number of other lectin receptors have been shown to bind with enhanced affinity to hyposialylated

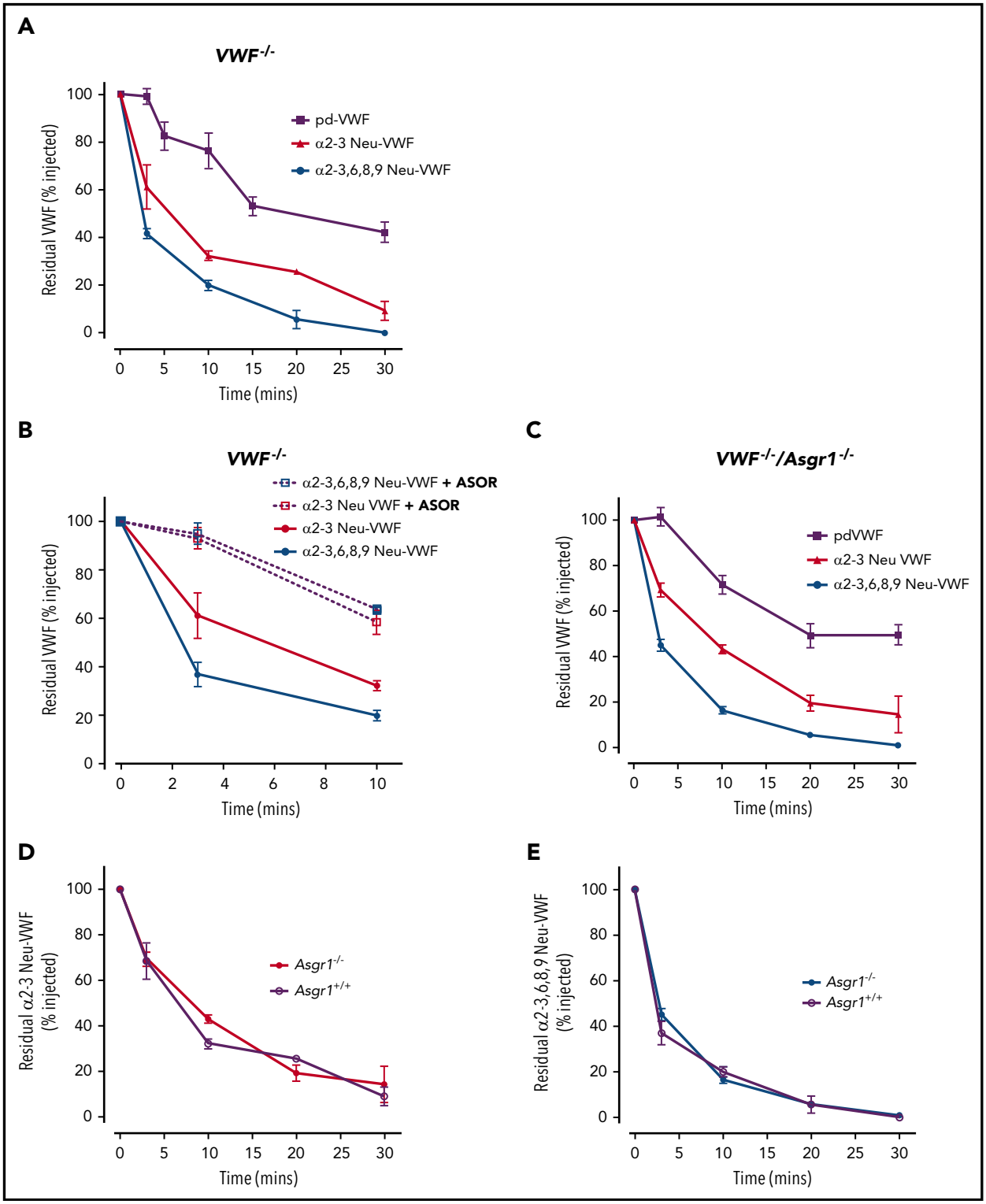

Figure 1. Clearance of hyposialylated VWF proceeds independently of AMR. (A) To study the effects of *N*- and *O*-linked sialylation on VWF clearance, purified human pd-VWF was treated with either α2-3,6,8,9 or α2-3 neuraminidase. In vivo clearance for each glycoform was then assessed in $VWF^{-/-}$ mice and compared with that of wild-type pd-VWF. At each time point, residual circulating VWF concentration was determined by VWF:Ag enzyme-linked immunosorbent assay. All results are plotted as percentage residual VWF:Ag levels relative to the amount injected. Three to 5 mice were used per time point. Data are represented as mean ± SEM. In some cases, the SEM cannot be seen because of its small size. (B) In the presence of ASOR, the enhanced in vivo clearance of both α2-3 Neu-VWF and α2-3,6,8,9 Neu-VWF was significantly attenuated (α2-3 Neu-VWF $t_{1/2}$ = 8.2 ± 1.4 minutes vs 12.4 ± 2.4 minutes, $P < .05$; and α2-3,6,8,9 Neu-VWF $t_{1/2}$ = 3.7 ± 0.7 minutes vs 14.4 ± 2.7 minutes, $P < .005$, respectively). (C) To determine whether AMR-independent pathways contribute to the enhance clearance of hyposialylated VWF, in vivo clearance studies were repeated in $VWF^{-/-}/Asgr1^{-/-}$ mice. Importantly, the markedly enhanced clearance of both α2-3 Neu-VWF and α2-3,6,8,9 Neu-VWF was still evident in the absence of the AMR ($t_{1/2}$ = 8.2 ± 0.6 and 3.2 ± 0.4 compared with 50.6 ± 2 minutes for pd-VWF; $P < .05$). Furthermore, the reduced half-life observed for α2-3 Neu-VWF (D) and α2-3,6,8,9 Neu-VWF (E) were not significantly different in the presence or absence of the AMR (α2-3 Neu-VWF $t_{1/2}$ = 8.2 ± 1.4 minutes vs 8.2 ± 0.6 minutes, $P = .96$; and α2-3,6,8,9 Neu-VWF $t_{1/2}$ = 3.7 ± 0.7 minutes vs 3.2 ± 0.4 minutes, $P = .42$, respectively).

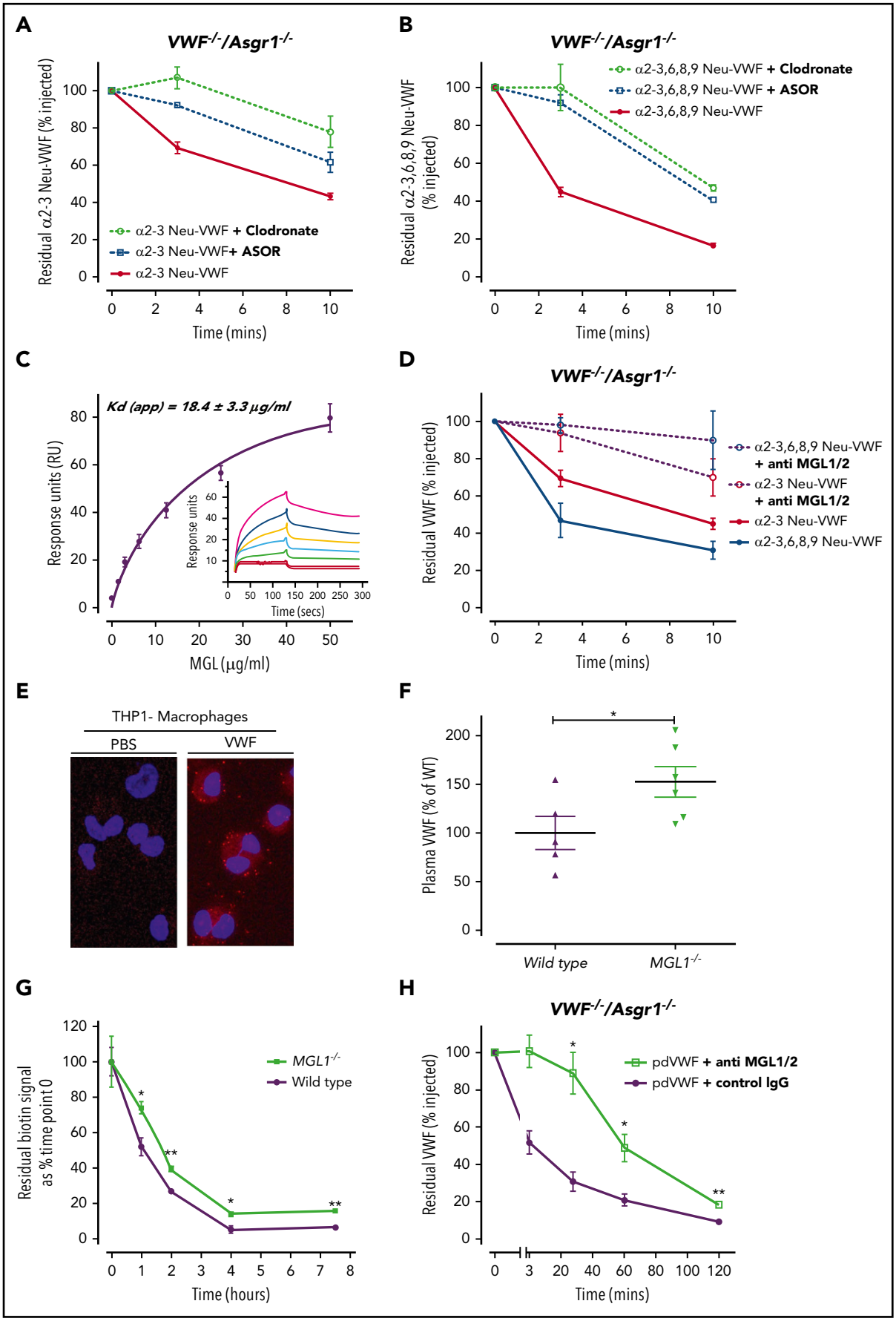

Figure 2.

glycoproteins.[11] In this study, we demonstrate a critical role for VWF *O*-linked sialylation in modulating in vivo clearance and further define a novel role for the macrophage galactose-type lectin (MGL) in regulating VWF clearance in a sialic acid–dependent manner.

Study design

Isolation and digestion of human plasma–derived VWF

As described in the supplemental Methods (available on the *Blood* Web site), plasma-derived VWF (pd-VWF) was purified from commercial concentrate Fandhi (Grifols, Barcelona, Spain) and subsequently treated with α2-3 neuraminidase (*Streptococcus pneumonia*; Sigma Aldrich, Ireland) or α2-3,6,8,9 neuraminidase (*Arthrobacter ureafaciens*; New England Biolabs, United Kingdom) as previously described.[5] VWF glycan expression was analyzed using lectin enzyme-linked immunosorbent assays (see supplemental Methods and supplemental Figure 1).[8]

VWF clearance studies

VWF$^{-/-}$ and *Asgr1*$^{-/-}$ mice on a C57BL/6J background were obtained from the Jackson Laboratory (Sacramento, CA) and crossbred to generate novel *VWF*$^{-/-}$/*Asgr1*$^{-/-}$ double-knockout mice. *MGL1*$^{-/-}$ mice were also obtained from the Jackson Laboratory. Where indicated, clearance studies were repeated in the presence of either clodronate or asialo-orosomucoid (ASOR) as previously described.[8,12] Specific clearance studies were performed after inhibition of MGL using a polyclonal goat anti-mouse MGL1/2 antibody. All in vivo clearance experiments were performed as detailed in the supplemental Methods in accordance with the Health Product Regulatory Authority, Ireland.

In vitro VWF binding studies

As described in the supplemental Methods, surface plasmon resonance (SPR) was used to evaluate MGL binding to VWF.[13] Briefly, purified pd-VWF was immobilized on a CM5 chip, and binding to recombinant MGL (R&D Systems, United Kingdom) was determined. Furthermore, proximity ligation assay (Duolink-PLA; Sigma Aldrich, Ireland) was performed to evaluate colocalization of VWF and MGL on THP1 macrophages.

Data presentation and statistical analysis

Experimental data were analyzed with GraphPad Prism version 5.0 (GraphPad Software, San Diego, CA). Data were expressed as mean values ± standard error of the mean (SEM). Data were analyzed with Student unpaired 2-tailed *t* test, and *P* values of $<.05$ were deemed significant.

Results and discussion

VWF sialylation modulates clearance through Ashwell-Morrell independent pathways

In keeping with previous studies, we observed that combined removal of *N*- and *O*-linked sialic acid by digestion with α2-3,6,8,9 neuraminidase resulted in markedly enhanced clearance of pd-VWF in *VWF*$^{-/-}$ mice (Figure 1A). Specific removal of α2-3-linked sialic acid was sufficient to markedly enhance VWF clearance ($t_{1/2}$ = 9.0 ± 1 minutes; $P < .05$) (Figure 1A). In fact, clearance of α2-3 Neu-VWF was almost as rapid as that of α2-3,6,8,9 Neu-VWF ($t_{1/2}$ = 4.0 ± 0.3 minutes). This finding is interesting because α2-3-linked sialic acid is predominantly located on the *O*-linked glycans of human VWF and accounts for <20% of total sialic acid expression.[5] Currently, the AMR is the only receptor described to regulate clearance of hyposialylated VWF.[10] We found that the enhanced clearance of α2-3 Neu-VWF and α2-3,6,8,9 Neu-VWF were both significantly attenuated in the presence of a hyposialylated inhibitor glycoprotein (ASOR) (Figure 1B). However, ASOR has a short plasma half-life and is not a specific AMR inhibitor.[14] Previous studies have shown that AMR demonstrates significantly greater affinity for exposed galactose residues on tri- and tetra-antennary galactoses (as present on VWF *N*-glycan) compared with terminal galactose moieties on mono- or biantennary galactoses (as present on VWF *O*-glycan).[15,16] We therefore hypothesized that other lectin receptors may contribute to the enhanced clearance of hyposialylated VW and be of particular importance in modulating the effects of *O*-linked sialylation on VWF clearance. To address this, in vivo clearance studies were repeated in dual *VWF*$^{-/-}$/*Asgr1*$^{-/-}$ knockout mice. Critically, we observed that markedly enhanced clearance of both α2-3 Neu-VWF and α2-3,6,8,9 Neu-VWF persisted in *VWF*$^{-/-}$/*Asgr1*$^{-/-}$ mice ($t_{1/2}$ = 8.2 ± 0.6 and 3.2 ± 0.4 vs 50.6 ± 2 minutes for pd-VWF; $P < .05$) (Figure 1C). Furthermore, the enhanced clearance rates observed for α2-3 Neu-VWF and α2-3,6,8,9 Neu-VWF were not significantly different in the presence or absence of the AMR (Figure 1D-E). Collectively, these data confirm that reductions in *N*- and/or *O*-linked sialylation have major effects on VWF half-life and demonstrate that α2-3-linked sialic acid expressed on *O*-linked glycans may be of particular importance in regulating pd-VWF clearance. Furthermore, our findings suggest that previously unrecognized AMR-independent pathways contribute to the enhanced clearance of hyposialylated VWF in vivo.

Figure 2. MGL facilitates VWF clearance in vivo. To investigate other receptors and/or cell types that modulate the enhanced clearance of hyposialylated VWF, α2-3 Neu-VWF (A) and α2-3,6,8,9 Neu-VWF (B) clearance studies in *VWF*$^{-/-}$*Asgr1*$^{-/-}$ mice were repeated in the presence of ASOR, or following clodronate-induced macrophage depletion. The enhanced clearance of both α2-3 Neu-VWF and α2-3,6,8,9 Neu-VWF was still inhibited by ASOR (blue lines) even in the absence of the AMR (α2-3 Neu-VWF $t_{1/2}$ = 8.2 ± 1.4 minutes vs 16.8 ± 1.6 minutes, $P < .005$; and α2-3,6,8,9 Neu-VWF $t_{1/2}$ = 3.7 ± 0.7 minutes vs 7.7 ± 1.3 minutes, $P < .05$, respectively). In addition, clodronate-induced macrophage depletion (green lines) also significantly attenuated the enhanced clearance of hyposialylated VWF (α2-3 Neu-VWF $t_{1/2}$ = 8.2 ± 1.4 minutes vs 24.0 ± 1.1 minutes, $P < .05$; and α2-3,6,8,9 Neu-VWF $t_{1/2}$ = 3.7 ± 0.7 minutes vs 9.6 ± 4.1 minutes, $P < .05$, respectively). Three to 5 mice were used per time point, and data are represented as mean ± SEM. (C) SPR was used to evaluate the binding of immobilized purified pd-VWF to recombinant human MGL. Dose-dependent binding were observed, with K_d (app) of 18.4 ± 3 μg/mL. (D) In mice, there are 2 homologs of human MGL, mMGL1 and mMGL2. Murine MGL1 shares significant sequence homology with human MGL and binds oligosaccharides with multiple terminal Gal residues including the T antigen. Interestingly, the markedly enhanced clearance of both α2-3 Neu-VWF and α2-3,6,8,9 Neu-VWF in *VWF*$^{-/-}$*Asgr1*$^{-/-}$ mice was significantly attenuated in the presence of an mMGL blocking antibody vs isotype immunoglobulin G (IgG) control antibody, respectively (α2-3 Neu-VWF $t_{1/2}$ = 21.9 ± 11.8 minutes vs 9.1 ± 1.5 minutes, $P < .05$; and α2-3,6,8,9 Neu-VWF $t_{1/2}$ = 24.4 ± 8.1 minutes vs 5.7 ± 2.1 minutes, $P < .05$, respectively). (E) THP1 macrophages incubated with VWF demonstrated VWF-MGL colocalization detected by Duolink-PLA, visualized as red spots via immunofluorescence microscopy. No signal was observed from cells incubated with phosphate-buffered saline (PBS) alone. (F) Plasma VWF:Ag levels were significantly elevated in MGL1$^{-/-}$ mice compared with wild-type (WT) littermate controls ($P < .05$). (G) The clearance of endogenous murine VWF in MGL1$^{-/-}$ mice was significantly attenuated compared with wild-type controls at all time points measured ($P < .05$). (H) In vivo clearance of wild-type pd-VWF in *VWF*$^{-/-}$*Asgr1*$^{-/-}$ mice was significantly attenuated in the presence of an mMGL blocking antibody compared with isotype control IgG ($t_{1/2}$ = 64.6 ± 18.4 minutes vs 42.8 ± 10.7 minutes; $P < .005$). A minimum of 3 mice were used per time point; data are plotted as mean ± SEM.

The macrophage galactose receptor regulates in vivo clearance of VWF

To investigate other receptors and/or cell types that modulate the enhanced clearance of hyposialylated VWF, α2-3 Neu-VWF and α2-3,6,8,9 Neu-VWF clearance studies in *VWF*$^{-/-}$/*Asgr1*$^{-/-}$ mice were repeated in the presence of ASOR, or following clodronate-induced macrophage depletion (Figure 2A-B). The enhanced clearance of both α2-3 Neu-VWF and α2-3,6,8,9 Neu-VWF was still inhibited by ASOR even in the absence of the AMR. Interestingly, in vivo macrophage depletion also significantly attenuated the enhanced clearance of hyposialylated VWF. Finally, in vitro binding studies demonstrated enhanced binding of asialo-VWF to differentiated THP1 macrophages (supplemental Figure 2). Collectively, these data demonstrate that additional asialo-receptors, at least in part expressed on macrophages, regulate the enhanced clearance of hyposialylated VWF in vivo.

MGL is a C-type lectin receptor expressed as a homo-oligomer on antigen-presenting cells such as macrophages and dendritic cells (supplemental Figure 3).[17] The carbohydrate recognition domain of MGL binds with high affinity to glycoproteins expressing terminal *N*-acetylgalactosamine or galactose (Gal) residues, and thus MGL can regulate glycoprotein endocytosis.[18-20] MGL binding to oligosaccharide chains is attenuated by terminal sialylation.[21] Importantly, given the putative role of VWF *O*-linked glycans in modulating clearance, MGL also recognizes the T antigen.[22] In mice, there are 2 homologs of human MGL, mMGL1 and mMGL2.[23] Murine MGL1 shares significant sequence homology with human MGL and has been shown to bind oligosaccharides with terminal Gal residues including the so called T antigen.[23] Of note, previous studies have demonstrated that ~70% of the *O*-glycans of VWF are composed of this sialylated tumor-associated T antigen structure.[4,7] Interestingly, the enhanced clearance of both α2-3 Neu-VWF and α2-3,6,8,9 Neu-VWF in *VWF*$^{-/-}$/*Asgr1*$^{-/-}$ mice was significantly attenuated in the presence of anti-mMGL1/2 inhibitory antibody, suggesting a novel role for MGL in regulating macrophage-mediated clearance of hyposialylated VWF (Figure 2D). Importantly, we observed dose-dependent binding of human pd-VWF to purified recombinant human MGL using SPR (Figure 2C). Moreover, Duolink-PLA analysis demonstrated that VWF colocalizes with MGL on the surface of THP1 macrophages, as indicated by the distinct red fluorescent dots (Figure 2E). Plasma VWF:Ag levels were significantly elevated in *MGL1*$^{-/-}$ mice compared with wild-type controls (152.6 ± 15.7% vs 100 ± 16.9%; $P < .05$) (Figure 2F). Furthermore, in vivo clearance of endogenous murine VWF was attenuated in *MGL1*$^{-/-}$ mice (Figure 2G), suggesting that MGL-mediated VWF clearance is important even in the presence of AMR. Finally, clearance of pd-VWF in *VWF*$^{-/-}$/*Asgr1*$^{-/-}$ mice was attenuated in the presence of mMGL1/2 inhibitory antibody (Figure 2H). Collectively, these findings reveal MGL as a novel macrophage lectin receptor for VWF that contributes to the clearance of both wild-type and hyposialylated VWF. Further studies will be required to determine the importance of MGL compared with other recently described receptors involved in regulating VWF clearance.[24] Nevertheless, the role of MGL in modulating VWF clearance has direct translational relevance in that quantitative variations in *N*- and *O*-linked sialylation have been described in patients with type 1 VWD.[7,9] In addition, desialylation of VWF has been described with glycoprotein ageing in plasma[25] and can also occur during infections with specific pathogens that are associated with significantly enhanced neuraminidase activity (eg, *Streptococcus* pneumonia).[10]

Acknowledgments

The authors thank Nico van Rooijen of the Foundation Clodronate Liposomes (Haarlem, The Netherlands) for generously providing the liposome-clodronate.

This work was supported by a Science Foundation Ireland Principal Investigator Award (11/PI/1066, J.S.O.).

Authorship

Contribution: S.E.W., J.M.O., S.A., C.D., C.N.J., J.S., P.G.F., T.M.B., P.S., O.S., and A.C. performed experiments; S.E.W., J.M.O., S.A., C.D., C.N.J., J.S., P.G.F., T.M.B., R.J.S.P., O.S., A.C., and J.S.O. designed the research and analyzed the data; and all authors were involved in writing and reviewing the manuscript.

Conflict-of-interest disclosure: J.S.O. has served on the speaker's bureau for Baxter, Bayer, Novo Nordisk, Boehringer Ingelheim, Leo Pharma, and Octapharma; has served on the advisory boards of Baxter, Bayer, Octapharma CSL Behring, Daiichi Sankyo, Boehringer Ingelheim, and Pfizer; and has received research grant funding awards from Baxter, Bayer, Pfizer, and Novo Nordisk. The remaining authors declare no competing financial interests.

Correspondence: Jamie M. O'Sullivan, Department of Molecular and Cellular Therapeutics, Irish Centre for Vascular Biology, Royal College of Surgeons in Ireland, 123 St Stephen's Green, Dublin 2, Ireland; e-mail: jamieosullivan@rcsi.ie.

Footnotes

Submitted 6 June 2017; accepted 12 December 2017. Prepublished online as *Blood* First Edition paper, 27 December 2017; DOI 10.1182/blood-2017-06-787853.

*S.E.W. and J.M.O. contributed equally to this study.

The online version of this article contains a data supplement.

There is a *Blood* Commentary on this article in this issue.

The publication costs of this article were defrayed in part by page charge payment. Therefore, and solely to indicate this fact, this article is hereby marked "advertisement" in accordance with 18 USC section 1734.

REFERENCES

1. Casari C, Lenting PJ, Wohner N, Christophe OD, Denis CV. Clearance of von Willebrand factor. *J Thromb Haemost.* 2013;11(suppl 1): 202-211.

2. Rawley O, O'Sullivan JM, Chion A, et al. von Willebrand factor arginine 1205 substitution results in accelerated macrophage-dependent clearance in vivo. *J Thromb Haemost.* 2015;13(5):821-826.

3. Canis K, McKinnon TAJ, Nowak A, et al. Mapping the N-glycome of human von Willebrand factor. *Biochem J.* 2012;447(2): 217-228.

4. Canis K, McKinnon TAJ, Nowak A, et al. The plasma von Willebrand factor O-glycome comprises a surprising variety of structures including ABH antigens and disialosyl motifs. *J Thromb Haemost.* 2010;8(1): 137-145.

5. McGrath RT, McKinnon TAJ, Byrne B, et al. Expression of terminal alpha2-6-linked sialic acid on von Willebrand factor specifically enhances proteolysis by ADAMTS13. *Blood.* 2010;115(13):2666-2673.

6. Sodetz JM, Pizzo SV, McKee PA. Relationship of sialic acid to function and in vivo survival of human factor VIII/von Willebrand factor protein. *J Biol Chem*. 1977;252(15):5538-5546.

7. van Schooten CJM, Denis CV, Lisman T, et al. Variations in glycosylation of von Willebrand factor with O-linked sialylated T antigen are associated with its plasma levels. *Blood*. 2007;109(6):2430-2437.

8. O'Sullivan JM, Aguila S, McRae E, et al. N-linked glycan truncation causes enhanced clearance of plasma-derived von Willebrand factor. *J Thromb Haemost*. 2016;14(12):2446-2457.

9. Ellies LG, Ditto D, Levy GG, et al. Sialyltransferase ST3Gal-IV operates as a dominant modifier of hemostasis by concealing asialoglycoprotein receptor ligands. *Proc Natl Acad Sci USA*. 2002;99(15):10042-10047.

10. Grewal PK, Uchiyama S, Ditto D, et al. The Ashwell receptor mitigates the lethal coagulopathy of sepsis. *Nat Med*. 2008;14(6):648-655.

11. Preston RJS, Rawley O, Gleeson EM, O'Donnell JS. Elucidating the role of carbohydrate determinants in regulating hemostasis: insights and opportunities. *Blood*. 2013;121(19):3801-3810.

12. Chion A, O'Sullivan JM, Drakeford C, et al. N-linked glycans within the A2 domain of von Willebrand factor modulate macrophage-mediated clearance. *Blood*. 2016;128(15):1959-1968.

13. O'Sullivan JM, Jenkins PV, Rawley O, et al. Galectin-1 and galectin-3 constitute novel-binding partners for factor VIII. *Arterioscler Thromb Vasc Biol*. 2016;36(5):855-863.

14. Wall DA, Wilson G, Hubbard AL. The galactose-specific recognition system of mammalian liver: the route of ligand internalization in rat hepatocytes. *Cell*. 1980;21(1):79-93.

15. Ashwell G, Harford J. Carbohydrate-specific receptors of the liver. *Annu Rev Biochem*. 1982;51(1):531-554.

16. Lodish HF. Recognition of complex oligosaccharides by the multi-subunit asialoglycoprotein receptor. *Trends Biochem Sci*. 1991;16(10):374-377.

17. Higashi N, Morikawa A, Fujioka K, et al. Human macrophage lectin specific for galactose/N-acetylgalactosamine is a marker for cells at an intermediate stage in their differentiation from monocytes into macrophages. *Int Immunol*. 2002;14(6):545-554.

18. van Vliet SJ, van Liempt E, Saeland E, et al. Carbohydrate profiling reveals a distinctive role for the C-type lectin MGL in the recognition of helminth parasites and tumor antigens by dendritic cells. *Int Immunol*. 2005;17(5):661-669.

19. van Vliet SJ, Aarnoudse CA, Broks-van den Berg VC, Boks M, Geijtenbeek TB, van Kooyk Y. MGL-mediated internalization and antigen presentation by dendritic cells: a role for tyrosine-5. *Eur J Immunol*. 2007;37(8):2075-2081.

20. Oo-puthinan S, Maenuma K, Sakakura M, et al. The amino acids involved in the distinct carbohydrate specificities between macrophage galactose-type C-type lectins 1 and 2 (CD301a and b) of mice. *Biochim Biophys Acta*. 2008;1780(2):89-100.

21. Yamamoto K, Ishida C, Shinohara Y, et al. Interaction of immobilized recombinant mouse C-type macrophage lectin with glycopeptides and oligosaccharides. *Biochemistry*. 1994;33(26):8159-8166.

22. Mortezai N, Behnken HN, Kurze AK, et al. Tumor-associated Neu5Ac-Tn and Neu5Gc-Tn antigens bind to C-type lectin CLEC10A (CD301, MGL). *Glycobiology*. 2013;23(7):844-852.

23. Tsuiji M, Fujimori M, Ohashi Y, et al. Molecular cloning and characterization of a novel mouse macrophage C-type lectin, mMGL2, which has a distinct carbohydrate specificity from mMGL1. *J Biol Chem*. 2002;277(32):28892-28901.

24. Pipe SW, Montgomery RR, Pratt KP, Lenting PJ, Lillicrap D. Life in the shadow of a dominant partner: the FVIII-VWF association and its clinical implications for hemophilia A. *Blood*. 2016;128(16):2007-2016.

25. Yang WH, Aziz PV, Heithoff DM, Mahan MJ, Smith JW, Marth JD. An intrinsic mechanism of secreted protein aging and turnover. *Proc Natl Acad Sci USA*. 2015;112(44):13657-13662.

2018 131: 911-916
doi:10.1182/blood-2017-06-787853 originally published online December 27, 2017

A novel role for the macrophage galactose-type lectin receptor in mediating von Willebrand factor clearance

Soracha E. Ward, Jamie M. O'Sullivan, Clive Drakeford, Sonia Aguila, Christopher N. Jondle, Jyotika Sharma, Padraic G. Fallon, Teresa M. Brophy, Roger J. S. Preston, Paul Smyth, Orla Sheils, Alain Chion and James S. O'Donnell

Blood (print ISSN 0006-4971, online ISSN 1528-0020), is published weekly by the American Society of Hematology, 2021 L St, NW, Suite 900, Washington DC 20036.

Editorial

Targeting von Willebrand Factor–Mediated Inflammation

Clive Drakeford, James S. O'Donnell

In this issue of *Arteriosclerosis, Thrombosis, and Vascular Biology*, Aymé et al[1] provide new insights into the role played by von Willebrand factor (VWF) in modulating in vivo inflammatory responses. In particular, a single-domain antibody against the VWF A1 domain is shown to markedly attenuate leukocyte recruitment and vascular permeability in 2 distinct murine models of inflammation. Collectively, these findings support the hypothesis that VWF is involved in regulating inflammation and suggest that novel VWF-targeted therapies may be useful inhibitors of this critical step in inflammatory pathogenesis.

See accompanying article on page 1736

VWF circulates in plasma as a large multimeric glycoprotein and plays critical roles in normal hemostasis.[2] At sites of vascular damage, VWF binds to exposed subendothelial collagen. Shear stress then triggers unwinding of the normal globular conformation of VWF, leading to conformational changes within the A domains and in particular exposure of the GPIbα (glycoprotein Ibα)-binding site within the A1 domain. Consequently, tethered VWF can recruit platelets to the site of injury. In addition, VWF also acts as a carrier for procoagulant FVIII, protecting it against premature proteolytic degradation and clearance.[3]

Besides these important roles in maintaining hemostasis, recent studies have identified novel roles for VWF in modulating inflammatory responses.[4–8] In vitro studies demonstrated that immobilized VWF binds directly to both polymorphonuclear leukocytes and monocytes under static and flow conditions.[4] Under flow conditions, this VWF-mediated interaction involved transient rolling (mediated in part though VWF binding to leukocyte P-selectin glycoprotein ligand-1) followed by stable adhesion (mediated in part through VWF interaction with leukocyte β2-integrins). VWF binding to P-selectin glycoprotein ligand-1 was dependent on the A1 domain, whereas several regions of VWF (including D'D3 and A1A2A3) were implicated in β2-integrin binding.[4]

Roles for VWF in modulating inflammatory responses have also been observed in vivo.[5–8] In an experimental sepsis model involving cecal ligation and puncture, Lerolle et al[5] observed significantly enhanced overall survival in VWF$^{-/-}$ mice compared with wild-type controls. Importantly, however, data derived from inflammation studies performed in VWF$^{-/-}$ mice are complicated by the fact that these mice also lack Weibel–Palade bodies and consequently have confounding P-selectin storage abnormalities. However, Petri et al[6] showed that VWF-blocking antibodies significantly inhibited neutrophil recruitment into thioglycollate-inflamed peritoneum and keratinocyte-derived chemokine–stimulated exposed cremaster muscle. In both murine models, the ability of the VWF-blocking antibody in reducing neutrophil extravasation was critically dependent on the presence of platelets and GPIbα.[6] In addition to VWF-mediated leukocyte binding, in vivo studies have further demonstrated that VWF-associated platelets are important in regulating permeability of the endothelial cell wall and, thus, also influence neutrophil extravasation.[6] VWF-blocking antibodies were also shown to attenuate neutrophil recruitment in a murine model of immune complex–mediated vasculitis.[7] Interestingly, in contrast to the critical need for platelet GPIbα in regulating VWF-induced neutrophil extravasation into inflamed peritoneum, Hillgruber et al[7] showed that VWF-modulated neutrophil recruitment in cutaneous inflammation was GPIbα-independent.

To further elucidate the role of VWF in regulating inflammation in vivo, Aymé et al[1] have developed a novel single-domain llama-derived antibody or nanobody that recognizes an epitope located within the A1 domain of VWF. Importantly, this A1 domain single-domain llama-derived antibody cross-reacts with both human and murine VWF. Consequently, a bivalent variant of the single-domain llama-derived antibody (KB-VWF-006bi) interfered with ristocetin-induced murine and human platelet aggregation and significantly attenuated VWF binding to collagen VI (but not to collagens I, III, or IV). In vivo, KB-VWF-006bi dose dependently increased bleeding time and blood loss in a tail-clip model and reduced the formation of occlusive thrombi in a ferric chloride–induced thrombosis model. In keeping with previous studies, KB-VWF-006bi was shown to markedly reduce leukocyte recruitment and vascular permeability in 2 distinct inflammation models of immune complex–mediated vasculitis and irritant contact dermatitis, respectively.[1] Given that KB-VWF-006bi binds only to the VWF A1 domain, this suggests that, at least in these animal models, the A1 domain plays a specific role in facilitating the proinflammatory effects of VWF. Perhaps unsurprisingly, this critical role for the A1 domain is at least partially dependent on the presence of platelets. Cumulatively, these findings suggest that VWF binding to GPIbα serves to tether platelets, which, in turn, modulates endothelial cell barrier wall permeability and thus leukocyte tissue extravasation into the tissues.

These emerging data demonstrate that VWF influences multiple different aspects of inflammation in vivo (Figure). Further studies will be essential in defining the molecular mechanisms through which these VWF-mediated immunomodulatory effects are mediated. On the basis of the current

From the Irish Centre for Vascular Biology, Royal College of Surgeons in Ireland, Dublin.

Correspondence to James O'Donnell, PhD, Irish Centre for Vascular Biology, Royal College of Surgeons in Ireland, Ardilaun House, 111 St. Stephen's Green, Dublin 2, Ireland. E-mail jamesodonnell@rcsi.ie

(*Arterioscler Thromb Vasc Biol*. 2017;37:1590-1591.
DOI: 10.1161/ATVBAHA.117.309817.)

Arterioscler Thromb Vasc Biol is available at http://atvb.ahajournals.org
DOI: 10.1161/ATVBAHA.117.309817

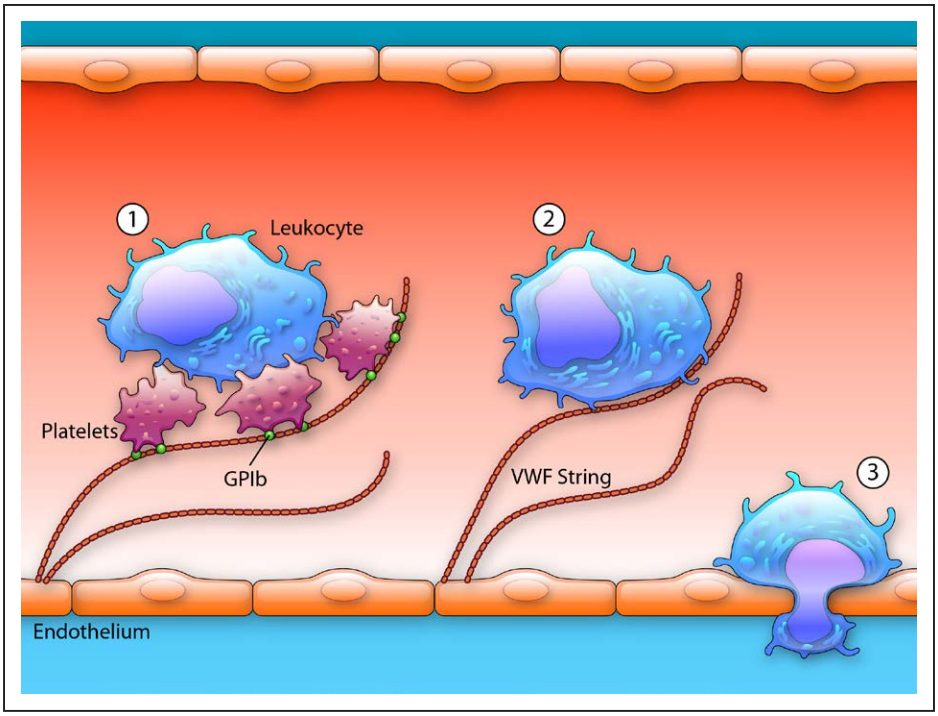

Figure. von Willebrand factor (VWF) modulates inflammation through multiple different mechanisms. (1) VWF released from activated endothelial cells, or bound to collagen at sites of vascular injury, interacts with platelet GPIbα (glycoprotein Ibα) and recruits platelets. The VWF-tethered platelets subsequently enable neutrophil recruitment. (2) VWF can also recruit leucocytes in a platelet-independent manner by directly interacting with leukocyte cell surface receptors including β2-integrins and P-selectin glycoprotein ligand-1. (3) VWF regulates endothelial wall permeability and influences leukocyte extravasation.

evidence, VWF clearly modulates inflammation through platelet-dependent and platelet-independent pathways.[4–8] Moreover, although the underlying biology remains unexplained, the animal data further suggest that the relative importance of these discrete VWF-mediated pathways varies between different types of inflammation. Further insights into the role played by VWF in regulating leukocyte extravasation and endothelial cell permeability and the complex cross-talk that exists in vivo between hemostasis and inflammation will undoubtedly emerge in the near future. Given the significant morbidity and mortality associated with inflammatory pathology, defining the roles of VWF may offer exciting opportunities to develop novel therapies to address a critical unmet clinical need.

Disclosures

None.

References

1. Aymé G, Adam F, Legendre P, Bazaa A, Proulle V, Denis CV, Christophe OD, Lenting PJ. A novel single-domain antibody against von Willebrand factor A1 domain resolves leukocyte recruitment and vascular leakage during inflammation—brief report. *Arterioscler Thromb Vasc Biol*. 2017;37:1736–1740. doi: 10.1161/ATVBAHA.117.309319.
2. Lenting PJ, Christophe OD, Denis CV. von Willebrand factor biosynthesis, secretion, and clearance: connecting the far ends. *Blood*. 2015;125:2019–2028. doi: 10.1182/blood-2014-06-528406.
3. Terraube V, O'Donnell JS, Jenkins PV. Factor VIII and von Willebrand factor interaction: biological, clinical and therapeutic importance. *Haemophilia*. 2010;16:3–13. doi: 10.1111/j.1365-2516.2009.02005.x.
4. Pendu R, Terraube V, Christophe OD, Gahmberg CG, de Groot PG, Lenting PJ, Denis CV. P-selectin glycoprotein ligand 1 and beta2-integrins cooperate in the adhesion of leukocytes to von Willebrand factor. *Blood*. 2006;108:3746–3752. doi: 10.1182/blood-2006-03-010322.
5. Lerolle N, Dunois-Lardé C, Badirou I, Motto DG, Hill G, Bruneval P, Diehl JL, Denis CV, Baruch D. von Willebrand factor is a major determinant of ADAMTS-13 decrease during mouse sepsis induced by cecum ligation and puncture. *J Thromb Haemost*. 2009;7:843–850. doi: 10.1111/j.1538-7836.2009.03313.x.
6. Petri B, Broermann A, Li H, Khandoga AG, Zarbock A, Krombach F, Goerge T, Schneider SW, Jones C, Nieswandt B, Wild MK, Vestweber D. von Willebrand factor promotes leukocyte extravasation. *Blood*. 2010;116:4712–4719. doi: 10.1182/blood-2010-03-276311.
7. Hillgruber C, Steingräber AK, Pöppelmann B, Denis CV, Ware J, Vestweber D, Nieswandt B, Schneider SW, Goerge T. Blocking von Willebrand factor for treatment of cutaneous inflammation. *J Invest Dermatol*. 2014;134:77–86. doi: 10.1038/jid.2013.292.
8. Adam F, Casari C, Prévost N, Kauskot A, Loubière C, Legendre P, Repérant C, Baruch D, Rosa JP, Bryckaert M, de Groot PG, Christophe OD, Lenting PJ, Denis CV. A genetically-engineered von Willebrand disease type 2B mouse model displays defects in hemostasis and inflammation. *Sci Rep*. 2016;6:26306. doi: 10.1038/srep26306.

Plasmin Cleaves Von Willebrand Factor at K1491-R1492 in the A1–A2 Linker Region in a Shear- and Glycan-Dependent Manner In Vitro

Teresa M. Brophy, Soracha E. Ward, Thomas R. McGimsey, Sonja Schneppenheim, Clive Drakeford, Jamie M. O'Sullivan, Alain Chion, Ulrich Budde, James S. O'Donnell

Objective—Previous studies have demonstrated a role for plasmin in regulating plasma von Willebrand factor (VWF) multimer composition. Moreover, emerging data have shown that plasmin-induced cleavage of VWF is of particular importance in specific pathological states. Interestingly, plasmin has been successfully used as an alternative to ADAMTS13 (a disintegrin and metalloproteinase with thrombospondin type 1 motif) in a mouse model of thrombotic thrombocytopenic purpura. Consequently, elucidating the molecular mechanisms through which plasmin binds and cleaves VWF is not only of basic scientific interest but also of direct clinical importance. Our aim was to investigate factors that modulate the susceptibility of human VWF to proteolysis by plasmin.

Approach and Results—We have adapted the VWF vortex proteolysis assay to allow for time-dependent shear exposure studies. We show that globular VWF is resistant to plasmin cleavage under static conditions, but is readily cleaved by plasmin under shear. Although both plasmin and ADAMTS13 cleave VWF in a shear-dependent manner, plasmin does not cleave at the Tyr1605-Met1606 ADAMTS13 proteolytic site in the A2 domain. Rather under shear stress conditions, or in the presence of denaturants, such as urea or ristocetin, plasmin cleaves the K1491-R1492 peptide bond within the VWF A1–A2 linker region. Finally, we demonstrate that VWF susceptibility to plasmin proteolysis at K1491-R1492 is modulated by local N-linked glycan expression within A1A2A3, and specifically inhibited by heparin binding to the A1 domain.

Conclusions—Improved understanding of the plasmin–VWF interaction offers exciting opportunities to develop novel adjunctive therapies for the treatment of refractory thrombotic thrombocytopenic purpura.

(*Arterioscler Thromb Vasc Biol*. 2017;37:845-855. DOI: 10.1161/ATVBAHA.116.308524.)

Key Words: glycosylation ■ heparin ■ plasmin ■ shear ■ von Willebrand factor

Von Willebrand factor (VWF) is a large plasma sialoglycoprotein that plays a critical role in primary hemostasis by mediating platelet adherence to exposed subendothelial collagen at sites of vascular injury.[1] In addition, VWF also acts as a carrier for procoagulant FVIII, protecting it against premature proteolytic degradation and clearance.[2] VWF is synthesized in endothelial cells and megakaryocytes initially as a monomer composed of a series of repeating domains (D′-D3-A1-A2-A3-D4-C1-C2-C3-C4-C5-C6-CK).[3] VWF monomers are assembled into dimers through the formation of C-terminal disulfide bonds in the endoplasmic reticulum.[4] Subsequently in the Golgi, a further round of N-terminal disulfide bond formation converts VWF dimers into longer multimeric structures.[5,6] Multimeric forms of up to 100- or 200-mers may be present in the circulation.[7] Multimeric composition is a critical determinant of VWF functional activity as high molecular weight (HMW) VWF multimers bind to both collagen and platelets with significantly increased affinities and are thus more efficient in inducing platelet aggregation.[1,8]

In normal plasma, pathological accumulation of HMW VWF multimers is prevented by proteolysis of multimers with the plasma metalloprotease, ADAMTS13 (a disintegrin and metalloproteinase with thrombospondin type-1 repeats), which cleaves a single peptide bond (Tyr1605-Met1606) within the A2 domain of VWF.[9,10] Inherited or acquired ADAMTS13 deficiency results in the accumulation of ultralarge VWF (UL-VWF) multimers in plasma.[11,12] These UL-VWF can trigger the formation of pathological platelet aggregates, which obstruct the microvasculature, thereby causing thrombotic thrombocytopenia purpura (TTP).[13,14] Congenital TTP has been associated with a series of different ADAMTS13 gene mutations.[11,15] Interestingly, although inherited TTP often presents during infancy, significant variability in both age of onset and disease severity have been reported.[16,17] Furthermore,

Received on: September 28, 2016; final version accepted on: February 23, 2017.

From the Haemostasis Research Group, Institute of Molecular Medicine, Trinity Centre for Health Sciences, St. James's Hospital, Trinity College Dublin, Ireland (T.M.B., S.E.W., T.R.M.G., C.D., J.M.O., A.C., J.S.O.); Medilys Laborgesellschaft mbH, Department of Hämostaseology, Hamburg, Germany (S.S., U.B.); National Centre for Hereditary Coagulation Disorders, St. James's Hospital, Dublin, Ireland (J.S.O.); and Irish Centre for Vascular Biology, Royal College of Surgeons in Ireland, Dublin (J.S.O.).

The online-only Data Supplement is available with this article at http://atvb.ahajournals.org/lookup/suppl/doi:10.1161/ATVBAHA.116.308524/-/DC1.

Correspondence to James O'Donnell, MB, PhD, Irish Centre for Vascular Biology, Royal College of Surgeons in Ireland, 123 St. Stephen's Green, Dublin 2, Ireland. E-mail jamesodonnell@rcsi.ie

Nonstandard Abbreviations and Acronyms	
ADAMTS13	a disintegrin and metalloproteinase with thrombospondin type 1 motif
HMW	high molecular weight
TTP	thrombotic thrombocytopenic purpura
VWF	von Willebrand factor
WT	wild type

ADAMTS13 deficiency and circulating UL-VWF multimers can be observed in patients with inherited ADAMTS13 deficiency during the periods of clinical remission.[14,18] Finally, complete deficiency of ADAMTS13 in transgenic mice models was not of itself sufficient to cause a TTP phenotype.[19,20] Collectively, these findings suggest that the loss of ADAMTS13 may be necessary but not sufficient to induce clinical TTP, and support the hypothesis that additional factors beyond ADAMTS13 may contribute to TTP pathogenesis in vivo.[14,21]

Interestingly, Tersteeg et al[22] recently showed that significant activation of plasminogen to plasmin constitutes a common feature in patients during acute episodes of TTP. This observation is important because plasmin has previously been shown to proteolyze ADAMTS13.[23] However, in vitro and in vivo studies have confirmed that plasmin can also successfully degrade UL-VWF platelet aggregates.[22,24] On the basis of these data, a possible role for plasmin as a novel therapy for patients with refractory TTP was proposed.[22] In addition, Herbig and Diamond[25] have further demonstrated that abnormal VWF fibers formed under pathological flow conditions are resistant to ADAMTS13 proteolysis, but remain susceptible to cleavage by plasmin. All together, these emerging data suggest that plasmin-induced cleavage of VWF may be of both physiological and pharmacological significance. Critically, however, the molecular mechanisms underlying VWF proteolysis by plasmin remain poorly understood.

Previous studies have demonstrated that shear may enhance proteolysis of VWF by plasmin, as well as several other plasma proteases.[22,24] In this study, we directly compared VWF proteolysis under static or shear conditions in the same assay and demonstrate that plasmin-mediated proteolysis of VWF is shear dependent. In addition, plasmin-mediated proteolysis of recombinant VWF truncated proteins was performed to localize a critical plasmin cleavage site to K1491-R1492 within the linker region between the A1 and A2 domains of VWF. Finally, we demonstrate that VWF susceptibility to plasmin proteolysis at K1491-R1492 is modulated by local N-linked glycan expression within A1A2A3 and is specifically inhibited by heparin binding to the A1 domain.

Materials and Methods

Materials and Methods are available in the online-only Data Supplement.

Results

pd-VWF Is Cleaved by Plasmin in a Shear-Dependent Manner

Recent studies have suggested that shear may influence the susceptibility of VWF to proteolysis by plasmin.[22,24] To investigate this hypothesis, we adapted the vortex-ADAMTS13 cleavage assay as previously described by the Long Zheng laboratory.[26,27] After incubation of pd-VWF with purified plasmin under static conditions for 5 minutes, no significant VWF proteolysis was observed (Figure 1A; Figure I in the online-only Data Supplement). In contrast, however, in the presence of vortex shear, a significant and time-dependent reduction in HMW multimers was apparent (0 minutes versus 5 minutes; P=0.005; Figure 1A and 1B; Figure I in the online-only Data Supplement). Moreover, a corresponding increase in low molecular weight multimers was also observed (0 minutes versus 5 minutes; P<0.0001). As the VWF preparation used was plasma-derived, and other plasma proteases can cleave VWF,[28,29] the vortex VWF proteolysis experiment was repeated in the absence of added plasmin. In the absence of plasmin, no significant reduction in HMW was observed despite 5 minutes vortex (0 minutes versus 5 minutes, P=0.64; Figure 1B). Furthermore, shear-related cleavage of VWF in this vortex assay was completely ablated in the presence of the known plasmin inhibitors aprotinin (0.5 μmol/L; P<0.0001) or ε-aminocaproic acid (50 mmol/L; P=0.006), respectively (Figure 1C). To determine whether the shear-induced ADAMTS13 cleavage site within the A2 domain of VWF is also cleaved by plasmin, immunoblotting was performed after vortexing using an antibody that specifically recognizes the ADAMTS13 140kDa N-terminal A2-cleavage product.[30] Following pd-VWF exposure to ADAMTS13 under shear, we observed a progressive increase in this cleavage product (Figure 1D). In contrast, however, in the presence of plasmin, no such cleavage band was seen despite the progressive loss in HMW multimers (Figure 1D). All together, these findings demonstrate that plasmin cleaves VWF in a shear-dependent manner. Moreover, although ADAMTS13 also cleaves VWF in a shear-dependent fashion, the plasmin-cleavage site(s) in VWF is distinct to that of ADAMTS13.

VWF Conformation Modulates Susceptibility to Plasmin Proteolysis

To further investigate how VWF conformation influences susceptibility to plasmin proteolysis, we studied VWF cleavage in the presence of the denaturant urea. Under static conditions, full-length VWF proteolysis by plasmin was significantly enhanced in the presence of increasing concentrations of urea (low molecular weight VWF after 120 minutes: 0 versus 1.5 mol/L urea P=0.027; Figure 2A). Ristocetin binding to the A1 domain causes a conformational change that enhances VWF binding to platelet glycoprotein Ibα.[31] Moreover, ristocetin binding also significantly enhances VWF proteolysis by ADAMTS13.[31] Similarly, we observed that plasmin-induced VWF proteolysis was also significantly increased in the presence of ristocetin (low molecular weight VWF after 120 minutes: 0 versus 1.5 mg/mL ristocetin P=0.006; Figure 2B; Figure II in the online-only Data Supplement). Previous studies have demonstrated that globular VWF is resistant to ADAMTS13 cleavage.[32] Similarly, our findings demonstrate that multimeric VWF is also resistant to plasmin proteolysis unless exposed to shear stress or in the presence of unfolding agents.

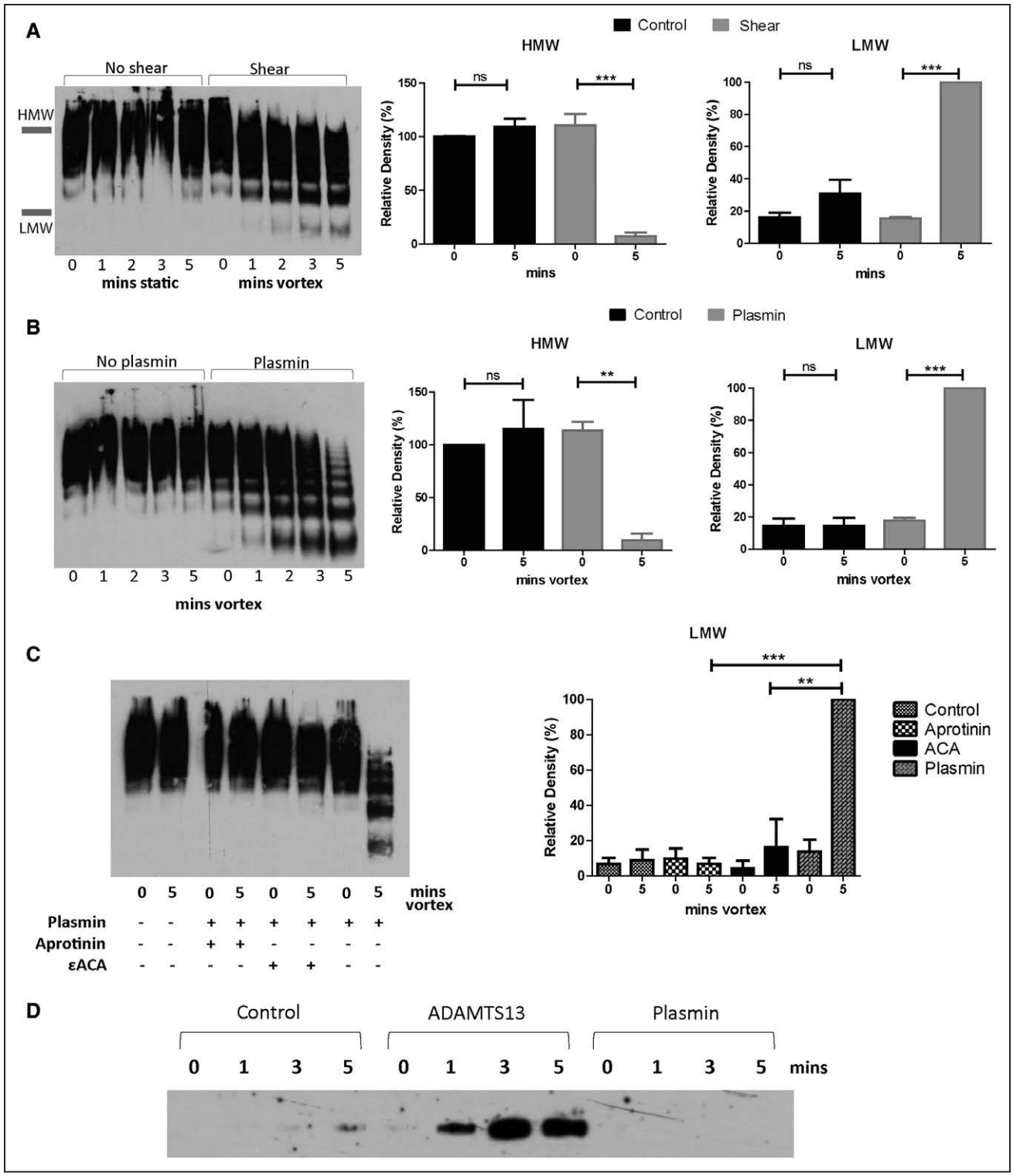

Figure 1. Human von Willebrand factor (VWF) is cleaved by plasmin in a shear-dependent manner. **A**, Purified human VWF (6 μg/mL) was incubated with plasmin (7.7 nmol/L) in the presence or absence of shear (vortexed at 2500 rpm). Samples are collected at 0, 1, 2, 3, and 5 minutes into tubes containing 15 μmol/L aprotinin. VWF proteolysis at each time point was analyzed by sodium dodecyl sulfate-agarose gel electrophoresis, immunoblotting, and densitometry as described in Materials and Methods section of this article. The area examined for densitometric analysis of high molecular weight (HMW) and low molecular weight (LWM) VWF is illustrated here and is applicable to all subsequent experiments. All experiments were performed in triplicate, and results described represent the means±SEM (**P<0.001 and ***P<0.0001 in comparison to control; ns, not significant). **B**, Purified pd-VWF was subjected to vortex-induced shear as before, in the presence or absence of added purified human plasmin (7.7 nmol/L). Samples were collected into aprotinin, and proteolysis assessed as above. **C**, Proteolysis of pd-VWF by plasmin under shear was repeated in the presence or absence of either aprotinin (0.5 μmol/L) or ε-aminocaproic acid (50 mmol/L) **D**, To investigate whether plasmin and ADAMTS13 (a disintegrin and metalloproteinase with thrombospondin type 1 motif) cleave VWF at the same site, pd-VWF was vortexed at 2500 rpm in the presence of either recombinant (*Continued*)

Figure 1. Continued human ADAMTS13 (3 nmol/L) or purified plasmin (7.7 nmol/L). Samples were collected at 0, 1, 3, and 5 minutes into either EDTA (50 mmol/L) for ADAMTS13-proteolysis studies, or aprotinin (15 μmol/L) for plasmin-proteolysis studies. All samples were then reduced with 100 mmol/L DTT (dithiothreitol), and analyzed by immunoblotting with a monoclonal antibody specific for the 140 kDa ADAMTS13-cleaved VWF product. ACA indicates aminocaproic acid.

Plasmin Cleaves VWF Within the A1–A2 Domains

Given the marked effect of ristocetin in enhancing VWF proteolysis by plasmin, we hypothesized that plasmin may cleave within the A1–A2–A3 domain region. To address this hypothesis, we examined plasmin-mediated proteolysis of recombinant VWF A domain truncated fragments (Figure 3A). In contrast to full-length VWF, recombinant A1A2A3-VWF was proteolyzed by plasmin under static conditions in the absence of any denaturants (Figure 3B). Moreover, this plasmin-mediated cleavage of A1A2A3-VWF was further enhanced in the presence of ristocetin (Figure 3C). Furthermore, although we observed plasmin-induced proteolysis of A1A2-VWF over time (Figure 3D), no significant cleavage of A2A3-VWF was seen (Figure 3D). Cumulatively, these data confirm a critical role for the A1 domain (aa1239–1494) in regulating VWF proteolysis by plasmin.

Plasmin Cleaves A1A2-VWF at K1491-R1492

As the A1A2 cleaved product is His-tagged at the C terminus, N-terminal sequencing of this product was performed to identify the site of proteolytic cleavage. RNSMV (Arg-Asn-Ser-Met-Val) were identified as the first five amino acids of the cleavage fragment. This sequence is only present in one location in human VWF, in the linker region between the A1 and A2 domains (^{1492}RNSMV^{1496}) (Figure 4A), and therefore suggests that plasmin cleaves between K1491 and R1492. Interestingly, both of these residues are highly conserved (Figure 4A). To confirm this putative plasmin cleavage site, K1491 was mutated to alanine in A1A2-VWF. In contrast to the plasmin-mediated proteolysis of wild-type (WT) A1A2, no proteolysis of A1A2-K1491A was observed over time (Figure 4B). Similarly, although WT D′D3A1A2A3-VWF was susceptible to plasmin cleavage, D'D3A1A2A3-K1491A/R1492A was resistant to plasmin proteolysis (Figure 4C).

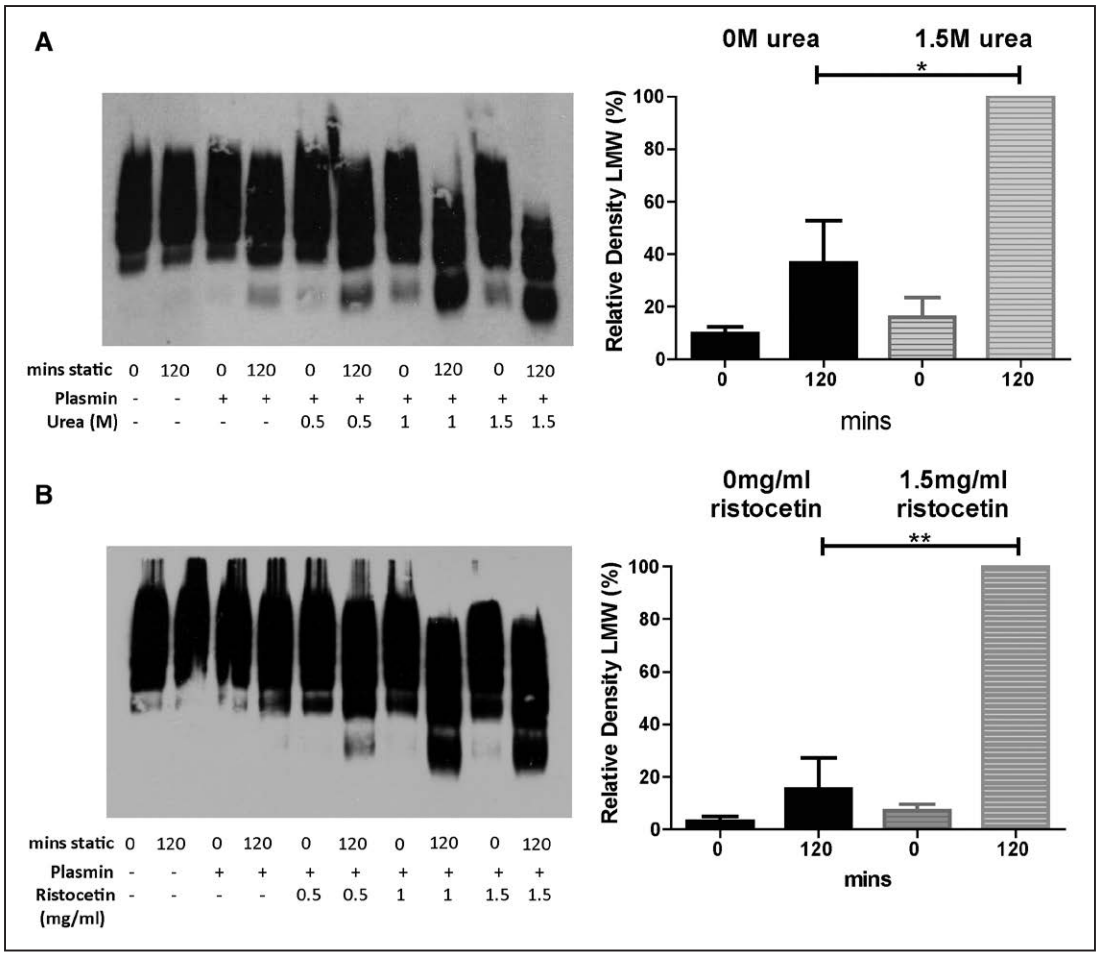

Figure 2. Von Willebrand factor (VWF) conformation modulates susceptibility to plasmin proteolysis. To investigate whether VWF conformation influences susceptibility to plasmin proteolysis, pd-VWF was incubated under static conditions with 7.7-nmol/L human plasmin in the presence of either (**A**) increasing concentrations of urea (0.5–1.5 mol/L) or (**B**) increasing concentrations of ristocetin (0.5–1.5 mg/mL). After incubation, samples were removed into aprotinin and rate of VWF multimer cleavage assessed by immunoblotting and densitometry. All experiments were performed in triplicate, and results described represent the means±SEM (*P<0.05, **P<0.001).

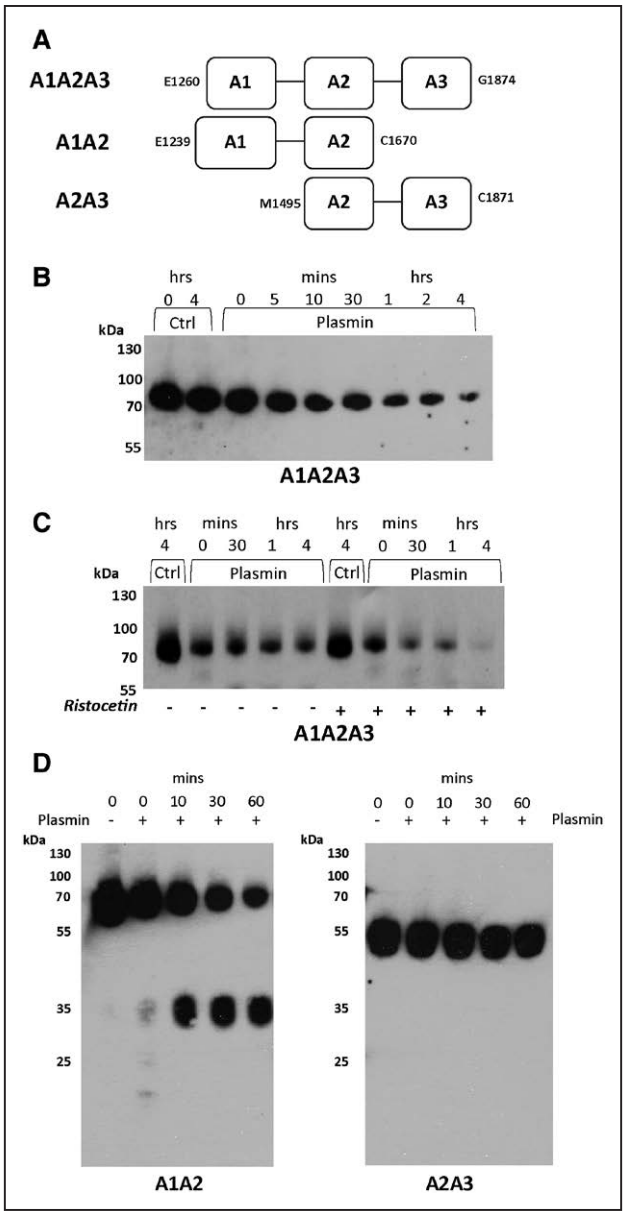

Figure 3. Plasmin cleaves within the A1–A2 domains of human von Willebrand factor (VWF). **A**, To investigate site(s) of plasmin-mediated proteolysis within VWF, a series of truncated VWF domain fragments were expressed and purified from HEK293T cells. **B**, Recombinant human A1A2A3-VWF was incubated with plasmin for up to 4 hours under static conditions. Samples were removed at specified time points for proteolysis analysis by immunoblotting as before. **C**, Recombinant A1A2A3-VWF was incubated with plasmin under static conditions in the absence or presence of ristocetin (1 mg/mL), and proteolysis analyzed on 4% to 12% Bis Tris acrylamide gels with immunoblotting. **D**, Recombinant human A1A2-VWF or A2A3-VWF were incubated with plasmin (12.8 nmol/L) for up to 1 hour. Samples were removed at each time point for analysis on 4% to 12% Bis Tris acrylamide gels with immunoblotting with anti-His horseradish peroxidase. WT indicates wild type.

Collectively, these findings demonstrate that plasmin cleaves VWF at the K1491–R1492 bond in the linker region between the A1 and A2 domains in this shear-sensitive region of VWF.

Heparin Inhibits Plasmin Cleavage of VWF

Several VWF-binding partners significantly enhance VWF susceptibility to ADAMTS13 proteolysis, including FVIII,[33] platelet glycoprotein Ibα,[34] ristocetin,[35] and heparin.[34] Both FVIII and glycoprotein Ibα are proteolyzed by plasmin.[36,37] Consequently, we further investigated whether heparin binding might also promote plasmin proteolysis of full-length VWF. Interestingly, in contrast to the effect of heparin in enhancing VWF proteolysis by ADAMTS13, we observed a significant and concentration-dependent inhibition of plasmin-mediated proteolysis of pd-VWF under shear by heparin (Figure 5A). Similarly, proteolysis of the truncated A1A2-VWF fragment by plasmin under static conditions was also inhibited by heparin (Figure 5B). Tersteeg et al[22] previously postulated that the lysine-rich ^{1405}KKKK^{1408} region in the A1 domain may be important in modulating plasminogen interaction with VWF. Interestingly, previous studies have also reported a heparin-binding role for this region.[38] To elucidate the mechanism underlying the inhibitory effect of heparin on plasmin-mediated VWF proteolysis, we investigated plasminogen binding to A1A2-VWF in the presence of heparin using the same assay as described by Tersteeg et al[22] In keeping with previous studies, immobilized recombinant A1A2-VWF bound to plasminogen in a saturable and concentration-dependent manner (Figure 5C). Moreover, this binding was inhibited by the soluble lysine analog ε-aminocaproic acid (data not shown). In the presence of heparin, binding of WT A1A2-VWF to plasminogen was markedly attenuated (Figure 5C). All together, these findings are consistent with the hypothesis that the lysine-rich ^{1405}KKKK^{1408} region in the A1 domain of VWF plays critical roles in modulating interaction with both heparin and plasmin. Importantly, we further observed that binding of the A1A2-K1491A VWF variant to plasminogen was similar to that of WT A1A2-VWF, despite the loss of the plasmin cleavage site (Figure 5D). This observation confirms that the plasmin(ogen) binding and proteolytic sites on VWF are distinct.

Plasmin Cleaves VWF in a Glycan-Dependent but ABO-Independent Manner

Previous studies from our laboratory and others have demonstrated that VWF glycan determinants play a major role in modulating susceptibility to ADAMTS13 proteolysis.[35,39,40] Given the role of N-linked glycans in modulating A2 domain conformation,[41] we hypothesized that local N-linked glycans within A1A2A3 might also be important in modulating VWF proteolysis by plasmin. Only two N-linked glycans are expressed on A1A2A3-VWF at N1515 and N1574, respectively, within the A2 domain. Specific removal of these 2 N-linked glycans from A1A2A3-VWF by PNGase F digestion resulted in significantly increased susceptibility to plasmin proteolysis (4 hours; WT versus PNGase-treated, P=0.013; Figure 6A).

ABO(H) blood determinants expressed on both the N- and O-linked glycans of human pd-VWF have been shown to modulate the susceptibility of pd-VWF to ADAMTS13 cleavage.[35,42] As ABO(H) determinants are not expressed on recombinant VWF,[43,44] we used blood group–specific pd-VWF to investigate whether ABO also influences plasmin-mediated proteolysis of VWF. Despite the significant effect of ABO blood group in regulating VWF proteolysis by ADAMTS13, no significant difference in plasmin-mediated proteolysis was observed for group AB VWF compared with group O

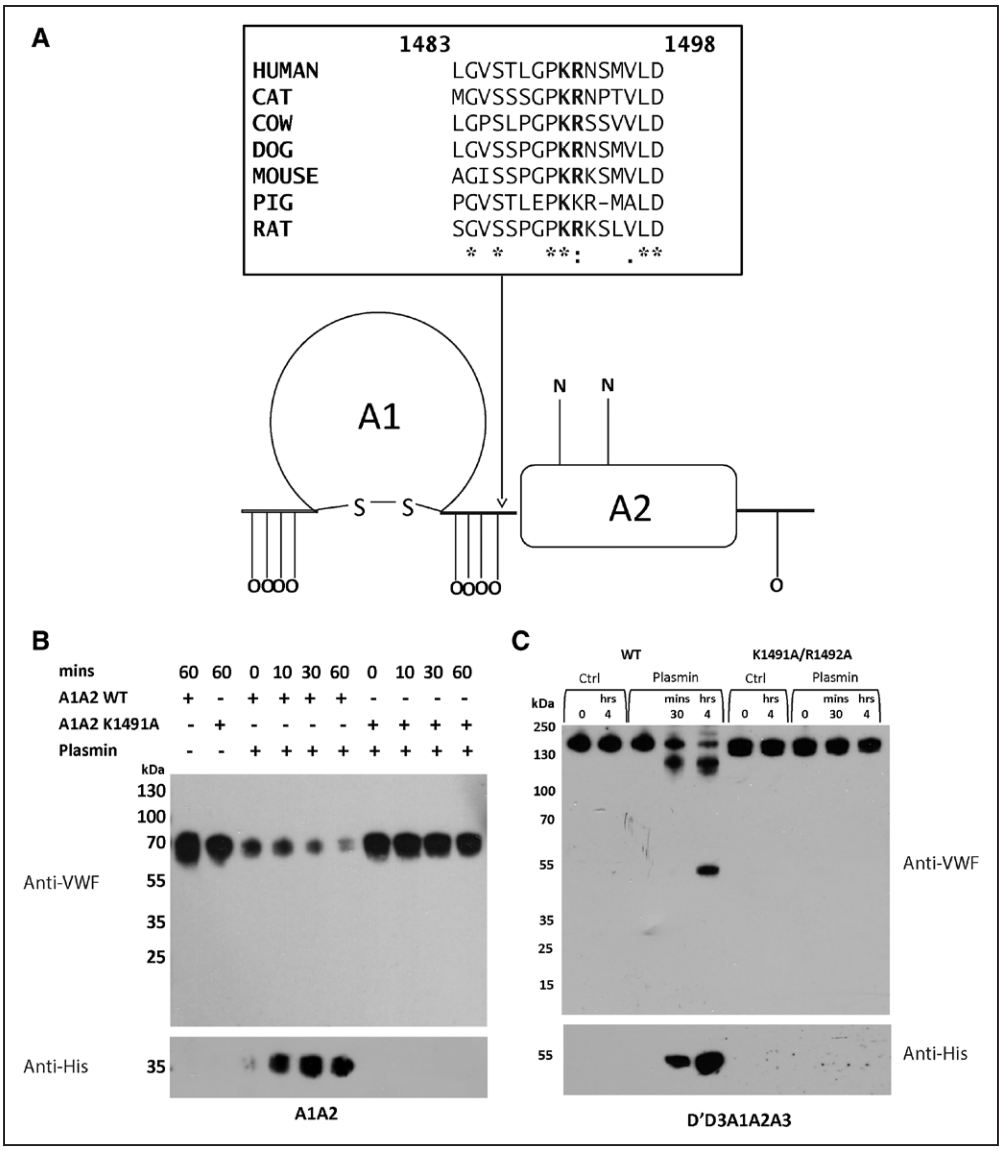

Figure 4. Plasmin cleaves A1A2-von Willebrand factor (VWF) at K1491-R1492. **A**, N-terminal sequencing of the C-terminally His-tagged product of plasmin-cleaved VWF identified RNSMV (Arg-Asn-Ser-Met-Val) as the first five amino acids of this protein band. This corresponds to a C-terminal region of the VWF A1 domain. The amino acid sequences of VWF protein from several species (human, feline, bovine, canine, murine, and porcine) were aligned using the T-Coffee multiple sequence alignment program. **B**, VWF A1A2 or A1A2 K1491A (10 μg/mL) were incubated with plasmin for up to 1 hour. Samples were removed at each time point and proteolysis analyzed by immunoblotting with anti-VWF horseradish peroxidase (HRP) or anti-His HRP. **C**, VWF D′A3 or D′A3 K1491A/R1492A (10 μg/mL) were incubated with plasmin for up to 4 hours. Samples were removed at each time point for analysis on 4% to 12% Bis Tris acrylamide gels with immunoblotting with anti-VWF HRP or anti-His HRP.

VWF (HMW 5 minutes AB versus O, P=0.1979; Figure 6C). Nevertheless, taken together, these data demonstrate that N- and O-glycans expressed within the A1A2A3 domains of VWF play important roles in modulating proteolysis by both plasmin and ADAMTS13.

Discussion

VWF multimer composition is a critical determinant of its hemostatic function.[1] The biological importance of regulating plasma VWF multimer distribution is illustrated by the fact that pathological accumulation of abnormal UL-VWF multimers is associated with thrombotic microangiopathy in TTP.[45,46] Conversely, in patients with type 2A von Willebrand disease, increased proteolysis results in loss of normal HMW VWF multimers, and confers a significant bleeding phenotype.[47] Under steady-state conditions, VWF multimer distribution in normal plasma is primarily regulated by ADAMTS13-mediated proteolysis. Nevertheless, other proteases can also cleave multimeric VWF in vitro.[21] Moreover, accumulating recent evidence suggests that these proteases may have roles in regulating VWF multimer composition in vivo under specific conditions.[22,48–52] For example, in a murine model of TTP, plasmin could regulate VWF multimer distribution in the absence of ADAMTS13.[22] Several other pathological conditions have also been associated with significant reductions in plasma ADAMTS13 levels, including acute

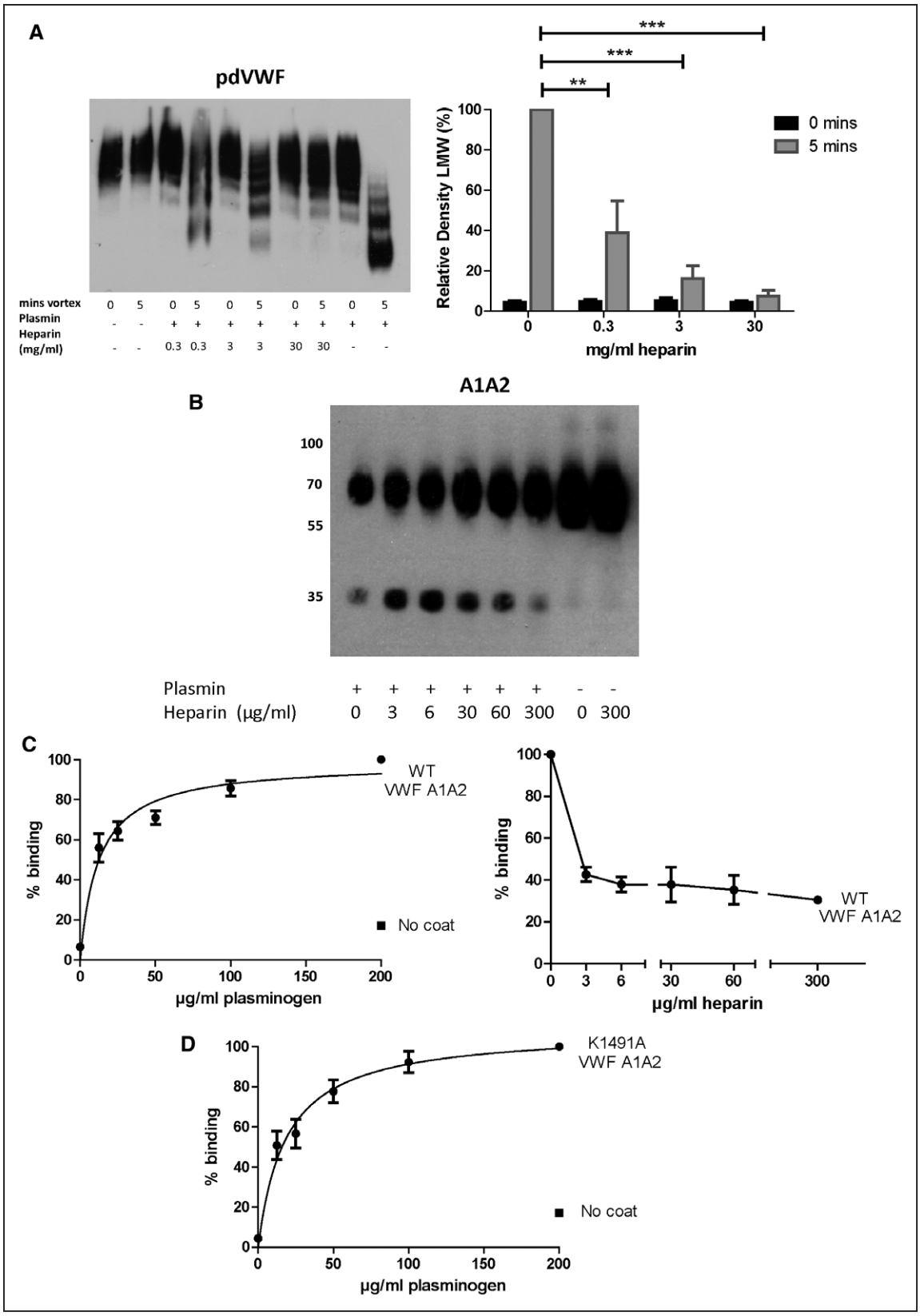

Figure 5. Heparin inhibits plasmin cleavage of von Willebrand factor (VWF). **A**, Full-length pd-VWF was vortexed at 2500 rpm in the absence or presence of plasmin or heparin (0.3–30 mg/mL). Samples are removed at 0 and 5 minutes for analysis on 1.8% sodium dodecyl sulfate-agarose gels with immunoblotting and densitometry. **B**, Recombinant A1A2-VWF (10 μg/mL) was incubated with plasmin in the presence of heparin (0–300 μg/mL) for 1 hour. Samples were removed at 1 hour for proteolysis analysis. **C**, Plate-binding of plasminogen (25–200 μg/mL) to immobilized recombinant human wild-type (WT) A1A2-VWF was detected by anti-plasminogen horseradish peroxidase (HRP). Binding experiments were repeated in the presence or absence of added heparin (0–300μg/mL). **D**, Binding of plasminogen (25–200μg/mL) to immobilized A1A2-K1491A (5 μg/mL) was detected by anti-plasminogen HRP as before.

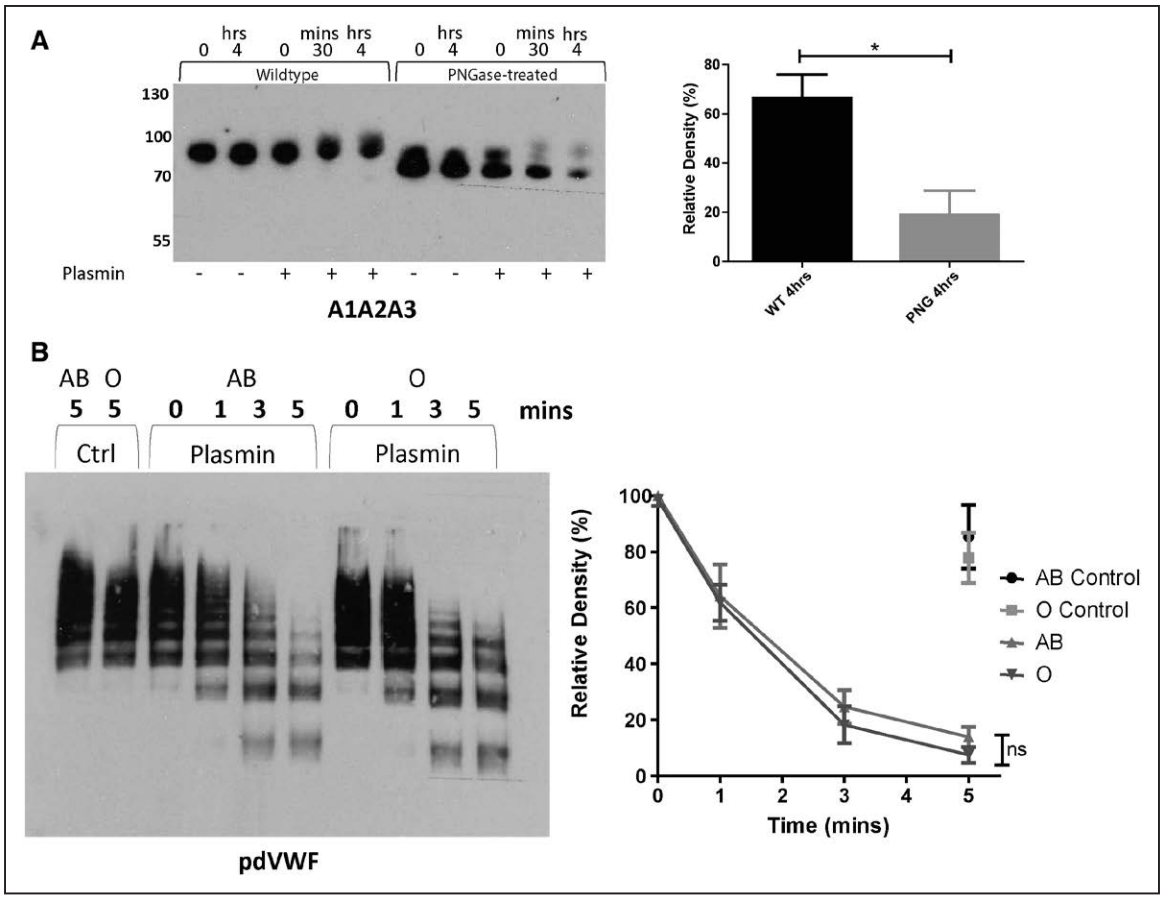

Figure 6. Plasmin cleaves von Willebrand factor (VWF) in a glycan-dependent but ABO-independent manner. **A**, N-linked glycans were removed from A1A2A3-VWF by digestion with PNGase F. Wild-type and PNGase F-treated A1A2A3-VWF (10 μg/mL) were then incubated with plasmin for up to 4 hours. Samples were removed at each time point for analysis on 4% to 12% Bis Tris acrylamide gels with immunoblotting. Samples were removed into aprotinin at each time point for analysis on 4% to 12% Bis Tris acrylamide gels with immunoblotting. **B**, Human pd-VWF was purified from pooled blood group AB or blood group O normal donors. The AB- and O-VWF preparations were then vortexed at 2500 rpm in the absence or presence of plasmin (7.7 nmol/L). Samples were removed at 0, 1, 3, and 5 minutes for analysis on 1.8% sodium dodecyl sulfate-agarose gels with immunoblotting. The loss of high molecular weight multimers over time was determined by densitometry.

liver injury,[48] cerebral malaria,[53] sickle cell disease,[54] and Dengue.[51] Importantly, however, despite low or even undetectable ADAMTS13 activity levels, UL-VWF multimers are not observed in many individuals with these conditions.[49] The absence of UL-VWF in these different patient cohorts is likely to be attributable to different molecular mechanisms, including consumption in platelet-rich microthrombi. Nevertheless, recent reports[21,22,48–52] have also postulated that VWF proteolysis through ADAMTS-13 independent pathways may be important in this context.

In the normal circulation, VWF adopts a globular conformation.[55] Shear stress triggers unwinding of globular VWF and conformational changes within the A domains,[32] exposing the glycoprotein Ibα–binding site in the A1 domain and the ADAMTS13 cleavage site in the A2 domain.[56,57] In this study, we directly compare plasmin-mediated proteolysis of VWF under both static and shear conditions in a controlled environment and show that human pd-VWF is relatively resistant to proteolysis by 7.7 nmol/L plasmin under static conditions. Previous studies reporting proteolysis of VWF by plasmin under static conditions have used significantly higher plasmin concentrations.[24,58] In contrast, however, our data show that HMW VWF is rapidly cleaved by 7.7 nmol/L plasmin under exposure to shear stress, which would parallel conditions present in stenosed arteries in vivo. Local plasmin concentrations of ≈10 nmol/L at sites of vascular injury, and >100 nmol/L after systemic thrombolytic therapy, have been estimated.[24,59] Although both plasmin and ADAMTS13 cleave VWF in a shear-dependent manner, our findings demonstrate that plasmin does not cleave VWF at the ADAMTS13 site (Tyr 1605-Met 1606 in A2).

Using a series of recombinant VWF truncated proteins, we have localized a plasmin cleavage site in VWF. Plasmin specifically cleaves VWF at the K1491-R1492 peptide bond that is located in the A1–A2 linker region. The lysine-rich ^{1405}KKKK^{1408} region in the VWF A1 domain was recently postulated to play a role in mediating interaction with plasmin.[22] Moreover, this region is important in modulating heparin binding to VWF.[38] Heparin has been reported to significantly enhance VWF proteolysis by ADAMTS13.[34] In contrast, our novel data demonstrate that heparin binding to the A1 domain of VWF attenuates plasmin-mediated VWF proteolysis in a dose-dependent manner. In binding studies, we confirmed that plasminogen binding to A1A2-VWF was significantly reduced in

the presence of heparin. Importantly, however, we observed that, despite site-directed mutagenesis of the plasmin cleavage site, A1A2-K1491A VWF binding to plasminogen was not reduced indicating that the plasmin(ogen)-binding site and the plasmin proteolysis sites within VWF are distinct. Therefore, our data show that under shear stress conditions, conformational changes in A1A2 facilitate plasmin binding to lysine-rich regions in the VWF A1 domain, and subsequently enable specific plasmin cleavage at the K1491–R1492 peptide bond within the VWF A1–A2 linker region. This pattern of distinct binding and cleavage sites as well as shear-enhanced and conformation-dependent cleavage has clear similarities to the VWF–ADAMTS13 interaction.[32,60]

To date, no VWF gene mutations involving the K1491-R1492 plasmin cleavage site have been described. However, both type 2A and type 2B von Willebrand disease are characterized by the loss of HMW multimers due, in part, to enhanced proteolysis.[61,62] On the basis of our data on the critical role of A1A2 conformation in regulating susceptibility to plasmin proteolysis, it seems likely that some type 2A and 2B mutations may lead to enhanced proteolysis by plasmin and ADAMTS13. Furthermore, given the importance of shear in regulating plasmin-mediated VWF proteolysis, it is plausible that plasmin cleavage may contribute to the loss of HMW multimers observed in patients in whom pathological local shear stress levels are generated (eg,) acquired von Willebrand disease secondary to aortic stenosis or left ventricular assist devices (LVADs).[63,64] Finally, plasmin-mediated VWF proteolysis after administration of thrombolytic treatment has been described in patients with myocardial infarction[65] and deep vein thrombosis,[61] and thus may be a contributing factor in the clinical bleeding risk associated with systemic thrombolysis.

In previous studies, we and others have shown an important role for VWF glycans in modulating VWF cleavage by ADAMTS13[39,40,42,66,67] and by plasmin.[29] Similarly, our novel findings demonstrate that VWF glycans also determine susceptibility to plasmin proteolysis, but in addition identify some important differences in the effects of VWF glycans in regulating proteolysis by plasmin compared with ADAMTS13. First, although the loss of terminal α2 to 6 linked sialic acid from human VWF significantly inhibits ADAMTS13 proteolysis,[66] desialylation actually enhances proteolysis by plasmin.[68] Second, N-linked glycans expressed at N1515 and N1574 within the A2 domain protect VWF against proteolysis by both plasmin and ADAMTS13.[67,69] Finally, ABO(H) blood group determinants modulate VWF susceptibility to proteolysis by ADAMTS13 (O≥B>A≥AB)[35] but do not influence plasmin-mediated cleavage. We hypothesize that VWF glycan determinants modulate interactions with both plasmin and ADAMTS13 by modifying protein conformation. Consequently, removal of specific glycans in the A1A2A3 domains result in conformations that are more permissive for either plasmin or ADAMTS13 cleavage. Further studies are necessary to define the molecular mechanism(s) through which glycans within the A domains of VWF regulate plasmin-mediated proteolysis. Nevertheless, these findings are of clinical relevance in that significant quantitative and qualitative variations in VWF glycan expression have been previously been reported in both the normal population[70,71] and in patients with different disease states.[72,73]

In conclusion, accumulating recent data have demonstrated that in addition to ADAMTS13, plasmin may also play an important role in regulating plasma VWF multimer distribution, particularly under specific pathological conditions that present with the accumulation of HMW VWF multimers.[22,48,50,51,54] Consequently, elucidating the molecular mechanisms through which plasmin binds and cleaves multimeric VWF is not only of basic scientific interest but also of direct translational importance. Improved understanding of the plasmin–VWF interaction may offer exciting opportunities to develop novel adjunctive therapies for the treatment of refractory TTP, which continues to be associated with significant morbidity and mortality. In addition, using thrombolytic therapy to lyse VWF-dependent platelet aggregates in sites of high shear stress may also be useful, particularly in pathological conditions where UL-VWF is resistant to ADAMTS13 proteolysis.[25,53]

Acknowledgments

This work was supported by a Science Foundation Ireland Principal Investigator Award (11/PI/1066; J.S. O'Donnell). J.S. O'Donnell has also received research grant funding awards from Baxter, Bayer, Pfizer and Novo Nordisk.

Disclosures

J.S. O'Donnell has served on the speaker's bureau for Baxter, Bayer, Novo Nordisk, Boehringer Ingelheim, Leo Pharma, and Octapharma. He has also served on the advisory boards of Baxter, Bayer, Octapharma CSL Behring, Daiichi Sankyo, Boehringer Ingelheim, and Pfizer. The other authors report no conflicts.

References

1. Lenting PJ, Christophe OD, Denis CV. von Willebrand factor biosynthesis, secretion, and clearance: connecting the far ends. *Blood*. 2015;125:2019–2028. doi: 10.1182/blood-2014-06-528406.
2. Terraube V, O'Donnell JS, Jenkins PV. Factor VIII and von Willebrand factor interaction: biological, clinical and therapeutic importance. *Haemophilia*. 2010;16:3–13. doi: 10.1111/j.1365-2516.2009.02005.x.
3. Zhou YF, Eng ET, Zhu J, Lu C, Walz T, Springer TA. Sequence and structure relationships within von Willebrand factor. *Blood*. 2012;120:449–458. doi: 10.1182/blood-2012-01-405134.
4. Kaufman RJ. Post-translational modifications required for coagulation factor secretion and function. *Thromb Haemost*. 1998;79:1068–1079.
5. Wagner DD, Mayadas T, Marder VJ. Initial glycosylation and acidic pH in the Golgi apparatus are required for multimerization of von Willebrand factor. *J Cell Biol*. 1986;102:1320–1324.
6. Springer TA. Biology and physics of von Willebrand factor concatamers. *J Thromb Haemost*. 2011;9 (Suppl 1):130–143. doi: 10.1111/j.1538-7836.2011.04320.x.
7. Schneider SW, Nuschele S, Wixforth A, Gorzelanny C, Alexander-Katz A, Netz RR, Schneider MF. Shear-induced unfolding triggers adhesion of von Willebrand factor fibers. *Proc Natl Acad Sci U S A*. 2007;104:7899–7903. doi: 10.1073/pnas.0608422104.
8. Arya M, Anvari B, Romo GM, Cruz MA, Dong JF, McIntire LV, Moake JL, López JA. Ultralarge multimers of von Willebrand factor form spontaneous high-strength bonds with the platelet glycoprotein Ib-IX complex: studies using optical tweezers. *Blood*. 2002;99:3971–3977. doi: 10.1182/blood-2001-11-0060.
9. Levy GG, Nichols WC, Lian EC, et al. Mutations in a member of the ADAMTS gene family cause thrombotic thrombocytopenic purpura. *Nature*. 2001;413:488–494. doi: 10.1038/35097008.
10. Zheng X, Chung D, Takayama TK, Majerus EM, Sadler JE, Fujikawa K. Structure of von Willebrand factor-cleaving protease (ADAMTS13), a metalloprotease involved in thrombotic thrombocytopenic purpura. *J Biol Chem*. 2001;276:41059–41063. doi: 10.1074/jbc.C100515200.

11. Zheng XL. ADAMTS13 and von Willebrand factor in thrombotic thrombocytopenic purpura. *Annu Rev Med*. 2015;66:211–225. doi: 10.1146/annurev-med-061813-013241.
12. Moake JL, Rudy CK, Troll JH, Weinstein MJ, Colannino NM, Azocar J, Seder RH, Hong SL, Deykin D. Unusually large plasma factor VIII:von Willebrand factor multimers in chronic relapsing thrombotic thrombocytopenic purpura. *N Engl J Med*. 1982;307:1432–1435. doi: 10.1056/NEJM198212023072306.
13. Sadler JE. Von Willebrand factor, ADAMTS13, and thrombotic thrombocytopenic purpura. *Blood*. 2008;112:11–18. doi: 10.1182/blood-2008-02-078170.
14. Desch KC, Motto DG. Thrombotic thrombocytopenic purpura in humans and mice. *Arterioscler Thromb Vasc Biol*. 2007;27:1901–1908. doi: 10.1161/ATVBAHA.107.145797.
15. Levy GG, Motto DG, Ginsburg D. ADAMTS13 turns 3. *Blood*. 2005;106:11–17. doi: 10.1182/blood-2004-10-4097.
16. Furlan M, Lämmle B. Aetiology and pathogenesis of thrombotic thrombocytopenic purpura and haemolytic uraemic syndrome: the role of von Willebrand factor-cleaving protease. *Best Pract Res Clin Haematol*. 2001;14:437–454. doi: 10.1053/beha.2001.0142.
17. Veyradier A, Lavergne JM, Ribba AS, Obert B, Loirat C, Meyer D, Girma JP. Ten candidate ADAMTS13 mutations in six French families with congenital thrombotic thrombocytopenic purpura (Upshaw-Schulman syndrome). *J Thromb Haemost*. 2004;2:424–429.
18. DE Meyer SF, Budde U, Deckmyn H, Vanhoorelbeke K. *In vivo* von Willebrand factor size heterogeneity in spite of the clinical deficiency of ADAMTS-13. *J Thromb Haemost*. 2011;9:2506–2508. doi: 10.1111/j.1538-7836.2011.04519.x.
19. Motto DG, Chauhan AK, Zhu G, Homeister J, Lamb CB, Desch KC, Zhang W, Tsai HM, Wagner DD, Ginsburg D. Shigatoxin triggers thrombotic thrombocytopenic purpura in genetically susceptible ADAMTS13-deficient mice. *J Clin Invest*. 2005;115:2752–2761. doi: 10.1172/JCI26007.
20. Banno F, Kokame K, Okuda T, Honda S, Miyata S, Kato H, Tomiyama Y, Miyata T. Complete deficiency in ADAMTS13 is prothrombotic, but it alone is not sufficient to cause thrombotic thrombocytopenic purpura. *Blood*. 2006;107:3161–3166. doi: 10.1182/blood-2005-07-2765.
21. Tersteeg C, Fijnheer R, Pasterkamp G, de Groot PG, Vanhoorelbeke K, de Maat S, Maas C. Keeping von Willebrand Factor under Control: Alternatives for ADAMTS13. *Semin Thromb Hemost*. 2016;42:9–17. doi: 10.1055/s-0035-1564838.
22. Tersteeg C, de Maat S, De Meyer SF, Smeets MW, Barendrecht AD, Roest M, Pasterkamp G, Fijnheer R, Vanhoorelbeke K, de Groot PG, Maas C. Plasmin cleavage of von Willebrand factor as an emergency bypass for ADAMTS13 deficiency in thrombotic microangiopathy. *Circulation*. 2014;129:1320–1331. doi: 10.1161/CIRCULATIONAHA.113.006727.
23. Crawley JT, Lam JK, Rance JB, Mollica LR, O'Donnell JS, Lane DA. Proteolytic inactivation of ADAMTS13 by thrombin and plasmin. *Blood*. 2005;105:1085–1093. doi: 10.1182/blood-2004-03-1101.
24. Wohner N, Kovács A, Machovich R, Kolev K. Modulation of the von Willebrand factor-dependent platelet adhesion through alternative proteolytic pathways. *Thromb Res*. 2012;129:e41–e46. doi: 10.1016/j.thromres.2011.11.021.
25. Herbig BA, Diamond SL. Pathological von Willebrand factor fibers resist tissue plasminogen activator and ADAMTS13 while promoting the contact pathway and shear-induced platelet activation. *J Thromb Haemost*. 2015;13:1699–1708. doi: 10.1111/jth.13044.
26. Han Y, Xiao J, Falls E, Zheng XL. A shear-based assay for assessing plasma ADAMTS13 activity and inhibitors in patients with thrombotic thrombocytopenic purpura. *Transfusion*. 2011;51:1580–1591. doi: 10.1111/j.1537-2995.2010.03020.x.
27. Zhang P, Pan W, Rux AH, Sachais BS, Zheng XL. The cooperative activity between the carboxyl-terminal TSP1 repeats and the CUB domains of ADAMTS13 is crucial for recognition of von Willebrand factor under flow. *Blood*. 2007;110:1887–1894. doi: 10.1182/blood-2007-04-083329.
28. Federici AB, Berkowitz SD, Lattuada A, Mannucci PM. Degradation of von Willebrand factor in patients with acquired clinical conditions in which there is heightened proteolysis. *Blood*. 1993;81:720–725.
29. Federici AB, Elder JH, De Marco L, Ruggeri ZM, Zimmerman TS. Carbohydrate moiety of von Willebrand factor is not necessary for maintaining multimeric structure and ristocetin cofactor activity but protects from proteolytic degradation. *J Clin Invest*. 1984;74:2049–2055. doi: 10.1172/JCI111628.
30. Zhou M, Dong X, Baldauf C, Chen H, Zhou Y, Springer TA, Luo X, Zhong C, Gräter F, Ding J. A novel calcium-binding site of von Willebrand factor A2 domain regulates its cleavage by ADAMTS13. *Blood*. 2011;117:4623–4631. doi: 10.1182/blood-2010-11-321596.
31. Chen J, Ling M, Fu X, López JA, Chung DW. Simultaneous exposure of sites in von Willebrand factor for glycoprotein Ib binding and ADAMTS13 cleavage: studies with ristocetin. *Arterioscler Thromb Vasc Biol*. 2012;32:2625–2630. doi: 10.1161/ATVBAHA.112.254144.
32. Crawley JT, de Groot R, Xiang Y, Luken BM, Lane DA. Unraveling the scissile bond: how ADAMTS13 recognizes and cleaves von Willebrand factor. *Blood*. 2011;118:3212–3221. doi: 10.1182/blood-2011-02-306597.
33. Cao W, Krishnaswamy S, Camire RM, Lenting PJ, Zheng XL. Factor VIII accelerates proteolytic cleavage of von Willebrand factor by ADAMTS13. *Proc Natl Acad Sci U S A*. 2008;105:7416–7421. doi: 10.1073/pnas.0801735105.
34. Nishio K, Anderson PJ, Zheng XL, Sadler JE. Binding of platelet glycoprotein Ibalpha to von Willebrand factor domain A1 stimulates the cleavage of the adjacent domain A2 by ADAMTS13. *Proc Natl Acad Sci U S A*. 2004;101:10578–10583. doi: 10.1073/pnas.0402041101.
35. Bowen DJ. An influence of ABO blood group on the rate of proteolysis of von Willebrand factor by ADAMTS13. *J Thromb Haemost*. 2003;1:33–40.
36. Nishiya K, Nogami K, Okada K, Matsuo O, Takeyama M, Ogiwara K, Shima M. Determination of a factor VIII-interactive region within plasmin responsible for plasmin-catalysed activation and inactivation of factor VIII(a). *Thromb Haemost*. 2010;104:105–117. doi: 10.1160/TH09-10-0715.
37. Adelman B, Michelson AD, Greenberg J, Handin RI. Proteolysis of platelet glycoprotein Ib by plasmin is facilitated by plasmin lysine-binding regions. *Blood*. 1986;68:1280–1284.
38. Rastegar-Lari G, Villoutreix BO, Ribba AS, Legendre P, Meyer D, Baruch D. Two clusters of charged residues located in the electropositive face of the von Willebrand factor A1 domain are essential for heparin binding. *Biochemistry*. 2002;41:6668–6678.
39. McGrath RT, McRae E, Smith OP, O'Donnell JS. Platelet von Willebrand factor–structure, function and biological importance. *Br J Haematol*. 2010;148:834–843. doi: 10.1111/j.1365-2141.2009.08052.x.
40. McGrath RT, van den Biggelaar M, Byrne B, O'Sullivan JM, Rawley O, O'Kennedy R, Voorberg J, Preston RJ, O'Donnell JS. Altered glycosylation of platelet-derived von Willebrand factor confers resistance to ADAMTS13 proteolysis. *Blood*. 2013;122:4107–4110. doi: 10.1182/blood-2013-04-496851.
41. Lynch CJ, Lane DA. N-linked glycan stabilization of the VWF A2 domain. *Blood*. 2016;127:1711–1718. doi: 10.1182/blood-2015-09-672014.
42. O'Donnell JS, McKinnon TA, Crawley JT, Lane DA, Laffan MA. Bombay phenotype is associated with reduced plasma-VWF levels and an increased susceptibility to ADAMTS13 proteolysis. *Blood*. 2005;106:1988–1991. doi: 10.1182/blood-2005-02-0792.
43. O'Donnell J, Mille-Baker B, Laffan M. Human umbilical vein endothelial cells differ from other endothelial cells in failing to express ABO blood group antigens. *J Vasc Res*. 2000;37:540–547. doi: 54087.
44. O'Donnell J, Laffan MA. Dissociation of ABH antigen expression from von Willebrand factor synthesis in endothelial cell lines. *Br J Haematol*. 2003;121:928–931.
45. Kremer Hovinga JA, Lämmle B. Role of ADAMTS13 in the pathogenesis, diagnosis, and treatment of thrombotic thrombocytopenic purpura. *Hematology Am Soc Hematol Educ Program*. 2012;2012:610–616. doi: 10.1182/asheducation-2012.1.610.
46. Crawley JT, Scully MA. Thrombotic thrombocytopenic purpura: basic pathophysiology and therapeutic strategies. *Hematology Am Soc Hematol Educ Program*. 2013;2013:292–299. doi: 10.1182/asheducation-2013.1.292.
47. Tsai HM, Sussman II, Ginsburg D, Lankhof H, Sixma JJ, Nagel RL. Proteolytic cleavage of recombinant type 2A von Willebrand factor mutants R834W and R834Q: inhibition by doxycycline and by monoclonal antibody VP-1. *Blood*. 1997;89:1954–1962.
48. Hugenholtz GC, Adelmeijer J, Meijers JC, Porte RJ, Stravitz RT, Lisman T. An unbalance between von Willebrand factor and ADAMTS13 in acute liver failure: implications for hemostasis and clinical outcome. *Hepatology*. 2013;58:752–761. doi: 10.1002/hep.26372.
49. Hugenholtz GC, Lisman T. Letter by Hugenholtz and Lisman regarding article, "plasmin cleavage of von Willebrand factor as an emergency bypass for ADAMTS13 deficiency in thrombotic microangiopathy". *Circulation*. 2015;131:e18. doi: 10.1161/CIRCULATIONAHA.114.009307.
50. O'Sullivan JM, Preston RJ, O'Regan N, O'Donnell JS. Emerging roles for hemostatic dysfunction in malaria pathogenesis. *Blood*. 2016;127:2281–2288. doi: 10.1182/blood-2015-11-636464.

51. Djamiatun K, van der Ven AJ, de Groot PG, Faradz SM, Hapsari D, Dolmans WM, Sebastian S, Fijnheer R, de Mast Q. Severe dengue is associated with consumption of von Willebrand factor and its cleaving enzyme ADAMTS-13. *PLoS Negl Trop Dis*. 2012;6:e1628. doi: 10.1371/journal.pntd.0001628.
52. Martin K, Borgel D, Lerolle N, Feys HB, Trinquart L, Vanhoorelbeke K, Deckmyn H, Legendre P, Diehl JL, Baruch D. Decreased ADAMTS-13 (A disintegrin-like and metalloprotease with thrombospondin type 1 repeats) is associated with a poor prognosis in sepsis-induced organ failure. *Crit Care Med*. 2007;35:2375–2382.
53. Larkin D, de Laat B, Jenkins PV, Bunn J, Craig AG, Terraube V, Preston RJ, Donkor C, Grau GE, van Mourik JA, O'Donnell JS. Severe Plasmodium falciparum malaria is associated with circulating ultra-large von Willebrand multimers and ADAMTS13 inhibition. *PLoS Pathog*. 2009;5:e1000349. doi: 10.1371/journal.ppat.1000349.
54. Chen J, Hobbs WE, Le J, Lenting PJ, de Groot PG, López JA. The rate of hemolysis in sickle cell disease correlates with the quantity of active von Willebrand factor in the plasma. *Blood*. 2011;117:3680–3683. doi: 10.1182/blood-2010-08-302539.
55. Siedlecki CA, Lestini BJ, Kottke-Marchant KK, Eppell SJ, Wilson DL, Marchant RE. Shear-dependent changes in the three-dimensional structure of human von Willebrand factor. *Blood*. 1996;88:2939–2950.
56. Baldauf C, Schneppenheim R, Stacklies W, Obser T, Pieconka A, Schneppenheim S, Budde U, Zhou J, Gräter F. Shear-induced unfolding activates von Willebrand factor A2 domain for proteolysis. *J Thromb Haemost*. 2009;7:2096–2105. doi: 10.1111/j.1538-7836.2009.03640.x.
57. Zhang X, Halvorsen K, Zhang CZ, Wong WP, Springer TA. Mechanoenzymatic cleavage of the ultralarge vascular protein von Willebrand factor. *Science*. 2009;324:1330–1334. doi: 10.1126/science.1170905.
58. Hamilton KK, Fretto LJ, Grierson DS, McKee PA. Effects of plasmin on von Willebrand factor multimers. Degradation *in vitro* and stimulation of release in vivo. *J Clin Invest*. 1985;76:261–270. doi: 10.1172/JCI111956.
59. Tanka-Salamon A, Kolev K, Machovich R, Komorowicz E. Proteolytic resistance conferred to fibrinogen by von Willebrand factor. *Thromb Haemost*. 2010;103:291–298. doi: 10.1160/TH09-07-0420.
60. Zander CB, Cao W, Zheng XL. ADAMTS13 and von Willebrand factor interactions. *Curr Opin Hematol*. 2015;22:452–459. doi: 10.1097/MOH.0000000000000169.
61. Berkowitz SD, Dent J, Roberts J, Fujimura Y, Plow EF, Titani K, Ruggeri ZM, Zimmerman TS. Epitope mapping of the von Willebrand factor subunit distinguishes fragments present in normal and type IIA von Willebrand disease from those generated by plasmin. *J Clin Invest*. 1987;79:524–531. doi: 10.1172/JCI112843.
62. Rayes J, Hommais A, Legendre P, Tout H, Veyradier A, Obert B, Ribba AS, Girma JP. Effect of von Willebrand disease type 2B and type 2M mutations on the susceptibility of von Willebrand factor to ADAMTS-13. *J Thromb Haemost*. 2007;5:321–328. doi: 10.1111/j.1538-7836.2007.02296.x.
63. Susen S, Rauch A, Van Belle E, Vincentelli A, Lenting PJ. Circulatory support devices: fundamental aspects and clinical management of bleeding and thrombosis. *J Thromb Haemost*. 2015;13:1757–1767. doi: 10.1111/jth.13120.
64. Van Belle E, Rauch A, Vincentelli A, et al. Von Willebrand factor as a biological sensor of blood flow to monitor percutaneous aortic valve interventions. *Circ Res*. 2015;116:1193–1201. doi: 10.1161/CIRCRESAHA.116.305046.
65. Federici AB, Berkowitz SD, Zimmerman TS, Mannucci PM. Proteolysis of von Willebrand factor after thrombolytic therapy in patients with acute myocardial infarction. *Blood*. 1992;79:38–44.
66. McGrath RT, McKinnon TA, Byrne B, O'Kennedy R, Terraube V, McRae E, Preston RJ, Laffan MA, O'Donnell JS. Expression of terminal alpha2-6-linked sialic acid on von Willebrand factor specifically enhances proteolysis by ADAMTS13. *Blood*. 2010;115:2666–2673. doi: 10.1182/blood-2009-09-241547.
67. McKinnon TA, Chion AC, Millington AJ, Lane DA, Laffan MA. N-linked glycosylation of VWF modulates its interaction with ADAMTS13. *Blood*. 2008;111:3042–3049. doi: 10.1182/blood-2007-06-095042.
68. Berkowitz SD, Federici AB. Sialic acid prevents loss of large von Willebrand factor multimers by protecting against amino-terminal proteolytic cleavage. *Blood*. 1988;72:1790–1796.
69. Nowak AA, Canis K, Riddell A, Laffan MA, McKinnon TA. O-linked glycosylation of von Willebrand factor modulates the interaction with platelet receptor glycoprotein Ib under static and shear stress conditions. *Blood*. 2012;120:214–222. doi: 10.1182/blood-2012-02-410050.
70. Canis K, McKinnon TA, Nowak A, Haslam SM, Panico M, Morris HR, Laffan MA, Dell A. Mapping the N-glycome of human von Willebrand factor. *Biochem J*. 2012;447:217–228. doi: 10.1042/BJ20120810.
71. Canis K, McKinnon TA, Nowak A, Panico M, Morris HR, Laffan M, Dell A. The plasma von Willebrand factor O-glycome comprises a surprising variety of structures including ABH antigens and disialosyl motifs. *J Thromb Haemost*. 2010;8:137–145. doi: 10.1111/j.1538-7836.2009.03665.x.
72. Ellies LG, Ditto D, Levy GG, Wahrenbrock M, Ginsburg D, Varki A, Le DT, Marth JD. Sialyltransferase ST3Gal-IV operates as a dominant modifier of hemostasis by concealing asialoglycoprotein receptor ligands. *Proc Natl Acad Sci U S A*. 2002;99:10042–10047. doi: 10.1073/pnas.142005099.
73. van Schooten CJ, Denis CV, Lisman T, Eikenboom JC, Leebeek FW, Goudemand J, Fressinaud E, van den Berg HM, de Groot PG, Lenting PJ. Variations in glycosylation of von Willebrand factor with O-linked sialylated T antigen are associated with its plasma levels. *Blood*. 2007;109:2430–2437. doi: 10.1182/blood-2006-06-032706.

Highlights

- An in vivo role for plasmin-mediated proteolysis of von Willebrand factor (VWF) has been demonstrated in a mouse model of thrombotic thrombocytopenic purpura.
- We examined plasmin-mediated proteolysis of VWF under shear and of recombinant VWF proteins.
- Plasmin cleaves VWF in a shear- and glycan-dependent manner at K1491-R1492.
- Heparin inhibits plasmin-mediated proteolysis of VWF.

Regular Article

blood

THROMBOSIS AND HEMOSTASIS

N-linked glycans within the A2 domain of von Willebrand factor modulate macrophage-mediated clearance

Alain Chion,[1,*] Jamie M. O'Sullivan,[1,*] Clive Drakeford,[1] Gudmundur Bergsson,[1] Niall Dalton,[1] Sonia Aguila,[1] Soracha Ward,[1] Padraic G. Fallon,[2] Teresa M. Brophy,[1] Roger J. S. Preston,[3,4] Lauren Brady,[5] Orla Sheils,[5] Michael Laffan,[6] Thomas A. J. McKinnon,[6] and James S. O'Donnell[1,7,8]

[1]Haemostasis Research Group, Institute of Molecular Medicine, Trinity Centre for Health Sciences, St. James's Hospital, [2]Inflammation and Immunity Research Group, Institute of Molecular Medicine, and [3]Department of Clinical Medicine, School of Medicine, Trinity College Dublin, Dublin, Ireland; [4]National Children's Research Centre, Our Lady's Children's Hospital, Crumlin, Dublin, Ireland; [5]Department of Histopathology, Sir Patrick Dun Research Laboratory, St. James's Hospital, Trinity College Dublin, Dublin, Ireland; [6]Faculty of Medicine, Imperial College, Hammersmith Hospital, London, United Kingdom; [7]National Centre for Hereditary Coagulation Disorders, St. James's Hospital, Dublin, Ireland; and [8]Irish Centre for Vascular Biology, Royal College of Surgeons in Ireland, Dublin, Ireland

Key Points

- The A1 domain of VWF contains a cryptic binding site that plays a key role in regulating macrophage binding and clearance.
- The N-linked glycans presented at N1515 and N1574 within the A2 domain of VWF modulate macrophage-mediated clearance.

Enhanced von Willebrand factor (VWF) clearance is important in the etiology of von Willebrand disease. However, the molecular mechanisms underlying VWF clearance remain poorly understood. In this study, we investigated the role of VWF domains and specific glycan moieties in regulating in vivo clearance. Our findings demonstrate that the A1 domain of VWF contains a receptor-recognition site that plays a key role in regulating the interaction of VWF with macrophages. In A1-A2-A3 and full-length VWF, this macrophage-binding site is cryptic but becomes exposed following exposure to shear or ristocetin. Previous studies have demonstrated that the N-linked glycans within the A2 domain play an important role in modulating susceptibility to ADAMTS13 proteolysis. We further demonstrate that these glycans presented at N1515 and N1574 also play a critical role in protecting VWF against macrophage binding and clearance. Indeed, loss of the N-glycan at N1515 resulted in markedly enhanced VWF clearance that was significantly faster than that observed with any previously described VWF mutations. In addition, A1-A2-A3 fragments containing the N1515Q or N1574Q substitutions also demonstrated significantly enhanced clearance. Importantly, clodronate-induced macrophage depletion significantly attenuated the increased clearance observed with N1515Q and N1574Q in both full-length VWF and A1-A2-A3. Finally, we further demonstrate that loss of these N-linked glycans does not enhance clearance in VWF in the presence of a structurally constrained A2 domain. Collectively, these novel findings support the hypothesis that conformation of the VWF A domains plays a critical role in modulating macrophage-mediated clearance of VWF in vivo. (*Blood*. 2016;128(15):1959-1968)

Introduction

Von Willebrand factor (VWF) is a large multimeric sialoglycoprotein that plays 2 key roles in normal hemostasis.[1,2] First, it mediates recruitment of platelets following injury to the vascular endothelium. Second, VWF also functions as a carrier molecule for factor VIII. In vivo expression of VWF occurs only within endothelial cells (ECs)[3] and megakaryocytes,[4] where VWF is initially synthesized as a monomer composed of a series of repeating domains in the order D′-D3-A1-A2-A3-D4-C1-C2-C3-C4-C5-C6-CK. VWF synthesized within ECs undergoes constitutive secretion into the plasma. Prior to this secretion, VWF undergoes complex posttranslational modification within ECs, including significant N- and O-linked glycosylation.[2,5,6]

The N- and O-linked glycans of human VWF have both been characterized and demonstrate significant heterogeneity.[7,8] Monosialylated or disialylated biantennary complex-type chains constitute the most common N-linked glycans expressed on VWF.[6,7,9-11] Although the O-linked glycans of VWF also demonstrate marked heterogeneity, disialyl core 1 structures account for ~70% of the total population.[8,12] Importantly, although the majority of its glycans are capped by negatively charged sialic acid,[7,13] VWF is unusual in that a minority of both N-linked and O-linked carbohydrate chains express terminal ABO(H) blood group determinants.[7,8,11]

Although substantial progress has been achieved in understanding the biosynthesis, structure, and functions of VWF, the biological mechanism(s) responsible for modulating VWF clearance from the plasma remain poorly understood.[14] Nevertheless, accumulating data have shown that enhanced VWF clearance plays an important role in the

Submitted 16 April 2016; accepted 16 August 2016. Prepublished online as *Blood* First Edition paper, 23 August 2016; DOI 10.1182/blood-2016-04-709436.

*A.C. and J.M.O. contributed equally to this study.

Presented in abstract form as an oral presentation at the 56th annual meeting of the American Society of Hematology, San Francisco, CA, 8 December 2014.

The online version of this article contains a data supplement.

The publication costs of this article were defrayed in part by page charge payment. Therefore, and solely to indicate this fact, this article is hereby marked "advertisement" in accordance with 18 USC section 1734.

etiology of both type 1 and type 2 VWD.[15-20] Recent evidence further suggests that hepatic and splenic macrophages may play key roles in mediating VWF clearance.[21-26] For example, differentiated primary human macrophages can bind and endocytose purified VWF in vitro.[21] Furthermore, macrophage depletion significantly prolonged the in vivo survival of VWF infused into VWF$^{-/-}$ mice.[21,24,25] In addition, the macrophage lipoprotein receptor (LRP1) has been shown to bind to VWF in a shear-dependent manner.[23] Critically however, the specific regions of the VWF glycoprotein involved in modulating macrophage interactions remain unclear.

More than 30 different *VWF* point mutations have already been associated with enhanced clearance in patients with VWD.[15,27,28] Intriguingly, the majority of VWF amino acid substitutions associated with enhanced clearance are clustered within the A1 domain.[14] Emerging evidence suggests that at least some of these VWF mutations result in enhanced macrophage-mediated clearance in vivo. For example, Wohner et al recently showed that specific type 2B VWD variants (R1306Q and V1316M within the A1 domain) result in increased VWF clearance that is predominantly modulated through the macrophage LRP1 receptor.[26] Nevertheless, the molecular mechanism through which so many different amino acid substitutions clustered within the A1 domain of VWF result in enhanced clearance remains poorly understood.

Variation in VWF glycosylation profile has also been shown to significantly influence the clearance rate.[29-34] For example, terminal ABO(H) blood group determinants significantly modulate in vivo clearance.[35] Consequently, plasma VWF levels are significantly lower in blood group O individuals than in non-O individuals.[5,36] The asialoglycoprotein or Ashwell receptor (ASGPR) is a C-type lectin predominantly expressed on hepatocytes and is composed of 2 transmembrane protein subunits (Asgr-1 and Asgr-2).[37] Importantly, a role for Asgr1 in modulating VWF clearance has recently been described.[34] In addition, a number of other carbohydrate receptors, including galectin-1 (Gal-1), galectin-3 (Gal-3), Siglec-5, and CLEC4M, have also been shown to bind VWF.[38-40] Furthermore, genome-wide association studies have reported associations between some of these receptors and plasma levels of the VWF–factor VIII complex.[41] Nevertheless, given the complexity and heterogeneity of the N- and O-linked glycans expressed on VWF, the biological mechanisms through which specific VWF carbohydrate structures serve to regulate in vivo clearance remain poorly defined. In this study, we have used a series of in vitro and in vivo methodologies to investigate the importance of specific domains and glycans in modulating VWF clearance. Our findings demonstrate that N-linked glycans at N1515 and N1574 within the A2 domain of VWF play a critical role in protecting VWF against macrophage-mediated clearance.

Materials and methods

Expression and purification of recombinant VWF

The expression vector pcDNA-VWF encoding full-length recombinant VWF (rVWF) has previously been described.[42] A DNA fragment containing VWFA1A2A3 (residues 1260-1874) was inserted into expression vector pEXPR-IBA 42 (IBA) via *Nhe*I and *Pme*I restriction sites. The same strategy was used for expressing VWFA1 (residues 1239-1472), VWFA2 (residues 1473-1668), and VWFA3 (residues 1671-1878). Human full-length rVWF, A1A2A3-VWF A1-VWF, A2-VWF, and A3-VWF were transiently expressed in HEK293T cells. Conditioned serum-free medium was harvested and concentrated as before.[24] A1-VWF, A2-VWF, A3-VWF, and A1A2A3-VWF variants were further purified via nickel affinity chromatography.

Site-directed mutagenesis of VWF was carried out to introduce point mutations at N1515 and N1574 within both full-length and truncated A1A2A3-VWF. In keeping with previous studies defining the biological significance of these glycans,[42-44] each asparagine residue was mutated to glutamine (N1515Q and N1574Q) to eliminate the N-linked glycans at these positions. Mutations were verified by DNA sequencing to ensure the absence of any other randomly introduced mutations. Similarly, mutagenesis of full-length VWF was carried out to introduce point mutations N1493C and C1670S. These mutations result in the creation of a homologous disulfide bond in the A2 domain of VWF between the cysteine at 1493 and the native cysteine at 1669. This cysteine clamp mutation has previously been described to prevent A2 domain unfolding and render VWF insensitive to ADAMTS13 cleavage.[45,46]

In vitro modification of VWF glycan structures

The N-linked glycan profile of rVWF and A1A2A3-VWF was modified using a specific exoglycosidase peptide N glycosidase F (PNGase F; New England Biolabs). VWF glycan digestions were carried out overnight under nondenaturing conditions at 37°C as previously reported.[42] After digestion, residual VWF glycan expression was quantified using specific lectin enzyme-linked immunosorbent assays (ELISAs) as described previously.[47,48]

Human RAP expression and purification

Low-density lipoprotein receptor-related protein-associated protein 1 (RAP) acts as a molecular chaperone by inhibiting ligand binding to LRP1, as well as other members of this receptor family. Human RAP complementary DNA coding Tyr35 to Leu357 (UNIPROTKB-P30533) was inserted into Novagen pET28a (+) bacterial expression vector (Novagen, Nottingham, UK) via *Bam*HI and *Sal*I restriction sites. Recombinant RAP protein was refolded from *Escherichia coli* inclusion bodies as described previously.[49]

THP-1 binding assay

THP-1 cells were seeded on microwell plates (Nunclon; Fisher Scientific) at a density of 5×10^6 cells/mL. For differentiation, media was supplemented with 20 ng/mL PMA (Sigma-Aldrich). After 72 hours, fresh growth medium was added to the cells, which were then rested for an additional 4 days before use.[50] VWF-THP-1 binding was performed at 4°C to prevent endocytosis. Full-length VWF or truncated A1A2A3-VWF variants were diluted in ice-cold serum-free growth medium incubated with the cells for 1 hour on ice. For analysis, the nuclei were stained with Hoechst 33342 (Thermo Fisher). Full-length bound VWF was detected using anti–human VWF (Dako) followed by Alexa Fluor 488 donkey anti–rabbit immunoglobulin G (IgG) (Life Technologies). Truncated A1A2A3-VWF variants were detected by Penta-His Alexa Fluor 488 conjugate (QIAGEN). THP-1 surface-bound VWF was quantified using the fluorescence microscopy IN Cell Analyzer 1000 (GE Healthcare). Eight fields of view were imaged per well at a magnification of ×20. Image analysis was carried out using high throughput IN Cell 1000 Image Analysis Software (GE Healthcare). Data were graphed as percentage fluorescently labeled VWF per cell relative to maximal VWF binding (mean ± standard error of the mean [SEM]).

VWF uptake by differentiated THP-1 cells was assessed using confocal microscopy. In brief, cells were seeded onto glass chamber sides and differentiated using PMA as above. Subsequently cells were incubated with VWF or glycoforms thereof in the presence of ristocetin (1 mg/mL) for 30 minutes at either 4°C or 37°C to assess binding and internalization, respectively. Cells were fixed with 4% paraformaldehyde for 20 minutes, in some cases permeabilized using 0.1% Triton X, and then incubated with 4,6-diamidino-2-phenylindole; polyclonal mouse anti-EEA1 (early endosomal antigen-1) (BD Biosciences); and/or polyclonal rabbit anti-VWF for 45 minutes. After washing, slides were stained with Alexa Flour 594–conjugated anti-mouse IgG (Invitrogen) and Alexa Flour 488–conjugated anti–rabbit IgG (Invitrogen, UK) for 15 minutes. Images were visualized using LSM700 (Carl Zeiss) Confocal Microscope, 63× plan-apochromat lens. Images were analyzed using ImageJ and Adobe Illustrator CC2015.3.

VWF clearance studies in VWF$^{-/-}$ mice

VWF$^{-/-}$ mice were obtained from The Jackson Laboratory (Sacramento, CA). All animal experiments were approved by the Animal Research Ethics Committee, Trinity College Dublin, and were performed in compliance with the Irish Medicines Board regulations. VWF clearance studies were performed using mice between 6 and 10 weeks of age. In brief, VWF$^{-/-}$ mice were injected intravenously with 30 nM (37.5 U/kg) of VWF or glycoforms thereof. At sequential time points, blood was collected into heparin-coated micro containers. Three to five mice per time point were used. Residual plasma VWF:antigen levels were determined by ELISA. In vivo macrophage depletion was performed as previously described,[24,51] using IV infusion of clodronate liposomes (100 μl/10 g body weight). Control mice were injected with PBS liposomes. To examine the role of the LRP1 clearance receptor, mice were administered 200 μM LRP1-antagonist RAP 1 minute prior to injection of VWF.

Data presentation and statistical analysis

All experimental data and statistical analysis were performed using the GraphPad Prism program. Data are expressed as mean ± SEM. To assess statistical differences for 2 data sets, data were analyzed using the Student unpaired 2-tailed *t* test. For multiple comparisons, data were analyzed using a one-way analysis of variance with post hoc Dunnett's test. For all statistical tests, $P < .05$ was considered significant.

Results

The A domains of VWF modulate macrophage-mediated clearance

Lenting et al previously reported that a truncated A1-A2-A3 VWF fragment expressed in BHK cells demonstrated a similar clearance pattern to that of full-length rVWF and postulated that a receptor-recognition site may be present within the A1-A3 region.[52] To further study this hypothesis, we first investigated the clearance of rVWF and A1-A2-A3 that was expressed in a different cell line (HEK293T). Following tail vein injection in VWF$^{-/-}$ mice, A1-A2-A3 (HEK) clearance was also similar to that of full-length VWF (HEK) (Figure 1A). Recent studies have shown that hepatic macrophages contribute to the clearance of full-length VWF.[21-26] To determine whether macrophages modulate A1-A2-A3 clearance in vivo, clearance studies were repeated following clodronate-induced macrophage depletion. In keeping with previous studies, clearance of full-length rVWF was significantly reduced following macrophage depletion (Figure 1B). Interestingly, in vivo clearance of A1-A2-A3 was also significantly attenuated following macrophage depletion (Figure 1B).

To further investigate a putative role for the A domains in regulating VWF clearance by macrophages, VWF binding to PMA-differentiated THP-1 cells in vitro was studied using HiContent image analysis. In preliminary studies, we observed that full-length plasma-derived VWF (pd-VWF) and rVWF both bound to THP-1 macrophages (supplemental Figure 1, available on the *Blood* Web site). In keeping with a role for the A domains in modulating macrophage interaction, full-length VWF binding was significantly enhanced in the presence of ristocetin (1 mg/mL) (supplemental Figure 1). Moreover, dose-dependent binding of the truncated A1-A2-A3 fragment to THP-1 macrophages in vitro was also observed (Figure 1C). Finally, the relative importance of the individual A domains within the A1-A2-A3 construct in determining macrophage binding was investigated. Significant in vitro binding of the A1 domain to THP-1 macrophages was observed (Figure 1D). However, in contrast, no significant binding was seen for the isolated A2 or A3 domains. Importantly, the macrophage binding of the isolated A1 domain was also significantly greater than that of the combined A1-A2-A3 fragment. Collectively, these data support the hypothesis that the A domains of VWF contain a receptor-recognition site important in regulating the interaction of VWF with macrophages and suggest that the VWF A1 domain plays a particular critical role in determining macrophage binding.

In previous studies, we observed that PNGase F digestion of human pd-VWF to remove the N-linked glycans resulted in markedly increased clearance. Similarly, clearance of rVWF was also significantly increased ~2.5-fold following PNGase digestion ($P < .05$) (Figure 1E). Given the important role of A1-A2-A3 in regulating VWF clearance by macrophages, it is interesting that only 2 N-linked glycan sites are located in this region (at N1515 and N1574 within the A2 domain).[7,42] To determine whether these N-linked glycans within A2 play a role in modulating VWF interaction with macrophages, binding of A1-A2-A3 before and after PNGase F digestion was investigated. Following PNGase treatment, in vitro binding of A1-A2-A3 to THP-1 macrophages was markedly increased (Figure 1F), suggesting that these N-linked glycans within A2 play a novel role in regulating macrophage interaction.

N-linked glycans at N1515 and N1574 are critical determinants of VWF clearance

Recent mass spectrometry analysis has demonstrated that both of the N-linked glycans at N1515 and N1574 within A2 are occupied by large complex carbohydrate structures (Figure 2A).[7] To further investigate the role of these glycans in modulating macrophage interaction, the asparagine residues at N1515 and N1574 were individually mutated to glutamine residues (VWF-N1515Q and VWF-N1574Q) and expressed in HEK293T cells. In accordance with previous studies,[42] VWF-N1515Q and VWF-N1574Q both displayed multimer distribution and collagen binding activities similar to wild-type (WT) VWF (data not shown). Following tail vein injection, in vivo clearance of VWF-N1515Q and VWF-N1574Q was markedly enhanced in VWF mice compared with WT-VWF (Figure 2B). Interestingly, clearance of VWF-N1515Q was faster than that of any other previously described VWF point mutations, including VWF-R1205H (data not shown; $P < .05$).[24] In keeping with previous studies, infusion of VWF-N1515Q and VWF-N1574Q had no significant effect on murine platelet counts (data not shown).[42] In addition, SDS-PAGE of murine plasma samples under reducing conditions demonstrated no significant evidence of in vivo proteolysis of either VWF-N1515Q or VWF-N1574Q.

To investigate the molecular mechanism responsible for the enhanced VWF clearance associated with the loss of A2 domain N-linked glycans, we further characterized the effects of introducing the VWF-N1515Q and VWF-N1574Q substitutions into the A2 domain of the A1-A2-A3 fragment (A1-A2-A3-N1515Q and A1-A2-A3-N1574Q). In keeping with their effect in reducing the survival of full-length rVWF, both mutations also resulted in significantly enhanced clearance of the A1-A2-A3 fragment (Figure 2C). Cumulatively, these novel findings demonstrate that both of the N-linked glycans located at N1515 and N1574 within the A2 domain of VWF play critical roles in regulating clearance in vivo. Furthermore, the increased clearance associated with loss of N-linked glycan structures at either N1515 or N1574 is modulated through local effects within the A1-A2-A3 region.

N-linked glycans within A2 regulate enhanced clearance

Besides the 2 N-linked glycans located within the A2 domain, another 10 N-linked glycans are present on the VWF monomer

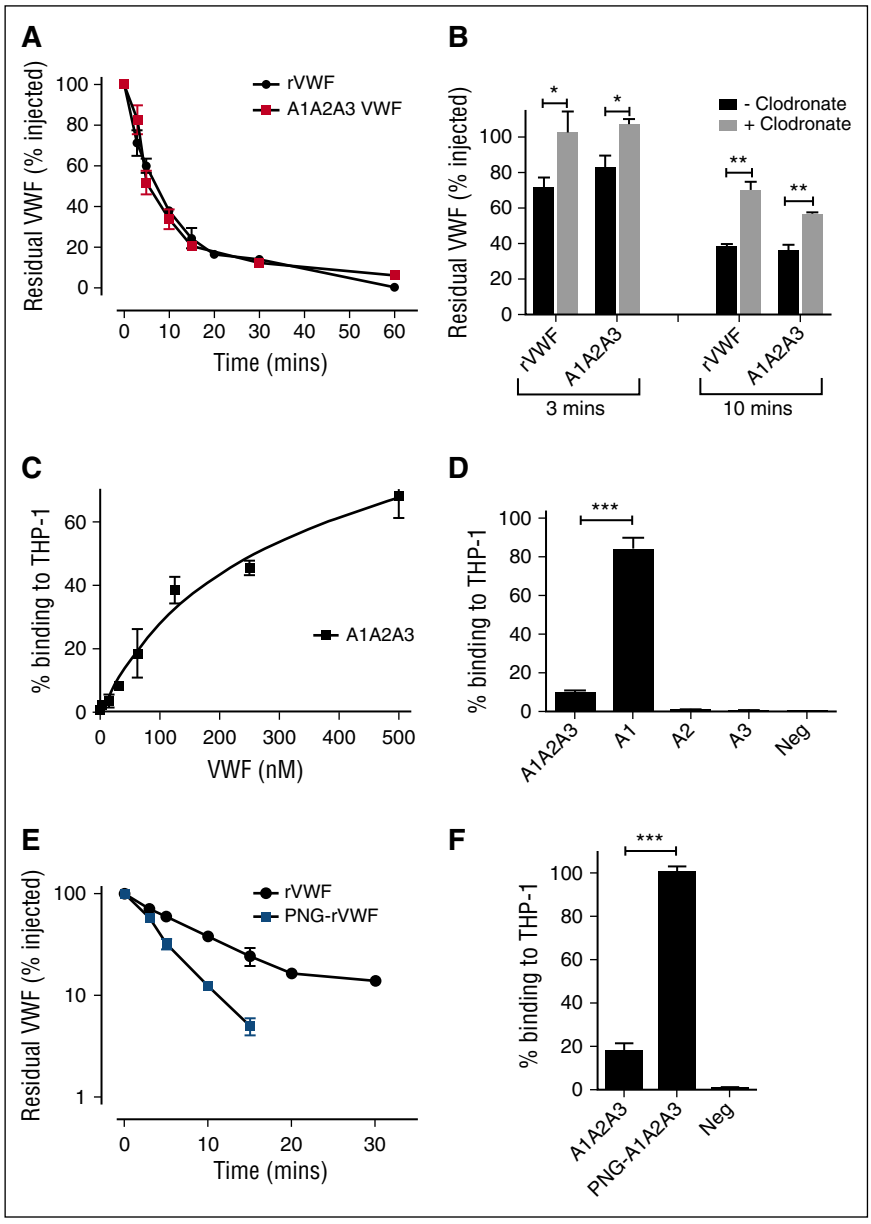

Figure 1. The A domains of VWF modulate macrophage-mediated clearance. (A) The in vivo clearance of a monomeric A1-A2-A3 VWF fragment in VWF$^{-/-}$ mice was compared with that of full-length rVWF. At each time point, the residual circulating VWF concentration was determined by VWF:antigen ELISA. All results are plotted as percentage residual VWF levels relative to the amount injected. Data are presented as mean ± SEM. In some cases, the SEM cannot be seen due to its small size. Mean residence times for full-length and A1-A2-A3 were 11.3 ± 0.6 and 10.0 ± 0.61 minutes, respectively. (B) To study the role of macrophages in modulating clearance of A1-A2-A3 and full-length rVWF, in vivo clearance studies were repeated in VWF$^{-/-}$ mice 24 hours following clodronate-induced macrophage depletion. Blood was collected at 3- and 10-minute time points, and residual VWF quantified by ELISA. (C) The in vitro binding of A1-A2-A3 to macrophages was assessed using THP-1 macrophage cells as detailed in "Materials and methods." (D) Individual A-domain proteins A1, A2, and A3 were examined for binding to THP-1 macrophages. Significant binding was observed for the A1 domain compared with the A2 and A3 domains (*$P < .05$, **$P < .01$, and ***$P < .001$, respectively; negative control is no VWF). (E) To investigate the role of VWF carbohydrate determinants in modulating VWF clearance, rVWF was treated with PNGase F (PNG-rVWF). N-linked glycan removal was confirmed using a specific lectin ELISA. In vivo survival was then measured in VWF$^{-/-}$ mice as before. Results are plotted as percentage residual VWF:antigen levels relative to the amount injected. Data are represented as mean ± SEM. (F) To assess a potential role for VWF N-linked glycans in the A domains in regulating macrophage binding, A1-A2-A3 was treated with PNGase to remove the N-linked glycans in the A2 domain at N1515 and N1574 (PNG-A1A2A3). The ability of PNG-A1A2A3 to bind to THP-1 macrophages in the presence of ristocetin was then compared with WT A1-A2-A3 using HiContent image analysis as before. Data are graphed as percentage binding relative to maximal (mean ± SEM) (****$P < .001$).

(Figure 3A).[7,43] To determine whether these additional N-linked glycans may also be important in regulating VWF clearance, we expressed a rVWF variant from which the A2 domain was deleted (ΔA2-VWF) (Figures 3A-B). Interestingly, in vivo clearance of ΔA2-VWF was not accelerated following PNGase F digestion (Figure 3C), suggesting that the N-linked glycans within the A2 domain play a critical role in modulating the enhanced clearance of PNG-VWF.

Accelerated clearance of VWF N1515Q and VWF N1574Q is mediated by macrophages

To investigate whether VWF A2 domain glycan expression influences macrophage-mediated clearance, studies were repeated in VWF$^{-/-}$ mice following clodronate administration. We found that the increased clearance phenotypes of both VWF-N1515Q and VWF-N1574Q were significantly attenuated following clodronate-induced macrophage depletion (Figure 4A). Similarly, the enhanced clearance of both A1-A2-A3-N1515Q and A1-A2-A3-N1574Q was also significantly reduced following macrophage depletion (Figure 4B). In keeping with previous reports,[21,22] confocal microscopy studies performed following incubation at 4°C demonstrated that VWF-WT, VWF-N1515Q, and VWF-N1574Q all bound to differentiated THP-1 cells in vitro (supplemental Figure 2). When incubation studies were performed at 37°C, confocal studies showed colocalization of VWF-WT, VWF-N1515Q, and VWF-N1574Q with early endosomes (supplemental Figure 2), demonstrating that both VWF-N1515Q and VWF-N1574Q are taken up by macrophages. To further study the molecular mechanism through which the N-linked glycans expressed at N1515 and N1574 influence macrophage-dependent clearance, we used HiContent image analysis to compare the in vitro binding of A1-A2-A3-N1515Q, A1-A2-A3-N1574Q, and WT A1-A2-A3 to THP-1 cells. WT A1-A2-A3 demonstrated minimal macrophage binding (Figure 5). However, this binding was significantly enhanced in the presence of ristocetin (1 mg/mL). Importantly, following PNGase digestion to remove the 2 N-linked glycans at

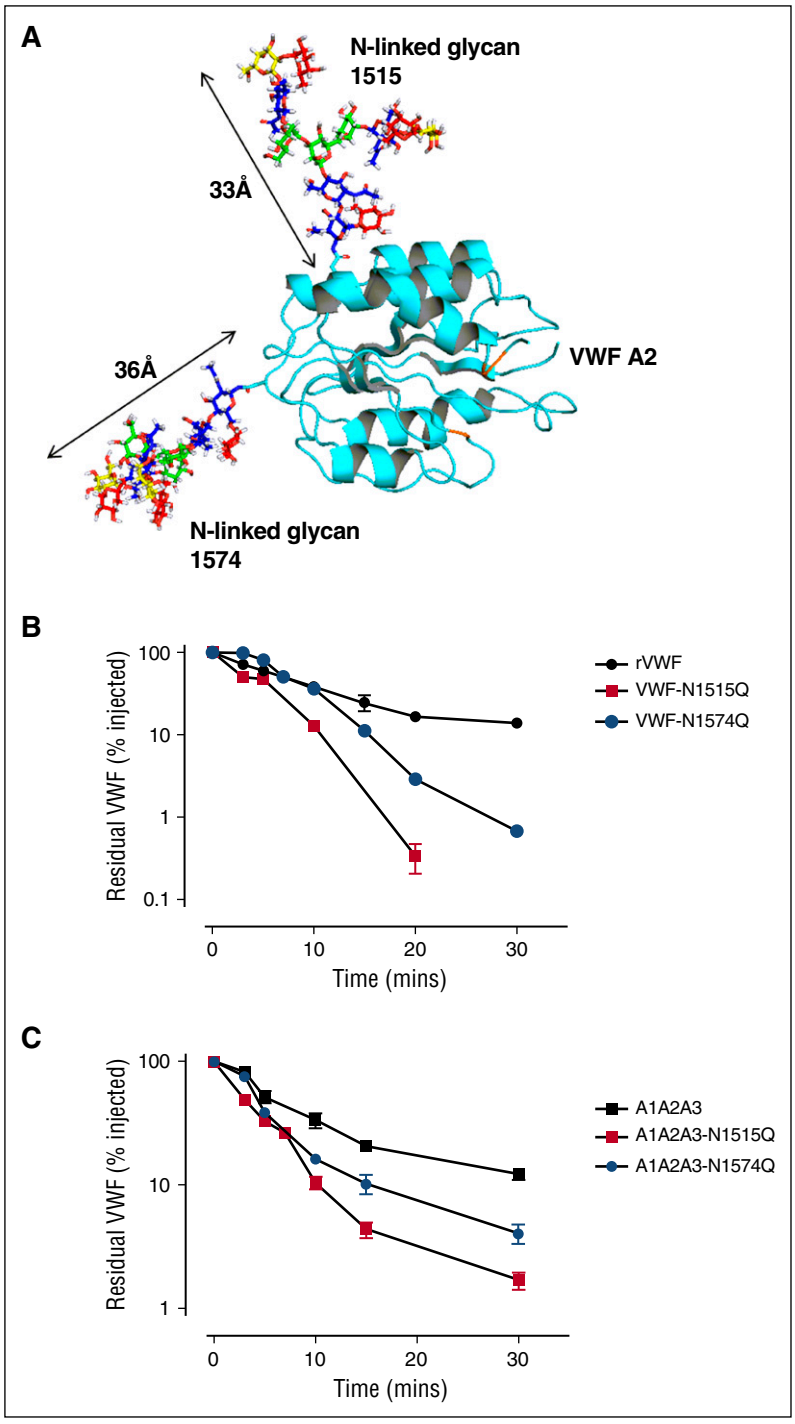

Figure 2. N-linked glycans at N1515 and N1574 are critical determinants of VWF clearance in vivo. (A) A model of the VWF A2 domain was prepared as previously described.[66] Mass spectrometry analysis of human pd-VWF has provided extensive information regarding the N-glycome of VWF. Utilizing this information, a model of the VWF A2 domain with its associated glycans was constructed using Glycam Glycoprotein Builder software. N1515 and N1574 glycans structures were mapped onto the A2 domain crystal structure using this glycan modeling. This in silico analysis revealed that the complex glycans at N1515 and N1574 were both of significant size, spanning ~33 Å and ~36 Å in length, respectively. (B) To investigate a potential role for specific glycan sites in influencing VWF clearance, N1515 and N1574 in the A2 domain were targeted for removal by site-directed mutagenesis (VWF-N1515Q and VWF-N1574Q, respectively). In vivo clearance studies of these VWF glycan variants were performed as before and compared with WT rVWF. (C) Given that the glycans N1515 and N1574 reside within the A2 domain of VWF, we further sought to examine if these glycans could also influence the in vivo survival of an A1A2A3 VWF truncated fragment. To this end, site-directed mutagenesis was performed to eliminate the glycan at N1515 (A1A2A3-N1515Q) and N1574 (A1A2A3-N1574Q). Clearance examined in VWF$^{-/-}$ mice as before. All results are plotted as percentage residual VWF:antigen levels relative to the amount injected. Data are presented as mean ± SEM.

N1515 and N1574, binding of A1-A2-A3 was dramatically increased, suggesting that the presence of these carbohydrate structures serves to prevent binding of A1-A2-A3 to macrophages. In keeping with this hypothesis, both A1-A2-A3-N1515Q and A1-A2-A3-N1574Q demonstrated significantly increased binding compared with WT A1-A2-A3 in either the presence or absence of ristocetin. Finally, PNGase treatment of both A1-A2-A3-N1515Q and A1-A2-A3-N1574Q served to further enhance macrophage binding, confirming that both N-linked glycans contribute to modulating macrophage interaction. Cumulatively, these in vivo and in vitro data confirm that the N-linked glycans within the A2 domain of play important roles in regulating macrophage-dependent VWF clearance

Glycan structures at N1515 and N1574 in the A2 domain influence LRP1-mediated clearance

Recent studies have demonstrated that macrophage LRP1 plays an important role in regulating VWF clearance.[23,26,53] In addition, LRP1 has been shown to bind to VWF in a shear-dependent manner. Importantly, Rastegarlari et al previously demonstrated that the inhibitory effects of RAP on VWF clearance were predominantly modulated through macrophage LRP1 rather than LRP1

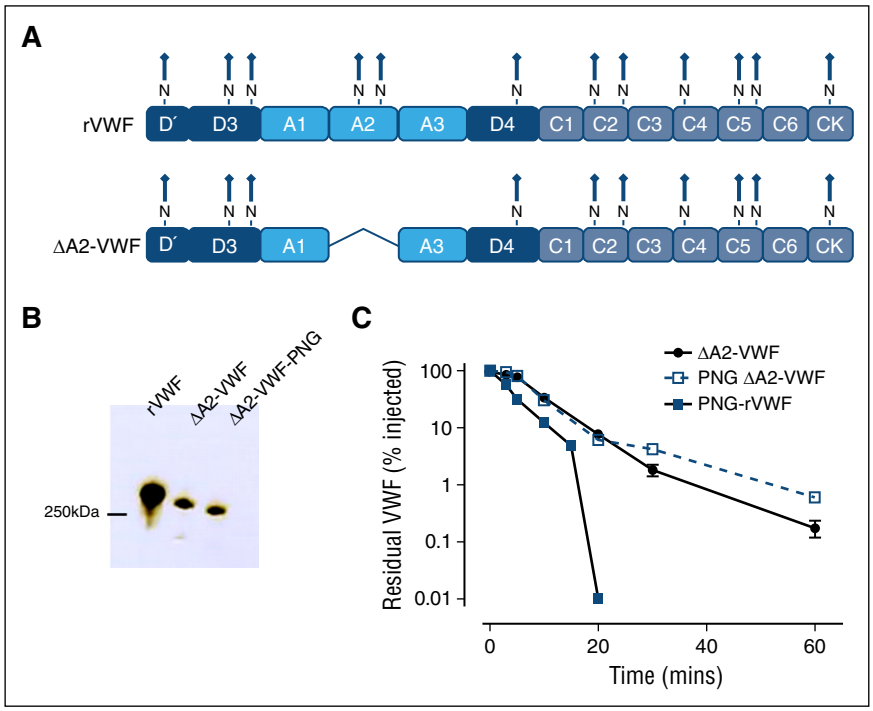

Figure 3. N-linked glycans within the VWF A2 domain regulate enhanced clearance. Our findings suggest that the N-linked glycan within A2 may have a specific role in modulating VWF clearance. To examine if glycans outside the A2 domain may also influence VWF survival, a fragment of VWF with the A2 domain deleted was constructed. (A) Consequently, this VWF variant (ΔA2-VWF) fails to express the N-linked glycans N1515 and N1574. (B) This VWF variant was subjected to PNGase F treatment (PNG ΔA2-VWF) to remove all remaining N-linked glycans. (C) Clearance was assessed in $VWF^{-/-}$ mice as before. All results are plotted as percentage residual VWF:antigen levels relative to the amount injected. Data are presented as mean ± SEM.

expressed in other cells or other macrophage lipoprotein receptors.[23] To further investigate whether VWF A2 domain glycans influence LRP1-mediated clearance in vivo, VWF-N1515Q and VWF-N1574Q clearance studies in $VWF^{-/-}$ mice were repeated in the presence or absence of RAP. In keeping with previous reports, we confirmed that clearance of WT-VWF was significantly reduced in the presence of RAP (Figure 6). Interestingly, the increased clearance of VWF-N1515Q and VWF-N1574Q were also both significantly attenuated in the presence of RAP (Figure 6). These findings are consistent with those observed above following clodronate-induced macrophage depletion (Figure 4A-B) and suggest that the VWF N-linked glycans at N1515 and N1574 modulate macrophage-dependent clearance at least in part through an LRP1-mediated mechanism.

Removal of the N-linked glycan at N1515 does not enhance clearance in VWF with a structurally constrained A2 domain

Large complex N-linked glycans, such as those expressed in the VWF A2 domain, have been previously shown to have important effects on glycoprotein conformation.[54-57] We hypothesized that loss of A2 domain N-linked glycans causes conformational changes that result in enhanced VWF clearance by macrophages. Interestingly, recent studies have described a structurally constrained VWF variant with an engineered long-range disulfide bond (Cys1493-Cys1669) within the A2 domain (Figure 7A).[45] To address our hypothesis, we therefore proceeded to express the N1515Q mutation in this cysteine-clamp VWF variant (VWF-CC-N1515). Insertion of the cysteine clamp alone in A2 (VWF-CC) had no significant effect upon A1-A2-A3 clearance compared with WT A1-A2-A3 (Figure 7B). Importantly however, the rapid in vivo clearance of A1-A2-A3 associated with loss of the N1515 glycan was ablated in the presence of this structurally constrained A2 domain (Figure 7B). Collectively, these data suggest that loss of the N-linked glycans in A2 trigger enhanced VWF clearance by macrophages through conformational changes.

Discussion

Although the biosynthesis, structure, and functional properties of VWF have been well characterized, the molecular mechanisms through which VWF is cleared remain poorly understood.[2,14] However, accumulating data have demonstrated that macrophages play important roles in regulating VWF clearance in vivo,[21-26] and a number of putative macrophage receptors for VWF have been identified.[23,26,38] Critically, however, the specific regions of the VWF glycoprotein involved in modulating interactions with these different macrophage receptors have not been determined. In this study, using a series of in vivo and in vitro methodologies, we demonstrate that the A1-A2-A3 domains of VWF contain a receptor-recognition site important in mediating VWF binding to macrophages in vitro and in regulating VWF clearance by macrophages in vivo. Furthermore, studies using isolated recombinant A domains demonstrated that the A1 domain plays a critical role in regulating macrophage binding. This observation is in keeping with previous studies demonstrating that full-length VWF binding to macrophages is significantly enhanced in the presence of ristocetin, botrecetin, or shear stress.[22,23,26] Importantly, however, our novel data further demonstrate that the ability of the isolated A1 domain to interact with macrophages is markedly attenuated when the A1 domain is linked to the other A domains (A1-A2-A3 truncation), suggesting that the receptor binding site may not be accessible in normal globular VWF.

Previous reports have demonstrated that desialylation of human VWF results in a marked reduction in plasma half-life.[29,32-34] In addition, although the molecular mechanisms involved were not elucidated, enhanced VWF clearance has also been associated with loss of specific O-linked glycans.[30,58] In this paper, we demonstrate that complete loss of N-linked glycan expression following PNGase F digestion also results in markedly enhanced macrophage-mediated VWF clearance. Interestingly, recent studies have reported that N-linked glycan expression on factor X also plays a key role in

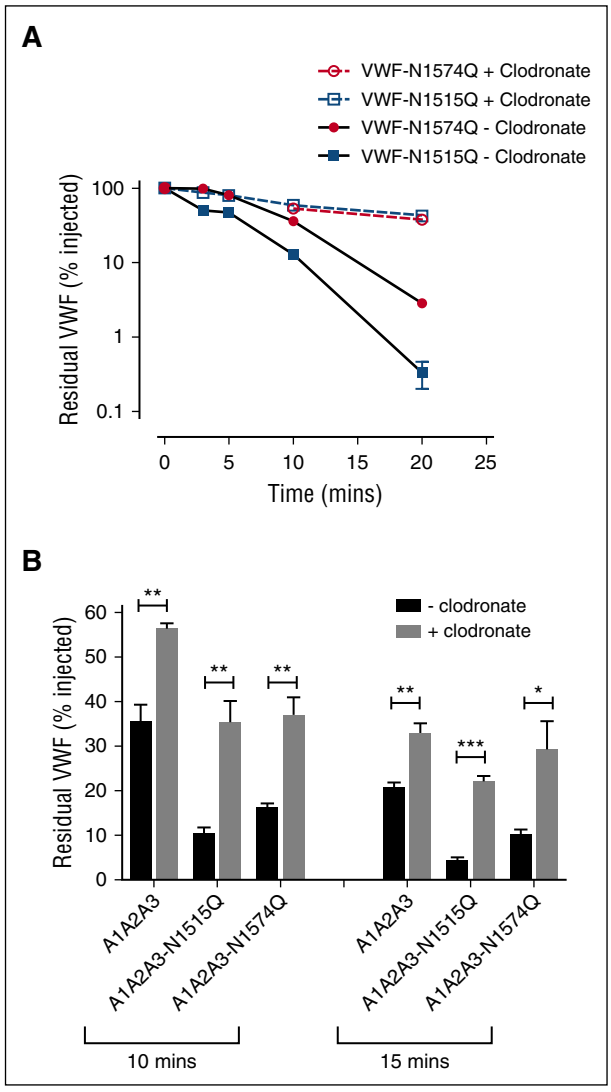

Figure 4. Accelerated clearance of VWF N1515Q and VWF N1574Q is mediated by macrophages. (A) In order to assess the potential contribution of macrophages in modulating the enhanced clearance of VWF glycan variants, clearance of VWF N1515Q and VWF N1574Q was repeated in VWF$^{-/-}$ mice 24 hours after clodronate-induced macrophage depletion. (B) To determine whether macrophages play a role in regulating the reduced survival of A1A2A3-N1515Q and A1A2A3-N1574Q, in vivo clearance studies were also re-assessed in VWF$^{-/-}$ mice following clodronate treatment. Data are graphed as percentage residual VWF relative to the amount injection (*$P < .05$, **$P < .01$, and ***$P < .001$).

regulating interaction with macrophages.[59] Although the molecular mechanism through which N-linked glycan determinants regulate coagulation glycoprotein clearance remains unknown, the effect may be due to general properties of the complex sugar chains or instead may be attributable to particular carbohydrate structures located at specific N-linked sites.[42,43] Given the role of the A1-A2-A3 domains in modulating the interaction of VWF with macrophages, we further investigated whether the 2 N-linked glycosylation sites located at N1515 and N1574, respectively, might play a particular role in regulating VWF clearance. Importantly, we observed that loss of N-linked glycans following site-directed mutagenesis at either N1515 or N1574 resulted in markedly enhanced clearance of full-length rVWF. Furthermore, introduction of the N1515Q or N1574Q substitutions into the A1-A2-A3 fragment also resulted in significantly enhanced clearance. In addition, the enhanced clearance phenotypes observed with N1515Q and N1574Q in full-length VWF, and also in the truncated A1-A2-A3 fragment, were all significantly attenuated following clodronate-induced macrophage depletion. Altogether, these novel findings therefore demonstrate that the N-linked glycan structures within the A2 domain play an important role in protecting VWF against macrophage-mediated clearance in vivo. Moreover, the reduced survival of VWF observed following loss of the N-linked glycan structures in A2 is predominantly due to local effects within the A1-A2-A3 region triggering enhanced macrophage clearance.

Accumulating data suggest that the LRP1 receptor may play a key role in regulating macrophage binding and clearance of VWF.[23,26] Furthermore, Wohner et al recently reported that the A1 domain of VWF (but not the isolated A2 or A3 domains) could bind to purified LRP1 in vitro.[26] Consequently, we investigated whether the LRP1 receptor may be involved in modulating the enhanced clearance of VWF-N1515Q and VWF-N1574Q. Interestingly, the reduced survival of both VWF-N1515Q and VWF-N1574Q was significantly attenuated in the presence of RAP. These findings suggest that the N-linked glycan expressed at N1515 and N1574 play a critical role in protecting VWF against LRP1-mediated macrophage clearance. Although the molecular mechanism(s) through which these N-linked glycans regulate LRP1-mediated clearance remain unclear, previous studies have demonstrated that expression of carbohydrate determinants can directly influence glycoprotein interactions through either charge-mediated mechanisms, or by modifying glycoprotein conformation.[54-57] Consequently, we hypothesize that the protective effect of the large complex N-linked glycan structures in the A2 domain may be due to steric hindrance, with covering of cryptic LRP1 binding sites. Alternatively, and perhaps more likely, variation in A2 domain carbohydrate structures may cause conformational changes that result in enhanced LRP1-modulated clearance. This hypothesis is supported by the observation that removal of the N-linked glycans at N1515 no longer enhances VWF clearance in the presence of a structurally constrained A2 domain. Although our findings

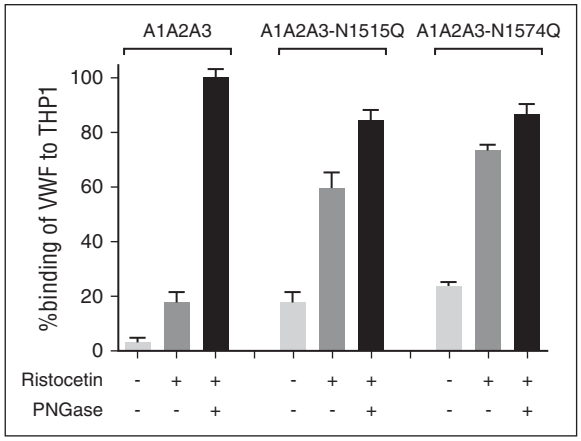

Figure 5. N-linked glycans N1515 and N1574 modulate in vitro binding of VWF to macrophages. To examine the biological mechanisms mediating the enhanced clearance of A1A2A3-N1515Q/N1574Q, we assessed binding to THP-1 macrophages in vitro. The binding of A1A2A3 VWF and the glycan variants A1A2A3-N1515Q and A1A2A3-N1574Q to THP-1 macrophages was examined in the presence or absence of 1mg/ml ristocetin. Additionally, all the A1A2A3 variants were subjected to PNGase treatment to remove both N-linked glycans (black columns) and THP-1 macrophage binding was measured. Data are graphed as percentage binding relative to maximal binding (mean ± SEM).

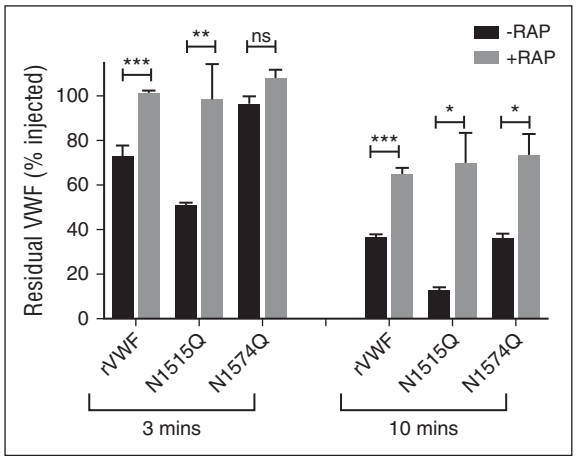

Figure 6. Glycan structures at N1515 and N1574 in the A2 domain influence LRP1-mediated clearance. Recent studies have shown that macrophage LRP1 plays an important role in regulating in vivo clearance of VWF. Moreover, RAP prolongs VWF survival in vivo predominantly by inhibiting this macrophage LRP1 mediated clearance. To investigate whether the effect of VWF glycans on macrophage-mediated clearance were modulated via LRP1, clearance studies for wild type rVWF and glycan variants N1515Q and N1574Q were repeated in VWF$^{-/-}$ mice in the presence or absence of the LRP1 antagonist RAP. Blood was collected at 3 and 10 minutes after injection, and data are graphed as percentage residual VWF relative to the amount injected (*$P < .05$, **$P < .01$, and ***$P < .001$; ns, not significant).

demonstrate a critical role for LRP1 in modulating macrophage-mediated clearance of VWF glycoforms, it is important to consider that a number of other macrophage receptors can also bind VWF.[38,39,60] Included among these macrophage receptors are the lectins ASGPR, Gal-1, and Gal-3. We observed that VWF binding to both galectins was significantly reduced following loss of N-linked glycans (data not shown). Moreover, ASGPR inhibition with asiolo-orosomucoid did not attenuate the enhanced in vivo clearance of VWF-N1515Q. Nevertheless, previous studies have shown that LRP1 can form heterologous functional complexes with a number of other macrophage receptors, including β2-integrins.[60] Additional studies will be necessary to determine whether the N1515 and/or N1574 glycans influence VWF interactions with any of these other macrophage receptors in addition to LRP1.

Previous studies have demonstrated that VWF clearance occurs independently of ADAMTS13 proteolysis and is not influenced by VWF multimer size.[52,61] Nonetheless, it is interesting that in addition to influencing VWF clearance by macrophages, the N-linked glycans expressed within the A2 domain of VWF have also been shown to modulate susceptibility to proteolysis by ADAMTS13.[42,62] In particular, McKinnon et al showed that loss of the N-linked glycan at N1574 resulted in significantly enhanced VWF proteolysis by ADAMTS13.[42] Furthermore, differential scanning fluorimetry has confirmed that glycosylation at N1574 plays an important role in stabilization of the A2 domain against unfolding.[44] However, in contrast to its marked effect upon clearance, loss of the VWF N1515 glycan did not significantly influence susceptibility to ADAMTS13 cleavage and did not have any significant effect on the thermostability of the A2 domain.[42,44] Further studies will be necessary to define the biological mechanisms through which the carbohydrate structures at N1515 and N1574 regulate macrophage-mediated clearance. However, it is interesting that ABO(H) blood group determinants, which influence both VWF proteolysis by ADAMTS13 and VWF clearance, are expressed on both of these complex N-linked glycans within the A2 domain of pd-VWF.[7,42]

In the normal circulation, VWF adopts a globular conformation, such that the glycoprotein Ibα (GPIbα) binding site in the VWF A1 domain remains largely hidden.[63] However, exposure to mechanical shear stress results in unwinding of globular VWF. As part of this unfolding process, previous studies have described both uncoupling of the A1A2A3 tridomain cluster, as well as conformational changes within the individual A domains.[64,65] Consequently the platelet binding site in A1 becomes exposed, and the ADAMTS13 cleavage site (Tyr1605-Met1606) that is buried within the A2 domain becomes accessible.[64,66] Our data, together with those recently published from other groups,[22,23,26] suggest that conformational changes in the VWF A domains lead to exposure of cryptic receptor binding sites within A1-A2-A3 that trigger macrophage clearance. Given the thrombotic potential of VWF in its active conformation, targeting of unfolded VWF for rapid macrophage-mediated clearance has biological plausibility. Our findings are also consistent with the hypothesis that specific mutations within the A1 domain result in enhanced clearance due to increased binding to both platelet Gp1bα and macrophage LRP1.[67] Further studies will be required to define the roles played by LRP1 and other macrophage receptors in modulating the enhanced clearance phenotypes associated with type 1C mutations located in other VWF domains. Interestingly however, preliminary data suggest that several other independent regions of VWF (including D′D3 and D4) are also able to bind to LRP1.[14]

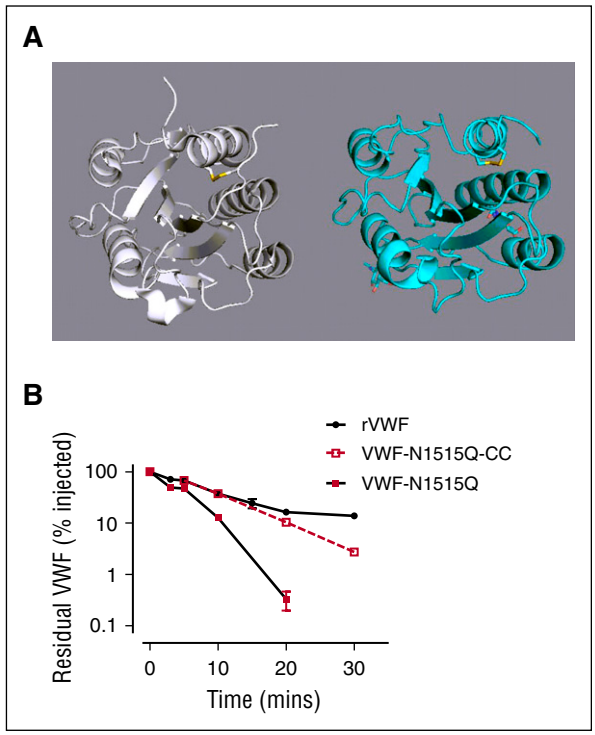

Figure 7. Removal of the N-linked glycans at N1515 does not enhance clearance in VWF with a structurally constrained A2 domain. (A) To examine a potential role for A2 domain conformation in modulating clearance VWF, a previously described cysteine-clamp mutation (N1493C/C1670S) was inserted into full-length rVWF (rVWF-CC) and VWF-N1515Q (VWF-N1515Q-CC). This mutation creates a structurally constrained A2 due to the presence of a long-range disulfide bridge, homologous to those present in the A1 and A3 domains. (B) Clearance was assessed in VWF$^{-/-}$ mice. All results are plotted as percentage residual VWF:antigen levels relative to the amount injected. Data are presented as mean ± SEM.

Acknowledgments

The authors thank Nico van Rooijen of the Foundation Clodronate Liposomes (Haarlem, The Netherlands) for generously providing the liposome-clodronate and Orla Rawley for technical assistance in expression studies.

M.L. and T.A.J.M. acknowledge support from the Imperial College Biomedical Research Centre. This work was supported by a Science Foundation Ireland Principal Investigator Award (11/PI/1066) (J.S.O.).

Authorship

Contribution: A.C., J.M.O., S.A., G.B., S.W., C.D., T.M.B., and T.A.J.M. performed experiments; A.C., J.M.O., P.G.F., T.M.B., R.J.S.P., M.L., T.A.J.M., and J.S.O. designed the research and analyzed the data; and all authors were involved in writing and reviewing the paper.

Conflict-of-interest disclosure: M.L. has received speaker fees from Bayer, Octapharma, and Pfizer; advisory board fees from CSL-Behring, Pfizer, Bayer, and Grifols; and research support from Bayer and CSL Behring. J.S.O. has served on the speaker's bureau for Baxter, Bayer, Novo Nordisk, Boehringer Ingelheim, Leo Pharma, and Octapharma; served on the advisory boards of Baxter, Bayer, Octapharma CSL Behring, Daiichi Sankyo, Boehringer Ingelheim, and Pfizer; and received research grant funding awards from Baxter, Bayer, Pfizer, and Novo Nordisk. The remaining authors declare no competing financial interests.

ORCID profiles: J.S.O., 0000-0003-0309-3313.

Correspondence: James S. O'Donnell, Irish Centre for Vascular Biology, Royal College of Surgeons in Ireland, 123 St. Stephen's Green, Dublin 2, Ireland; e-mail jamesodonnell@rcsi.ie.

References

1. Lillicrap D. von Willebrand disease: advances in pathogenetic understanding, diagnosis, and therapy. *Blood.* 2013;122(23):3735-3740.
2. Lenting PJ, Christophe OD, Denis CV. von Willebrand factor biosynthesis, secretion, and clearance: connecting the far ends. *Blood.* 2015; 125(13):2019-2028.
3. Wagner DD, Marder VJ. Biosynthesis of von Willebrand protein by human endothelial cells: processing steps and their intracellular localization. *J Cell Biol.* 1984;99(6):2123-2130.
4. Sporn LA, Chavin SI, Marder VJ, Wagner DD. Biosynthesis of von Willebrand protein by human megakaryocytes. *J Clin Invest.* 1985;76(3): 1102-1106.
5. Jenkins PV, O'Donnell JS. ABO blood group determines plasma von Willebrand factor levels: a biologic function after all? *Transfusion.* 2006; 46(10):1836-1844.
6. Titani K, Kumar S, Takio K, et al. Amino acid sequence of human von Willebrand factor. *Biochemistry.* 1986;25(11):3171-3184.
7. Canis K, McKinnon TA, Nowak A, et al. Mapping the N-glycome of human von Willebrand factor. *Biochem J.* 2012;447(2):217-228.
8. Canis K, McKinnon TA, Nowak A, et al. The plasma von Willebrand factor O-glycome comprises a surprising variety of structures including ABH antigens and disialosyl motifs. *J Thromb Haemost.* 2010;8(1):137-145.
9. Debeire P, Montreuil J, Samor B, et al. Structure determination of the major asparagine-linked sugar chain of human factor VIII–von Willebrand factor. *FEBS Lett.* 1983;151(1):22-26.
10. Samor B, Michalski JC, Debray H, et al. Primary structure of a new tetraantennary glycan of the N-acetyllactosaminic type isolated from human factor VIII/von Willebrand factor. *Eur J Biochem.* 1986;158(2):295-298.
11. Matsui T, Titani K, Mizuochi T. Structures of the asparagine-linked oligosaccharide chains of human von Willebrand factor. Occurrence of blood group A, B, and H(O) structures. *J Biol Chem.* 1992;267(13):8723-8731.
12. Samor B, Michalski JC, Mazurier C, et al. Primary structure of the major O-glycosidically linked carbohydrate unit of human von Willebrand factor. *Glycoconj J.* 1989;6(3):263-270.
13. McGrath RT, McKinnon TA, Byrne B, et al. Expression of terminal alpha2-6-linked sialic acid on von Willebrand factor specifically enhances proteolysis by ADAMTS13. *Blood.* 2010;115(13): 2666-2673.
14. Casari C, Lenting PJ, Wohner N, Christophe OD, Denis CV. Clearance of von Willebrand factor. *J Thromb Haemost.* 2013;11(suppl 1):202-211.
15. Casonato A, Pontara E, Sartorello F, et al. Reduced von Willebrand factor survival in type Vicenza von Willebrand disease. *Blood.* 2002; 99(1):180-184.
16. Castaman G, Tosetto A, Rodeghiero F. Reduced von Willebrand factor survival in von Willebrand disease: pathophysiologic and clinical relevance. *J Thromb Haemost.* 2009;7(Suppl 1):71-74.
17. Schooten CJ, Tjernberg P, Westein E, et al. Cysteine-mutations in von Willebrand factor associated with increased clearance. *J Thromb Haemost.* 2005;3(10):2228-2237.
18. Haberichter SL, Castaman G, Budde U, et al. Identification of type 1 von Willebrand disease patients with reduced von Willebrand factor survival by assay of the VWF propeptide in the European study: molecular and clinical markers for the diagnosis and management of type 1 VWD (MCMDM-1VWD). *Blood.* 2008;111(10): 4979-4985.
19. Pruss CM, Golder M, Bryant A, et al. Pathologic mechanisms of type 1 VWD mutations R1205H and Y1584C through in vitro and in vivo mouse models. *Blood.* 2011;117(16):4358-4366.
20. Eikenboom J, Federici AB, Dirven RJ, et al; MCMDM-1VWD Study Group. VWF propeptide and ratios between VWF, VWF propeptide, and FVIII in the characterization of type 1 von Willebrand disease. *Blood.* 2013;121(12): 2336-2339.
21. van Schooten CJ, Shahbazi S, Groot E, et al. Macrophages contribute to the cellular uptake of von Willebrand factor and factor VIII in vivo. *Blood.* 2008;112(5):1704-1712.
22. Castro-Núñez L, Dienava-Verdoold I, Herczenik E, Mertens K, Meijer AB. Shear stress is required for the endocytic uptake of the factor VIII-von Willebrand factor complex by macrophages. *J Thromb Haemost.* 2012;10(9):1929-1937.
23. Rastegarlari G, Pegon JN, Casari C, et al. Macrophage LRP1 contributes to the clearance of von Willebrand factor. *Blood.* 2012;119(9): 2126-2134.
24. Rawley O, O'Sullivan JM, Chion A, et al. von Willebrand factor arginine 1205 substitution results in accelerated macrophage-dependent clearance in vivo. *J Thromb Haemost.* 2015;13(5): 821-826.
25. Groeneveld DJ, van Bekkum T, Cheung KL, et al. No evidence for a direct effect of von Willebrand factor's ABH blood group antigens on von Willebrand factor clearance. *J Thromb Haemost.* 2015;13(4):592-600.
26. Wohner N, Legendre P, Casari C, Christophe OD, Lenting PJ, Denis CV. Shear stress-independent binding of von Willebrand factor-type 2B mutants p.R1306Q & p.V1316M to LRP1 explains their increased clearance. *J Thromb Haemost.* 2015; 13(5):815-820.
27. Casari C, Berrou E, Lebret M, et al. von Willebrand factor mutation promotes thrombocytopathy by inhibiting integrin αIIbβ3. *J Clin Invest.* 2013;123(12):5071-5081.
28. Haberichter SL, Balistreri M, Christopherson P, et al. Assay of the von Willebrand factor (VWF) propeptide to identify patients with type 1 von Willebrand disease with decreased VWF survival. *Blood.* 2006;108(10):3344-3351.
29. Sodetz JM, Pizzo SV, McKee PA. Relationship of sialic acid to function and in vivo survival of human factor VIII/von Willebrand factor protein. *J Biol Chem.* 1977;252(15):5538-5546.
30. Stoddart JH Jr, Andersen J, Lynch DC. Clearance of normal and type 2A von Willebrand factor in the rat. *Blood.* 1996;88(5):1692-1699.
31. Mohlke KL, Purkayastha AA, Westrick RJ, et al. Mvwf, a dominant modifier of murine von Willebrand factor, results from altered lineage-specific expression of a glycosyltransferase. *Cell.* 1999;96(1):111-120.
32. Ellies LG, Ditto D, Levy GG, et al. Sialyltransferase ST3Gal-IV operates as a dominant modifier of hemostasis by concealing asialoglycoprotein receptor ligands. *Proc Natl Acad Sci USA.* 2002;99(15):10042-10047.
33. van Schooten CJ, Denis CV, Lisman T, et al. Variations in glycosylation of von Willebrand factor with O-linked sialylated T antigen are associated with its plasma levels. *Blood.* 2007; 109(6):2430-2437.
34. Grewal PK, Uchiyama S, Ditto D, et al. The Ashwell receptor mitigates the lethal coagulopathy of sepsis. *Nat Med.* 2008;14(6): 648-655.
35. Gallinaro L, Cattini MG, Sztukowska M, et al. A shorter von Willebrand factor survival in O blood group subjects explains how ABO determinants

influence plasma von Willebrand factor. *Blood.* 2008;111(7):3540-3545.

36. Gill JC, Endres-Brooks J, Bauer PJ, Marks WJ Jr, Montgomery RR. The effect of ABO blood group on the diagnosis of von Willebrand disease. *Blood.* 1987;69(6):1691-1695.
37. Harris RL, van den Berg CW, Bowen DJ. ASGR1 and ASGR2, the genes that encode the asialoglycoprotein receptor (Ashwell receptor), are expressed in peripheral blood monocytes and show interindividual differences in transcript profile. *Mol Biol Int.* 2012;2012:283974.
38. Saint-Lu N, Oortwijn BD, Pegon JN, et al. Identification of galectin-1 and galectin-3 as novel partners for von Willebrand factor. *Arterioscler Thromb Vasc Biol.* 2012;32(4):894-901.
39. Pegon JN, Kurdi M, Casari C, et al. Factor VIII and von Willebrand factor are ligands for the carbohydrate-receptor Siglec-5. *Haematologica.* 2012;97(12):1855-1863.
40. Rydz N, Swystun LL, Notley C, et al. The C-type lectin receptor CLEC4M binds, internalizes, and clears von Willebrand factor and contributes to the variation in plasma von Willebrand factor levels. *Blood.* 2013;121(26):5228-5237.
41. Smith NL, Chen MH, Dehghan A, et al; Wellcome Trust Case Control Consortium. Novel associations of multiple genetic loci with plasma levels of factor VII, factor VIII, and von Willebrand factor: The CHARGE (Cohorts for Heart and Aging Research in Genome Epidemiology) Consortium. *Circulation.* 2010;121(12):1382-1392.
42. McKinnon TA, Chion AC, Millington AJ, Lane DA, Laffan MA. N-linked glycosylation of VWF modulates its interaction with ADAMTS13. *Blood.* 2008;111(6):3042-3049.
43. McKinnon TA, Goode EC, Birdsey GM, et al. Specific N-linked glycosylation sites modulate synthesis and secretion of von Willebrand factor. *Blood.* 2010;116(4):640-648.
44. Lynch CJ, Lane DA. N-linked glycan stabilization of the VWF A2 domain. *Blood.* 2016;127(13):1711-1718.
45. Baldauf C, Schneppenheim R, Stacklies W, et al. Shear-induced unfolding activates von Willebrand factor A2 domain for proteolysis. *J Thromb Haemost.* 2009;7(12):2096-2105.
46. Luken BM, Winn LY, Emsley J, Lane DA, Crawley JT. The importance of vicinal cysteines, C1669 and C1670, for von Willebrand factor A2 domain function. *Blood.* 2010;115(23):4910-4913.
47. McGrath RT, McRae E, Smith OP, O'Donnell JS. Platelet von Willebrand factor–structure, function and biological importance. *Br J Haematol.* 2010;148(6):834-843.
48. McGrath RT, van den Biggelaar M, Byrne B, et al. Altered glycosylation of platelet-derived von Willebrand factor confers resistance to ADAMTS13 proteolysis. *Blood.* 2013;122(25):4107-4110.
49. Zanardelli S, Crawley JT, Chion CK, Lam JK, Preston RJ, Lane DA. ADAMTS13 substrate recognition of von Willebrand factor A2 domain. *J Biol Chem.* 2006;281(3):1555-1563.
50. Daigneault M, Preston JA, Marriott HM, Whyte MK, Dockrell DH. The identification of markers of macrophage differentiation in PMA-stimulated THP-1 cells and monocyte-derived macrophages. *PLoS One.* 2010;5(1):e8668.
51. van Rooijen N, Kors N, Kraal G. Macrophage subset repopulation in the spleen: differential kinetics after liposome-mediated elimination. *J Leukoc Biol.* 1989;45(2):97-104.
52. Lenting PJ, Westein E, Terraube V, et al. An experimental model to study the in vivo survival of von Willebrand factor. Basic aspects and application to the R1205H mutation. *J Biol Chem.* 2004;279(13):12102-12109.
53. Bovenschen N, Herz J, Grimbergen JM, et al. Elevated plasma factor VIII in a mouse model of low-density lipoprotein receptor-related protein deficiency. *Blood.* 2003;101(10):3933-3939.
54. Narhi LO, Arakawa T, Aoki KH, et al. The effect of carbohydrate on the structure and stability of erythropoietin. *J Biol Chem.* 1991;266(34):23022-23026.
55. Wyss DF, Choi JS, Li J, et al. Conformation and function of the N-linked glycan in the adhesion domain of human CD2. *Science.* 1995;269(5228):1273-1278.
56. Kimura N, Uchida M, Nishimura S, Yamaguchi H. Promotion of polypeptide folding by interactions with Asn-Glycans. *J Biochem.* 1998;124(4):857-862.
57. Mitra N, Sinha S, Ramya TN, Surolia A. N-linked oligosaccharides as outfitters for glycoprotein folding, form and function. *Trends Biochem Sci.* 2006;31(3):156-163.
58. Badirou I, Kurdi M, Legendre P, et al. In vivo analysis of the role of O-glycosylations of von Willebrand factor. *PLoS One.* 2012;7(5):e37508.
59. Kurdi M, Cherel G, Lenting PJ, Denis CV, Christophe OD. Coagulation factor X interaction with macrophages through its N-glycans protects it from a rapid clearance. *PLoS One.* 2012;7(9):e45111.
60. Pendu R, Terraube V, Christophe OD, et al. P-selectin glycoprotein ligand 1 and beta2-integrins cooperate in the adhesion of leukocytes to von Willebrand factor. *Blood.* 2006;108(12):3746-3752.
61. Badirou I, Kurdi M, Rayes J, et al. von Willebrand factor clearance does not involve proteolysis by ADAMTS-13. *J Thromb Haemost.* 2010;8(10):2338-2340.
62. Preston RJ, Rawley O, Gleeson EM, O'Donnell JS. Elucidating the role of carbohydrate determinants in regulating hemostasis: insights and opportunities. *Blood.* 2013;121(19):3801-3810.
63. Crawley JT, de Groot R, Xiang Y, Luken BM, Lane DA. Unraveling the scissile bond: how ADAMTS13 recognizes and cleaves von Willebrand factor. *Blood.* 2011;118(12):3212-3221.
64. Kim J, Zhang CZ, Zhang X, Springer TA. A mechanically stabilized receptor-ligand flex-bond important in the vasculature. *Nature.* 2010;466(7309):992-995.
65. Wu T, Lin J, Cruz MA, Dong JF, Zhu C. Force-induced cleavage of single VWFA1A2A3 tridomains by ADAMTS-13. *Blood.* 2010;115(2):370-378.
66. Zhang X, Halvorsen K, Zhang CZ, Wong WP, Springer TA. Mechanoenzymatic cleavage of the ultralarge vascular protein von Willebrand factor. *Science.* 2009;324(5932):1330-1334.
67. Rayes J, Hollestelle MJ, Legendre P, et al. Mutation and ADAMTS13-dependent modulation of disease severity in a mouse model for von Willebrand disease type 2B. *Blood.* 2010;115(23):4870-4877.

2016 128: 1959-1968
doi:10.1182/blood-2016-04-709436 originally published online August 23, 2016

N-linked glycans within the A2 domain of von Willebrand factor modulate macrophage-mediated clearance

Alain Chion, Jamie M. O'Sullivan, Clive Drakeford, Gudmundur Bergsson, Niall Dalton, Sonia Aguila, Soracha Ward, Padraic G. Fallon, Teresa M. Brophy, Roger J. S. Preston, Lauren Brady, Orla Sheils, Michael Laffan, Thomas A. J. McKinnon and James S. O'Donnell

Blood (print ISSN 0006-4971, online ISSN 1528-0020), is published weekly by the American Society of Hematology, 2021 L St, NW, Suite 900, Washington DC 20036.